Identification of Antibiotic-Resistant Staphylococci and Epidemiological Typing of Methicillin-Resistant *Staphylococcus aureus* by Fourier Transform Infrared Spectroscopy

By

Mohamed Nassim Amiali

Department of Food Science and Agricultural Chemistry

Macdonald Campus, McGill University

Montreal, Quebec

A Thesis submitted to the Faculty of Graduate Studies and Research in partial fulfillment of the requirements for the degree of Doctor of Philosophy

June, 2003

Short title:

DIFFERENTIATION OF STAPHYLOCOCCI STRAINS BY FTIR SPECTROSCOPY

ABSTRACT

Staphylococci strains are among the most widespread multidrug-resistant nosocomial pathogens in Canada. Rapid and accurate identification and epidemiological typing of methicillin-resistant *S. aureus* (MRSA) and its discrimination from coagulase-negative staphylococci (CNS) and glycopeptide-intermediate *S. aureus* (GISA) are crucial for appropriate therapy and for monitoring and limiting intra- and inter-hospital spread of epidemic MRSA strains. Although pulsed-field gel electrophoresis and polymerase chain reaction methods for the identification of MRSA are reliable, they are technically demanding, time-consuming and inappropriate for routine clinical diagnosis. Moreover, no reliable method exists for discrimination of epidemic MRSA from sporadic MRSA and from GISA strains. The objective of the research described in this thesis was to investigate whether Fourier transform infrared (FTIR) spectroscopy could be used to distinguish MRSA from methicillin-susceptible *S. aureus*, borderline oxacillin-resistant *S. aureus* (BORSA), CNS, including methicillin-resistant CNS, and GISA. The application of FTIR spectroscopy for epidemiological typing of Canadian epidemic MRSA (CMRSA) strains as well as their discrimination from sporadic MRSA was also assessed. FTIR spectra were recorded from intact stationary-phase cells grown on Universal Medium (UM™) and deposited and dried on a ZnSe optical window, normalized, and converted to first-derivative spectra. Various chemometric approaches were employed to cluster the different phenotypes of staphylococci species and to subtype five CMRSA strains based on the similarity of their infrared spectral fingerprints in narrow spectral regions selected by visual inspection and by employing a singular-value decomposition (SVD) algorithm. Pairwise separation of MRSA from MSSA, BORSA, CNS, MRCNS, and GISA was accomplished by using principal component analysis (PCA), self-organizing maps (SOM), and the K-nearest neighbors (KNN) algorithm. These chemometric techniques were also successfully employed for epidemiological typing of the five CMRSA strains and their discrimination from sporadic MRSA strains using a combination of different optimal spectral regions selected by SVD. These results demonstrate that FTIR spectroscopy has considerable potential as a rapid method for the identification of different phenotypes of staphylococci and epidemiological typing of MRSA.

RÉSUMÉ

Les souches de staphylocoques multirésistantes aux antibiotiques sont les bactéries pathogènes qui génèrent le plus d'infections nosocomiales au Canada. L'identification et le typage épidémique des souches de *Staphylococcus aureus* résistantes à la méthicilline (SARM) ainsi que leur discrimination des souches staphylocoques à coagulase-négative (SCN) et des souches de *S. aureus* à résistance intermédiaire aux glycopeptides (SAIG) sont des étapes cruciales pour assurer une thérapie appropriée et pour contrôler et limiter leur propagation dans les hôpitaux. Bien que les méthodes d'électrophorèse en champ pulsés («PFGE») et de la réaction à chaîne de polymérase («PCR») sont efficaces et fiables pour l'identification et le typage des souches de SARM respectivement, elles s'avèrent cependant, techniquement très laborieuses exigeant beaucoup de temps et ne sont pas appropriés pour des diagnostics clinique de routine. De plus, l'existence d'une méthode efficace et fiable pour la discrimination des souches épidémiques de SARM des souches sporadiques de SARM ainsi que l'identification des souches de SAIG n'a pas été rapportée à ce jour. L'objectif de la recherche décris dans cette thèse était de vérifier la capacité de la méthode d'infrarouge à transformée de Fourier (IRTF) à distinguer entre les souches SARM, des souches de *S. aureus* à résistance sensible à la méthicilline (SASM), des souches de *S. aureus* à résistance limitrophe («borderline») à la méthicilline («BORSA» pour «borderline methicillin-resistant *S. aureus*»), de celles des souches SCN y compris les souches de SCN à méthicilline résistante (SCN-RM) et des souches de SAIG. L'application de l'IRTF pour le typage épidémiologique des souches épidémiques canadiennes de SARM (CSARM) ainsi que leur discrimination des souches sporadiques a également été investigués. Les spectres de IRTF normalisés et convertis à la dérivé première ont été acquis à partir d'une suspension de cellules bactériennes provenant de la phase stationnaire de croissance sur le milieu universel (UM^{TM}) et déposer ainsi que sécher sur un cristal optique de ZnSe. Différentes méthodes de chémométrie ont été utilisées pour grouper les différents phénotypes de staphylocoques et pour sous-typer les cinq souches de CSARM, en se basant sur la similarité de leur empreinte spectrale infrarouge dans des régions spectrales étroites sélectionnées par inspection visuelle et par l'emploie de l'algorithme décomposition en valeurs singulières (DVS) «Singular value decomposition» («SVD»). La séparation par paire des SARM, de ceux des SASM,

«BORSA», SCN, SCN-RM et SAIG a été accomplie par l'utilisation de l'algorithme de l'analyse en composantes principales (ACP), du réseaux auto-organisés (RAO) «Self-organizing maps» («SOM») et du K plus proches voisins (KPPV) «K-nearest neighbor» («KNN»). Ces techniques de chémométrie ont aussi été employées avec succès pour le typage épidémiologique des cinq souches épidémiques de CSARM ainsi que leur discrimination de celles des souches sporadiques de SARM en utilisant différentes combinaisons optimales de régions spectrales sélectionnées par DVS. Ces résultats démontrent que la spectroscopie à IRTF offre un potentiel considérable du fait que cette méthode est unique, rapide et économique pour l'identification des différents phénotypes de staphylocoques et le typage épidémiologique des souches de SARM.

STATEMENT FROM THE THESIS OFFICE

In accordance with the regulations of the Faculty of Graduate Studies and Research of McGill University, the following statement from the Guidelines for Thesis Preparation (McGill University, October, 1999) is included:

Candidates have the option of including, as part of the thesis, the text of one or more papers submitted, or to be submitted, for publication, or the clearly-duplicated text of one or more published papers. These texts must conform to the "Guidelines for Thesis Preparation" and must be bound together as an integral part of the thesis.

The thesis must be more than a collection of transcripts. All components must be integrated into a cohesive unit with a logical progression from one chapter to the next. In order to ensure that the thesis has continuity, connecting texts that provide logical bridges between the different papers are mandatory.

The thesis must conform to all other requirements of the "guidelines for Thesis Preparation" in addition to the manuscripts.

As manuscripts for publication are frequently very concise documents, where appropriate additional material must be provided in sufficient detail to allow a clear and precise judgement to be made of the importance and originality of the research reported in the thesis.

In general, when co-authored papers are included in a thesis, the candidate must have made a substantial contribution to all papers included in the thesis. In addition, the candidate is required to make an explicit statement in the thesis as to who contributed to such work and to what extent. This statement should appear in a single section entitled "Contribution of Authors" as a preface to the thesis.

When previously published copyright material is presented in a thesis, the candidate must obtain, if necessary, signed waivers from the co-authors and publishers and submit these to the Thesis Office with the final deposition.

ACKNOWLEDGEMENTS

I would like to express my deepest gratitude to my supervisor Professor Ashraf. A. Ismail for giving me the opportunity to conduct this research project in the R&D department of Quelab Laboratories Inc. as well for the support, guidance, encouragement, and advice that he has given me to make this thesis possible. I would like also to thank Dr. Jacqueline Sedman for her help, support, valuable advice, and encouragement and appreciate her judicious editing assistance in the preparation of papers, posters and this thesis.

The contributions of Dr. Michael R. Mulvey and Dr. Andrew Simor, who did some of the microbiological analysis, and the Canadian Nosocomial Infection Surveillance Program are gratefully acknowledged. I would also like to thank Dr. Brigitte Berger-Bächi for sharing with me her expertise and biochemical knowledge about staphylococci species and Dr. Kerstin Ehlert for the extraction of MRSA cell walls.

I must also acknowledge the members of my committee for the assistance they provided at all levels of the research project. I would like to express my appreciation to Mrs. Lise Stiebel, Mrs. Barbara Laplaine and Dr. Inteaz. Alli in the departmental office for their helpfulness and kindness. I would like also to thank Mr. Eby Noroozi and my colleagues in the McGill IR Group.

A special thanks also goes out to Dr. David Burns, Dr. Martin Gander and Dr. Juha Vesanto, who provided with me with advice on chemometrics and MATLAB programming at times of critical need.

Special thanks goes to Dr. Hammiche Bouzid and Mr. Abdelfatah Zinet; without their motivation, help and encouragement I would not have considered a graduate career in Microbiology research. Also very special thanks go out to Dr. Antoine Karam for his moral support, understanding, kindness, and guidance. Without his support and encouragement, I would not have pursued a *Ph.D.* degree. I doubt that I will ever be able to convey my appreciation fully, but I owe him an eternal gratitude.

I would like to thank my parents, my sister and my brothers and also my family for the support they provided me throughout my graduate studies and entire life. Special thanks to my brother Malek, for his help in formatting the thesis and for helping to make the years that I have spent with him stimulating and rewarding. I must acknowledge my wife for her patience during the stressful moments of writing the thesis and I dedicate this thesis to our lovely daughter, Ines Amelia.

Finally, I recognize that this research would not have been possible without the financial assistance of Quelab Laboratories Inc. and express my sincere gratitude to the President, Mr. Roger Boulais, for having confidence in my progress throughout the course of the research project I conducted and for his moral support and encouragement.

CONTRIBUTION OF AUTHORS

Chapters 3-7 of this thesis are the text of papers to be submitted for publication, as listed below. The present author was responsible for the concepts, design of experiments, experimental work, and manuscript preparation. Dr. Ashraf. A. Ismail is the thesis supervisor and had direct advisory input into the work as it progressed. Dr. B. Berger-Bächi and Dr. J. Sedman contributed their expertise and knowledge of staphylococci strains and FTIR spectroscopy, respectively, in the interpretation and discussion of the results. Dr. M. Mulvey, L. Louie, and Dr. A. Simor provided most of the staphylococci strains employed in this research and some of the microbiological data presented in Chapters 3-7. Dr. K. Ehlert provided samples of cell-wall extracts of MRSA (BB270) and MSSA (BB255) employed in part of the research described in Chapter 3.

Chapter 3
M.N. Amiali, B. Berger-Bächi, K. Ehlert, M.R. Mulvey, A.A. Ismail, J. Sedman and A.E. Simor. Rapid Identification of Methicillin-Resistant *Staphylococcus aureus* (MRSA) by Fourier Transform Infrared (FTIR) Spectroscopy

Chapter 4
M.N. Amiali, B. Berger-Bächi, M.R. Mulvey, A.A. Ismail, J. Sedman, L. Louie and A.E. Simor. Rapid and Accurate Identification of Coagulase-Negative Staphylococci (CNS) and Methicillin-Resistant CNS (MRCNS) by Fourier Transform Infrared (FTIR) Spectroscopy

Chapter 5
M.N. Amiali, B. Berger-Bächi, M.R. Mulvey, A.A. Ismail, J. Sedman and A.E. Simor. Evaluation of Fourier Transform Infrared (FTIR) Spectroscopy for the Rapid Identification of Glycopeptide-Intermediate *Staphylococcus aureus* (GISA)

Chapter 6
M.N. Amiali, M.R. Mulvey, B. Berger-Bächi, A.A. Ismail, J. Sedman and A.E. Simor. Epidemiological Typing of Methicillin-Resistant *Staphylococcus aureus* (MRSA) Strains by Fourier Transform Infrared (FTIR) Spectroscopy

Chapter 7
M.N. Amiali, M.R. Mulvey, B. Berger-Bächi, A.A. Ismail, J. Sedman and A.E. Simor. Discrimination between Epidemic and Sporadic Isolates of Methicillin-Resistant *Staphylococcus aureus* (MRSA) Strains by Fourier Transform Infrared (FTIR) Spectroscopy

TABLE OF CONTENTS

LIST OF TABLES

LIST OF FIGURES

LIST OF ABREVIATIONS

ANN	Artificial neural network
AP-PCR	Arbitrary primed polymerase chain reaction
BHI	Brain heart infusion
BMU	Best matching unit
BORSA	Borderline oxacillin-resistant *Staphylococcus aureus*
CDC	Centers for Disease Control and Prevention
CMRSA	Canadian epidemic methicillin-resistant *Staphylococcus aureus*
CNISP	Canadian Nosocomial Infection Surveillance Program
CNS	Coagulase-negative staphylococci
coa	Genes encoding coagulase
CSV	Comma-separated values
DTGS	Deuterated triglycine sulfate
EDTA	Ethylenediaminetetraacetic acid
EMRSA	Epidemic methicillin-resistant *Staphylococcus aureus*
FTIR	Fourier transform infrared
GISA	Glycopeptide-intermediate *Staphylococcus aureus*
HCA	Hierarchical cluster analysis
h-GISA	Heterogeneous glycopeptide-intermediate *Staphylococcus aureus*
h-VRSA	Heterogeneous vancomycin-resistant *Staphylococcus aureus*
IR	Infrared
KNN	K-Nearest neighbors
mec	Methicillin resistance gene
MIC	Minimum inhibitory concentration
MLEE	Multilocus enzyme electrophoresis
MRCNS	Methicillin-resistant coagulase-negative staphylococci
MRSA	Methicillin-resistant *Staphylococcus aureus*
MS	Mass spectroscopy
MSCNS	Methicillin-sensitive coagulase-negative staphylococci
MSSA	Methicillin-sensitive *Staphylococcus aureus*
NARSA	Network on Antimicrobial Resistance in *Staphylococcus aureus*
NCCLS	National Committee for Clinical Laboratory Standards
NIPALS	Nonlinear iterative partial least squares
nuc	Gene encoding nuclease
PBP	Penicillin binding protein
PC	Principal component
PCA	Principal component analysis
PCR	Polymerase chain reaction
PFGE	Pulsed-field gel electrophoresis
RAPD	Random amplification of polymorphic DNA
Rep-PCR	Repetitive element sequence-based polymerase chain reaction
RFLP	Restriction fragment length polymorphism
RTD	Standard routine test dilution
SDS	Sodium dodecyl sulfate
SMRSA	Sporadic methicillin-resistant *Staphylococcus aureus*
SOM	Self-organizing map

SPC	Single point comma
SVD	Singular-value decomposition
TSA	Tryptic soy with sheep blood agar
TSB	Tryptic soy broth
UM™	Universal Medium™
U-matrix	Unified distance matrix
van	Vancomycin resistance genes
VISA	Vancomycin-intermediate *Staphylococcus aureus*
VRSA	Vancomycin-resistant *Staphylococcus aureus*

CHAPTER 1

INTRODUCTION

1.1 GENERAL INTRODUCTION

The research described in this thesis concerns the evaluation of FTIR spectroscopy as a tool for the identification of methicillin-resistant staphylococci and epidemiological typing of methicillin-resistant *Staphylococcus aureus* (MRSA) strains. *Staphylococcus aureus* and coagulase negative staphylococci (CNS) are the most prevalent pathogens causing both nosocomial and epidemic community-acquired infections. The incidence of MRSA in Canadian hospitals increased sixfold from 1995 to 1999 with 4,507 infected patients [1] and with treatment costing between $50 million and $60 million per year. Much of the increase in MRSA prevalence in Canada is due to specific strains of MRSA that are termed epidemic (EMRSA) strains [2,3] owing to their ease and rate of transmission, long-term persistence, rapid inter-hospital spread, and ability to cross geographic and continental boundaries compared to sporadic MRSA (SMRSA) strains [4,5]. Outbreaks of hospital-acquired infections due to EMRSA are also being reported with increasing frequency throughout the world, challenging clinicians and infection control teams [6-9]. Furthermore, the recent emergence and spread of glycopeptide-intermediate *Staphylococcus aureus* (GISA) isolates among MRSA clinical isolates are expected to raise the morbidity and mortality rates of nosocomial infection significantly, since glycopeptides (vancomycin and teicoplanin) have been the drugs of choice for the treatment of multiresistant MRSA infections in the last three decades [10].

With the emergence of methicillin-resistant staphylococci as worldwide nosocomial pathogens [11,12], highly specific and fast identification and typing methods for MRSA strains and discrimination of MRSA from CNS are needed for infection control and epidemiological surveillance purposes. The ability to rapidly differentiate *S. aureus* from CNS in blood cultures and other specimens is essential for selecting the appropriate treatment. *S. aureus* typing is often required for the tracking of an outbreak or

as part of ongoing surveillance, whereas CNS typing is often used to determine whether two or more strains from a patient represent contamination or infection. In addition, rapid and accurate discrimination between EMRSA and SMRSA strains would allow a more selective implementation of infection control measures in order to prevent dissemination of MRSA strains within hospitals. Finally, before the prevalence and clinical relevance of GISA strains can be assessed, a reliable method for their detection must be established.

Presently, no single definitive diagnostic and typing system exists for both identification of methicillin-resistant staphylococci and epidemiological surveillance of MRSA, although a hierarchical approach using two or more methods sequentially has been advocated [13]. Most public health laboratory services use phenotypic (antimicrobial susceptibility and phage typing) as well as genotypic [polymerase chain reaction (PCR)-based and pulsed field gel electrophoresis (PFGE)] methods for characterization and typing of MRSA strains. The ideal method to replace these labor-intensive procedures for routine clinical diagnosis of methicillin-resistant staphylococcal infections and clinical epidemiology purposes would (i) require minimal sample preparation, (ii) produce results within seconds, (iii) analyze samples directly without the need of reagents, (iv) be amenable to automation, and (v) be relatively inexpensive.

With the recent improvements in analytical instrumentation, these requirements are being fulfilled by physicochemical "whole-organism fingerprinting" methods [14]. These methods are based on various types of spectroscopy, most commonly pyrolysis mass spectrometry [15], electrospray ionization mass spectrometry [16], ultraviolet (UV) resonance Raman spectroscopy [17], proton magnetic resonance spectroscopy [18], and Fourier transform infrared (FTIR) spectroscopy [19,20]. In the case of FTIR spectroscopy, whole-organism fingerprinting is based on measurement of the absorption of infrared light due to the excitation of the molecular vibrations of the various biomolecules present in the cell. Infrared absorption intensities provide quantitative information while the absorption frequencies give qualitative information about molecular structure and, because molecular vibrations are perturbed by intermolecular interactions, are sensitive to the environment of the molecule. Thus, infrared spectra

provide an enormous amount of information about the biochemistry of the intact viable organism. The infrared spectrum of a whole intact organism can be considered to be the sum of the infrared spectra of all the cellular components (nucleic acids, cytoplasmic proteins, membrane and cell wall components). The complex superposition of the individual contributions of these constituents yields broad and complex absorption bands throughout the entire infrared spectrum. Accordingly, the infrared spectrum in essence provides quantitative information about the total biochemical composition of a sample, and variations in biochemical composition among different organisms should result in differences in their infrared spectra. Based on the recognition of this fact, the potential use of infrared spectroscopy to differentiate microorganisms was studied as early as the 1950s [21-25]. These early studies established that, just as the infrared spectrum of a chemical compound is considered to be its most unique physical characteristic and is often considered to be equivalent to a fingerprint in unequivocally identifying the compound [26,27], so the infrared spectrum of an organism can serve as its fingerprint. However, because the dispersive spectrometers available at that time were inadequate in terms of sensitivity, speed, and reproducibility and lacked data handling capabilities, the identification of bacteria by infrared spectroscopy was regarded as too time-consuming and impractical.

In the 1980s, interest in the possibility of employing infrared spectroscopy for bacteria identification revived after the performance of infrared instruments was improved through the development of FTIR spectroscopy, coupled with efficient low-cost computers capable of generating and processing high-quality spectra. Since that time, increasing efforts have been made to develop FTIR spectroscopy as a diagnostic tool in microbiology. Much of this research has concerned the application of chemometrics to address the problems associated with processing the complex infrared spectra of microorganisms for purposes of classification and identification. Chemometrics can generally be described as the application of mathematical and multivariate statistical methods to: (i) improve chemical measurement process and (ii) extract more useful chemical information from chemical and physical measurement data [28,29]. The latter is particularly relevant to infrared spectroscopy, which can produce

large data sets of multidimensional complexity. Infrared spectra of microorganisms have extensive overlap of absorptions from the various biomolecules present in the cells. The subtle differences in the infrared spectra among different strains may not be perceptible, but can be revealed by detailed examination, often with the aid of chemometric tools such as genetic algorithms [30] and supervised neural networks [31]. The capability to differentiate between different strains on the basis of their infrared spectra may then be investigated by judiciously using specific spectral regions in combination with chemometrics [32-34]. Principal component analysis (PCA), unsupervised neural networks such as self-organized maps (SOM), supervised neural networks (ANNs), and the K-nearest neighbors (KNN) algorithm have all been applied in the analysis of infrared spectra of a variety of different microorganisms within the fields of medicine and agriculture [20]. For example, FTIR spectroscopy has been successfully used for the discrimination of some species of the genus *Staphylococcus* [31,35,36], other clinical pathogens [37,38], food poisoning bacteria [31,35,39-43], and food spoilage microorganisms [43].

FTIR spectroscopy has also been used for the detection of antibiotic resistance in bacteria for the identification of imipenem-resistant *Pseudomonas aeruginosa* species [44,45], ß-lactam-resistant *E. coli* [44,46,47], and MRSA [36,48] as well as for the detection of drug resistance in human cells [30,49]. However, these studies were based on very limited numbers of resistant species; numbers that are too small and insignificant to allow the FTIR methods to be compared with phenotypic methods such as antibiotic susceptibility testing or to genotypic gold-standard methods such as PCR. Moreover, regarding the identification of MRSA, the classification trial failed when larger and new data sets were included in the analysis due to the heterogeneous nature of some MRSA strains [36]. Examples of epidemiological typing and subtyping of microorganisms by FTIR spectroscopy are also scarce and have been reported only recently for some nosocomial [50,51] and foodborne yeasts [52] and for bacteria such as *Salmonella enteritidis* [53] and *Acinetobacter baumannii* [54].

1. 2 OVERVIEW AND OBJECTIVES OF THE RESEARCH PROJECT

1.2.1 Goal of the research project

The overall objective of this thesis is to evaluate the feasibility of employing FTIR spectroscopy for identification of methicillin-resistant staphylococci and epidemiological typing of MRSA strains. The research includes the differentiation between the various phenotypes of clinical methicillin-resistant staphylococcal species that arise from the heterogeneous nature of the resistance mechanism [55-58]. This heterogeneity is an inherent limitation to the accuracy of susceptibility testing and automated systems. Among the phenotypes that are addressed in this work are GISA, which exhibits low-level resistance to glycopeptide antibiotics (teicoplanin MIC 8-16 μg/ml and vancomycin MIC ≥8 μg/ml) [10], and borderline oxacillin-susceptible *S. aureus* (BORSA: oxacillin MICs of 2-8 μg/ml), which exhibits methicillin resistance overlapping with low-level methicillin resistance of MRSA [59] but can be effectively treated with ß-lactamase-resistant penicillins and cephalosporins [60,61], unlike MRSA, which is resistant to all ß-lactam antibiotics, including cephalosporins, carbapenems, and monocarbactams. Though several screening methods have been suggested for BORSA [62] and GISA strains [63,64], no standardized method to screen for them in the clinical laboratory is available. Thus, the rapid and accurate identification of MRSA strains and discrimination of MRSA from MSSA, BORSA, GISA, and CNS species by FTIR spectroscopy could not only provide a tool to control the spread of MRSA strains but could also decrease unnecessary use of glycopeptide antibiotics, thereby both reducing the cost of care and minimizing the rate of development of bacterial resistance to glycopeptides.

1.2.2 Specific objectives of the research

(i) To discriminate MRSA from MSSA and BORSA strains by employing FTIR spectroscopy.

(ii) To discriminate CNS species from *S. aureus* (MRSA, MSSA) strains by using FTIR spectroscopy.

(iii) To evaluate the capability of FTIR spectroscopy for the identification of methicillin-resistant CNS strains.

(iv) To assess the feasibility of employing FTIR spectroscopy for the accurate differentiation of GISA/heterogeneous-GISA (h-GISA) strains from MRSA and MSSA strains.

(v) To evaluate the discriminatory power of FTIR spectroscopy for epidemiological typing of five Canadian epidemic MRSA strains (CMRSA-1 to CMRSA-5) and compare the FTIR typing approach to the reference typing methods.

(vi) To differentiate between epidemic (EMRSA) and sporadic (SMRSA) strains based on differences between their infrared spectra.

1.3 REFERENCES

1. Simor, A.E., D. Boyd L. Louie, A. McGeer, M.R. Mulvey, and B.M. Willey for the Canadian Hospital Epidemiology Committee and the Canadian Nosocomial Infection Surveillance Program, 1999. Characterization and proposed nomenclature of epidemic strains of MRSA in Canada. *Can. J. Infect. Dis.* 10:333-336

2. McGeer, A., D. Low, and J. Conly. 1997. Methicillin-resistant *Staphylococcus aureus* in Ontario. *Can. Commun. Dis. Rep.* 23:45-46

3. Preston, M., A. Borezyk, and F. Jamieson 1998. Epidemic methicillin-resistant *Staphylococcus aureus* strain-Ontario. *Can. Commun. Dis. Rep.* 24:47-49

4. Roman, R.S., J. Smith, and M. Walker, 1997. Rapid geographic spread of methicillin-resistant *Staphylococcus aureus* strain. *Clin. Infect. Dis.* 25:698-705

5. Teixeira, L.A., C.A. Resende, and L.R. Ormonde, 1995. Geographic spread of epidemic multiresistant *Staphylococcus aureus* clone in Brazil. *J. Clin Microbiol.* 33:2400-2404

6. Brumfit W, and J. Hamilton-Miller, 1989. Methicillin-resistant *Staphylococcus aureus. N. Engl. J. Med.* 320:1188-1196

7. Struelens, M.J., O. Ronveaux, B. Jans, and R. Mertens, 1996. Methicillin-resistant *Staphylococcus aureus* epidemiology and control in Belgium, 1991 to 1995. *Infect. Control Hosp. Epidemiol.* 17:503-508

8. Thompson, R.L., M.D. Cabezudo, and R.P. Wenzel, 1982. Epidemiology of nosocomial infections caused by methicillin-resistant *Staphylococcus aureus. Ann. Int. Med.* 1982:309-316

9. Voss, A, D. Milatovic, C. Wallrauch-Schwarz, V.T. Rosdahl, and I. Braveny, 1994. Methicillin-resistant *Staphylococcus aureus* in Europe. *Eur. J. Clin. Microbiol. Infect. Dis.* 13:50-55

10. Hiramatsu, K., H. Hanaki, T. Ino, K. Yabuta, Y. Oguri, and F.C. Tenover, 1997. Methicillin-resistant *Staphylococcus aureus* clinical strain with reduced vancomycin sisceptibility. *J. Antimicrob. Chemother.* 40:135-136

11. Boyce, J.M., 1990. Increasing prevalence of MRSA in the USA. *Infect. Control Hosp. Epidemiol.* 11:639-642

12. Keane, C.T., D.C. Coleman, and M.T. Cafferkey, 1991. Methicillin-resistant *Staphylococcus aureus* affecting patients in England and Wales. *J. Hosp. Infect.* 16:35-48

13. Tenover, F.C., D. Arbeit, R. V. Goering, P.A. Mickelsen, B.E. Murray, D.H. Persing, and B. Swaminathan, 1995. Interpreting chromosomal DNA restriction patterns produced by pulsed-field gel electrophoresis: criteria for bacterial strain typing. *J. Clin. Microbiol.* 33:2233-2239

14. Magee, J.T., 1993. Whole-organism fingerprinting, *in* M. Goodfellow and A.G. O'Donnel (eds.), *Handbook of New Bacterial Systematics*. London: Academic Press. pp. 383-427

15. Goodacre, R., and D.B. Kell, 1996. Pyrolysis mass spectrometry and its applications in biotechnology. *Curr. Opin. Biotechnol.* 7:20-28

16. Goodacre, R., J.K. Heald, and D.B. Kell, 1999. Characterization of intact microorganism using electrospray ionisation mass spectrometry. *FEMS Microbiol. Lett.* 176:17-24

17. Nelson, W.H., R. Manoharan, and J.F. Sperry, 1992. U.V. resonance Raman studies of bacteria. *Appl. Spectrosc. Rev.* 27:67-124

18. Bourne, R., U. Himmelreich, A. Sharma., C. Mountford, and T. Sorrel, 2001. Identification of *Enterococcus*, *Streptococcus*, and *Staphylococcus* by multivariate analysis of proton magnetic resonance spectroscopic data from plate cultures. *J. Clin. Microbiol.* 39:2916-2923.

19. Naumann, D., D Helm, and H. Labischinski, 1991. Microbiological characterization by FT-IR spectroscopy. *Nature* 351:81-82

20. Mariey, L., J.P. Signolle, C. Amiel, and J. Travert, 2001. Discrimination, classification, identification of microorganisms using FTIR spectroscopy and chemometrics. *Vibr. Spectrosc.* 26:151-159

21. Thomas, L.C., and J.E.S. Greenstreet, 1954. The identification of microorganisms by infrared spectrophotometry. *Spectrochim. Acta.* 6:302-319.

22. Riddle, J.W., P.W. Kabler, B.A. Kenner, R.H. Bordner, S.W. Rockwood, and H.J.R. Stevenson, 1956. Bacterial identification by infrared spectrophotometry. *J. Bacteriol.* 72:593-603

23. Goulden, J.D.S., and M.E. Sharpe, 1958. The infra-red absorption spectra of lacto-bacilli. *J. Gen. Microbiol.* 19:76-86

24. Norris, K.P., 1959. Infra-red spectroscopy and its application to microbiology. *J. Hyg.* 57:326-345

25. Scopes, A.W., 1962. The infrared spectra of some acetic acid bacteria. *J. Gen. Microbiol.* 28:69-79.

26. Colthup, N.B., L.H. Daly, and S. E. Wiberly, 1995. *Introduction to Infrared and Raman Spectroscopy.* New York: Academic Press

27. Griffith, P.R., and J.A. de Haseth, 1986. *Fourier Transform Infrared Spectrometry.* New York: John Wiley and Sons

28. Defernez, M., and R.H. Kemsley, 1997. The use and misuse of chemometrics for treating classification problems. *Trends Anal. Chem.* 16:216-221

29. Workman, J.J., P.R. Mobley, B.R. Kowalski, and R..Bro, 1996. Review of chemometrics applied to spectroscopy - 1985-95. *Appl. Spectrosc. Rev.* 31:73-124.

30. Gaigneaux, A., J.M. Ruysschaert, and E. Goormaghtigh. 2002. Infrared spectroscopy as a tool for discrimination between sensitive and multiresistant K562 cells. *Eur. J. Biochem.* 269:1968-1973

31. Udelhoven, T., D. Naumann, and J. Shmitt. 2000. Development of a hierarchical classification system with artificial neural networks and FTIR spectra for the identification of bacteria. *Appl. Spectrosc.* 54:1471-1479

32. Goodacre, R., E.M. Timmins, P.J. Rooney, J.J. Rowland, and D.B. Kell, 1996. Rapid identification of *Streptococcus* and *Enterococcus* species using diffuse reflectance-absorbance Fourier transform infrared spectroscopy and artificial neural networks. *FEMS Microbiol. Lett.* 140:233-239

33. Naumann, D, D. Helm, H. Labischinski, and P.Giesbrecht, 1991. The characterization of microorganisms by Fourier-transform infrared spectroscopy (FT-IR), *in* W.H. Nelson (ed.), *Modern Techniques for Rapid Microbiological Analysis.* New York: VCH. Publishers. pp. 43-96

34. Surewicz, W.K, H.H. Mantsch, and D. Chapman, 1993. Determination of protein secondary structure by Fourier transform infrared spectroscopy. A critical assessment. *Biochemistry.* 32:389-394

35. Helm, D., H. Labischinski, and D. Naumann. 1991. Classification and identification of bacteria by Fourier transform spectroscopy. *J. Gen. Microbiol.* 137:69-79

36. Kirschner, C., Ngoc Anh Ngo Thi, and D. Naumann, 1999. FT-IR spectroscopic investigations of antibiotic sensitive and resistant microorganisms. *2nd Workshop on FT-IR Spectroscopy in Microbiology and Medical Diagnostics.* Robert Koch-Institute, Berlin

37. Goodacre, R., E.M. Timmins, R. Burton, N. Kaderbhai, A.M. Woodward, D.B. Kell, and P.J. Rooney, 1998. Rapid identification of urinary tract infection bacteria using hyperspectral whole-organism fingerprinting and artificial neural networks. *Microbiology* 144:1157-1170

38. Oberreuteur, H., J. Chaezinski, and S. Scherer. 2002. Intraspecific diversity of *Brevibacterium lines*, *Corynebacterium glutamicum* and *Rhodococcus erythropolis* based on partial 16S rDNA sequence analysis and Fourier-transform infrared (FTIR) spectroscopy. *Microbiology* 148:1523-1532

39. Helm, D., and D. Naumann, 1995. Identification of some bacterial cell components by FTIR spectroscopy. *FEMS Microbiol. Lett.* 126:75-80

40. Franz, M., 1994. Identifizierung von Clostridien mittels FT-IR-Spektroskopie. *Dtsch. Milchwirtsch.* 3:130-132

41. Holt, C., D. Hirst, A. Sutherland, and F. MacDonald, 1995. Discrimination of species in the genus *Listeria* by Fourier transform infrared spectroscopy and canonical variate analysis. *Appl. Environ. Microbiol.* 61:377-378

42. Lefier, D., D. Hirst, C. Holt, and A.G. Williams, 1997. Effect of sampling procedure and strain variation in *Listeria monocytogenes* on the discrimination of species in the genus *Listeria* by Fourier transform infrared spectroscopy and canonical variate analysis. *FEMS Microbiol. Lett.* 147:45-50

43. Mossoba, M.M., F.M. Khambaty, and F.S. Fry, 2002. Novel application of a disposable optical film to the analysis of bacterial strains: a chemometric classification of mid-infrared spectra. *Appl. Spectrosc.* 56:732-736

44. Sockalingum, G.D., W. Bouhedja, P. Pina, P. Allouch, C. Mandray, R. Labia, J.M. Millot, and M. Manfait, 1997. ATR-FTIR spectroscopic investigation of imipenem-susceptible and-resistant *Pseudomonas aeruginosa* isogenic strains. *Biochem. Biophys. Res. Commun.* 232:240-246

45. Sockalingum, G.D., W. Bouhedja, P. Pina, P. Allouch, C. Bloy, and M. Manfait, 1998. FT-IR spectroscopy as an emerging method for rapid characterization of microorganisms. *Cell. Mol. Biol.* 44:261-269

46. Zeroual, W, M. Manfait, and C. Choisy, 1995. FT-IR spectroscopy study of perturbations induced by antibiotic on bacteria (*E. coli*). *Path. Biol.* 43:300-305

47. Bouhedja, W., G.D. Sockalingum, P. Pina, P. Allouch, C. Bloy, R. Labia, J.M. Millot, and M. Manfait, 1997. ATR-FTIR spectroscopy investigation of *E. coli* transconjugants β-lactams-resistance phenotype. *FEBS Lett.* 412:39-42

48. Goodacre, R., P.J. Rooney, and D.B. Kell, 1998. Rapid analysis of microbial systems using vibrational spectroscopy and supervised learning methods: application to the discrimination between methicillin-resistant and methicillin-susceptible *Staphylococcus aureus*. *Proc. SPIE* 3257 *(IR Spectroscopy: New Tool in Medicine)*: 220-229

49. Le Gal, J.M., H. Morjani, and M. Manfait, 1993. Ultrastructural appraisal of multidrug resistance in K562 and LR73 cell lines from Fourier transform infrared spectroscopy. *Cancer Res.* 53:3681:3686

50. Schmalrek, A., P. Tränkle, E. Vanca, and R. Blaschke-Hellmessen, 1998. Differentiation and characterization of *Candida albicans, Exophila dermatidis* and *Prototheca* spp. by Fourier-transform infrared spectroscopy (FTIR) in comparison with conventional methods. *Mycoses* 41:71-77

51. Sockalingum, G.D., C. Sandt, D. Gomez, P. Pina, I. Beguinot, F. Witthuhn, D Aubert, P. Allouch, J.M. Pinon, and M. Manfait. 2002. FTIR characterization of *Candida* species: a study on some reference strains and pathogenic *C. albicans* isolates from HIV+ patients. *Vibr. Spectrosc.* 28:137-146

52. Kümmerle, M., S. Scherer, and H. Seiler, 1998. Rapid and reliable identification of food-borne yeasts by Fourier-transform infrared spectroscopy. *Appl. Environ. Microbiol.* 64:2207-2214

53. Seltmann, G., W. Voigt, and W. Beer, 1994. Application of physico-chemical typing methods for the epidemiological analysis of *Salmonella enteritidis* strains of phage type 25/17. *Epidemiol. Infect.* 113:411-424

54. Seltmann, G., W. Beer, H. Claus, and H. Seifert 1995. Comparative classification of *Acinetobacter baumannii* strains using seven different typing methods. *Zbl. Bakteriol.* 282:372-383

55. Matthews, P.R, and P.R. Stewart, 1984. Resistance heterogeneity in methicillin-resistant *Staphylococcus aureus*. *FEMS Microbiol. Lett.* 22:161-166

56. Chambers, H.F. 1997. Methicillin-resistance in staphylococci: molecular and biochemical basis and clinical implication. *Clin. Microbiol. Rev.* 10:781-791

57. Hartman, B.J., and A. Tomasz, 1986. Expression of methicillin-resistance in heterogeneous strains of *Staphylococcus aureus*. *Antimicrob. Agents Chemother.* 29:85-92

58. Matthews, P.R., K.C. Reed, and P.R. Stewart, 1987. The cloning of chromosomal DNA associated methicillin and other resistances in *Staphylococcus aureus*. *J. Gen. Microbiol.* 133:1919-1929

59. McDougal, L.K., and C. Thornsberry, 1986. The role of β-lactamase in staphylococcal resistance to penicillinase-resistant penicillin and cephalosporin. *J. Clin. Microbiol.* 23:832-839

60. Montanari, M.P., E. Tonin, F. Biavasco, and P.E. Varaldo, 1990. Further characterization of borderline methicillin-resistant *Staphylococcus aureus* and analysis of penicillin-binding proteins. *Antimicrob. Agents Chemother.* 34: 911-913

61. Pefanis, A., C. Thauvin-Eliopoulos, G.M. Eliopoulos, and R.C. Moellering, 1993. Activity of ampicillin-sulbactam and oxacillin in experimental endocarditis caused by ß lactamase hyperproducing *Staphylococcus aureus*. *Antimicrob Agents Chemother.* 37:507

62. Louie, L., S.O. Matasumura, E. Choi, M. Louie, and A.E. Simor, 1999. Evaluation of three rapid methods for detection of methicillin-resistance in *Staphylococcus aureus*. *J. Clin. Microbiol.* 38:2170-2173

63. Tenover, F.C., 2000. VRSA, VISA, and GISA, the dilemma behind the name game. *Clin. Microbiol. Newslett.* 22:49-53

64. Tenover, F.C., M.V. Lancaster, B.C. Hill, C.D. Steward, S.A. Stocker, G.A. Hancock, C.M. O'Hara, S.K. McAllister, N.C. Clark, and K. Hiramatsu, 1998. Characterization of staphylococci with reduced susceptibilities to vancomycin and other glycopeptides. *J. Clin. Micrbiol.* 36:1020-1027

CHAPTER 2

LITERATURE REVIEW

2.1 TAXONOMY AND SYSTEMATICS OF STAPHYLOCOCCI

Bacteria that are members of the genus *Staphylococcus,* belonging to the family Micrococcaceae, are Gram-positive cocci about 1 μm in diameter, characteristically dividing in more than one plane to form grape-like clusters. They have a unique cell wall peptidoglycan characterized by multiple glycine residues in the interpeptide bridge, which renders them susceptible to lysostaphin. Members of the genus *Staphylococcus* are usually facultative anaerobes, capable of generating energy by respiratory or fermentative pathways. Most species have relatively complex nutritional requirements, usually requiring several of the amino acids and B vitamins for growth. They are catalase-positive and usually oxidase-negative. Staphylococci are tolerant of high concentrations of NaCl (up to 10% w/v) and can grow over a temperature range of 10-45 °C. The G + C content of *Staphylococcus* DNA is within the range of 30-38 mol %, which is considered relatively low for Gram-positive bacteria [1].

Classification of staphylococci was traditionally based on colony morphology and simple biochemical and physiological tests [2]. Finer subdivisions are possible using contemporary molecular genetics techniques (e.g., DNA-DNA hybridization [3], ribotyping [4], and pulsed-field gel electrophoresis (PGFE) of *Sma*I digests of chromosomal DNA [5)]), as well as detailed chemical analysis of cellular fatty acids [5], microbial proteins [6], and composition of the peptidoglycan [7]. A number of staphylococci species as well as subspecies have been defined on the basis of their DNA relatedness as established by DNA-DNA hybridization [8].

Typically, staphylococci are found in association with the skin, skin glands, and mucous membranes of warm-blooded animals, although some species can be isolated from processed animal sources such as meat and dairy products or from environmental sources such as soil, dust, air, and water. The staphylococci are among the most prominent of all nosocomial pathogens throughout the world. Among staphylococci

species, *S. aureus* has the greatest pathogenic potential and diversity. *S. aureus* causes disease by exotoxin production (toxic shock and staphylococcal scalded-skin syndromes) and direct invasion and systematic dissemination (bacteremia, urinary tract infections) and has the ability to clot blood plasma. The latter property, with its connotations of virulence, has been used to divide staphylococci into two major groups: the coagulase-positive (*S. aureus*) and the coagulase-negative staphylococci (CNS). The distinction of the species *S. aureus* from other staphylococci was of considerable importance, since *S. aureus* was recognized as a common opportunistic pathogen causing morbidity and mortality, whereas other staphylococci were generally regarded as commensal or saprophytic. Although *S. aureus* is clearly the primary pathogen, the coagulase-negative staphylococci are also capable of causing infections associated with indwelling medical devices [9,10]. However, the prevalence of CNS species as commensal bacteria has the adverse diagnostic consequence of false-positive culture results owing to contamination of the specimen during collection [11]. For this reason, it is important to distinguish between *S. aureus* and CNS in clinical samples and to confirm the presence of CNS before making a diagnostic decision [11,12]. Misidentification of *S. aureus* as a CNS can result in a costly search for other pathogens or unwarranted broad-spectrum empiric antimicrobial coverage [13].

The major concern with regard to the treatment of staphylococcal infection is the continued emergence of antibiotic-resistant strains. Indeed, over 90% of all nosocomial isolates are resistant to penicillin, and as increasing number are resistant to the semi-synthetic, β lactamase-resistant derivatives represented by oxacillin or methicillin [14, 15]. Moreover, oxacillin-resistant strains are often resistant to other antimicrobial agents commonly used to treat staphylococcal infection [16]. Therapeutic options in such cases are often limited to the glycopeptide antibiotics (e.g., vancomycin) or the newly approved drugs linezolid [17] and quinupristin-dalfopristin [18]. Recent reports describing *S. aureus* with reduced susceptibility to vancomycin emphasize the tenuous nature of our reliance on such a limited group of drugs [19,20]. To delay the emergence of resistant strains and prolong the utility of currently available antibiotics, it is imperative that the

use of these drugs be restricted to those cases in which they are absolutely necessary, the primary example being a serious infection caused by an oxacillin-resistant strain.

2.2 ANTIMICROBIAL RESISTANCE IN STAPHYLOCOCCI

2.2.1 General mechanisms of bacterial resistance to antimicrobial agents

Antibiotics have been available for the treatment of bacterial infections for more than fifty years. However, even during the initial period surrounding the commercial development of benzylpenicillin, it was realized that certain bacteria were not killed by the antibiotic, i.e., that antibiotic-resistant bacteria existed already. Nowadays, two broad categories of antibiotic resistance are recognized: intrinsic (or intrinsic insusceptibility) and acquired. The term "intrinsic" is used to indicate that inherent features of the cell are responsible for preventing antibiotic action and distinguishes this situation from acquired resistance, which occurs when resistant strains emerge from previously sensitive bacterial populations, usually after exposure to the agents concerned. Intrinsic resistance is usually expressed by chromosomal genes, whereas acquired resistance may result from mutations in chromosomal genes or by acquisition of plasmids and transposons. In a clinical setting, acquired antibiotic resistance results primarily from selective pressure exerted on bacteria during antibiotic administration for chemotherapy.

Mechanisms of antimicrobial resistance include alterations in membrane permeability [21], active antimicrobial extrusion or efflux [22,23], antimicrobial target alteration, metabolic bypass [24], and enzymatic modification of the antimicrobial [24]. Alterations in membrane permeability may prohibit influx of certain antimicrobials, e.g., aminoglycosides [25]. Antimicrobial target alteration results in a lowered affinity for the antimicrobial (e.g., ß-lactams and macrolides). Enzymatic modification of antimicrobials (e.g., ß-lactams and chloramphenicol) may inhibit membrane permeability or ability to interact with the target of action. Genes conferring antimicrobial resistance often have a metabolic purpose in that organism or a different organism. For example, the gene *mecA*, which confers methicillin resistance to *S. aureus*, probably encodes a cell wall transpeptidase from a nonstaphylococcal organism [26].

Bacteria can acquire resistance by mutation, conjugation, transduction, or transformation, although transduction and transformation are rare resistance-acquisition mechanisms for staphylococci [27]. Chromosomal mutation usually causes an alteration in the antimicrobial target site but also can affect bacterial membrane permeability to an antimicrobial agent, or enzymatically inactivate it. Conjugation between two microorganisms is not as common among Gram-positive microorganisms as it is among Gram-negative microorganisms but does occur. Conjugation may transfer chromosomal or plasmid-borne genes. Transposons are DNA sequences that move between chromosomes and plasmids. Plasmids are extrachromosomal DNA that can self-replicate. Plasmids can acquire multiple resistance genes, giving the microorganism additional genetic material to use. Plasmids have less deleterious effect on the organism and facilitate acquisition of multiple effective antimicrobial resistance genes en bloc [27].

2.2.2 Overview of methicillin resistance in staphylococci

Methicillin and other ß-lactam antibiotics interact with the penicillin-binding proteins (PBPs), enzymes anchored in the cytoplasmic membrane that are involved in the last stages of peptidoglycan biosynthesis. The PBPs are responsible for the polymerization of peptide moieties of the peptidoglycan chains, which in *S. aureus* are cross linked by a characteristic pentaglycyl side chain [28]. Penicillin reduces the cross linking of the peptidoglycan and inhibits new septum initiation [29,30]. The effect of ß-lactams in staphylococci is dose dependent, extending with increasing concentration from growth inhibition, through lytic death, to nonlytic death [31]. The lethal target of ß-lactams has not been identified, and penicillin-induced death does not necessarily correlate with bacteriolysis [32].

Staphylococci become resistant to ß-lactam antibiotics by various mechanisms. Resistance may be due to ß-lactamases that open the ß-lactam ring, inactivating the antibiotic. The genes for ß-lactamase production are usually on a plasmid. Because ß-lactamases are structurally similar to PBPs but are not associated with cell wall transpeptidation [33], penicillins bind to them, and are thereby rendered inactive, without metabolic consequences in the bacteria; i.e., the β-lactamases are essentially PBP

antimicrobial targets freed of their metabolic action. Alteration of the ß-lactam target site can also cause resistance, and this is the mechanism of methicillin resistance in *S. aureus*. This can occur either by mutation or more efficiently, and of greater clinical relevance, by acquisition of a foreign DNA element coding for methicillin resistance. The methicillin-resistance determinant *mec* encodes a low-affinity penicillin-binding protein, referred to as PBP2a or PBP2', and confers to the staphylococci an intrinsic resistance against all ß-lactams, including cephalosporins and carbapenems. Resistance is termed "intrinsic" because it is not due to destruction of the antibiotic by ß-lactamases [34]. The first methicillin-resistant *S. aureus* (MRSA) containing the *mec* determinant was isolated in 1960, shortly after the introduction of methicillin into clinical use. At that time, MRSA strains comprised less than 0.1% of all isolates but have since spread all over the world. MRSA strains reside mainly in environments in which there is a constant strong antibiotic pressure, such as in hospitals. Once established, they are difficult to eradicate and have become a serious problem because of their multi-resistance and their intrinsic resistance to all ß-lactams, ruling out therapy with currently available ß-lactam antibiotics. Another genetically distinct and clinically less important class of staphylococci exhibits borderline resistance to methicillin. Although these isolates can sometimes be mistaken for MRSA in susceptibility tests, they carry no *mec* determinant, are usually not multi-resistant, and arise by mutation at additional non-*mec* loci and as a result of selection of resistance. For treatment and epidemiologic purposes, it is important to differentiate between *mec*-dependent and non-*mec*-dependent methicillin resistance because in the latter case infections appear to be effectively treated with ß-lactamase-resistant penicillins and cephalosporins [35,36].

In summary, at least three different mechanisms are thought to account for methicillin resistance in staphylococci: (i) the production of low-affinity penicillin binding protein, referred to as PBP2a or PBP2' and encoded by the *mecA* gene; (ii) ß-lactamase production [37-39]. and (iii) production of PBPs with modified penicillin-binding capacity or increased levels of production of PBPs [37,40,41].

2.2.2.1 Heterogeneity in expression of methicillin resistance

A distinctive feature of methicillin resistance is its heterogeneous nature [42,43], with the level of resistance varying according to the culture conditions and ß-lactam antibiotic. The majority of cells in heterogeneous strains (typically 99.9% or more) are susceptible to low concentrations of ß-lactam antibiotics (e.g., 1-5 μg/ml of methicillin), with only a small proportion of cells (e.g., 1 in 10^6) growing at methicillin concentrations of 50 μg/ml or greater. Most clinical isolates exhibit this heterogeneous pattern of resistance under routine growth conditions. Heterogeneous strains can, however, appear homogeneous (i.e., 1% or more of cells grow at methicillin concentrations of 50 μg/ml) under certain culture conditions, such as growth in hypertonic culture medium supplemented with NaCl or sucrose or incubation at 30 °C [44]. Addition of EDTA or incubation at 37-43 °C favors a heterogeneous pattern and may suppress resistance entirely.

These changes in expression of resistance with different culture conditions are transient and entirely phenotypic. Passage of a heterogeneous strain in the presence of ß-lactam antibiotic alters the resistance phenotype by selecting for highly resistant mutant clones [26,44]. These clones produce a homogeneous population of highly resistant cells that can grow at methicillin concentrations of 50-100 μg/ml. The trait tends to be unstable in these laboratory-selected clones. With repeated subculture in antibiotic-free medium, the proportion of highly resistant cells gradually diminishes and the original heterogeneous pattern reemerges.

The phenomenon of heterogeneous versus homogeneous resistance in wild-type strains is completely unexplained. Heterogeneous strains may be deficient in a factor or lack a critical modification in a biochemical pathway, possibly for cell wall synthesis, that is important to the functions of PBP2a, which is, in effect, a "foreign" PBP. Homogeneous strains may result from ß-lactam antibiotic selective pressure favoring mutants whose genetic background allows for a fully functional PBP2a [45,46].

2.2.2.2 *mecA*-Associated intrinsic resistance to ß-lactams

Methicillin resistance in staphylococci is due to the acquisition of the chromosomal gene *mecA* and its flanking sequences (*mec* DNA) [47]. The *mecA* gene is highly conserved among staphylococci species, being virtually identical in both MRSA and coagulase-negative staphylococci that have the characteristic methicillin resistance phenotype. There is no *mecA* homologue in susceptible strains. The *mecA* gene encodes PBP2a (also termed PBP2'), an inducible high-molecular-weight (76-kDa) class B PBP [48]. PBP2a has a low binding affinity for β-lactams, thereby allowing cell wall transpeptidation to proceed in the presence of β-lactam antibiotics at concentrations that would inactivate high-affinity PBPs and hence be lethal to the cell. The precise structural basis for its low affinity is not understood, as the same penicillin binding motifs as found in the penicillin-binding domains of high-affinity PBPs also are present in PBP2a [49].

2.2.2.3 Non-*mecA*-mediated intrinsic resistance to ß-lactams

Standard susceptibility tests sometimes fail to distinguish between an MRSA with a very low-level basal resistance and the clinically less relevant borderline resistant strains that carry no *mec* determinant. Two types of borderline resistant strains can be encountered:

(i) The first type of borderline resistant isolates, termed BORSA, are hyperproducers of β-lactamase [37] or strains producing a methicillinase [50]. This resistance mechanism cannot be defined as intrinsic, because it involves partial hydrolysis of penicillinase-resistant penicillins. However, it appears that hyperproduction of ß-lactamase is not sufficient, but specific, yet-to-be defined, host background factors are also needed to establish borderline resistance [50,51].

(ii) The second types of borderline resistant isolates, termed MODSA, are strains with modifications in their own PBPs [52]. Such strains can also be obtained *in vitro* starting from a susceptible *S. aureus* and selecting for growth on increasing concentrations of ß-lactams [53]. Multiple factors that have not yet been identified are involved in this process, and changes in the amount and/or affinity of the existing PBPs

of the cell, mainly in PBP2 and PBP4, have been described [54,40]. Increase in resistance by this mechanism is usually paired with decreased growth rates. In contrast to *mec*A-dependent methicillin resistance, no heteroresistance is observed in MODSA strains; all descendants of culture are uniformly resistant clinically.

Neither BORSA nor MODSA have become as relevant clinically as MRSA, but, because of the phenotypic overlap of BORSA and MODSA with low-level-resistant MRSA, identification methods have to be used that can distinguish between the presence and absence of the *mecA* gene.

2.2.3 Staphylococci with reduced susceptibility to glycopeptides

Glycopeptides (vancomycin and teicoplanin) have been the drugs of choice for treating MRSA infections for the last decade. However, the frequency of staphylococci isolates with reduced susceptibility to glycopeptides has been increasing [55,56]. The emergence and spread of such strains are expected to raise significantly the morbidity and mortality rates of nosocomial infections. Strains of *S. aureus* exhibiting intermediate resistance to glycopeptides (termed GISA), defined as vancomycin MICs of 8 μg/ml, have been reported in Japan [55], the United States [57-59], France [60], the United Kingdom [61] Hong Kong [62], and Korea [63]. The isolates from the United States, France, and Japan appear to have developed from pre-existing MRSA infections. The strains from the United Kingdom and additional strains from Spain [64] appear heteroresistant to vancomycin with MICs in the 1-4 μg/ml range. MRSA with subpopulations exhibiting reduced susceptibility to glycopeptides have been reported worldwide [55,61,63-66]. Heteroresistance to vancomycin was found among 1-20% of MRSA strains isolated in Japanese hospitals in 1997 [55]. However, a lower range (0.5-1.5%) was reported in the majority of European countries and the United States [59,66-68]. The reduced susceptibility of GISA strains to glycopeptides has been associated with therapeutic failures with vancomycin, and these strains have shown resistance to many other antimicrobial agents, limiting therapeutic alternatives to fewer antimicrobials Currently, there are no recommended therapy guidelines for GISA infections [69]. Although nosocomial spread of GISA strains has not been observed in North America

and Europe, spread of heteroresistant *S. aureus* has apparently occurred in Japan [55]. Infection control measures, rational antibiotic policies, including the reduction of glycopeptide use, and rapid laboratory detection of GISA and heterogeneous GISA (h-GISA) strains (h-GISA: vancomycin MIC of 1-4 μg/ml and teicoplanin MIC of 16 μg/ml, with resistant subpopulations that can grow in the presence of >4 μg/ml vancomycin being present at a frequency of 10^{-6}) are the key measures in preventing the spread of these strains. h-GISA isolates might be precursors of GISA, as has been suggested previously [55], and can be associated with treatment failures.

2.2.3.1 Classification of glycopeptide-resistant staphylococci

On the basis of phenotypic differences with respect to vancomycin and teicoplanin susceptibility and bacterial population analysis, three distinct classes of resistant isolates have been defined: class A, vancomycin intermediate, teicoplanin intermediate; class B, vancomycin intermediate, teicoplanin susceptible; class C, vancomycin susceptible, teicoplanin intermediate [70]. *S. aureus* strains with reduced susceptibility to vancomycin have been defined in the literature using different acronyms, such as VRSA, VISA, and GISA, which correspond to different breakpoint criteria in different countries, causing confusion among infectious disease and microbiology specialists.

Vancomycin-intermediate S. aureus (VISA)

The National Committee for Clinical Laboratory Standards [71] defines those *S. aureus* strains requiring 8-16 μg/ml of vancomycin for inhibition as "intermediate" (VISA), those requiring ≤4 μg/ml as "susceptible", and those requiring ≥32 μg/ml as "resistant" strains. Since most VISA strains are also resistant to teicoplanin, the term GISA (glycopeptide-intermediate *S. aureus*) is more appropriate.

Vancomycin-resistant S. aureus (VRSA)

Japanese investigators [55] have defined vancomycin-resistant *S. aureus* (VRSA) as staphylococcal isolates with a vancomycin MIC of ≥8 μg/ml according to the NCCLS method. This term suggests the failure of vancomycin treatment even when administered in appropriate doses and for appropriate periods of time [56]. However, in North America, the term VRSA defines staphylococci with vancomycin MICs of ≥32 μg/ml.

Heterogeneous vancomycin-resistant S. aureus (h-VRSA, h-VISA, h-GISA)

Heterogeneous resistance to vancomycin has been reported in Japan [55] and was defined as staphylococcal strains that grow on brain heart infusion (BHI) screening agar plates supplemented with 4 μg/ml of vancomycin at a frequency of $1/10^6$ colonies or higher. These subpopulations have MICs of 8 μg/ml, higher than the parent clinical isolate (MICs 1-4 μg/ml). This type of resistance appears to be much more common and is termed heterogeneous vancomycin-resistant *S. aureus* (h-VRSA), heterogeneous vancomycin-intermediate *S. aureus* (h-VISA), or heterogeneous glycopeptide-intermediate *S. aureus* (h-GISA) [55,64,65,72]. Often, the vancomycin MICs reported for hetero-VRSA in published reports are those for the daughter colonies, not for the original clinical isolate (i.e., the parent strain).

2.2.3.2 Mechanism of glycopeptide resistance in staphylococci

The mechanism of resistance in clinical GISA isolates is not yet known, but the low level of resistance and the lack of hybridization with enterococcal vancomycin resistance genes *vanA*, *vanB*, *vanC*, *vanD*, and *vanE* suggest that the mechanism(s) is distinct from those that mediate vancomycin resistance in enterococci [73]. Briefly, GISA is associated with an increased proportion of glutamine-nonamidated muropeptides in the cell-wall peptidoglycan synthesis pathway and increased levels of penicillin-binding proteins (PBP2), resulting in thickened or aggregated cell walls. These alterations in cell-wall composition and upregulation of cell wall synthesis presumably result in triggering the overproduction of false target sites (affinity trapping of glycopeptide molecules) that may decrease the access of glycopeptides to their lethal target, the D-alanyl-D-alanine of

the lipid-II-linked muropeptide precursor [74]. The potential mechanisms of resistance in GISA include increases in cell wall turnover that lead to an increase of non-cross-linked D-alanyl-D-alanine side chains; these chains are capable of binding vancomycin outside of the cell wall, making less vancomycin available for intracellular target molecules. In addition, greater autolytic activity and increased *Sigma*B activity have also been reported [75]. The first GISA strain (Mu-50), which was reported in Japan [55], showed the following characteristics: (a) the cell wall appeared twice as thick as the cell wall of vancomycin-susceptible strains on electron microscopy; (b) penicillin-binding protein production (PBP2 and PBP2a) was increased; (c) nonhydrolytic trapping capacity for glycopeptides; (d) activity of cell-wall synthesis enzymes was enhanced; and (e) *vanA*, *vanB*, *vanC*, *vanD* and *vanE* genes from vancomycin-resistant enterococci were not present. Recently, other investigators demonstrated that the vancomycin resistance phenotype is unstable in clinical GISA isolates. A decrease of glycopeptide MICs was observed by nonselective serial passage of GISA strains [76]. Much research needs to be done to better understand the mechanisms of resistance.

2.3 EPIDEMIOLOGY OF NOSOCOMIAL STAPHYLOCOCCI INFECTIONS

S. aureus is one of the most common causes of both endemic nosocomial infections and epidemics of hospital-acquired infection [77]. On the other hand, most nosocomial infections caused by CNS represent endemic infections. In fact, epidemics due to these pathogens have not been reported in Canada [78].

S. aureus may be introduced into hospitals by colonized health care workers [79, 80]. Transmission of S. aureus in hospitals may occur by direct or indirect contact and by airborne transmission [81]. Some strains of *S. aureus* such as type 80/81 strains that were prevalent during the 1950s and 1960s had the propensity to cause serious infections in patients and personnel and spread rapidly through hospitals [82]. More recently, certain strains of MRSA [so-called "epidemic MRSA" (EMRSA)] have spread through hospitals despite the use of measures that effectively controlled transmission of other strains [83, 84]. The characteristics responsible for rapid spread of such organisms are not clear, although it has been suggested that strains that produce large amounts of coagulase or

with multiple copies of the protein A gene may be more likely to cause outbreaks [85-87]. Since most strains of MRSA are multidrug resistant, utilization of a variety of different agents can exert selection pressure that would favor spread of MRSA. Also, the efficacy of infection control measures can greatly affect the incidence of MRSA in hospitals.

The epidemiologic goal of bacterial typing is to accurately identify the source, extent, and mechanism(s) of transmission of outbreaks of infection. Investigations are typically triggered by an increase in the prevalence of *S. aureus* infection or by the appearance of isolates with a distinctive biotype or antibiotic susceptibility pattern. Thus, basic infection control surveillance and routine laboratory evaluation of isolates are practical epidemiologic screening tools. Putative outbreaks are most appropriately corroborated by detailed epidemiologic investigation; molecular typing studies can effectively verify that the isolates represent an outbreak due to a single strain, as was well demonstrated in a recently reported investigation of a nosocomial outbreak of *S. aureus* [88].

2.4 STANDARD METHODS FOR IDENTIFICATION AND EPIDEMIOLOGICAL TYPING OF ANTIBIOTIC-RESISTANT STAPHYLOCOCCI

2.4.1 Phenotypic methods

A variety of well-known phenotypic methods have been used for the detection and/or epidemiological typing of MRSA, including antibiogram susceptibility testing, phage typing, serotyping, and protein electrophoresis [whole cell protein, immunoblotting, multilocus enzyme electrophoresis (MLEE), and zymotyping]. Among these, antibiogram susceptibility testing and phage typing are the most widely used in clinical and routine diagnostic laboratories.

2.4.1.1 Antimicrobial susceptibility testing

Clinical microbiology laboratories routinely test most bacterial isolates for susceptibility to a panel of antimicrobial agents. The identification of a new or unusual pattern of antibiotic resistance among isolates cultured from multiple patients is often the first indication of an outbreak [89]. Both manual and automated methods are widely available, rigorously quality controlled, typically easily performed, and relatively inexpensive. The major disadvantages are poor discriminatory ability and lack of reproducibility. Different strains may develop similar resistance patterns, or sequential clinical isolates representing the same strain may differ in their resistance to one or more antibiotics [90, 91] owing to the acquisition or loss of plasmids or transposons carrying resistance genes. Thus, in most circumstances, the antibiogram cannot be used as the sole typing method for MRSA [6].

2.4.1.2 Bacteriophage typing

Phage typing reflects the outcome of a complex biologic process in which a freshly plated lawn of bacteria is spotted with a suspension of 23 different standard phages and then examined after 24 hours of incubation. An isolate is considered to be sensitive to a particular phage if the growing organisms are lysed, leaving a defect in the lawn, and resistant if growth is unaffected. Resistance may reflect a variety of circumstances, including the absence of an appropriate cell surface receptor for the phage, restriction-modification systems that prevent replication of phage DNA, or the presence of an incompatible lysogenic phage. The phage types assigned to an isolate indicate those phages to which the isolates are determined to be sensitive. Typically, the response to a particular phage is consistent for isolates representing the same strain, and thus a panel of diverse phages can be used to identify and differentiate distinct strains. For many years, phage typing was the method of choice for epidemiological investigations of MRSA. However, in addition to being time-consuming and technically demanding, phage typing suffers from a lack of reproducibility, and the value of this approach is further diminished by the high proportion (20-30%) of non-typable strains of MRSA. Although phage typing has been replaced in many reference laboratories by molecular typing systems, it provided critical insights not only into the basic

epidemiology of staphylococcal transmission, but also into the kinds of problems, many still unresolved, inherent in numerous typing methods.

2.4.2 Genotypic methods

Advances in molecular biology have provided new sets of tools that have been used to develop a wide variety of DNA-based strain-typing systems. Initially restricted largely to research settings, technologies such as plasmid analysis, chromosomal DNA restriction enzyme analysis (REA), Southern hybridization (ribotyping, insertion sequences, *mecA*: *Tn554* probe typing, binary typing), pulsed-field gel electrophoresis (PFGE), PCR typing (coagulase gene typing; *coa* gene), Protein A gene typing, random amplified polymorphic DNA (RAPD) or arbitrary primed-PCR (AP-PCR), and repetitive element sequence-based PCR (rep-PCR) have disseminated, so that genotypic methods are increasingly performed in clinical laboratories. Although these approaches avoid the problems inherent in phenotypic systems, they are, nevertheless, subject to natural and, in some cases, experimental sources of variation. In addition, substantial complexities are involved in interpreting genotyping data and applying them consistently and effectively to epidemiologic studies. Among these genotypic methods, PCR and PFGE are the gold-standard methods in the clinical laboratory.

2.4.2.1 Polymerase chain reaction (PCR)

The essential feature of PCR is the ability to replicate ("amplify") rapidly and exponentially a particular DNA sequence ("the template"). The basic procedure involves several distinct components:

1. The template is typically a relative small fragment of DNA, 0.5 to 2.0 kb, as larger sequences are difficult to amplify efficiently. Only minute quantities of the template need be present.
2. Two small oligonucleotides, termed "primers", corresponding to sequences at opposite ends of the template, define the sites at which replication is initiated. The primers should be long enough to define those sites uniquely; based on statistical considerations, 18 to 20 bp is typically sufficient. A cycle of replication involves denaturing the double-stranded DNA template and binding of the primers to each

strand of the template, followed by synthesis ("polymerization") of the complementary strand.

3. A rapid, self-contained "chain reaction" is achieved by using thermostable DNA polymerases and programmable thermocyclers. An entire procedure, consisting of 20-30 cycles, can be conducted in a small closed container (microfuge tube) and within a few hours will generate sufficient product ("amplicon") to be visualized and sized directly in an agarose or polyacrylamide gel.

PCR is highly useful for diagnostic detection of infectious agents [92]. Strain typing, however, requires additional information beyond the presence or absence of the target sequences.

There are numerous reports describing the use of PCR for the identification and characterization of staphylococcal isolates [12,93-95]. To maximize sensitivity, most of the reported PCR protocols focused on amplification of conserved regions of eubacterial *rRNA* genes and required additional steps (e.g., hybridization with species-species probes) to establish a diagnosis [93,96-99]. Other protocols were directed toward the specific detection of *S. aureus* and focused on amplification of genes found only in that species. Specific examples include the genes encoding nuclease (*nuc*) and coagulase (*coa*), an undefined 442-bp DNA fragment amplified from the *S. aureus* chromosome [99-101], and the *S. aureus* specific *clfA* gene, encoding a surface-associated fibrinogen-binding protein [102]. However, reports describing polymorphisms within *coa* [103-105] suggest that protocols that focus on *coa* as a distinguishing characteristic might be subject to errors of amplification and/or interpretation. Given the importance of detecting oxacillin resistance, some protocols focused directly on amplification of the *mecA* gene, either alone or in multiplex format capable of simultaneously amplifying additional markers [12,93,95,99,106,107].

2.4.2.2 Pulsed-field gel electrophoresis (PFGE)

Pulsed-field gel electrophoresis (PFGE), developed by Schwartz and Cantor [108], is a variation of agarose gel electrophoresis in which the orientation of the electric field across the gel is changed periodically ("pulsed"), rather than being kept constant as in conventional agarose gel electrophoresis used for Southern blot. For technical reasons [109], this modification enables DNA fragments as large as megabases to be separated effectively by size. Suitable unshared DNA is obtained by embedding intact organisms in agarose plugs ("insert"), and enzymatically lysing the cell wall and digesting the cellular proteins. The isolated genomes are then digested *in situ* with restriction enzymes that have few recognition sites [110,111]. When a staphylococcal chromosome of about 2800 kb with a G+C content of approximately 34% is digested with restriction enzyme *Sma*I (recognition sequence CCCGGG), PFGE analysis provides a chromosomal restriction profile composed of 15-20 distinct, well-resolved fragments ranging from approximately 10 to 800 kb.

PFGE has two notable limitations. First, because of the need to diffuse all buffers and enzymes into the agarose insert, the preparation of suitable DNA involves several extended incubation periods and takes 2-4 days [111]. Second, PFGE requires relatively expensive specialized equipment [109]. Nevertheless, PFGE has emerged as the technique of choice for many laboratories and has been used to investigate MRSA in numerous studies [90,112,113]. Although a variety of restriction enzymes have been used, none has been found to be better than *Sma*I [114-116]. All staphylococcal isolates are typable by PFGE, and the pattern is reproducible even after many subcultures [90,113]. Discriminatory ability is high and has been shown superior to that of bacteriophage typing, antibiogram susceptibility testing, RAPD, ribotyping, and zymotyping [114]. Results are also more reliable than for standard REA as there is no interference from plasmid DNA, the fragments being too small to affect the pattern [117]. Thus, PFGE has many of the features associated with the ideal typing method, and it has been proposed that it be regarded as the "gold standard" for delineation of the epidemiology of both endemic and epidemic MRSA.

2.4.3 Commercial rapid identification kits and automated systems

To expedite the process of identification of staphylococci in the clinical laboratory, several manufacturers have developed rapid identification kits and automated systems that allow tests to be completed in only a few hours to one day. With these products, identification of most species and subspecies can be made with an accuracy of 70 to >90% [113,118]. Several manual and automated methods for rapid identification of staphylococci based on biochemical screening are commercially available, including the API STAPH-IDENT kit identification system [118], the STAPH Tract system, and ID 32 STAPH kits (for a much larger range of staphylococcal species) and automated systems such as the MicroScan system [119] and Vitek GPS-SA cards. These methods have excellent specificity but often lack sensitivity in detecting methicillin-resistant staphylococci, particularly coagulase-negative strains [44]. Other commercial systems include the Alamar panel system (Alamar, Sacramento, CA), E-test quantitative antimicrobial susceptibility testing (with 2% NaCl in Mueller-Hinton agar; AB Biodisk, Solona, Sweden) [120], and the BBL crystal MRSA ID system (Becton Dickinson, Cockeysville, MD).

The heterogeneous resistance to methicillin or oxacillin manifested by strains of MRSA (see Section 2.2.2.1) made detection of these organisms problematic for early versions of rapid, automated susceptibility testing systems. The currently available automated systems such as Vitek GPS-SA cards or the MicroScan system have excellent specificity but often lack sensitivity in detecting methicillin-resistant staphylococci, particularly coagulase-negative strains [121]. It has been reported that, except for unusual *mecA*-positive *S. aureus* strains for which MICs of oxacillin are <2 mg/ml, MRSA strains are detected accurately by the Vitek system [122]. It has been recommended that laboratories using automated systems (and probably other commercial methods as well) for detecting methicillin resistance should confirm the results with a second test before a strain is reported as methicillin-susceptible. PCR assays for the *mecA* gene are currently considered a "gold standard" for identifying MRSA, as they will correctly identify even the most heterogeneous of strains [26], However, for laboratories where such assays are

not available, oxacillin-salt agar screen plates have been recommended as probably the best alternative [44,122].

Over the years, many manufacturers have developed commercial kits for the rapid identification of *S. aureus* based on agglutination tests. The earliest of these tests employed erythrocytes sensitized with fibrinogen for the detection of clumping factor. Thereafter, a second generation of products was marketed which employed coated latex particles and/or sensitized sheep erythrocytes to identify *S. aureus* by the simultaneous detection of clumping factor and protein A [123]. Initially, these tests were reported to be very accurate, but later reports documented false-negative results among MRSA strains [124-128]. It was hypothesized that these false-negative MRSA strains do not expose clumping factor or protein A on their surface, which might be explained by the presence of a large amount of capsular polysaccharides masking other cell wall structures. The observation that capsular polysaccharide serotype 5 predominated among MRSA isolates that were not identified by rapid agglutination methods offered a target for improvement of the available tests [124]. Third-generation tests were developed, which incorporated antibodies against group-specific antigens on the *S. aureus* cell surface [123,129]. Well-known commercial agglutination kits for the identification of *S. aureus* include Slidex Staph-Plus (bioMérieux), Staphaurex Plus (Murex Diagnostics Ltd.), and Pastorex Staph-Plus (Sanofi Diagnostics Pasteur, SA). All three tests detect clumping factor and staphylococcal protein A; in addition, Slidex Staph-Plus and Staphaurex Plus detect group-specific antigens on the *S. aureus* cell surface, and Pastorex Staph-Plus detects capsular polysaccharides.

Another standard test kit for differentiating *S. aureus* from CNS species is the traditional tube coagulase test for the detection of free coagulase. However, the time-consuming nature of the test (incubation for 4-24 h is required) often forces clinical microbiology laboratories to use more rapid alternatives. The slide coagulase test, which detects bound coagulase (clumping factor), is rapid (<1 min), but 10-15% of *S. aureus* strains may yield a false-negative result [130]. Accurate differentiation of *S. aureus* from other *Staphylococcus* spp. was achieved by using PCR to detect the presence of the *nuc*

gene, which codes for an extracellular thermostable nuclease [130,130]. However, this method would not be considered suitable for routine diagnostic tests since it is tedious and time-consuming.

2.4.4. Laboratory detection of GISA

The difficulties of laboratory detection of GISA have been reviewed in several recent articles [56,132-134]. Routine methods for antibiotic susceptibility testing, such as disk diffusion and rapid automated methods (MicroScan rapid panels and Vitek cards [132]), fail to detect staphylococci with reduced susceptibility to glycopeptides. Several screening methods to detect GISA isolates have been reported [45,59,132-134], and it has been recommended that quantitative susceptibility testing should be used routinely, with confirmatory testing done only on isolates with MICs $\geq$ 4 μg/ml [56,59,132]. The U.S. Centers for Disease Control (CDC) has specified three requirements to confirm an isolate as GISA [56]: (1) broth microdilution vancomycin MIC of 8-16 μg/ml; (2) E-test vancomycin MIC $\geq$ 6 μg/ml on Mueller Hinton agar (MHA) plates; and (3) growth on commercially prepared BHI screen plate containing 6 μg/ml of vancomycin (inoculum of 10^8 CFU/ml; 24 h of incubation). The Emerging Infections Program of the CDC found that although 84% of U.S. laboratories had the capacity to screen for GISA (i.e., they did not rely solely on the use of disk diffusion without supplemental testing), only 60% recognized the need to perform supplemental testing on selected isolates [135]. Although routine population analysis profiles (PAP) testing is not recommended, because of the technical difficulties, all GISA isolates should be confirmed by this method [136]. Identification of subpopulations that demonstrate heterogeneous resistance to vancomycin is difficult, and there is currently no clinical method for routine screening of *S. aureus* for hetero-resistance [137].

2.5 FTIR SPECTROSCOPY

The last two decades have witnessed the emergence of sensitive, rapid, and increasingly precise physical techniques for microbiological analysis. These new techniques include mass spectrometry (MS), molecular spectroscopy [including fluorescence, Fourier transform infrared (FTIR), and Raman spectroscopy], the application of laser technologies, flow cytometry, and separation techniques such as gas chromatography and high-performance liquid chromatography [138]. Although FTIR spectroscopy is included in this list of "new" techniques, the use of infrared (IR) spectroscopy as a means of differentiating and identifying bacteria was extensively reported as early as the 1950s [139,140]. However, in a critical review on this subject published in 1959, it was concluded that, although individual strains of bacteria definitely exhibit unique IR spectra, the identification of bacteria by IR spectroscopy could not be regarded as a useful technique, as the procedure was too time-consuming and impractical [139]. Indeed, reports on the study of microorganisms by IR spectroscopy became less frequent in the 1960s and virtually ended in the mid-1970s. However, interest in this technique revived in the 1990s, when the development of FTIR spectroscopy in combination with new emerging techniques of chemometrics opened a wide range of new applications for IR spectroscopy.

This revitalization of IR spectroscopy was made possible by the vastly superior performance of FTIR spectrometers in comparison to the dispersive IR instruments that they replaced. The advantages of FTIR spectrometers include excellent photometric and wavelength accuracy, improved spectral quality and reproducibility, and very rapid spectral acquisition. The fundamental basis for these advantages is the use of interferometeric modulation (e.g., a Michelson interferometer) to resolve the radiation from an IR source into its component wavelengths. Thus, as illustrated in Figure 2.1, absorption of IR radiation by the sample is measured simultaneously at all wavelengths by recording an interferogram, which can be acquired in less than one second. The IR spectrum of the sample is then calculated from the interoferogram by a fast Fourier transform algorithm [141]. In addition to the availability of FTIR spectrometers, the interfacing of low-cost minicomputers with these instruments and the development of

Figure 2.1: Systematic diagram illustrating principle of FTIR spectral acquisition

Light emitted from the IR source (**1**) is passed into an interferometer (**2**), where "spectral encoding" takes place, producing an interferogram signal. The beam enters the sample compartment, where it is transmitted through the surface of the sample (**3**). The interferogram signal is altered by absorption of energy of specific frequencies by the sample. The beam then passes to the detector (**4**), which measures the interferogram signal. The measured signal is digitized and sent to the computer (**5**), where it is Fourier transformed to yield an FTIR spectrum

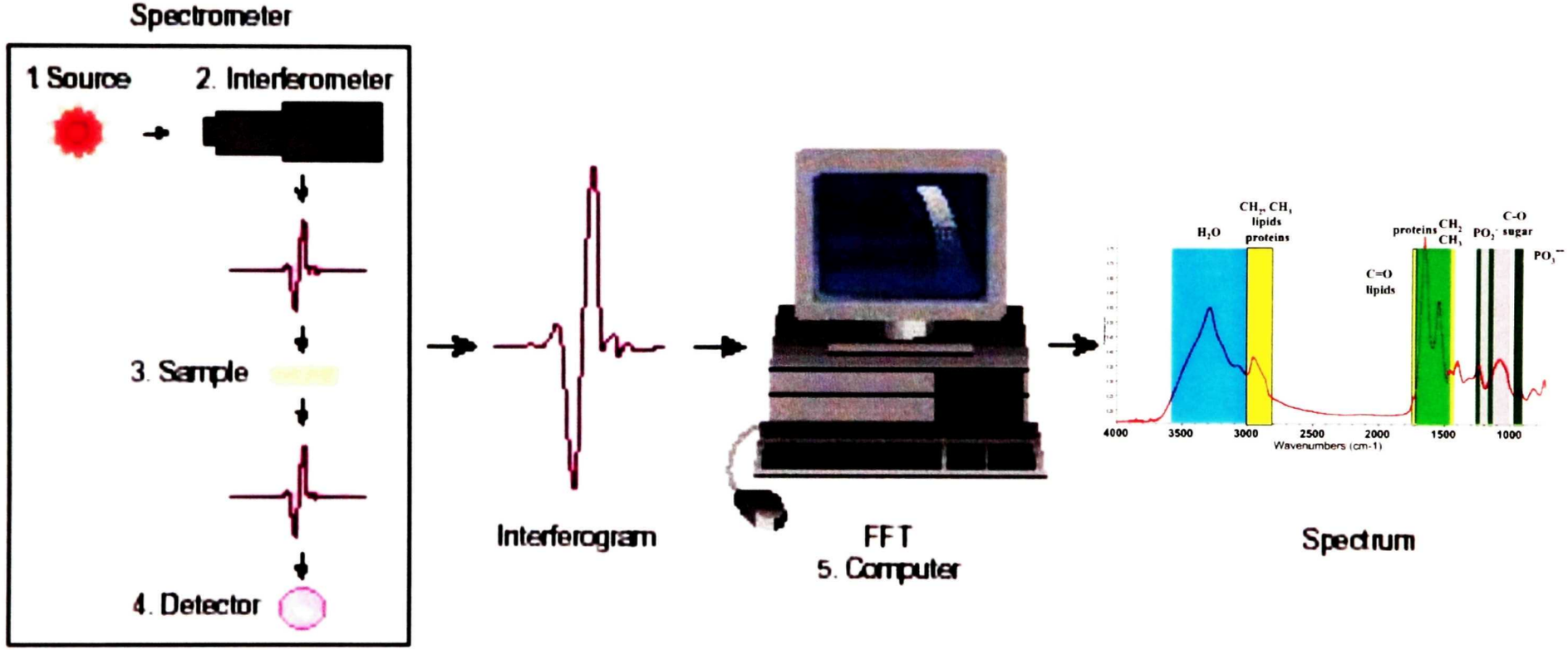
Spectrometer
1 Source
2. Interferometer
3. Sample
4. Detector
Interferogram
FFT
5. Computer
H2O
CH2, CH3
lipids
proteins
C=O
lipids
proteins
CH2
CH3
PO2-
C-O
sugar
PO3-
4000
3500
3000
2500
2000
1500
1000
Wavenumbers (cm-1)
Spectrum

new algorithms for multivariate statistical analysis and pattern recognition also all contributed to the revival of interest in IR spectroscopy as a means of characterizing microbial samples.

2.5.1 Principles of IR spectroscopy

The infrared region of the electromagnetic spectrum extends from the visible region to the microwave, or very short radar, region at wavelengths of some millimeters and is subdivided into the near-infrared (NIR), mid-infrared (MIR), and far-infrared (FIR) regions. The mid-infrared region, corresponding to the wavelength range between 2.5 and 20 μm, is of special interest because absorption of IR radiation in this region results in excitation of the fundamental vibrational modes of molecules. According to quantum mechanics, a molecule can take up an amount of energy to reach the first vibrationally excited state of one of its vibrational modes. A molecule that is irradiated with a continuous spectrum of IR energy will absorb light quanta that have this energy, resulting in an absorption band in the IR spectrum at the vibrational frequency, ν_s. A nonlinear molecule composed of N atoms has $3N - 6$ fundamental vibrational modes, corresponding to various internal stretching and bending vibrations. Although not all of these vibrational modes give rise to IR absorption bands, since only vibrations that are accompanied by a change in the molecular dipole moment are infrared-active, complex molecules display numerous bands in their IR spectra.

It has been internationally accepted that the position of IR absorption bands is expressed in wavenumbers (cm^{-1}), which is the reciprocal of the wavelength. This unit of measurement has the advantage of being directly proportional to the absorbed energy. In general, the frequency of an absorption band in the IR spectrum increases with increasing force constant of the bond(s) involved and decreases with increasing mass of the atoms. This allows the interpretation of a spectrum according to a rough pattern: bands observed between 4000 and 2800 cm^{-1} are due to the stretching vibrations of bonds linking hydrogen to another atom, the stretching vibrations of double and triple bonds occur between 2500 and 1500 cm^{-1}, and the stretching vibrations of single bonds as well as deformation, bending, and ring-breathing vibrations occur in the range below 1500 cm^{-1}

[148]. Some vibrational bands can be assigned to specific bonds or functional groups and are especially valuable in elucidating the structure of a compound, whereas the entire IR spectrum of a particular compound is unique to that compound and is thus of great use in the identification of unknowns. In particular, the range below 1000 cm^{-1} is frequently referred to as the "fingerprint region" of the spectrum.

2.5.2 Characterization of bacteria based on their IR spectra

IR spectroscopy has been applied to the study of bacteria for over 50 years [142] and is based on the observation that different bacteria display different IR spectra. However, bacterial cells represent an extremely complex biochemical system. Many different signals arise from vibrations of molecules of the cell wall, membrane, and polymeric substances in the cytoplasm. This leads to an overlapping and broadening of bands in the spectra. Despite the availability of several resolution enhancement techniques, it is still not possible to completely separate these spectral bands from each other. Nevertheless, the region between 4000 and 500 cm^{-1} contains characteristic bands of peptide and protein structures, of polysaccharides, of phospholipids, and of nucleic acids and is suitable for the characterization of microorganisms.

The high information content of the IR spectra of bacteria has already been exploited for the classification of microorganisms of clinical relevance [143]. Most of the structural and functional groups in different bacteria are identical, and thus the spectra of bacteria are very similar. However, the relative distribution of different functional groups varies among microbial strains, and the availability of software and statistical algorithms for analyzing IR spectra allows the detection of subtle differences in the IR spectra of different bacterial strains. Furthermore, once a spectral library has been established using authenticated strains, mathematical and statistical methods allow the identification of unknowns by comparison of their spectra to those in the library.

2.5.2.1 Spectral acquisition and processing

The fundamental requirement for IR analysis of microorganisms is that the variance within the spectra of one taxon must be smaller than the variance among spectra

of different taxa. Although the variations in biochemical composition among different taxa will result in differences in their IR spectra, these differences may be very slight (e.g., between different strains). Thus, the requirement stated above imposes stringent conditions on spectral reproducibility, and interest in IR bacteria identification, which waned in the 1960s largely because these conditions could not be achieved with the IR instrumentation available at the time, was renewed only when FTIR spectrometers that could provide the required spectral reproducibility were developed. However, many factors other than instrument performance affect spectral reproducibility, and these must all be carefully considered and controlled.

IR spectra of bacteria are usually recorded from intact cells taken directly from culture plates. As early as the 1950s, it was recognized that the IR spectra of living bacterial cells strongly depend on the composition of the growth medium and time of growth. In a more recent study of these types of effects, differences in the spectra of *S. aureus* grown in two different broth media (brain heart infusion versus peptone) and at different times of growth (stationary growth phase versus exponential growth phase) were examined; it was found that the relative peak intensities were affected much more significantly (due to changes in metabolite pool sizes) than the peak positions [144]. These differences suggest that FTIR analysis is dependent on the constraint that all cultures must be grown on the same growth medium under identical conditions. Consequently, extremely precise metabolic control and strict standardized handling of all samples are necessary to yield sufficient reproducibility for the interpretation and comparison of IR spectra of various bacterial cells [144-147]. For the work described in this thesis, an "IR grade" standard growth medium developed by Quelab Laboratories (Monreal, PQ, Canada) to ensure reproducibility of IR spectra for the use of FTIR spectroscopy in routine microbiological analysis was employed.

The reproducibility of the sample-handling technique employed to acquire the FTIR spectra of bacteria is also of critical importance. FTIR spectra of microorganisms are commonly acquired in the transmission mode, although various other techniques such as attenuated total reflectance (ATR) and diffuse reflectance spectroscopy (DRIFT) have also been employed. For spectra acquired in the transmission mode, spectral

reproducibility depends mainly on the uniformity of the sample (sample homogeneity, particle size) and sample thickness (or pathlength) [148]. Sample nonuniformity leads to baseline variations owing to the scattering, diffraction, and refraction that occur as the infrared beam passes through the sample, whereas variations in sample thickness result in variations in band intensity, although consistency in relative peak intensities is maintained. Such variations between replicate spectra can be minimized by normalization and transformation to derivative spectra, assuming the spectra possess very high signal-to-noise ratio. In addition, other types of mathematical preprocessing are frequently applied to facilitate subsequent data analysis aimed at the differentiation of different phenotypes of bacteria on the basis of their spectral profiles. The main types of preprocessing algorithms that have been applied for these purposes are briefly described below.

(i) Smoothing

Smoothing is a useful treatment for allowing visual recognition of trends in spectral data. It is important that smoothing be carried out in an objective manner. One very well recognized method of smoothing is to apply a Savitzky-Golay filter to the data in order to reduce the spectral noise. Commonly, a 5-point Savitzky-Golay filter is appropriate as higher orders of smoothing may result in the loss of useful spectral information [150].

(ii) Normalization

Normalization makes the lengths of all the data vectors in a data set equal; that is, the sum of the squares of the elements of each data vector is the same for all of the samples in the entire data set. Normalization of a set of spectra can be based on the height or area of a single peak or the integrated area under the entire spectrum, depending on the nature of the spectral data set. With an appropriately chosen normalization procedure, normalization effectively removes the variance due to differences in pathlength [150].

(iii) Spectral derivatives

Raw absorption spectra may be transformed to first- or second-derivative spectra to mathematically enhance their spectral resolution, highlighting differences in band shapes and contours of spectra, as well was to eliminate baseline offsets (first-derivative spectra) or tilts (second-derivative spectra). Derivative spectra are commonly computed by using the algorithm published by Savitzky and Golay in 1964 [151]. Because spectral noise is increased by derivatization, first-derivative spectra provide a higher signal-to-noise ratio than second-derivative spectra.

(iv) Mean centering

Mean centering of spectra involves the subtraction of the mean absorbance at each data point for the entire data set from the absorbance at that data point in each individual spectrum Thus, use of mean-centered data facilitates the extraction of spectral information relevant to the variability in the data set, as such data represent the variation around the mean [150].

(v) Variance scaling

Variance scaling, also termed autoscaling to unit variance, is applied to mean-centered spectra and involves dividing the absorbance at each data point in each individual spectrum by the standard deviation of the absorbance values at that data point for the entire data set. Thus, variance-scaling gives equal weighting to all data points in the spectrum, thereby eliminating the effect of inherent differences in band intensities.

2.5.3. Discrimination, classification, and identification of microorganisms based on their IR spectra

The high information content of the IR spectra of microorganisms may be exploited for the discrimination, classification, and identification of microorganisms. Indeed, FTIR spectroscopy has been shown to have sufficient discriminatory power to distinguish between microbial cells even at the strain level, without any preclassification on the basis of other taxonomic criteria [149]. The extensive work conducted in this field

during the past decade has recently been reviewed by Mariey *et al.* [152], and investigations of potential clinical relevance have been discussed by Maquelin *et al.* [153].

The application of various chemometric tools has played a major role in the advancement of FTIR techniques for the identification and classification of microorganisms. Chemometrics can generally be described as the application of mathematical and multivariate statistical methods to: (i) improve chemical measurement process and (ii) extract more useful chemical information from chemical and physical measurement data [150,154]. The latter is particularly relevant to infrared spectroscopy, which can produce large data sets of multidimensional complexity. Infrared spectra of microorganisms have extensive overlap of absorptions from the various biomolecules present in the cells, and the subtle differences in the infrared spectra among different strains may not be perceptible. Thus, identification and classification of microorganisms on the basis of their FTIR spectra can be categorized as pattern recognition tasks, and, as in any such task, feature extraction is an important stage. Chemometric techniques that may be employed for feature extraction include singular-value decomposition (SVD) of the spectral data matrix; genetic algorithms; fractal dimensions; sequential feature selection algorithms such as forward, backward, and bidirectional sequential searches; and feature weighting. The capability to differentiate between different strains on the basis of specific spectral features may then be investigated by various chemometric approaches [149,155]. Principal component analysis (PCA), hierarchical cluster analysis (HCA), discriminant analysis, supervised neural networks (ANNs), and the K-nearest neighbors (KNN) algorithm have all been applied in the analysis of infrared spectra of a variety of different microorganisms within the fields of medicine and agriculture [152].

In the work described in this thesis, singular-value decomposition (SVD) was utilized to assist in the selection of appropriate spectral regions for differentiation of particular staphylococcal strains. PCA was then used to achieve data reduction and a preliminary idea about the distribution of the data. An unsupervised ANN method developed by Kohonen [156] to allow the visualization of high-dimensional data via

generation of a self-organizing map (SOM) was also employed to examine the distribution of the data. Subsequent cluster analysis was performed by partitioning the SOM with the use of the *k*-means algorithm. Although the SOM approach has seldom been employed in the analysis of FTIR data, it has been applied successfully to multidimensional flow-cytometric data for the identification of seven species of fresh water phytoplankton [157] and to pyrolysis mass-spectrometric data for the classification of *Propionibacterium acnes* isolates [158,159]. In parallel, a robust supervised cluster analysis algorithm (KNN), which was previously employed to discriminate between cyanobacterial strains and yielded a high rate (99-100%) of correct classification [160], was applied to confirm the results obtained by exploratory data analysis. The basic principles of these chemometric techniques are presented in the following sections.

2.5.3.1 Exploratory data analysis

2.5.3.1a Principal component analysis (PCA)

In spectroscopy, computational chemistry, image analysis, and process control, a large number of variables describing the samples can be collected. A major problem is to find ways of dealing with these large numbers of variables and eliminate correlations between variables that may lead to invalid results. The aim of analyzing data is often to find the underlying structure of a data set and to describe it in the simplest possible way in order to find patterns and trends in the data as well as to interpret which variables contribute most strongly to these patterns and trends.

PCA is a well-known and effective technique for reducing the dimensionality of multivariate data, including FTIR data, while preserving most of the variance [161,162]. By using PCA, most of the variation in the data is described by a few orthogonal principal components (PCs), or latent variables, which are linear combinations of the original variables. The data are characterized by (a) scores, which are projections of objects (such as spectra) onto each PC, and (b) loadings, which represent the contributions of the variables to each PC. Because the PCs are orthogonal to each other, PCA removes collinearities from the data.

In mathematical terms, PCA is an eigenanalysis technique. It extracts a set of eigenvectors and their associated eigenvalues by a sequential or non-sequential procedure, depending on the algorithm used. The nonlinear iterative partial least squares (NIPALS) algorithm is most commonly employed and extracts the eigenvectors sequentially in order of explained variance. Thus, the first eigenvector accounts for the maximum amount of variance in the data. After each eigenvector is extracted, a residual data matrix is calculated and the procedure is repeated, until there are no significant eigenvalues left. The variance accounted for by each eigenvector is equal to the square of the eigenvalue. Examination of the eigenvalues and their relative magnitudes allows an estimation of the number of significant "factors" or components in the data matrix.

2.5.3.1b Self-organizing map (SOM)

In this section, only the basic principles of SOM, also known as Kohonen networks, will be presented owing to the mathematical complexity of the topic. For a detailed discussion of self-organization, the reader may refer to the monograph by Kohonen [163]. The principal chemical applications of Kohonen networks have been reviewed by Gasteiger and Zupan [164].

The SOM algorithm is an unsupervised neural network algorithm. The neurons are regularly spaced on a low-dimensional grid (one-, two-, or three-dimensional), and each neuron k is represented by an n-dimensional prototype vector $m_k = [m_{k1}, \ldots\ldots, m_{kn}]$, where n is the dimension of the input space. On each training step, a data sample x is selected and the nearest neuron m_c (referred to as the best matching unit, BMU) is found from the map. The prototype vectors of the BMU and its neighbors on the grid are moved toward the sample vector:

$$m_k = m_k + \alpha(t)h_{ck}(t)(x - m_k)$$

where $\alpha(t)$ is the learning rate and $h_{ck}(t)$ is a neighborhood kernel centered on the BMU. Both learning rate and neighborhood kernel radius decease monotonically with time. Thus, during iterative training of the network, the neurons are organized into a meaningful two-dimensional order in which similar neurons are closer to each other in

the grid than the more dissimilar ones. The SOM may thus be regarded as a clustering diagram. There are a variety of methods to visualize the SOM. The two methods used in this work are the U-matrix (unified distance matrix) [165] and component planes [166] methods. In the U-matrix method, color is used to show the distances between neighboring map units: longer distances are represented by shades of yellow and red, while shorter distances are represented by shades of blue. Thus, the U-matrix shows the cluster structure of the map, with a uniform area being blue (designating a cluster) while border areas are yellow and red. Component planes show the values of the individual variables (i.e., PC scores) in each map unit and provide an idea of the spread of values of each variable. By comparing the U-matrix with the component planes, it is possible to identify which variables contribute strongly to a cluster observed in the U-matrix. When the number of SOM units is large, standard clustering algorithms such as the *k*-means algorithm described in the following section may be applied to partition the SOM [166]. The number of clusters can then be evaluated using some kind of validity index such as the Davies-Bouldin index [167].

2.5.3.2 Cluster analysis

Clustering is a statistical technique that classifies objects into groups characterized by their qualitative or quantitative properties [168]. A clustering Q involves partitioning a data set into a set of clusters Q_i, $i = 1 \ldots\ldots\ldots, C$. Most clustering algorithms produce crisp partitionings, where each data sample belongs to exactly one cluster. In the case of ambiguity in assigning a particular data point to a specific cluster, the use of fuzzy clustering algorithms, where a data object may belong to several clusters [169], is warranted. Cluster analysis algorithms may also be characterized as hierarchical or partititive. Agglomerative hierarchical clustering algorithms cluster objects one by one using some measure of similarity, usually the Euclidean distance. The next most similar object is then grouped to form a larger cluster. This process is continued until all the objects have been grouped together to build a hierarchical clustering tree (dendrogram). Divisive hierarchical algorithms are similar but work in the opposite direction, starting from a single cluster and dividing each cluster into sub-clusters until each sub-cluster contains a single object. On the other hand, partitive clustering algorithms divide a data

set directly into a (given) number of clusters, usually based on an implicit assumption on the form of the clusters (e.g., spherical in the case of the *k*-means algorithm employed in this thesis). If the number of clusters is unknown, the partitioning can be repeated for different numbers of clusters, typically ranging from two to the square root of N, where N is the number of samples in the data set. The application of some validity measure is then required to evaluate which partitioning is the best. For example, in the case of the widely used Davies-Bouldin index [167], the best partitioning is that which minimizes:

$$I_{DB} = 1/C \sum \max S_c(C_i) + S_c(C_j)/ d_{ce}(C_i, C_j)$$

where C is the number of clusters, S_c is within-cluster distance, and $d_{ce}(C_i, C_j)$ is between-clusters distance. Because the Davies-Bouldin index uses centroid distance for within-cluster distance and centroid linkage for between-clusters distance, it makes the implicit assumption that the clusters are hyperspheres and thus is suitable for evaluation of *k*-means partitioning.

2.5.3.3 K-nearest neighbors (KNN) algorithm

The K-nearest neighbors algorithm [170,171] is a similarity-based classification method that attempts to categorize unknown samples exclusively on the basis of their proximity to other samples of pre-assigned categories (the training set) in n-dimensional space. It consists of drawing a circle (sphere for $n = 3$; "hypersphere" for $n > 3$) around a point to be classified. The circle is drawn to encompass K nearest neighbors, where K is a user-set parameter. The unclassified point is then assigned to the class to which the majority of its K nearest neighbors belong. If the vote is split, the decision will be based on average distance. The performance of this classification method is assessed by using samples of known category in an independent prediction set as test points and counting the number of correctly classified test points.

2.5.4 Advantages and disadvantages of FTIR spectroscopy in microbiological analysis

Among the advantages of FTIR spectroscopy for investigating microorganisms, the following are the most noteworthy:

1- The method is uniformly applicable to virtually all microorganisms that can be grown in culture. IR spectra can be recorded from intact cells taken directly from culture plates, and biomass requirement can be scaled down to single colonies. With the use of an IR microscope, even microcolonies as small as 20 μm in diameter, corresponding to a few hundred cells, can be analyzed [149].

2- Spectra are available within minutes after obtaining an adequate sample of a pure culture.

3- Detection, enumeration, classification, and identification can be integrated in a single instrument. With the use of an IR-microscope, results are available within one working day in a clinical setting, including isolation, cultivation, and identification.

4- IR spectroscopy can classify microorganisms at very different levels of taxonomic discrimination without any preselection of strains by other taxonomic criteria. In contrast to most other techniques, IR spectroscopy is useful at the strain, species, and genus level. The specificity of the method is generally extremely high, allowing differentiation at the strain and/or serogroup/serotype level.

5- The above advantages make IR spectroscopy useful for (i) very rapid identification of life-threatening pathogens, (ii) epidemiological investigations, conductance of case studies, screening of pathogens, hygiene control, elucidation of infection chains, therapy control, and detection of recurrent infections, (iii) characterization and screening of microorganisms from the environment, (iv) monitoring of biotechnological processes, (v) microbiological quality control in the food and pharmaceutical industries, and (vi) maintenance of strain collections.

6- In a number of cases, *in situ* detection of specific cell components is possible (e.g., storage materials, spore formation, encapsulation of microorganisms), and drug resistance and cell-drug interactions can be monitored and characterized.

The limitations of this technique include the following:

1- Only microorganisms that can be grown in culture can be analyzed. Mixed cultures can only be investigated with the use of an IR microscope provided single colony growth is obtained.
2- Classification and identification are based on the analysis of spectral fingerprints. Specific information on specific compounds present in the whole cells is generally not available.
3- Since the technique provides a spectral fingerprint of cell constituents, reliable identification of unknowns can only be obtained provided the microbiological parameters (culture medium, cultivation time and temperature) can be rigorously controlled. Development of spectral databases for use in different laboratories requires the use of the accepted culture media available on the market.
4- While the strength of the technique is its ability to differentiate microorganisms very rapidly below the species level, classification at the genus level may not be taxonomically relevant in all cases [149].

2.5.5 Application of FTIR spectroscopy in identification and differentiation of staphylococcal species, identification of antibiotic-resistant bacteria, and typing of bacteria

As previously mentioned, the extensive work on the discrimination, classification, and identification of microorganisms based on their IR spectra that has been conducted during the past decade has recently been reviewed in the literature [152,153]. Accordingly, the review of the literature in this section will be limited to a brief survey of work related to the specific applications of FTIR spectroscopy described in Chapters 3-7 of this thesis.

(i) Identification and differentiation of staphylococcal species

Numerous studies have shown the capability of infrared spectroscopy to differentiate bacteria at the genus level [140,149,172-176], and staphylococci have been included in many of these studies, owing to their prevalence [44]. In all cases, the spectral

data in broad regions of the infrared spectra of the bacteria (3000-2800, 1750-1500, 1500-1200, 1200-900, and 900-700 cm^{-1}) were utilized. In some cases, each spectral region was given a weighting factor to augment the performance of the data analysis algorithms [149,172-174]. More recently, ANN was utilized to automatically predict the weighting factors [176]. In all cases reported to date, a correct classification rate of >93% was achieved in the differentiation of staphylococcal species from other bacteria.

In one of the above studies, various staphylococcal species were also successfully distinguished from each other by FTIR spectroscopy [172]. In this study, 11 strains of *S. aureus* and 12 strains of coagulase-negative staphylococci (CNS) were separated by hierarchical cluster analysis (HCA) into two well-separated subclusters by applying both the average linkage method (UMPGA) and Ward's algorithm to the first-derivative spectral data in three broad spectral ranges (weighting factors in parentheses): 3000-2800 cm^{-1} (3.0), 1200-900 cm^{-1} (1.0), and 900-700 cm^{-1} (3.0).

(ii) Antibiotic resistance

Several groups have investigated the feasibility of employing FTIR spectroscopy for the differentiation between antibiotic-resistant and sensitive strains. Significant differences between the FTIR spectra of *E. coli* susceptible to ß-lactams and those of resistant transconjugants were reported [177,178], and the strains were separated from each other employing cluster analysis based on spectral differences in the region 1800-950 cm^{-1}. Similarly, discrimination between four isogenic imipinem-susceptible and resistant *Pseudomonas aeruginosa* strains was achieved using PCA and HCA, employing a single broad spectral region (1800-900 cm^{-1}) [178,179].

An alternative approach to the differentiation between antibiotic-resistant and susceptible strains makes use of an observation made by Zeroual *et al.* [180] that the infrared spectra of *E. coli* were significantly affected by addition of sublethal doses of β-lactam (penicillins G and A) and quinolone (nalidixic acid) antibiotics to the growth medium. Kirschner *et al.* [181] failed to separate 20 strains of MRSA from 18 strains of MSSA by PCA, HCA, and ANN, utilizing either broad or narrow regions of their infrared

spectra. However, by growing the microorganisms in the presence of sublethal doses of the antibiotic oxacillin, a significant change in the infrared spectra (between 1175-875 cm^{-1}) of the MSSA strains in comparison to those of the MRSA strains was observed which allowed for the complete separation of MRSA from MSSA.

(iii) Bacteria typing

FTIR spectroscopy was recently employed for typing of *Legionella pneumophila* [182], *Salmonella enteritidis* [183], *Acinetobacter baumannii* [184], and *Serratia marcescens* [185]. Horbach *et al.* [182] demonstrated the utility of FTIR spectroscopy to differentiate between four different serogroups of *Legionella pneumophila* (based on differences in the spectral region 1200-900 cm^{-1}). They separated the strains based on a differentiation index (D) calculated from the equation $D = (1-\alpha) \times 1000$, where α is Pearson's moment correlation coefficient [172]. Seltmann *et al.* [183] reported a complete separation of 89 strains of *Salmonella enteritidis* into two subgroups based on the differences in their infrared spectra between 1185 and 1120 cm^{-1} employing HCA. It was concluded that the sensitivity of the FTIR-based method was equal to that of whole cell protein pattern (WCPP) analysis and multilocus enzyme electrophoresis (MLEE) for typing of bacteria. Seltmann *et al.* [184] also demonstrated that FTIR spectroscopy could be employed to type 49 *Acinetobacter baumannii* strains into three biotypes (biotypes 2, 6, and 9). Multiple spectral regions were employed (3000-2800, 1500-1200, and 1200-900 cm^{-1}) with a different weighting factor for the 1200-900 cm^{-1} spectral region. While FTIR spectroscopy proved to be a very rapid and reproducible method, it was limited in its discriminating power as compared to PFGE since only 43 out of the 49 strains were correctly typed. Irmscher *et al.* [185] evaluated the efficacy of FTIR spectroscopy relative to MLEE and PFGE to type 66 isolates of *Serratia marcescens* obtained from 46 patients. They concluded that FTIR spectroscopy was easy to use and highly reproducible but that its discriminatory power was limited relative to that of the other two techniques.

2.6 REFERENCES

1. Maidak, B.L, N. Larsen, and M.J. McCaughey, 1994. The ribosomal database project. *Nucleic Acids Res.* 22:3485

2. Baird-Parker, A.C., 1974. The basis for the present classification of staphylococci and micrococci. *Ann. N.Y. Acad. Sci.* 263:7

3. Kloos, W.E. 1980. Natural populations of the genus *Staphylococcus*. *Annu. Rev Microbiol.* 34:559

4. De Buyser, M.-L., A. Morvan, S. Auber *et al.*, 1992. Evaluation of a ribosomal gene probe for the identification of species and subspecies within the genus *Staphylococcus*. *J. Gen. Microbiol.* 138:889

5. Kotilainen, P., P. Huovinen, and E. Eerola, 1991. Application of gas-liquid chromatographic analysis of cellular fatty acids for species identification and typing of coagulase-negative staphylococci. *J. Clin. Microbiol.* 29:315

6. Weller, T.M.A., 2001. Methicillin-resistant *Staphylococcus aureus* typing methods: which should be the international standards?. *J. Hosp. Infect.* 44:160

7. Endl, J., P.H. Seidl, F. Fiedler, and K.H. Schleifer, 1983. Chemical composition and structure of cell wall teichoic acids of staphylococci. *Arch. Microbiol.* 135:215

8. Kloos., W., 1997. Taxonomy and systematics of staphylococci indigeneous to humans, *in* K.B. Crossley and G.L. Archer (eds.), *The Staphylococci in Human Disease*. New York: Churchill Livingstone.

9. Archer, G.L., 1990. *Staphylococcus epidermidis* and other coagulase-negative staphylococci, *in* G.L. Mandell, R.G. Douglas, Jr., and J.E. Bennett (eds.), *Principles and Practice of Infectious Diseases.* New York: Churchill Livingstone. pp. 1511-1518

10. Foster, T.J., and D. Mcdevitt, 1994. Molecular basis of adherence of staphylococci to biomaterials, *in* A.L. Bisno and F.A. Waldvogel (eds.), *Infections Associated with Indwelling Medical Devices*. Washington, D.C.: American Society for Microbiology. pp. 31-44.

11. Weinstein, RA., 1998. Nosocomial infection update. *Emerging Infect. Dis.* 4:416-420

12. Mason, W.J., J. Jon, K. Beenken, N. Wibowo, N. Ojha, and M.S. Smeltzer, 2001. Multiplex PCR protocol for the diagnostic of staphylococcal infection. *J. Clin. Microbiol.* 39:3332-3338

13. Papasian, C.J., and B. Garrison, 1999. Evaluation of a rapid slide agglutination test for identification of *Staphylococcus aureus*. *Diagn. Microbiol. Infect. Dis.* 33(3):201-203

14. Berger-Bachi, B., 1997. Resistance not mediated by beta-lactamase (methicillin resistance), *in* K.B. Crossley and G.L. Archer (eds.), *The Staphylococci in Human Disease*. New York: Churchill Livingstone. pp.158-174

15. Hussain, Z., L. Stoakes, R. Lannigan, S. Longo, and B. Nancekivell, 1998. Evaluation of screening and commercial methods for detection of methicillin resistance in coagulase-negative staphylococci. *J. Clin. Microbiol.* 36:273-274

16. Waldvogel, F.A., 1990. *Staphylococcus aureus* (including toxic shock syndrome), *in* G.L. Mandell, R.G. Douglas, Jr., and J.E. Bennett (eds.), *Principles and Practice of Infectious Diseases*. New York: Churchill Livingstone. pp. 1489-1510

17. Noskin, G.A., F. Siddiqui, V. Stosor, D.L.R. Hacek, and L.R. Peterson, 1999. In vitro activities of linezolid against important gram-positive bacterial pathogens including vancomycin-resistant enterococci. *Antimicrob. Agents Chemother.* 43:2059-2062

18. Von Eiff, C., R.R. Reinert, M. Kresken, J. Brauers, D. Hafner, and G. Peters, 2000. Nationwide German multicenter study on prevalence of antibiotic resistance in staphylococcal bloodstream isolates and comparative in vitro activities of quinpristin-dalfopristin. *J. Clin. Microbiol.* 38:2819-2823.

19. Hiramatsu, K., H. Hanaki, T. Ino, K. Yabuta, T. Oguri, and F.C. Tenover, 1997. Methicillin-resistant *Staphylococcus aureus* clinical strain with reduced vancomycin susceptibility. *J. Antimicrob. Chemother.* 40:135-136

20. Tenover, F.C., R. Arbeit, G. Archer, J. Biddle, S. Byrne, R. Goering, G. Hancock, G.A. Hebert, B. Hill, R. Hollis *et al.*, 1994. Comparison of traditional and molecular methods of typing isolates of *Staphylococcus aureus*. *J. Clin. Microbiol.* 32:407-415

21. Lyon, B.R., and R.A. Skurray, 1987. Antimicrobial resistance of *Staphylococcus aureus*: genetic basis. *Microbiol. Rev.* 51:88

22. Tennent, J.M., B.R. Lyon, M. Midgley *et al.*, 1989. Physical and biochemical characterization of the *qacA* gene encoding antiseptic and disinfectant resistance in *Staphylococcus aureus*. *J. Gen. Microbiol.* 135:1

23. Littlejohn, T.G., I.T. Paulsen, M.T. Gillespie *et al.*, 1992. Substrate specificity and energetics of antiseptic and disinfectant resistance in *Staphylococcus aureus*. *FEMS Microbiol. Lett.* 95:259

24. Young, H., R.A. Skurray, and S.G.B. Amyes, 1987. Plasmid-mediated trimethoprim-resistance in *Staphylococcus aureus*. *Biochem. J.* 243:309

25. Shaw, K.J., P.N. Rather, R.S. Hare, and G.H. Miller, 1993. Molecular genetics of aminoglycoside resistance genes and familial relationships of the aminoglycoside-modifying enzymes. *Microbiol Rev.* 57:138

26. Chambers, H.F., and C.J. Hackbarth, 1987. Effect of NaCl and nafcillin on penicillin-binding protein 2a and heterogeneous expression of methicillin resistance in *Staphylococcus aureus*. *Antimicrob. Agents Chemother.* 31:1982-1988

27. Al-Masaudi, S.B., M.J. Day, and A.D. Russell, 1991. Antimicrobial resistance and gene transfer in *Staphylococcus aureus*. *J. Appl. Bacteriol.* 70(4):279-290

28. Schleifer, K.H., and O. Kandler, 1972. Peptidoglycan types of bacterial cell walls and their taxonomic implications. *Bacteriol. Rev.* 36:407

29. Sidow, T., L. Johannsen, and H. Labischinki, 1990. Penicillin-induced changes in the cell wall composition of *Staphylococcus aureus* before the onset of bacteriolysis. *Arch. Microbiol.* 154:73

30. Wilkinson, B.J., and M.J. Nadakavukaren, 1983. Methicillin-resistant septal peptidoglycan synthesis in a methicillin-resistant *Staphylococcus aureus* strain. *Antimicrob. Agents Chemother.* 23:610

31. Labischinski, H., H. Maidhof, M. Franz *et al*, 1988. Biochemical and biophysical investigations into the cause of penicillin-induced lytic death of staphylococci: checking predictions of the murosome model, *in* P. Actor, L. Daneo-Moore, M.L. Higgins, M.R.J. Salton, and G.D. Shockman (eds.), *Antibiotic Inhibition and Function of Bacterial Cell Surface Assembly and Function.* Washington, D.C.: American Society for Microbiology. p. 242

32. Giesbrecht, P., T. Kersten, and H. Maidhof, 1994. A novel "hidden" penicillin-induced death of staphylococci at high drug concentration, occurring earlier than murosome-mediated killing process. *Arch. Microbiol.* 161:370

33. Massova, I., and S. Mobashery, 1998. Kinship and diversification of bacterial penicillin-binding proteins and beta-lactamases. *Antimicrob. Agents Chemother.* 42:1-17

34. Seligman, S.J., 1966. Penicillinase-negative variants of methicillin-resistant *Staphylococcus aureus*. *Nature* (London) 209:994-996

35. Montanari, M.P., E. Tonin, F. Biavasco, and P.E. Varaldo, 1990. Further characterization of borderline methicillin-resistant *Staphylococcus aureus* and analysis of penicillin-binding proteins. *Antimicrob. Agents Chemother.* 34:911-913

36. Pefanis, A., C. Thauvin-Eliopoulos, G.M. Eliopoulos, and R.C. Moellering, 1993. Activity of ampicillin-sulbactam and oxacillin in experimental endocarditis caused by β lactamase hyperproducing *Staphylococcus aureus*. *Antimicrob. Agents Chemother.* 37:507

37. McDougal, L.K., and C. Thornsberry, 1986. The role of β-lactamase in staphylococcal resistance to penicillinase-resistant penicillin and cephalosporin. *J. Clin. Microbiol.* 23:832-839

38. Massidda, O., M.P. Montanari, and P.E. Valrado, 1992. Evidence for a methicillin-hydrolyzing beta-lactamase in *Staphylococcus aureus* strains with borderline susceptibility to this drug. *FEMS Microbiol. Lett*: 92:223-227

39. Tomasz, A., H.B. Drugeon, H.M. de Lancaster, D. Jabes, L. McDougal, and J. Bille, 1989. New mechanism for methicillin resistance in *Staphylococcus aureus*: clinical isolates that lack the PBP 2a gene and contain normal penicillin binding proteins with modified penicillin-binding capacity. *Antimicrob. Agents Chemother.* 33:1899-1874

40. Henze, U.U., and B. Berger-Bachi, 1995. *Staphylococcus aureus* penicillin-binding protein 4 and intrinsic β lactam resistance. *Antimicrob. Agents Chemother.* 39:2415

41. Hartman, B.J., and A. Tomasz, 1986. Expression of methicillin-resistance in heterogeneous strains of *Staphyococcus aureus*. *Antimicrob. Agents Chemother*: 29:85-92

42. Matthews, P.R., and P.R. Stewart, 1984. Resistance heterogeneity in methicillin resistant *Staphylococcus aureus*. *FEMS Microbiol. Lett.* 22:161-166

43. Sabath, L.D., and S.J. Wallace, 1974. Factors influencing methicillin-resistance in staphylococci. *Ann. N. Y. Acad. Sci.* 263:258-266

44. Chambers, H.F., 1997. Methicillin-resistance in staphylococci: molecular and biochemical basis and clinical implication. *Clin. Microbiol. Rev.* 10:781-791

45. Hiramatsu, K., 1995. Molecular evolution of MRSA. *Microbiol Immunol.* 39:531-543

46. Suzuki, E., K. Kuwahara-Arai, J.F. Richardson, and K. Hiramatsu, 1993. Distribution of *mec* regulator genes in methicillin-resistant clinical strains. *Antimicrob. Agents Chemother.* 37:1219-1226

47. Berger-Bachi, B., 1994. Expression of resistance to methicillin. *Trends Microbiol.* 2:389.

48. Ghysen, J-M., 1994. Molecular structures of penicillin-binding proteins and beta-lactamases. *Trends Microbiol.* 2:372-380

49. Wu, C.Y., W.E. Alborn, Jr., J.E. Flokowitsch, J. Hoskins, S. Unal, L.C. Blaszczak, D. A. Preston, and P.L. Skatrud, 1994. Site-directed mutagenesis of the *mec A* gene from a methicillin-resistant strain of *Staphylococcus aureus. J. Bacteriol.* 176:443-449

50. Massida, O., M.P. Montanari, M. Mingoia, and P.E. Valrado, 1994. Cloning and expression of the penicillinase from a borderline methicilllin-resistant *Staphylococcus aureus* strains in *Escherichia coli. FEMS Microbiol. Lett.* 119:263-270

51. Varaldo, P.E., P.M. Montanari, F. Biavasco *et al.*, 1993. Survey of clinical isolates of *Staphylococcus aureus* for borderline susceptibility to antistaphylococcal penicillins. *Eur. J. Clin. Microbiol. Infect. Dis.* 12:677

52. Tomasz, A., H.B. Drugeon, H.M. de Lancaster, D. Jabes, L. McDougal, and J. Bille, 1989. New mechanism for methicillin resistance in *Staphylococcus aureus*: clinical isolates that lack the PBP 2a gene and contain normal penicillin binding proteins with modified penicillin-binding capacity. *Antimicrob. Agents Chemother.* 33:1899-1874

53. Berger-Bächi, B., A. Strassle, and F.H. Kayser, 1989. Natural methicillin resistance in comparison with that selected by in vitro drug exposure in *Staphylococcus aureus. J. Antimicrob. Chemother.* 23:179

54. Georgopapadakou, G., *et al.*, 1988. Overproduction of penicillin-binding protein 4 in *Staphylococcus aureus* is associated with methicillin resistance, *in* P. Actor, L. Daneo-Moore, M.L. Higgins, M. Salton, and G.D. Shockman (eds.), *Antibiotic Inhibition and Function of Bacterial Cell Surface Assembly and Function.* Washington, D.C.: Society for Microbiology. p. 597

55. Hiramatsu, K., N. Aritaka, H. Hanaki, S. Kawasaki, Y. Hosoda, S. Hori, Y. Fukuchi, and I. Kobayashi, 1997. Dissemination in Japanese hospitals of strains of *Staphylococcus aureus* heterogeneously resistant to vancomycin. *Lancet* 350:1670-1673

56. Tenover, F.C., 2000. VRSA, VISA and GISA, the dilemma behind the name game. *Clin Microbiol Newslett.* 22:49-53

57. Smith, T.L., M.L. Pearson, K.R. Wilcox *et al.*, 1999. Emergence of vancomycin resistance in *Staphylococccus aureus. N. Engl. J. Med.* 340:493-501

58. Sieradzki, K., and A. Tomasz, 1999. Gradual alterations in cell wall structure and metabolism in vancomycin-resistant mutants of *Staphylococcus aureus*. *J. Bacteriol.* 181:7566-7570

59. Fridkin, S.K., 2001. Vancomycin-intermediate and resistant *Staphylococcus aureus*: what the infectious disease specialist needs to know. *Clin. Infect. Dis.* 32:108-115

60. Ploy, M.C., C. Gréland, C. Martin, L. de Lumley, and F. Denis, 1998. First clinical isolate of vancomycin-intermediate *Staphylococcus aureus* in a French hospital. *Lancet* 351:1212

61. Howe, R.A, K.E. Bowker, T.R. Wash, T.G. Feest, and A.P. MacGowan, 1998. Vancomycin-resistant *Staphylococcus aureus*. *Lancet* 351:601-602

62. McManus, J., 1999. Vancomycin-resistant *Staphylococcus* reported in Hong Kong. *BMJ* 318:626

63. Mi-Na, K., C.H. Pai, J.H. Woo, J.S. Ryu, and K. Hiramatsu, 2000. Vancomycin intermediate *Staphylococcus aureus* in Korea. *J. Clin. Microbiol.* 38:3879-3881

64. Ariza, J., M. Pujol, J. Cabo *et al.*, 1999. Vancomycin in surgical infections due to methicillin-resistant *Staphylococcus aureus* with heterogeneous resistance to vancomycin. *Lancet* 353:1587-1588

65. Hiramatsu, K., H. Hanaki, T. Ino, K. Yabuta, T. Oguri, and F.C. Tenover, 1997. Methicillin-resistant *Staphylococcus aureus* clinical strain with reduced vancomycin susceptibility. *J. Antimicrob Chemother.* 40:135-136

66. Bierbaum, G., K. Fuchs, W. Lenz, C. Szekar, and H.G. Sahl, 1999. Presence of *Staphylococcus aureus* with reduced susceptibility to vancomycin in Germany. *Eur. J. Clin. Microbiol.* 38:2985-2988

67. Geisel, R., F. Schmitz, L. Thomas, G. Berns *et al.*, 1999. Emergence of heterogeneous intermediate vancomycin resistance in *Staphylococcus aureus* isolates I the Dusseldorf area. *J. Antimicrob. Chemother.* 43:846-848

68. Chesneau, O., A. Morvan, and N. El Sohl, 2000. Retrospective screening for heterogeneous vancomycin resistance in diverse *Staphylococcus aureus* clones dissiminated in French hospitals. *J. Antimicrob. Chemother.* 45:887-890

69. Rybak, M.J., and R.L. Akins, 2001. Emergence of methicillin-resistant *Staphylococcus aureus* with intermediate glycopeptide resistance. Clinical significance and treatment options. *Drugs* 61:1-7

70. Boyle-Vavra, S., H. Labischinski, C. Ebert, K. Ehlert, and R. Daum, 2001. A spectrum of changes occurs in peptidoglycan composition of glycopeptide-

intermediate clinical *Staphylococcus aureus* isolates. *Antimicrob. Agents Chemother.* 45:280-287

71. National Committee for Clinical Laboratory Standards, NCCLS, 2000. Methods for dilution antimicrobial susceptibility tests for bacteria that grow aerobically, Approved Standard M7-A5.

72. Trakulsomboon, S., S. Danchaivijitr, Y. Rongrungruang *et al.*, 2001. First report of methicillin-resistant *Staphylococcus aureus* with reduced susceptibility to vancomycin in Thailand. *J. Clin. Microbiol.* 39:591-595

73. Murray, B.E., 2000. Drug therapy: vancomycin-resistant enterococcal infections. *N. Engl. J. Med.* 342:710-721

74. Sieradzki, K., and A. Tomasz, 1999. Inactivation of methicillin-resistance gene *mec*A in vancomycin-resistant *Staphylococcus aureus*. *Microb. Drug Resist.* 5:253-257

75. Hiramatsu, K., 1998. The emergence of *Staphylococcus aureus* with reduced susceptibility to vancomycin in Japan. *Am. J. Med.* 104:7S-10S

76. Boyle-Vavra, S., S. Berke, J.C. Lee, and R.S. Daum, 2000. Reversion of glycopeptide resistance phenotype in *Staphylococcus aureus* clinical isolates. *Antimicrob Agents Chemother.* 44:272-277

77. Patti, J.M, B.L. Allen, M.J. McGavin, and M. Hook, 1994. MSCRAMM-mediated adherence of microorganisms to host tissues. *Annu. Rev. Microbiol.* 43:585

78. Louie, L., A. Majury, J. Goodfellow, M. Louie, and A.E. Simor, 2001. Evaluation of a latex agglutination test (MRSA-Screen) for detection of oxacillin resistance in coagulase-negative staphylococci. *J. Clin. Microbiol.* 39:4149-4151

79. Strausbaugh, L.J., C. Jacobson, and T. Yost, 1993. Methicillin resistant *Staphylococcus aureus* in a nursing home and affiliated hospital: a four-year perspective. *Infect. Control Hosp. Epidemiol.* 14:331

80. Bradley, S.F., M.S. Trepenning, M.A. Ramsey *et al.*, 1991. Methicillin-resistant *Staphylococcus aureus*: colonization and infection in a long-term care facility. *Ann. Intern. Med.* 115:417

81. Thompson, R.L, M.D. Cabezudo, and R.P. Wenzel, 1982. Epidemiology of nosocomial infections caused by methicillin-resistant *Staphylococcus aureus*. *Ann. Int. Med.* 1982:309-316

82. Shanson, D.C., 1981. Antibiotic-resistant *Staphylococcus aureus*. *J. Hosp. Infect.* 2:11-36.

83. Casewell, M.W., 1986. Elimination of nasal carriage of *Staphylococcus aureus* with mupirocin ("pseudo acid") – a control trial. *J. Antimicrob. Chemother.* 17:365

84. Marples, R.R, J.F. Richardson, and M.J. DeSaxe, 1986. Bacteriological characters of strains of *Staphylococcus aureus* submitted to a reference laboratory related to methicillin resistance. *J. Hyg.* 96:217

85. Kluytmans, J., W. van Leeuwen, and W. Goessens, 1995. Food-initiated outbreak of methicillin-resistant *Staphylococcus aureus* analyzed by pheno- and genotyping. *J. Clin. Microbiol.* 33:1121

86. Jordens, J.Z., G.J. Duckworth, and R.J. Williams, 1989. Production of "virulence factors" by "epidemic" methicillin-resistant *Staphylococcus aureus* in vitro. *J Med. Microbiol.* 30:245

87. Frénay, H.M.E., J.P.G. Theelen, L.M. Schouls, C.M.J.E. Vandenbrouke-Grauls, J. Verhoef, W.J. van Leeuwen, and F.R. Mooi, 1994. Discrimination of epidemic and non epidemic methicillin-resistant *Staphylococcus aureus* strains on the basis of protein A gene polymorphism. *J. Clin. Microbiol.* 32:846-847

88. Boyce, J.M., S.M. Opal, G. Potter-Bynoe, and A.A. Medeiros, 1993. Spread of methicillin-resistant *Staphylococcus aureus* in a hospital after exposure to a health care worker with chronic sinusitis. *Clin. Infect. Dis.* 17:496

89. Back, N.A., C.C. Linnemann, Jr., M.A. Pfaller *et al.*, 1993. Recurrent epidemics caused by single strain of erythromycin-resistant *Staphylococcus aureus*: the importance of molecular epidemiology. *JAMA* 270:1329

90. Tenover, F.C., R. Arbeit, G. Archer *et al.*, 1994. Comparison of traditional and molecular methods of typing isolates of *Staphylococcus aureus. J. Clin. Microbiol.* 32:407-415

91. Mickelsen, P.A., J.J. Plorde, and K.P. Gordon, 1985. Instability of antibiotic resistance in a strain *of Staphylococcus epidemidis* isolated from an outbreak of prosthetic valve endocarditis. *J. Infect Dis.* 152:50

92. Persing, D.H., T.F. Smith, F.C. Tenover, and T.J. White, 1993. *Diagnostic Molecular Microbiology: Principles and Application.* Washington, D.C.: American Society of Microbiology.

93. Geha, D.J., J.R Uhl, C.A. Gustaferro, and D.H. Persing, 1994. Multiplex PCR for identification of methicillin-resistant staphylococci in the clinical laboratory. *J. Clin. Microbiol.* 32:1768-1772

94. Brakstad, O.G., K. Aasbakk, and J.A. Maeland, 1992. Detection of *Staphylococcus aureus* by polymerase chain reaction amplification of *nuc* gene. *J. Clin. Microbiol.* 30:1654

95. Wallet, F., M. Rousseldelvallez , and R.J. Courcol, 1996. Choice of a routine method for detecting methicillin-resistance in staphylococci. *J. Antimicrob. Chemother.* 37:901-909

96. Greisen, K., M. Loeffelholz, A. Purohit, and D. Leong, 1994. PCR primers and probes for the 16s RNA gene of most species of pathogenic bacteria, including bacteria found in cerebrospinal fluid. *J. Clin. Microbiol.* 32:335-351

97. Gribaldo, S., B. Cookson, N. Saunders, R. Marples, and J. Stanley, 1997. Rapid identification by specific PCR of coagulase-negative staphylococcal species important in hospital infection. *J. Med. Microbiol.* 46:45

98. Mariani, B.D., D.S. Martin, M.J. Levine, R.E. Booth, and R.S Tuan, 1996. Polymerase chain reaction detection of bacterial infection in total knee arthroplasty. *Clin. Orthop. Relat. Res.* 331:11-22

99. Schmitz, F.J., C.R. Mackenzie, B. Hofmann, J. Verhoef, M. Finkeneigen, H.P. and K. Kohrer, 1997. Specific information concerning taxonomy, pathogenicity and methicillin resistance of staphylococci obtained by a multiplex PCR. *J. Med. Microbiol.* 46:773-778

100. Carroll, K.C., R.B. Leonardo, P.L. Newcomb-Gayman, and D.R. Hillyard, 1996. Rapid detection of the staphylococcal *mecA* gene from BACTEC blood culture bottles by the polymerase chain reaction. *Am. J. Clin. Pathol.* 106:600-605

101. Martineau, F., F.J. Picard, P.H. Roy, M. Ouellete, and M.G. Bergeron, 1998. Species-specific and ubiquitous-DNA-based assays for rapid identification of *Staphylococcus aureus*. *J. Clin. Microbiol.* 36:618-623

102. Mcdevitt, D., P. Francois, P. Vaudaux, and T.J. Foster, 1994. Molecular characterization of the clumping factor (fibrinogen receptor) of *Staphylococcus aureus*. *Mol. Microbiol.* 11(2):237-248

103. Goh, S.-H., S.K. Byrne, J.L. Zhang, and A.W. Chow, 1992. Molecular typing of *Staphylococcus aureus* on the basis of coagulase gene polymorphisms. *J. Clin. Microbiol.* 30:1642

104. Hookey, J.V., J.F. Richardson, and B.D. Cookson, 1998. Molecular typing of *Staphylococcus aureus* based on PCR restriction fragment length polymorphism and DNA sequence analysis of the coagulase gene. *J. Clin. Microbiol.* 36:1083-1089

105. Schwarzkopf, A., and H. Karch, 1994. Genetic variation in *Staphylococcus aureus* coagulase genes - potential and limits for use as epidemiological marker. *J. Clin. Microbiol.* 32:2407-2412

106. Kampf, G., K. Weist, S. Swidsinski, M. Kegel, and H. Ruden, 1997. Comparison of screening methods to identify methicillin-resistant *Staphylococcus aureus*. *Eur. J. Clin. Microbiol. Infect. Dis.* 16(4):301-307.

107. Salisbury, S.M., L.M. Sabatini, and C.A. Spiegel, 1997. Identification of methicillin-resistant staphylococci by multiplex polymerase chain reaction assay. *Am. J. Clin. Pathol.* 107(3):368-373

108. Schwartz, D.C., and C.R. Cantor, 1984. Separation of yeast chromosome-sized DNAs by pulsed field gradient gel electrophoresis. *Cell* 37:67

109. Birren, B., and E. Lai, 1993. *Pulsed Field Gel Electrophoresis: A Practical Guide.* San Diego: Academic Press.

110. Arbeit, R.D., M. Arthur, R.D. Dunn *et al.*, 1990. Resolution of recent evolutionary divergence among *Escherichia coli* from related lineages: the application of pulsed field electrophoresis to molecular epidemiology. *J. Infect Dis.* 161:230

111. Maslow, J.N., M.E. Mulligan, and R.D. Arbeit, 1993. Molecular epidemiology - application of contemporary techniques to the typing of microorganisms. *Clin. Infect. Dis.* 17(2):153-164

112. Mulvey, M. R., L. Chui, J. Ismail, L. Louie, C. Murphy, N. Chang, M. Alfa, and Canadian Committee for the Standardization of Molecular Methods, 2001. Development of a Canadian standardization protocol for subtyping methicillin-resistant *Staphylococcus aureus* (MRSA) using pulsed-field gel electrophoresis. *J. Clin. Microbiol.* 39:3481-3485

113. Bannerman, T.L., G.A. Hancock, F.C. Tenover, and J.M. Miller, 1995. Pulsed-field gel electrophoresis as a replacement for bacteriophage typing of *Staphylococcus aureus*. *J. Clin. Microbiol.* 33:551-555

114. Prevost, G., B. Jaulhac, and Y. Piemont, 1992. DNA fingerprinting by pulsed field gel electrophoresis is more effective than ribotyping in distinguishing among methicillin-resistant *Staphylococcus aureus* isolates. *J. Clin. Microbiol.* 30:967

115. Carles-Nurit, M.J., B. Christophle, S. Broche *et al.*, 1992. DNA polymorphisms in methicillin-susceptible and methicillin-resistant strains of *Staphylococcus aureus* strains. *J. Clin. Microbiol.* 30:2092

116. Ichiyama, S., M. Ohta, K. Shimokata *et al.*, 1991. Genomic DNA fingerprinting by pulsed-field gel electrophoresis as an epidemiological marker for study of

nosocomial infections caused by methicillin resistant *Staphylococcus aureus*. *J. Clin. Microbiol.* 29:2690

117. Struelens, M.J., A. Deplano, C. Godard, N. Maes, and E. Serruys, 1992. Epidemiologic typing and delineation of genetic relatedness of methicillin-resistant *Staphylococcus aureus* by macrorestriction analysis of genomic DNA by using pulsed-field gel electrophoresis. *J. Clin. Microbiol.* 30:2599-2605

118. Kloos, W.E., and J.F. Wolfshohl, 1982. Identification of *Staphylococcus* species with the API STAPH-IDENT system. *J. Clin. Microbiol.* 16:509-516

119. Hussain, Z., L. Stockes, D.L. Stevensen, B.C. Shieven, R. Lannigan, and C. Jones, 1986. Comparison of the Microscan system with the API Staph-Ident system for species identification of coagulase-negative staphylococci. *J. Clin. Microbiol.* 16:105-113

120. Novak, S.M., J. Hindler, and D.A. Bruckner, 1993. Reliability of 2 novel methods, Alamar and E-test, for detection of methicillin-resistant *Staphylococcus-aureus*. *J. Clin. Microbiol.* 31:3056-3057

121. Chambers, H.F., 1993. Detection of methicillin-resistant staphylococci. *Infect. Dis. Clin. North Am.* 7:425-433

122. Frebourg, N.B., D. Nouet, L. Lemee, E. Martin, and J.F. Lemeland, 1998. Comparison of ATB staph, rapid ATB staph, Vitek, and E-test methods for detection of oxacillin heteroresistance in staphylococci possessing *mecA*. *J. Clin. Microbiol.* 36:52-57

123. Personne, P., M. Bes, G. Lina, F. Vandenesch, Y. Brun, and J. Etienne, 1997. Comparative performances of six agglutination kits assessed by using typical and atypical strains of *Staphylococcus aureus*. *J. Clin. Microbiol.* 35:1138-1140

124. Fournier, J.M., A. Boutonnier, and A. Bouvet, 1989. *Staphylococcus aureus* strains which are not identified by rapid agglutination methods are of capsular serotype 5. *J. Clin. Microbiol.* 27:1372-1374

125. Luijendijk, A., A. Vanbelkum, H. Verbrugh, and J. Kluytmans, 1996. Comparison of five tests for identification of *Staphylococcus aureus* from clinical samples. *J. Clin. Microbiol.* 34:2267-2269

126. Mathieu, D., and V. Picard, 1991. Comparative evaluation of five agglutination techniques and a new miniaturized system for rapid identification of methicillin-resistant strains of *Staphylococcus aureus*. *Zbl. Bakteriol.* 276:46-53

127. Piper, J., T. Hadfield, F. McCleskey, M. Evans, S. Friedstrom, P. Lauderdale, and R. Winn, 1998. Efficacies of rapid agglutination tests for identification of methicillin-

resistant staphylococcal strains as *Staphylococcus aureus*. *J. Clin. Microbiol.* 26:1907-1909

128. Ruane, P.J., M.A. Morgan, D.M. Citron, and M.E. Mulligan, 1986. Failure of rapid agglutination methods to detect oxacillin-resistant *Staphylococcus aureus*. *J. Clin. Microbiol.* 24:490-492

129. Fournier, J.M., A. Bouvet, D Mathieu *et al.*, 1993. New latex reagent using monoclonal antibodies to capsular polysaccharides for reliable identification of both oxacillin-susceptible and oxacillin-resistant *Staphylococcus aureus*. *J. Clin. Microbiol.* 31:1342

130. Kloos, W.E., and T.L. Bannerman, 1999. *Staphylococcus* and *Micrococcus*, *in* P.R. Murray, E.J. Baron, M.A. Pfaller, F.C. Tenover, and R.H. Yolken (eds.), *Manual of Clinical Microbiology*, 7th ed. Washington, D.C.: American Society for Microbiology. pp. 264-282

131. Brakstad, O.G., and J.A. Maeland, 1995. Direct identification of *Staphylococcus aureus* in blood cultures by detection of the gene encoding the thermostable nuclease or the gene product. *APMIS* 103(3):209-218

132. Tenover, F.C., M.V. Lancaster, B.C. Hill *et al.*, 1998. Characterization of staphylococci with reduced susceptibilities to vancomycin and other glycopeptides. *J. Clin. Microbiol.* 36:1020-1027

133. Howe, R.A,. M. Wootton, T.R. Walsh, P.M. Bennett, and A.P. MacGowan, 1999. Expression and detection of hetero-vancomycin resistance in *Staphylococcus aureus*. *J. Antimicrob Chemother*. 44:675-678

134. Hubert, S.K., J.M. Mohammed, S.K. Fridkin, R.P. Gaynes, and J.E. McGowan, Jr., 1999. Glycopeptide-intermediate *Staphylococcus aureus*; evaluation of a novel screening method and results of a survey. *J. Clin Microbiol.* 37:3590-3593

135. Centers for Disease Control and Prevention (CDC), 2000. *Staphylococcus aureus* with reduced susceptibility to vancomycin: Illinois. *Morbid. Mortal. Wkly. Rep.* 48:1165-1167

136. Tomasz, F.C., S. Nachman, and H. Leaf, 1991. Stable classes of phenotypic expression in methicillin-resistant clinical isolates of staphylococci. *Antimicrob. Agents Chemother*. 35:124-129

137. Tenover, F.C., 1999. Implications of vancomycin-resistant *Staphylococcus aureus*. *J Hosp. Infect*. 43(Suppl 1):3-7

138. Nelson, W.H., R. Manoharan, and J.F. Sperry 1992. U.V. resonance Raman studies of bacteria. *Appl. Spectrosc. Rev.* 27:67-124

139. Norris, K.P., 1959. Infra-red spectroscopy and its application to microbiology. *J. Hyg.* 57:326-345

140. Riddle J.W., P.W. Kabler, B.A. Kenner, R.H. Bordner, S.W. Rockwood, and H.J.R. Stevenson, 1956. Bacterial identification by infrared spectrophotometry. *J. Bacteriol.* 72:593-603

141. Griffith, P.R., and J.A. de Haseth, 1986. *Fourier Transform Infrared Spectrometry.* New York: John Wiley and Sons

142. Heber, J.R., R. Sevenson, and O. Boldman, 1952. Infrared spectroscopy as a means for identification of bacteria. *Science* 116:111-112

143. Naumann, D., D. Helm, and H. Labischinski, 1990. Einsatzmöglichkeiten der FTIR-Spectroscopie in Diagnostik und Epidemiologie. *Bundesges.* 9(90):387-393

144. Naumann, D., 1984. Some ultrastructural information on intact, living bacterial cells and related cell-wall fragments as given by FTIR. *Infrared Phys.* 24:233-238

145. Kummerle, M., S. Sherer, and H. Seiler, 1998. Rapid and reliable identification of food-borne yeast by Fourier-transformed infrared spectroscopy. *Appl. Environ. Microbiol.* 64:2207-2214.

146. Magee, J.T., 1993. Whole-organism fingerprinting, *in* M. Goodfellow and A.G. O'Donnel (eds.), *Handbook of New Bacterial Systematics.* London: Academic Press. pp. 383-427

147. Bourne, R., U. Himmelreich, A. Sharma, C. Mountford, and T. Sorrel, 2001. Identification of *Enterococcus, Streptococcus,* and *Staphylococcus* by multivariate analysis of proton magnetic resonance spectroscopic data from plate cultures. *J. Clin. Microbiol.* 39:2916-2923.

148. Diem, M., 1994. *Introduction to Modern Vibrational Spectroscopy.* New York: John Wiley and Sons

149. Naumann, D, D. Helm, H. Labischinski, and P. Giesbrecht, 1991. The characterization of microorganisms by Fourier-transform infrared spectroscopy (FT-IR), *in* W.H. Nelson (ed.), *Modern Techniques for Rapid Microbiological Analysis.* New York: VCH Publishers. pp. 43-96

150. Workman, J.J., P.R. Mobley, B.R. Kowalski, and R. Bro, 1996. Review of chemometrics applied to spectroscopy - 1985-95. *Appl. Spectrosc. Rev.* 31:73-124

151. Savitzky, A., and M.J.E. Golay, 1964. Smoothing and differentiation of data by simplified least squares procedures. *Anal. Chem.* 36:1627-1633

152. Mariey, L., J.P. Signolle, C. Amiel, and J. Travert, 2001. Discrimination, classification, identification of microorganisms using FTIR spectroscopy and chemometrics. *Vibr. Spectrosc.* 26:151-159

153. Maquelin, K., C. Kirschner, L.-P. Choo-Smith, N. van den Braak, H.P. Endtz, D. Naumann, and G.J. Puppels, 2002. Identification of medically relevant microorganisms by vibrational spectroscopy. *J. Microbiol. Methods* 51:255-271

154. Defernez, M., and R. H. Kemsley, 1997. The use and misuse of chemometrics for treating classification problems. *Trends Anal. Chem.* 16:216-221

155. Goodacre, R., E. M. Timmins, P.J. Rooney, J.J. Rowland, and D.B. Kell. 1996. Rapid identification of *Streptococcus* and *Enterococcus* species using diffuse reflectance-absorbance Fourier transform infrared spectroscopy and artificial neural networks. *FEMS Microbiol. Lett.* 140:233-239

156. Kohonen, T., 1984. *Self Organization and Associative Memory*, 3rd ed. New York Springer

157. Wilkins, M.F., L. Boddy, C.W. Morris, and R. Jonker, 1996. A comparison of some neural and non-neural methods for identification of phytoplankton from flow cytometry data. *Comput. Appl. Biosci.* 12(1):9-18

158. Goodacre, R., M.J. Neal, D.B. Kell, L.W. Greenham, W.C. Noble, and R.G. Harvey, 1994. Rapid identification using pyrolysis mass spectrometry and artificial neural networks of *Propionibacterium acnes* isolated from dogs. *J. Appl. Bacteriol.* 76(2):124-134

159. Goodacre, R., S.A. Howell, W.C. Noble, and M.J. Neal, 1996. Sub-species discrimination, using pyrolysis mass spectrometry and self-organising neural networks, of *Propionibacterium acnes* isolated from normal human skin. *Zbl. Bakteriol. – Int. J. Med. Microbiol. Virol. Parasitol. Infect. Dis.* 284:501-515

160. Kansiz, M., P. Heraud, B. Wood, F. Burden, J. Beardall, and D. McNaughton, 1999. Fourier transform infrared microspectroscopy and chemometrics as a tool for the discrimination of cyanobacterial strains. *Phytochemistry* 52:407-417

161. Causton, D.R., 1987. *A Biologist's Advanced Mathematics*. London: Allen & Unwin

162. Jolliffe, I. T., 1986. *Principal Component Analysis*. New York: Springer

163. Kohonen, T, 2001. *Self-Organizing Maps*, Volume 30 of Springer Series in Information Sciences, 3rd ed. Berlin, Heidelberg: Springer

164. Gasteiger, J., and J. Zupan, 1993. On the topology distortion in self-organizing feature maps. *Biol. Cybernet.* 70(2):189-198

165. Ultsch, A., and H.P. Siemon, 1990. Kohonen's self organizing feature maps for extrapolatory data analysis, *Proceedings of International Neural Network Conference (INNC'90)*. Dordrecht: Kluwer. pp. 305-308

166. Vesanto, J., and E. Alhoniemi, 2000. Clustering of the self-organizing map. *IEEE Trans. Neural Networks* 11(3):586-600

167. Davies, D.L., and D.W. Bouldin, 1979. A cluster separation measure. *IEEE Trans. Patt. Anal. Machine Intell.*, Vol. PAMI-1, pp.224-227

168. Massart, D.L., and L. Kauffman, 1983. *The Interpretation of Analytical Chemical Data by the Use of Cluster Analysis*. New York: John Wiley and Sons

169. Bezdek, C.J., and K.P. Sankar (eds.), 1992. *Fuzzy Models for Pattern Recognition: Methods That Search for Structures in Data*. New York: IEEE Press

170. Adams, M.J., 1995. *Chemometrics in Analytical Spectroscopy*. Cambridge: The Royal Society of Chemists

171. Brereton, R.G., 1993. *Chemometrics – Applications of Mathematics and Statistics to Laboratory Systems*. New York: Ellis Horwood

172. Helm, D., H. Labischinski, and D. Naumann. 1991. Classification and identification of bacteria by Fourier transform spectroscopy. *J. Gen. Microbiol.* 137:69-79

173. Helm, D., H. Labischinski, and D. Naumann. 1991. Elaboration of a procedure for identification of bacteria using Fourier-transform IR spectral libraries: a stepwise correlation approach. *J. Microbiol. Methods* 14:127-142

174. Lang, P.L., and S.C. Sang, 1998. The *in situ* infrared microspectroscopy of bacterial colonies on agar plates. *Cell. Mol. Biol.* 44 (1):231

175. Lipkus, A.H., K. C. Krishnan, S.J. Vesper, J. B. Robinson, and G. E. Pierce, 1990. Evaluation of infrared spectroscopy as a bacterial identification method. *J. Ind. Microbiol.* 6:71-75

176. Udelhoven, T., D. Naumann, and J. Shmitt, 2000. Development of a hierarchical classification system with artificial neural networks and FTIR spectra for the identification of bacteria. *Appl. Spectrosc.* 54:1471-1479

177. Bouhedja, W., G.D. Sockalingum, P. Pina, P. Allouch, C. Bloy, R. Labia, J.M. Millot, and M. Manfait, 1997. ATR-FTIR spectroscopy investigation of *E. coli* ranscon-jugants β-lactams-resistance phenotype. *FEBS Lett.* 412:39-42

178. Sockalingum, G.D., W. Bouhedja, P. Pina, P. Allouch, C. Bloy, and M. Manfait, 1998. FT-IR spectroscopy as an emerging method for rapid characterization of microorganisms. *Cell. Mol. Biol.* 44:261-269

179. Sockalingum, G.D., W. Bouhedja, P. Pina, P. Allouch, C. Mandray, R. Labia, J. Millot, and M. Manfait, 1997. ATR-FTIR spectroscopic investigation of imipenem-susceptible and -resistant *Pseudomonas aeruginosa* isogenic strains. *Biochem. Biophys. Res. Commun.* 232:240-246

180. Zeroual, W., M. Manfait, and C. Choisy, 1995. FTIR spectroscopy study of perturbations induced by antibiotic on bacteria (*Escherichia coli*). *Path. Biol.* 43:300-305

181. Kirschner, K., N.A. Ngo Thi, and D. Naumann, 1999. *In* J. Greve, G.J. Puppels, and C. Otto (eds.), *Spectroscopy of Biological Molecules: New Directions*. Dordrecht: Kluwer. p. 469

182. Horbach, I., D. Naumann, and F.J. Fehrenbach, 1988. Simultaneous infections with different serogroups of *Legionella pneumophila* investigated by routine methods and Fourier transform infrared spectroscopy. *J. Clin. Microbiol.* 26: 1106-1110

183. Seltmann, G., W. Voigt, and W. Beer, 1994. Application of physico-chemical typing methods for the epidemiological analysis of *Salmonella enteritidis* strains of phage type 25/17. *Epidemiol. Infect.* 113:411-424

184. Seltmann, G., W. Beer, H. Claus, and H. Seifert, 1995. Comparative classification of *Acinetobacter baumannii* strains using seven different typing methods. *Zbl. Bakteriol.* 282:372-383

185. Irmscher, H-M., R. Fischer, W. Beer, and G. Seltmann, 1999. Characterization of nosocomial *Serratia marcescens* isolates: comparison of Fourier-transform infrared spectroscopy with pulsed-field gel electrophoresis of genomic DNA fragments and multilocus enzyme electrophoresis. *Zbl. Bakteriol.* 289:249-263

CHAPTER 3

RAPID IDENTIFICATION OF METHICILLIN-RESISTANT *STAPHYLOCOCCUS AUREUS* (MRSA) BY FOURIER TRANSFORM INFRARED (FTIR) SPECTROSCOPY

3.1 ABSTRACT

Methicillin-resistant *Staphylococcus aureus* (MRSA) has become a worldwide nosocomial pathogen. The feasibility of employing Fourier transform infrared (FTIR) spectroscopy as a rapid, single-step method for the detection of MRSA and differentiation of MRSA from borderline oxacillin-resistant *S. aureus* (BORSA) and methicillin-sensitive *S. aureus* (MSSA) was investigated. The FTIR spectra of whole cells from stationary-phase cultures, grown on a universal growth (UM™) medium, of 26 MRSA, 25 MSSA, and 15 BORSA (*mecA* negative, oxacillin MICs of 2-8 μg/ml) strains were recorded in quadruplicate and normalized to unit height. Principal component analysis (PCA), self-organizing maps (SOM), and the K-nearest neighbors (KNN) algorithm were investigated to cluster the different phenotypes of *S. aureus* strains based on the similarity of their infrared spectral fingerprints obtained from whole cells. Visual inspection of the spectra revealed clear differences in the region of 1080-1050 cm^{-1} (containing absorption bands assigned to the phosphodiester backbone of nucleic acids, polysaccharides, and phosphorylated proteins). When PCA was performed on first-derivative spectra using this single narrow spectral range, a scores plot of the first two PCs yielded three clusters corresponding to MRSA, MSSA, and BORSA strains. However, one MRSA strain did not fall in the MRSA cluster, nine MSSA and five BORSA (phage group 94/96) strains were misclassified as MRSA, and three BORSA strains fell between the MSSA and MRSA clusters, yielding an overall correct classification rate of 76%. Similar results, with slightly higher overall rates of correct classification, were obtained when the same spectral data were used to generate an SOM or were subjected to cluster analysis using the KNN algorithm. With the use of additional spectral regions selected by employing singular-value decomposition (SVD), pairwise differentiation of the three strains by PCA, SOM, and KNN all yielded >90% correct classification, and, of particular significance from a clinical perspective, only a single

MRSA strain was misclassified. Furthermore, in a separate validation study, 166 *S. aureus* clinical isolates were all correctly classified. The FTIR spectra of cell walls extracted from one MRSA and one MSSA strain showed differences in the same spectral regions as those employed for the discrimination of MSSA and MRSA, consistent with the fact that the structural modifications associated with methicillin resistance are localized within the cell wall. The results obtained in this study demonstrate that FTIR spectroscopy has considerable potential as an alternative rapid (1-hr) method for the differentiation of MRSA from BORSA and MSSA strains.

3.2 INTRODUCTION

The increasing incidence of nosocomial infections caused by methicillin-resistant *S. aureus* (MRSA) makes it essential to have a rapid, simple and reliable method for detection of MRSA so that appropriate therapy and intervention for cross-infection control can be initiated in a timely manner. Methicillin resistance is caused exclusively by production of an altered penicillin binding protein (PBP2a) in the cell wall encoded by the *mecA* gene [1]. Most diagnostic laboratories use traditional antimicrobial susceptibility methods to detect MRSA. However, these methods are technically demanding and time-consuming (48 hr). In addition, the differentiation of MRSA from methicillin-sensitive *S. aureus* (MSSA) may be further obscured by the presence of borderline oxacillin-resistant *S. aureus* (BORSA) strains that overlap with low-level resistant MRSA [2]. Detection of the *mecA* gene by PCR appears to most accurately detect methicillin resistance in *S. aureus* [1,2]. However, the *mecA* gene occurs in some strains of *S. aureus* that are phenotypically methicillin sensitive [3]. Moreover, PCR assays are not currently utilized by most routine diagnostic laboratories.

The application of FTIR spectroscopy for the discrimination, classification, and identification of microorganisms has been increasingly investigated during the past decade [4]. FTIR spectroscopy is a biophysical method that provides quantitative information about the total biochemical cellular composition [5]. As illustrated in Figure 3.1, the absorption bands in the FTIR spectra of whole cells are assigned to major cellular constituents such as proteins, lipids, polysaccharides, and nucleic acids. The FTIR spectra of different strains exhibit distinct and unique patterns that are highly reproducible, thereby providing a means for differentiation between strains. FTIR spectroscopy has a number of advantages over conventional methods of biochemical analysis: it is rapid and reliable, sample preparation is relatively simple, and no reagents are required. FTIR spectroscopy has proved to be successful in bacterial classification at different levels of taxonomic discrimination without any preselection of strains based on other taxonomic criteria [6].

Recently, several studies have been reported on the application of FTIR spectroscopy for the detection of antibiotic-resistant microorganisms, including imipenem-resistant *Pseudomonas aeruginosa* species [7], ß-lactam-resistant *Escherichia*

coli [8], and MRSA [9,10]. However, the previous work on the differentiation of MRSA from MSSA was inconclusive and the possible presence of BORSA strains was not considered in the data analysis. Thus, the present study was undertaken to evaluate more fully the potential utility of FTIR spectroscopy for the rapid identification of MRSA strains by investigating the capability of this technique to distinguish MRSA from MSSA and BORSA strains.

3.3 MATERIALS AND METHODS

3.3.1 Strains

Twenty-six strains of MRSA and twenty-five strains of MSSA were obtained from the Royal Victoria Hospital (Montreal, PQ, Canada). Fifteen strains of BORSA were obtained from the Laboratoire de Santé Publique du Québec (Pointe-Claire, PQ, Canada) culture collection. All strains were stored in brain heart infusion (BHI) supplemented with 15% glycerol at -70°C.

3.3.2 Sample preparation and FTIR spectral acquisition

After an overnight subculture of *S. aureus* strains on tryptic soy with sheep blood agar (Quelab Laboratories Inc., Montreal, QC, Canada) at 37 °C, followed by culture on Universal Medium (UM™) agar plates (Quelab Laboratories Inc., Montreal, QC, Canada) for 18 h at 37 °C, four loops-full of stationary-phase cells were carefully collected using a 10-mm-diameter loop and suspended in 200-µl aliquots of sterile physiological saline (0.9%). A 25-µl aliquot of the 10-fold diluted bacterial suspension (approximately 5×10^{11} cells ml^{-1}) was evenly applied onto a zinc selenide (ZnSe) optical window and then oven-dried at 48 °C for 1 hour. For each of the 66 strains employed in this study, four samples were prepared in this manner from different culture plates. IR spectra were recorded using a Bomem MB-104 (ABB-Bomem, Quebec, PQ, Canada) FTIR spectrometer equipped with a deuterated triglycine sulfate (DTGS) detector and a KBr beamsplitter and operating under Bomem-Grams/386 software (Galactic, Salem, NH). The spectrometer was purged with dry, CO_2-free air from a Balston dryer (Balston, Lexington, MA). A total of 64 scans were co-added at 4 cm^{-1} resolution in the mid-IR

region (4000-400 cm^{-1}) and ratioed against an open-beam background to produce an absorbance spectrum.

3.3.3 Mathematical processing

The collected spectral data, stored in Grams SPC format, were converted into CSV format and then into MAT format using Matlab version 5.1 (The MathWorks, Inc. Natick, MA). Spectra were normalized to unit height and were transformed to first-derivative spectra using the Savitzky-Golay algorithm to maximize peak separation and minimize baseline shifts. Exploratory data analysis was performed using principal component analysis (PCA) based on both singular-value decomposition (SVD) and the nonlinear iterative partial-least-squares (NIPALS) algorithm and self-organizing maps (SOM), using data processing routines written in Matlab for this study. Cluster analysis was performed by using the K-nearest neighbors (KNN) algorithm (written in Matlab).

3.3.4 Microbiological analysis of selected strains

Strains that were not properly classified in the initial analysis of the FTIR data were subsequently characterization by antimicrobial susceptibility testing, phage typing, and multiplex PCR, as described below.

3.3.4 1 Antimicrobial susceptibility testing

Antimicrobial susceptibility testing was performed by the disk diffusion method of Kirby-Bauer [11], using breakpoints according to National Committee for Clinical Laboratory Standards (NCCLS) guidelines [12].

3.3.4.2 Phage typing

Strains were phage typed by the standard method of Blair and Williams [13] with the basic international set of 23 phages. The set of phages included the lytic groups I (29, 52, 52A, 79 and 80), II (3A, 3C, 55 and 71), III (6, 42E, 47, 53, 54, 75, 77, 83A, 84 and 85), and V (94, 96) and miscellaneous or non-allocated phages 81 and 95. Susceptibility

to phages was determined at the standard routine test dilution (RTD) and at 100 × RTD concentrations.

3.3.4.3 Multiplex PCR

Multiplex PCR reactions were performed for the simultaneous detection of the *mecA* and *nucA* gene sequences [14,15]. Bacterial DNA was extracted using 2-3 colonies of a test organism and boiled in 100 µl of Triton X-100 lysis buffer. One microliter of the cooled, centrifuged suspension was used as template, and PCR was performed in a 25-µl volume, with 10 mM Tris–HCl, 50 mM KCl, 1.5 mM $MgCl_2$, 200 µM dNTP's, 2.5 U of *Taq* polymerase, and 0.2 µM of each primer. Thermocycling conditions in a Gene-Amp 9600 thermocycler were as follow: 94 °C for 2 min followed by 30 cycles of 94 °C for 1 s and 55 °C for 15 s, with a final 10-min extension at 72 °C. Amplicons were detected on a 1% agarose gel after electrophoresis and stained with ethidium bromide.

3.3.5 Cell wall extraction

Following the procedure for cell wall extraction described by Stranden *et al.* [16], MRSA BB270 and MSSA BB255 strains were grown in 500 ml of brain heart infusion (Difco) to an optical density at 600 nm of 0.9 and harvested by centrifugation. Cells were resuspended in 10 ml of 1 M NaCl and mechanically disrupted by glass beads (0.1 mm), using a cell grinder for 5 min at 4 °C. The glass beads were separated by filtration and washed with 0.5% sodium dodecyl sulfate (SDS). The collected cell suspension was incubated at 60 °C for 30 min to remove noncovalently bound components. The cell walls were isolated by centrifugation and washed three times with water to remove SDS prior to lyophilization. The cell wall extracts obtained by this procedure have previously been shown to contain murein with teichoic acids and proteins covalently attached via interpeptide chains [16].

3.4 RESULTS

The primary aim of this study was to investigate the feasibility of employing FTIR spectroscopy for the rapid identification of MRSA strains. The following strategy

was employed to ascertain whether MRSA could be discriminated from MSSA and BORSA utilizing the spectra of whole cells. First, the spectra of 26 MRSA, 25 MSSA, and 15 BORSA strains were collected in quadruplicate to generate a spectral database comprising 263 spectra (one improperly collected spectrum having been rejected). The effects of various types of spectral processing on spectral reproducibility, as assessed by examination of variations between replicate spectra, were studied to select the most suitable spectral preprocessing tools to be employed prior to data analysis. Analysis of the FTIR data commenced with visual inspection of a subset of 30 spectra in an attempt to identify specific spectral regions containing information that would allow for discrimination between MRSA, MSSA, and BORSA strains. Prior to data processing, the most significant spectral region for differentiation of MRSA, MSSA and BORSA was selected by visual inspection of the spectra. Various chemometric techniques were applied in the analysis of the spectral data within the selected region(s) to cluster the different phenotypes of *S. aureus* strains. The results obtained in each of the above stages are presented in the following sections.

3.4.1 Spectral reproducibility

The discrimination, classification, and identification of microorganisms by FTIR spectroscopy requires that the variance within the spectra of one taxon must be less than the variance between the spectra of different taxa. Accordingly, a high level of spectral reproducibility is required, and the sources of spectral variability must be identified and controlled. These include variations in plating conditions (growth media, growth temperature, incubation time) and sampling methodology (transfer of bacteria from an agar plate to a ZnSe optical window, drying of the bacterial suspension on the optical window). Thus, FTIR spectroscopy, as well as other whole-organism fingerprinting techniques, such as pyrolysis-mass spectrometry and UV resonance spectroscopy, has been reported to require strict metabolic control of growth media and standardization of growth conditions [17-20]. The selection of a universal growth medium (UM^{TM}) and appropriate standard growth conditions for the present study was thus of prime importance in order for the IR spectra of various bacterial strains to be reliably compared and interpreted. In addition, as the quality of the IR spectra of bacterial films deposited

on an optical window depends on the sample homogeneity, particle size, and film thickness, a standardized sampling methodology was established, whereby a single drop of a diluted bacterial suspension was deposited onto the window and dried for 1 hr at 48 °C to form a transparent and homogeneous film suitable for FTIR measurements.

To assess the level of spectral reproducibility achieved under the conditions selected for this study, quadruplicate spectra of each of the strains investigated were recorded by depositing samples from four different culture plates on four different optical windows. Figure 3.2 presents quadruplicate spectra in the 1800-800 cm^{-1} region obtained for cells taken from a stationary-phase MRSA culture. Although there is some spectral variability due to baseline shifts and sampling-associated factors such as sample thickness, these spectra show excellent reproducibility in terms of the relative peak intensities. Pairwise comparison of quadruplicate spectra yielded an average correlation coefficient of r = 0.97. The variation between replicate spectra was minimized by normalization to unit height and the use of the first-order spectral derivatives [21], which highlight shapes and contours of spectra and remove the effects of baseline shifts. Other spectral processing techniques, including mean centering, autoscaling, and second-order spectral derivatives, were evaluated but were not found to be helpful.

3.4.2 Discrimination of MRSA from MSSA and BORSA

3.4.2.1 Spectral differences of MRSA, MSSA and BORSA strains

Visual inspection over the full spectral range (4000-400 cm^{-1}) of 30 randomly selected raw spectra of MRSA, MSSA and BORSA strains among the 263 spectra collected revealed clear differences in the region between 1080 and 1050 cm^{-1} (Figure 3.3). Absorptions in this range in the spectra of bacteria may be attributed mainly to the symmetric P=O stretching vibration of the phosphodiester backbone of nucleic acids and phosphorylated proteins and C-O-C stretching vibrations of polysaccharides [5,6]. For the analysis of the full spectral data set using the specific narrow spectral region of 1080-1050 cm^{-1} for discrimination, multivariate analysis was performed because of the large number of spectra.

3.4.2.2 Principal component analysis (PCA)

PCA is a technique used for reducing the dimensionality of multivariate data while preserving most of the variance. It compresses data by producing linear combinations of the original variables ("scrambles" them) and removes collinearities [22]. The variation in the data is thus described in a few orthogonal principal components (PCs), or latent variables, characterized by (a) scores, which are projections of objects (in the present case, spectra) onto the PCs, and (b) loadings, which represent the contributions of the original variables to each PC. A scores plot is a projection of the original data onto the PC(s) and allows for the visualization of the relationship between samples, thereby providing possibilities to find patterns and trends in the data and interpret which variables contribute most strongly to these patterns and trends, as well as to identify outliers in the data set.

PCA was applied, using the nonlinear iterative partial least squares (NIPALS) algorithm, to the first derivatives of the complete set of 263 peak-height-normalized spectra in the spectral range of 1080-1050 cm^{-1} selected by visual inspection of a subset of 30 spectra. The first three principal components captured almost 99.9% of the total variance. The first component (PC1) by itself accounted for over 98.1% of the total variance. The PC1 vs. PC2 scores plot displayed three distinct clusters corresponding to MRSA, BORSA, and MSSA strains (Figure 3.4). However, one MRSA strain fell between the BORSA and MSSA clusters, and nine MSSA strains fell within the MRSA cluster. Moreover, five BORSA strains of phage group 94/96 were within the MRSA cluster, and two BORSA strains belonging to phage group 75 and one BORSA strain belonging to phage group 29 fell between the MSSA and MRSA clusters. Although the five misclassified BORSA strains of phage group 94/96 were clustered together, this cluster was not distinct from the MRSA cluster. Overall, a correct classification rate of 76% was obtained, indicating that a more sophisticated classification technique would be required.

3.4.2.3 Self-organizing map (SOM)

An SOM, also known as a Kohonen map, is the product of a neural network algorithm based on unsupervised learning that was developed to allow the visualization of high-dimensional data [23]. The SOM employed in this work was based on a two-dimensional grid of neurons, and the network was trained using the PC scores obtained as described above as input data. In the SOM algorithm, initially the neurons are regularly spaced, and each neuron k is represented by an n-dimensional weight vector $m_k = [m_{k1}, \ldots\ldots\ldots, m_{kn}]$, where n is the dimension of the input space (i.e., in the present case, the number of PC scores selected to describe the spectra, typically 2-3). On each training step, a data sample x is selected and the nearest unit m_c (the best matching unit, BMU) is found from the map. The weight vectors of the BMU and its neighbors on the grid are moved toward the sample vector:

$$m_k = m_k + \alpha(t)h_{ck}(t)(x - m_k)$$

where $\alpha(t)$ is the learning rate and $h_{ck}(t)$ is a neighborhood kernel centered on the BMU. Both learning rate and neighborhood kernel radius decease monotonically with time. Thus, during iterative training of the network, the neurons are organized into a meaningful two-dimensional order in which similar neurons are closer to each other in the grid than the more dissimilar ones. The SOM may thus be regarded as a clustering diagram. There are a variety of methods to visualize the SOM. The two methods used in this work are the U-matrix (unified distance matrix) [24] and component planes [25] methods. In the U-matrix method, color is used to show the distances between neighboring map units: longer distances are represented by shades of yellow and red, while shorter distances are represented by shades of blue. Thus, the U-matrix shows the cluster structure of the map, with a uniform area being blue (designating a cluster) while border areas are yellow and red. Component planes show the values of the individual variables (i.e., PC scores) in each map unit and provide an idea of the spread of values of each variable. By comparing the U-matrix with the component planes, it is possible to identify which variables contribute strongly to a cluster observed in the U-matrix. When the number of SOM units is large, standard clustering algorithms such as the k-means algorithm may be applied to partition the SOM [25]. The number of clusters can be evaluated using some kind of validity index such as the Davies-Bouldin index [26].

An SOM of size [10 × 8] was trained using a rough training phase of 4 and a fine-tuning phase of 13 epochs. The learning rate decreased linearly to zero during the fine-tuning phase with a final quantization error of 0.434 and final topographic error of 0.057. From the U-matrix (Figure 3.5a), three distinct clusters were detected, two large clusters and one small cluster. The labeled SOM (Figure 3.5b) shows that most of the interpolating units (empty hexagonal neurons) are positioned neatly along the border of cluster R (MRSA). Following partitioning of the map by using the *k*-means clustering algorithm, computation of the Davies-Bouldin index confirmed that there are three clusters on the map, as indicated by the minimum on the plot on the left-hand side of Figure 3.6a. Based on the three clusters on the partitioned SOM (Figure 3.6a, 3.6b), 100% of R (MRSA) map units, 80% of B (BORSA) map units, and 60% of S (MSSA) map units were correctly classified. Overall, using the SOM algorithm for the classification of MRSA, MSSA, and BORSA, 80% correct classification was obtained with no false negatives (i.e., no misclassification of MRSA strains).

3.4.2.4 K-Nearest neighbors (KNN) algorithm

The KNN algorithm is a similarity-based classification method [27,28] that attempts to categorize unknown samples exclusively on the basis of their proximity in *n*-dimensional space to other samples of pre-assigned categories, which constitute the training set [27,28]. It consists of drawing a circle (a sphere for $n = 3$ and a "hypersphere" for $n > 3$) around a point to be classified. The circle is drawn to encompass K nearest neighbors, where K is a user-set parameter. The category to which an unknown is assigned is based on a majority vote of its K nearest neighbors; if the vote is split, the decision is based on average distance.

In the present study, the data set of 263 spectra was split into subsets 1 and 2 (containing 132 and 131 spectra, respectively), each of which served alternately as the training set and the prediction set, and classification of the spectra in the prediction set was performed with K ranging from 1 to 10. The highest percentage of correctly classified spectra was achieved with K = 3 and K = 4 for subsets 1 and 2, respectively. Although KNN gave a slightly higher percentage of correct classification (79%) than

PCA, the nine MSSA and five BORSA strains that were misclassified as MRSA by PCA were also misclassified by the KNN algorithm.

3.4.2.5 Genotypic characterization and antibiogram testing

A genotypic study was undertaken to investigate the reason for the misclassification of nine MSSA and five BORSA strains as MRSA by FTIR spectroscopy, irrespective of the multivariate technique employed in the analysis of the spectral data in the 1080-1050 cm^{-1} region. In a study on methicillin resistance in *S. aureus*, it was reported that the *mecA* gene occurs in some coagulase-negative staphylococci and in some (13%) strains of *S. aureus* that are phenotypically methicillin-sensitive [3]. Thus, the possibility that the misclassified MSSA and BORSA strains carry the *mecA* gene without producing the altered penicillin binding protein PBP2a was first considered. However, when multiplex PCR reactions were performed for the simultaneous detection of the *mecA* and *nucA* gene sequences, no such mutants were found (Figure 3.7). A second possibility was suggested by recent findings at Health Canada (M.R. Mulvey, personal communication), where several MSSA strains were found by PFGE to have identical DNA profiles as MRSA; these strains had, in fact, been provided to Health Canada for epidemiological study, having been incorrectly classified as MRSA. If similar findings were to be obtained for the MSSA and BORSA strains misclassified as MRSA by FTIR spectroscopy, it would indicate that the spectral information in the 1080–1050 cm^{-1} range was in effect serving for DNA typing. However, PFGE showed that the DNA profiles of all the misclassified strains were quite different from those of MRSA (Figure 3.8), demonstrating that the 1080–1050 cm^{-1} spectral range does not contain the information required for representative DNA typing. Finally, antibiotic susceptibility testing of the misclassified strains was performed and revealed that the MSSA strains falling within the MRSA cluster were resistant to erythromycin and some other aminoglycosides. Accordingly, it was concluded that the spectral differences observed in the 1080–1050 cm^{-1} range appear to be related to antibiotic resistance but are not specific to methicillin resistance. Therefore, a search for other spectral regions that would allow for the complete separation of the MRSA, MSSA, and BORSA strains into distinct clusters was undertaken by randomly selecting pairs of

spectra (i.e., MRSA/MSSA, MRSA/BORSA, or MSSA/BORSA pairs) and performing singular-value decomposition (SVD) of these spectral data matrices.

3.4.2.6 Spectral regions selected using the SVD algorithm for the pairwise differentiation of MRSA, MSSA, and BORSA

Application of SVD to randomly selected pairs of spectra suggested the potential utility of three regions for the pairwise discrimination of MRSA vs. MSSA (1070-1000, 1732-1708, and 2968-2958 cm^{-1}), one region for the pairwise discrimination of MSSA vs. BORSA (1732-1708 cm^{-1}), and two regions for the pairwise discrimination of MRSA vs. BORSA (1118-1112 and 2622-2552 cm^{-1}) (Table 3.1). PCA, SOM, and KNN were then employed to examine the clustering of the strains based on the spectral data in these specific regions.

3.4.2.7 Discrimination of MRSA from MSSA

The pairwise discrimination of MRSA and MSSA strains was investigated employing a data set of 200 spectra acquired from four replicate test portions of 25 MSSA and 25 MRSA strains. The PCA scores plot (PC1 vs. PC2) generated from the normalized and first-derivatized spectral data in the spectral regions of 1070-1000, 1732-1708, and 2968-2958 cm^{-1}, as selected by using SVD, showed two distinct clusters, corresponding to MRSA and MSSA strains (Figure 3.9). Two MSSA strains fell in the MRSA cluster, and a single MRSA strain was misclassified as MSSA, yielding an overall correct classification rate of 94%. The separation of the two clusters was also evident by visual inspection of the SOM (Figure 3.10), with a similar rate of correct classification (95%) and similar misclassified strains as in PCA. Cluster analysis using the KNN algorithm was performed using half of the data set (n = 100) as the training set and the other half as the prediction set; the best results were obtained with K = 4. Two MSSA strains were misclassified as MRSA, and a single MRSA strain was misclassified as MSSA, again yielding an overall correct classification rate of 95%.

3.4.2.8 Discrimination of MSSA from BORSA

A spectral data set consisting of 159 spectra acquired from four replicate test portions of 25 MSSA and 15 BORSA strains was used in the pairwise differentiation of these two groups of strains. The data for the single spectral region (1732-1708 cm^{-1}) selected for the discrimination of MSSA and BORSA strains were employed in exploratory data analysis by PCA. Plots of the linear projection of the scores of the first two PCs (PC1 vs. PC2) showed clustering of MSSA and BORSA strains (Figure 3.11). However, two BORSA strains were misclassified within the MSSA cluster and five MSSA strains were within the BORSA cluster, yielding a correct classification rate of 83%. The SOM generated by nonlinear projection of the scores of the first two PCs (Figure 3.12) yielded the same rate of correct classification with the same misclassified strains. The clustering indicated by visual inspection of the SOM was also confirmed by the partitioning of the SOM using the *k*-means algorithm and the Davies-Bouldin index (not shown). Supervised clustering performed with the KNN algorithm using half of the data set (n = 80) as the training set and the rest (n = 79) as the prediction set yielded a correct classification rate of 90%, obtained with K = 4. In this case, only one MSSA strain and three BORSA strains were misclassified.

3.4.2.9 Discrimination of MRSA from BORSA

A data set of 163 spectra consisting of four replicate spectra of 26 MRSA and 15 BORSA strains was investigated for the pairwise discrimination of MRSA and BORSA strains using the regions of 1118-1112 and 2622-2552 cm^{-1} selected with the use of the SVD algorithm. The PCA scores plot (PC1 vs. PC2) revealed two distinct clusters, corresponding to MRSA and BORSA strains (Figure 3.13). A single MRSA strain was misclassified within the BORSA cluster and two BORSA strains fell within the MRSA cluster, yielding an overall rate of correct classification of 94%. Similarly, the SOM generated using the scores of the first two PCs as input data showed visually the existence of two clusters of MRSA and BORSA strains (Figure 3.14). The same strains of MRSA and BORSA misclassified in PCA were also misclassified when using SOM, yielding 93% correct classification. Supervised cluster analysis using the KNN algorithm was performed using 82 spectra as the training set and the remaining 81 spectra as the

prediction set. The highest rate of correct classification (97%) was achieved with K = 1 and K = 2. Although no false negatives (misclassified MRSA) were obtained, the same BORSA strains misclassified as MRSA by PCA and SOM were misclassified in the supervised cluster analysis.

In summary, the use of SVD to select spectral regions for the pairwise discrimination of MRSA, MSSA, and BORSA yielded much higher correct classification rates than were obtained using the single region of 1080-1050 cm^{-1} selected by visual inspection of the spectra. This finding highlights the importance of identifying appropriate spectral regions for the differentiation of MRSA from MSSA and BORSA.

3.4.3 Validation of FTIR method

The potential of FTIR spectroscopy to discriminate MRSA clinical strains from MSSA and BORSA strains was assessed in a validation study performed with 166 *S. aureus* isolates. These included 100 epidemic MRSA, 25 sporadic MRSA, 22 clinical BORSA strains, and 10 *S. aureus* strains from hospitals across Canada and 9 mutant strains from Switzerland, comprising 6 MRSA and 3 MSSA strains. With the use of the spectral regions listed in Table 3.1, all these strains were correctly classified by PCA, SOM, and KNN. These results confirmed the utility of the FTIR method for the discrimination of MRSA from MSSA and BORSA strains.

3.4.4 FTIR spectroscopic analysis of cell walls

Since the structural modifications associated with methicillin resistance are within the cell wall [1], the FTIR spectra of the cell walls extracted from one MRSA (BB270) and one MSSA (BB255) strain were recorded. These spectra exhibited discernible differences in all the regions selected using SVD for the discrimination of the 26 MRSA and 25 MSSA strains. The major differences between the spectra were observed at 1018-978, 1074-1018, 1276-1214, 1540-1500, and 1756-1726 cm^{-1} (Figure 3.15). and at 3190-3170 cm^{-1} (not shown in Figure 3.15). These findings provide evidence that the specific markers for the discrimination of MRSA from MSSA from the spectra of whole cells are localized within the cell wall.

3.5 DISCUSSION

In previous FTIR studies [9,10], attempts to differentiate MRSA from MSSA by applying cluster analysis techniques were unsuccessful and were thus abandoned in favor of neural network approaches, which yielded better results but did not provide 100% correct classification. The present study indicates that achieving accurate classification appears to rely mainly on the appropriate selection of specific spectral regions and less on the choice of chemometric method since exploratory data analysis (PCA), an unsupervised neural network (SOM), and supervised cluster analysis (KNN) gave similar results. Consequently, the use of SVD to select spectral regions containing features that are specifically related to methicillin resistance was a key element of this work. Thus, although spectral differences among MRSA, MSSA, and BORSA strains were visually discernible in the 1080-1050 cm^{-1} region of the spectrum, the results obtained when differentiation was based on this region alone indicated that these differences were not specific to methicillin resistance. Therefore, it was necessary to select additional spectral regions that were not evident by visual inspection, and SVD proved very effective in identifying optimal spectral regions that allowed for the pairwise differentiation of the three *S. aureus* phenotypes. Cell walls extracted from MRSA and MSSA strains exhibited spectral differences in all the regions selected by SVD for the discrimination of MRSA from MSSA, consistent with the localization of methicillin resistance in the cell wall of MRSA strains.

Another important aspect of this work was the strategy employed to ensure the high degree of spectral reproducibility required to reliably detect the spectral features that differentiate MRSA, MSSA, and BORSA. Excellent spectral reproducibility was attained through the rigorous control of growth conditions, including the use of a universal growth medium (UM™), and the selection of appropriate spectral preprocessing tools (normalization and first-order derivatization) to minimize spectral variability arising from baseline shifts and sampling-associated factors such as sample thickness.

3.6 CONCLUSION

This study has demonstrated the potential utility of FTIR spectroscopy as a rapid method for the accurate classification of MRSA, MSSA, and BORSA strains. Pairwise discrimination of MRSA, MSSA, and BORSA yielded high rates of correct classification; the lowest rate of correct classification (90%) was for the discrimination of MSSA from BORSA, which is not important from a clinical perspective since infections due to BORSA strains are treated in the same way as those due to MSSA and do not require the use of vancomycin as for MRSA infections. In addition, 166 *S. aureus* isolates were all correctly classified in a separate validation study. Furthermore, the speed of the FTIR method, with results being obtained within 1 hour from a stationary-phase culture, make it highly suitable for application in a clinical setting.

3.7 REFERENCES

1. Chambers, H.F., 1997. Methicillin-resistance in staphylococci: molecular and biochemical basis and clinical implication. *Clin. Microbiol. Rev.* 10: 781-791

2. Berger-Bächi, B., 1997. Resistance not mediated by ß-lactamase (methicillin-resistance), *in* K. B. Crossley and G. L. Archer (eds.), *The Staphylococci in Human Disease*. New York: Churchill Livingstone.

3. Kobayachi, N., K. Kojima, K. Taniguchi, S. Urasawa, N. Uehara, Y. Omizu, Y. Kishi, A. Yagihashi, and I. Kurokawa, 1994. Detection of *mecA*, *femA*, *femB* genes in clinical strains of staphylococci using polymerase chain reaction. *Epidemiol. Infect.* 113:259-266.

4. Mariey, L., J.P. Signolle, C. Amiel, and J. Travert, 2001. Discrimination, classification, identification of microorganisms using FTIR spectroscopy and chemometrics. *Vibr. Spectrosc.* 26:151-159.

5. Naumann, D., D Helm, and H. Labischinski, 1991. Microbiological characterization by FT-IR spectroscopy. *Nature* 351:81-82.

6. Helm, D., H. Labischinski, G. Schallehn, and D. Naumann, 1991. Classification and identification of bacteria by Fourier transform spectroscopy. *J. Gen. Microbiol.* 137:69-79.

7. Sockalingum, G.D., W. Bouhedja, P. Pina, P. Allouch, C. Mandray, R. Labia, J. Millot, and M. Manfait, 1997. ATR-FTIR spectroscopic investigation of imipenem-susceptible and -resistant *Pseudomonas aeruginosa* isogenic strains. *Biochem. Biophys. Res. Commun.* 232:240-246

8. Bouhedja, W., G.D. Sockalingum, P. Pina, P. Allouch, C. Bloy, R. Labia, J.M. Millot, and M. Manfait, 1997. ATR-FTIR spectroscopy investigation of *E. coli* transconjugants β-lactams-resistance phenotype. *FEBS Lett.* 412:39-42

9. Kirschner C., Ngoc Anh Ngo Thi, and D. Naumann, 1999. FT-IR spectroscopic investigations of antibiotic sensitive and resistant microorganisms. *2nd Workshop on FT-IR Spectroscopy in Microbiology and Medical Diagnostics*. Robert Koch-Institute, Berlin.

10. Goodacre, R., P.J. Rooney, and D.B. Kell, 1998. Rapid analysis of microbial systems using vibrational spectroscopy and supervised learning methods: Application to the discrimination between methicillin-resistant and methicillin-susceptible *Staphylococcus aureus*. *Proc. SPIE* 3257 *(IR Spectroscopy: New Tool in Medicine)*:220-229

11. Bauer, AW., W.M. Kirby, and J.C. Sherris, 1966. Antibiotic susceptibility testing by a standard single disk method. *Am. J. Clin. Pathol.* 45:493-496

12. National Committee for Clinical Laboratory Standards, 1999. *Performing Standards for Antimicrobial Susceptibility Testing-Eighth Informational Supplement*: Approved Standards M7-A4. NCCLS, Wayne, PA

13. Blair, J.E., and R.E.O. Williams, 1961. Phage typing of staphylococci. *Bull. WHO* 24:771-784

14. Murakami, K., W. Minamide, K. Wada, N. Nakamura, H. Teraoka, and S. Watanabe, 1991. Identification of methicillin-resistant staphylococci by polymerase chain reaction. *J. Clin. Microbiol.* 29:2240-2244

15. Brakstad, O.G., K. Aasbakk, and J.A. Maeland, 1992. Detection of *Staphylococcus aureus* by PCR amplification of the *nuc* gene. *J. Clin. Microbiol.* 30:1654-1660

16. Stranden, A.M., K. Ehlert, H. Labischinski, and B. Berger-Bächi, 1997. Cell wall monoglycine cross-bridges and methicillin hypersusceptibility in a *femAB* null mutant of methicillin-resistant *Staphylococcus aureus*. *J. Bacteriol.* 179:9-16

17. Naumann, D., 1984. Some ultrastructural information on intact, living bacterial cells and related cell-wall fragments as given by FTIR. *Infrared Phys.* 24:233-238

18. Kummerle, M., S. Sherer, and H. Seiler, 1998. Rapid and reliable identification of food-borne yeast by Fourier-transformed infrared spectroscopy. *Appl. Environ. Microbiol.* 64:2207-2214

19. Magee, J., 1993. Whole-organism fingerprinting, *in* M. Goodfelow and A.G. O'Donnell (eds.), *Handbook of New Bacterial Systematics*. New York: Harcourt Brace. pp. 383-427

20. Bourne, R., U. Himmelreich., A. Sharma., C. Mountford, and T. Sorrel, 2001. Identification of *Enterococcus*, *Streptococcus*, and *Staphylococcus* by multivariate analysis of proton magnetic resonance spectroscopic data from plate cultures. *J. Clin. Microbiol.* 39:2916-2923

21. Savitzky, A., and M.J.E. Golay, 1964. Smoothing and differentiation of data by simplified least squares procedures. *Anal. Chem.* 36:1627-1633

22. Jolliffe, I.T., 1986. *Principal Component Analysis*. New York: Springer.

23. Kohonen, T., 1995. *Self–Organizing Maps*, Vol. 30 of Springer Series in Information Sciences. Berlin, Heidelberg: Springer.

24. Ultsch, A., and H.P. Siemon, 1990. Kohonen's self organizing feature maps for extrapolatory data analysis. *Proceedings of International Neural Network Conference (INNC'90)*. Dordrecht: Kluwer. pp. 305-308

25. Vesanto, J., and E. Alhoniemi, 2000. Clustering of the self-organized map. *IEEE Trans. Neural Networks* 11(3):586-600

26. Davies, D.L., and D.W. Bouldin, 1979. A cluster separation measure. *IEEE Trans. Patt. Anal. Machine Intell.*,Vol. PAMI-1, pp.224-227

27. Adams, M.J., 1995. *Chemometrics in Analytical Spectroscopy*. Cambridge: The Royal Society of Chemists.

28. Brereton, R.G., 1993. *Chemometrics – Applications of Mathematics and Statistics to Laboratory Systems*. New York: Ellis Horwood Ltd.

Table 3. 1. Spectral regions selected using SVD for the pairwise differentiation of MRSA MSSA and BORSA

Strains differentiated	**Spectral region(s)* (cm-1)**
MRSA vs. MSSA	1070-1000 1732-1708 2968-2958
MSSA vs. BORSA	1732-1708
MRSA vs. BORSA	1118-1112 2622-2552

*Assignment of the major bands in these regions can be seen in Figure 3.1

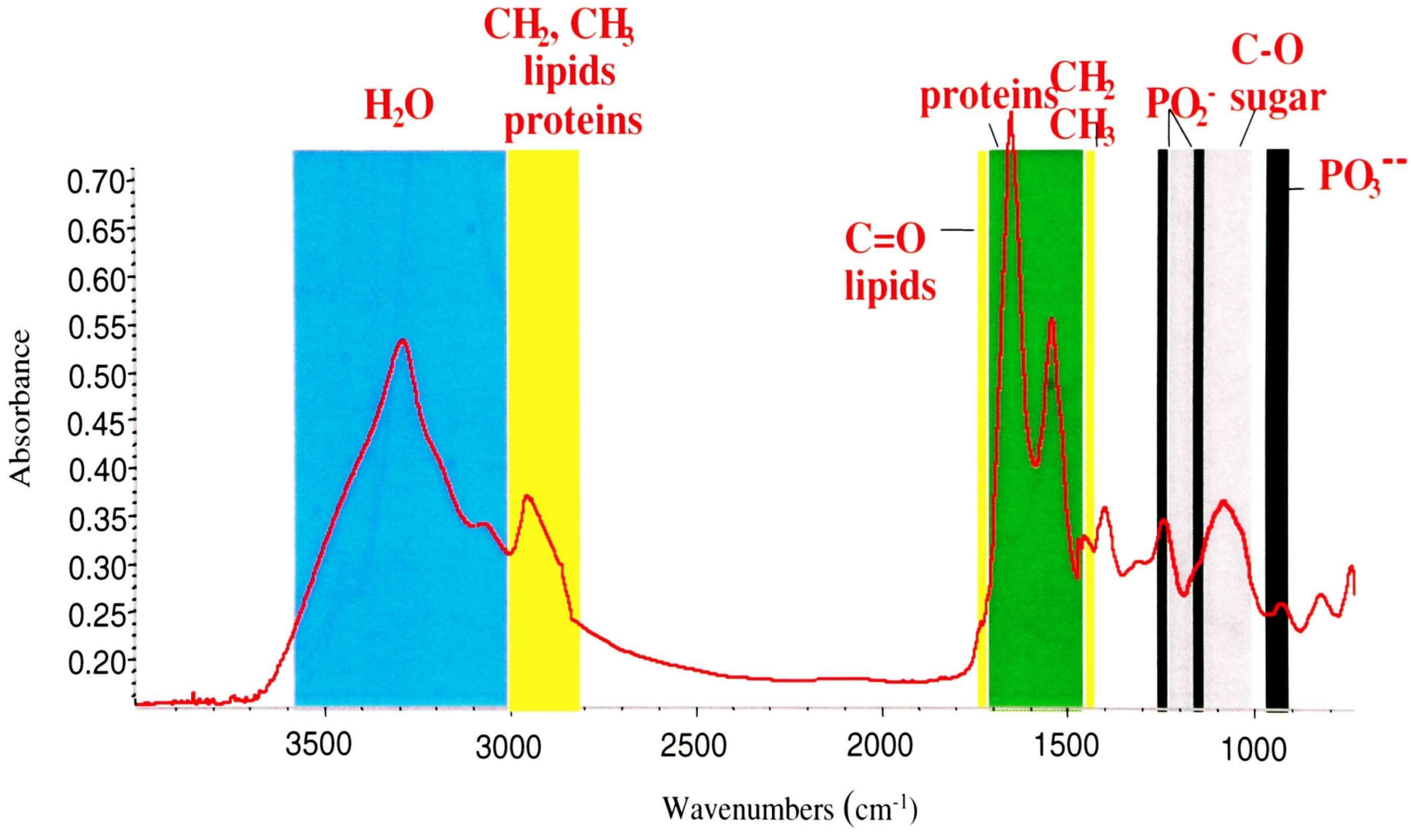

Figure 3.1: Typical FTIR spectrum of bacteria cells

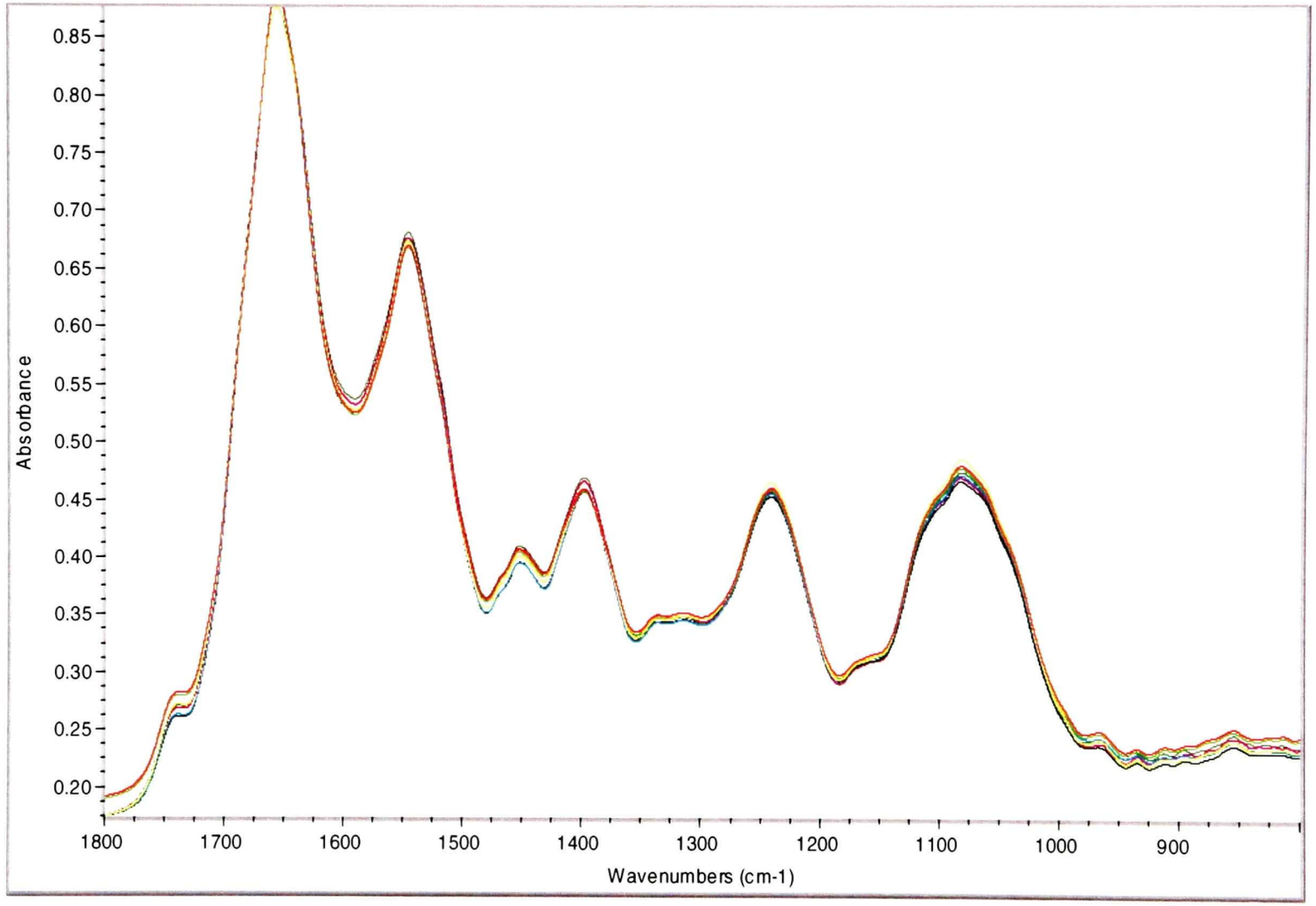

Figure 3. 2: Overlaid FTIR spectra in the region 1800-800 cm^{-1} of a single MRSA strain obtained for cells taken from four culture plates

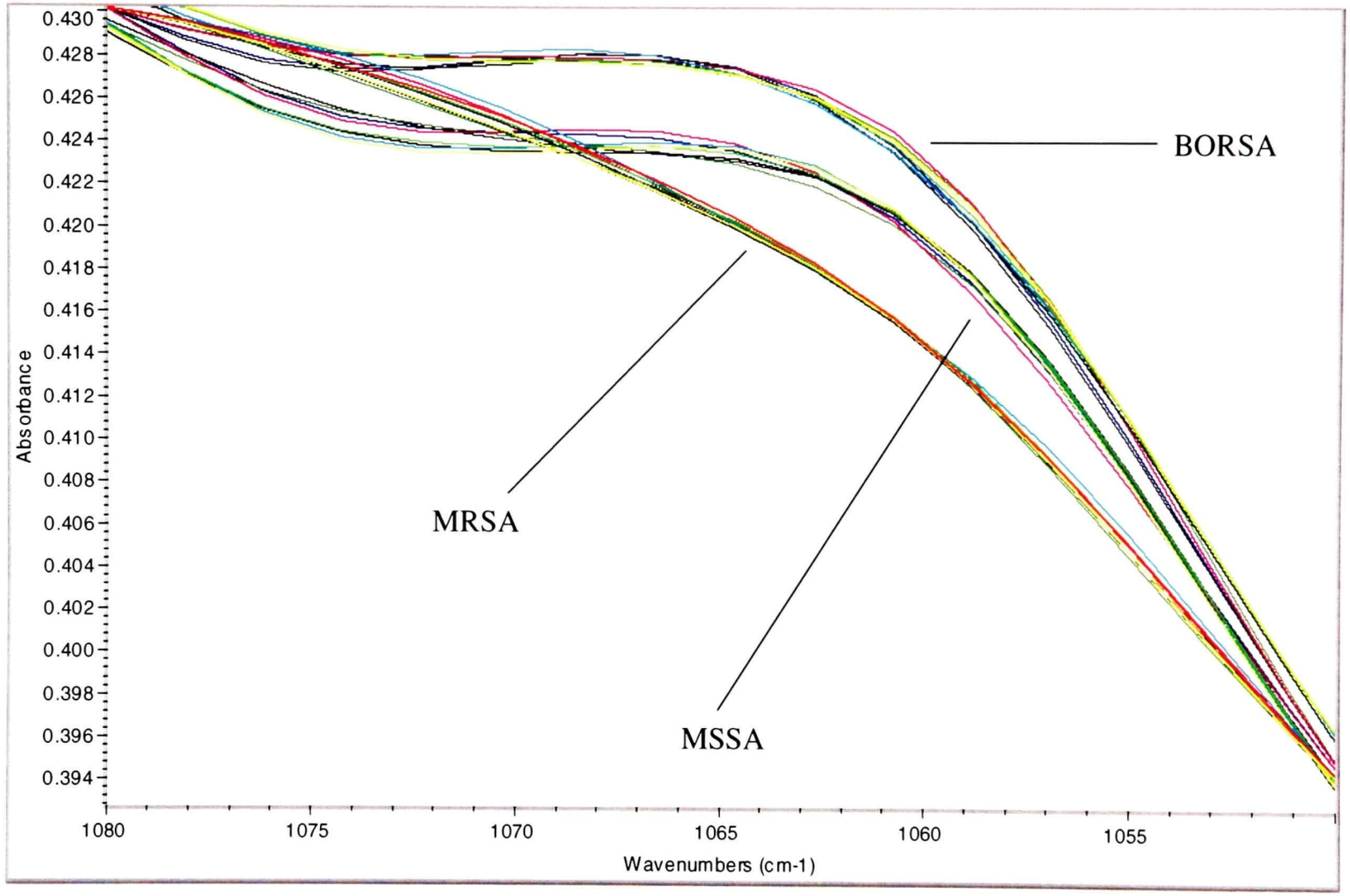

Figure 3.3: FTIR spectra of MRSA, MSSA and BORSA strains in the region 1080-1050 cm^{-1}

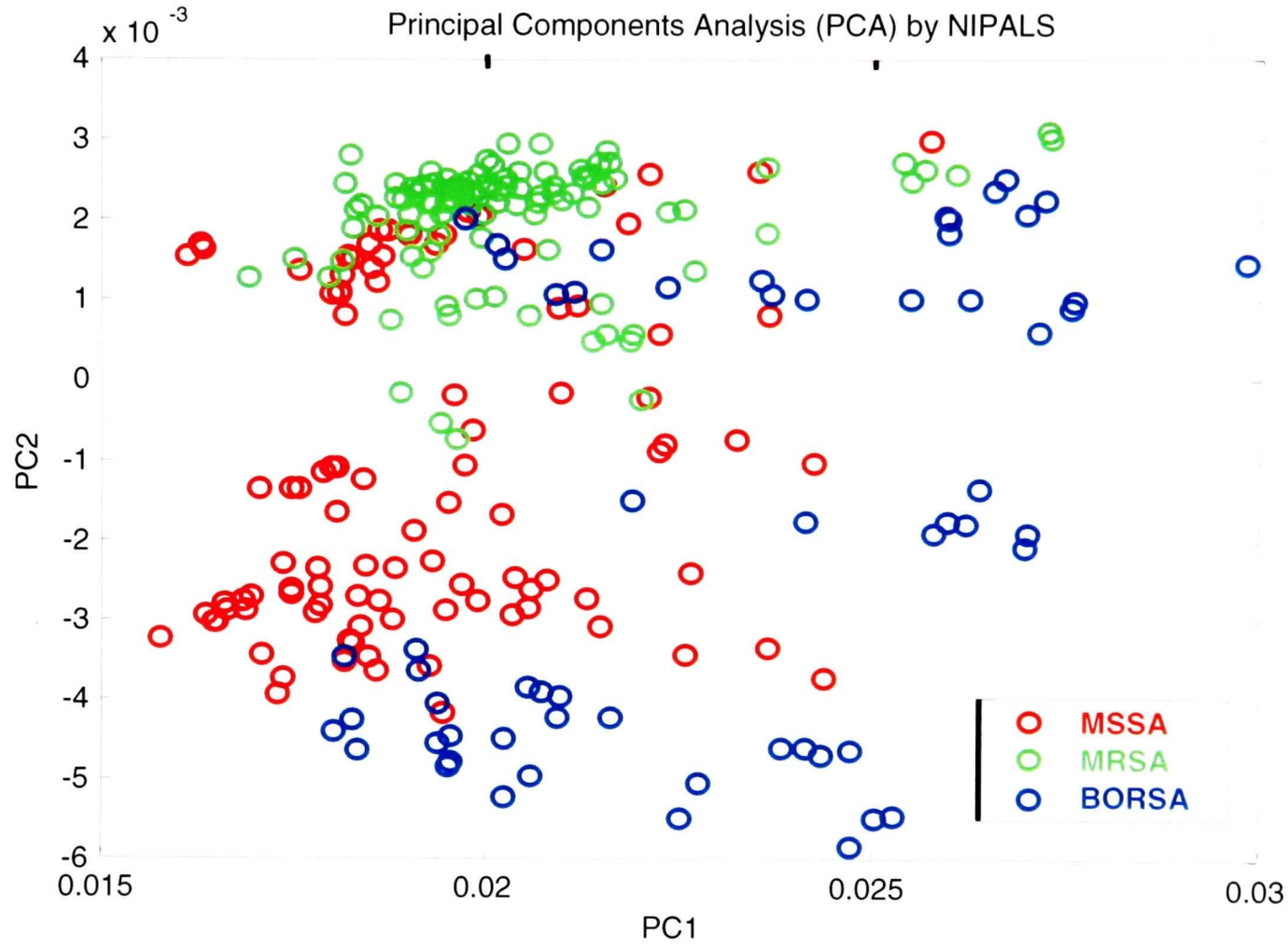

Figure 3.4: Scores plot for first two PCs obtained from the spectral data for 26 MRSA, 25 MSSA and 15 BORSA strains in the region 1080-1050 cm^{-1} by PCA using the NIPALS algorithm

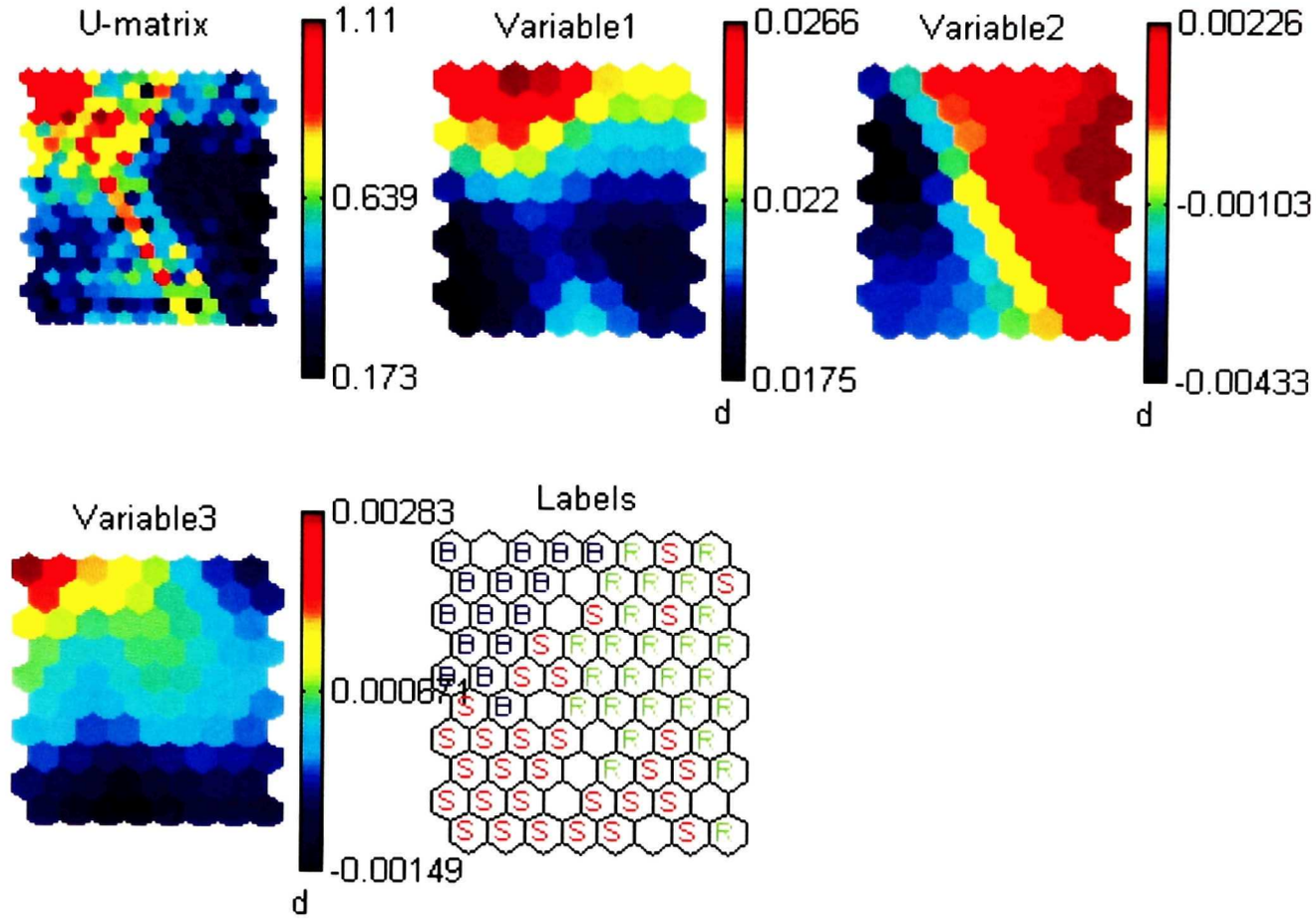

Figure 3.5a: U-matrix, component planes, and SOM obtained by application of the SOM algorithm using the spectral data for 25 MRSA (R), 25 MSSA (S) and 15 BORSA (B) strains in the region 1080-1050 cm^{-1}

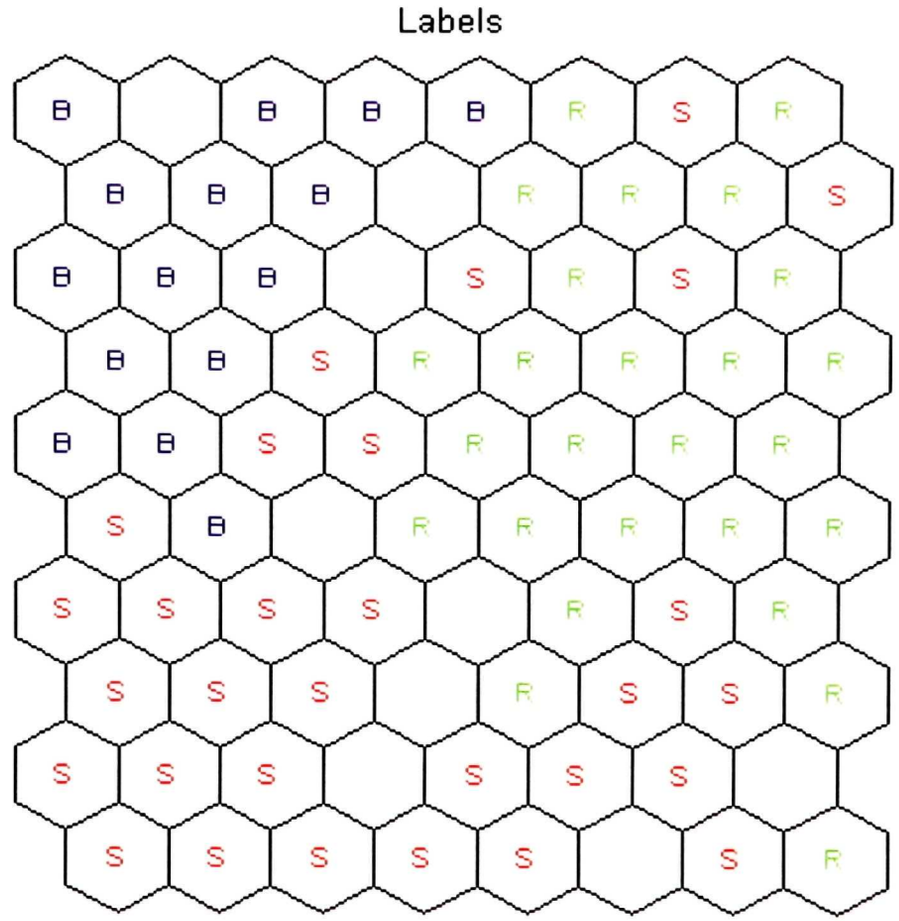

Figure 3.5b: Expanded view of the SOM shown in Figure 3.5a

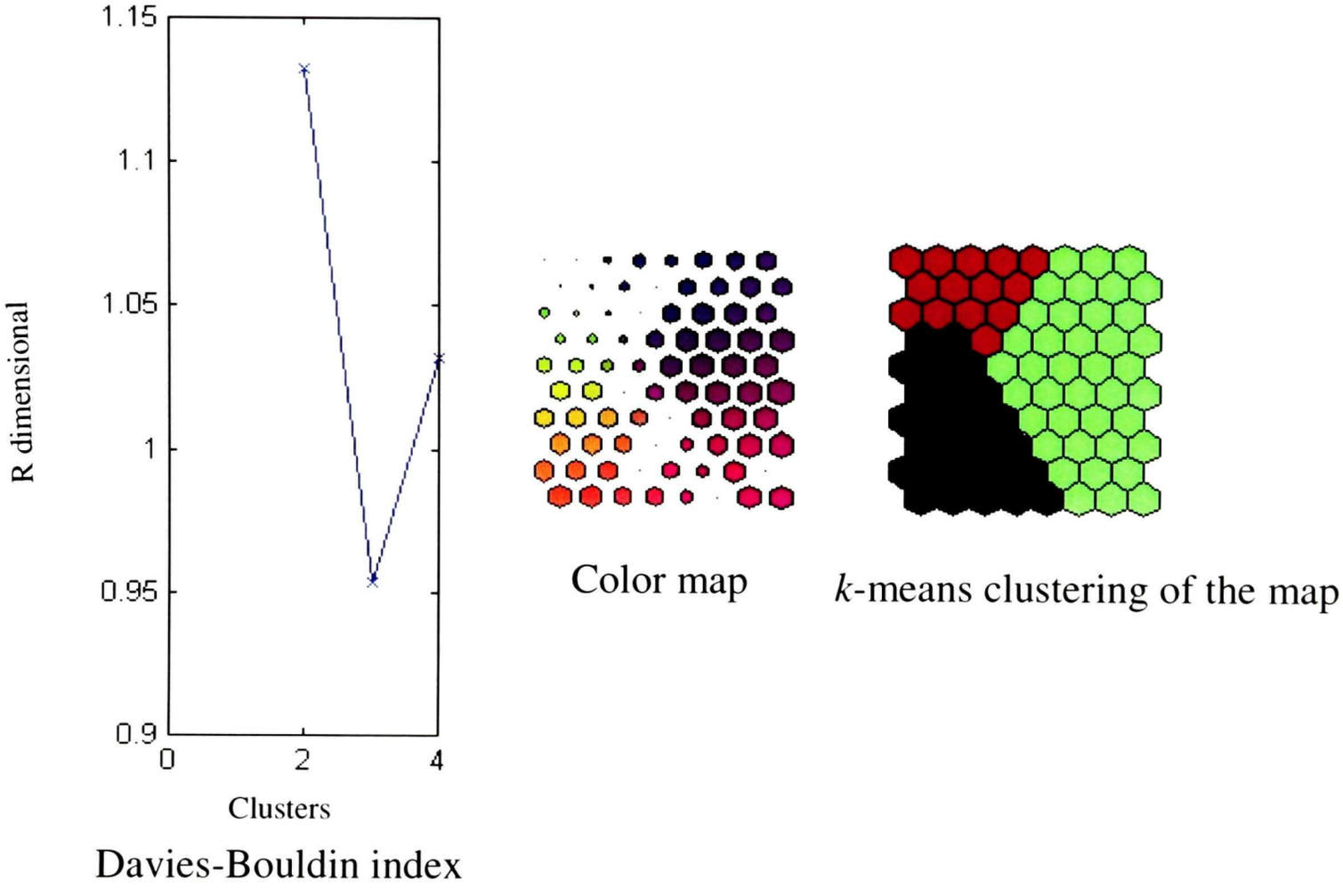

Figure 3.6a: Partitioned SOM for the spectral data in the region 1080-1050 cm^{-1} obtained by applying the *k*-means algorithm and the Davies-Bouldin index

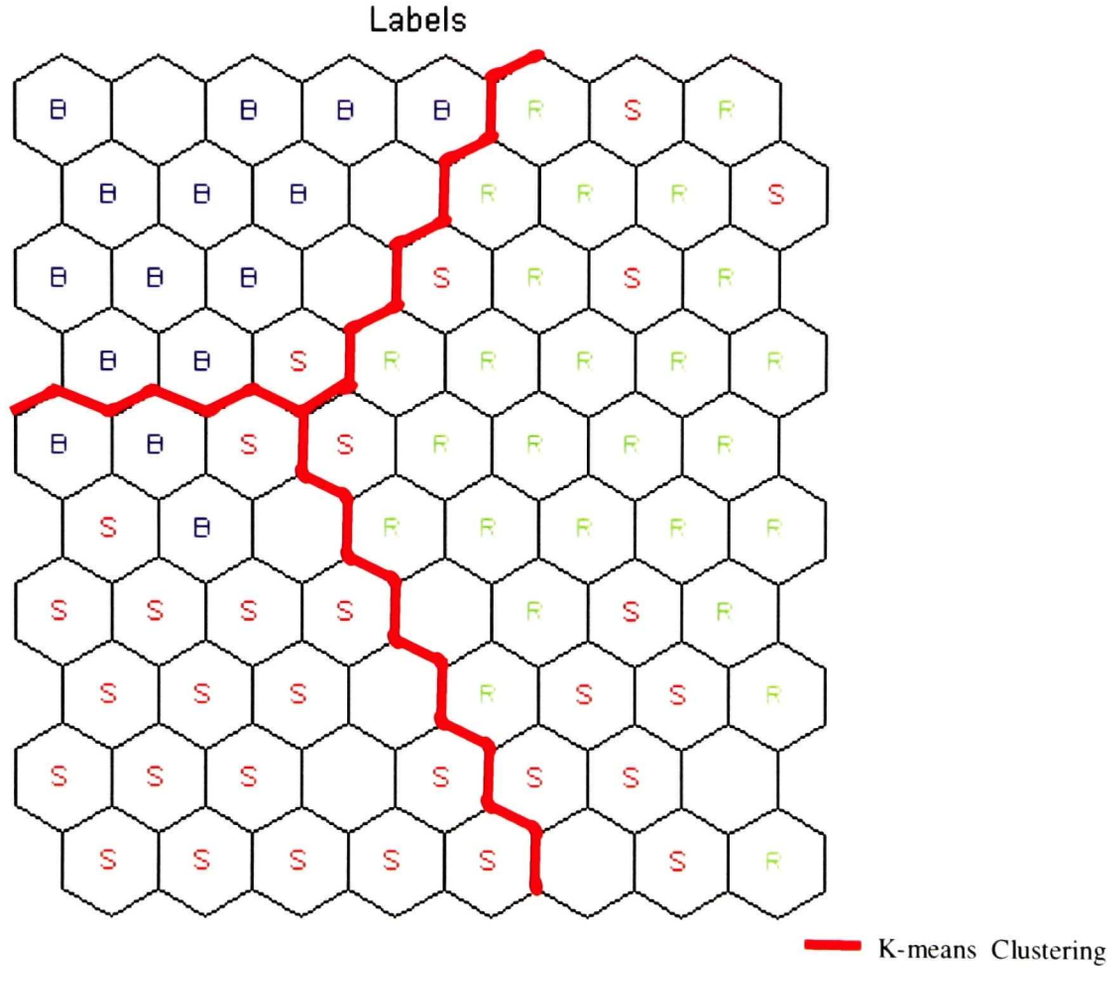

Figure 3.6b: Labeling of the partitioned map units shown in Figure 3.6a., R, S and B represent MRSA, MSSA and BORSA respectively

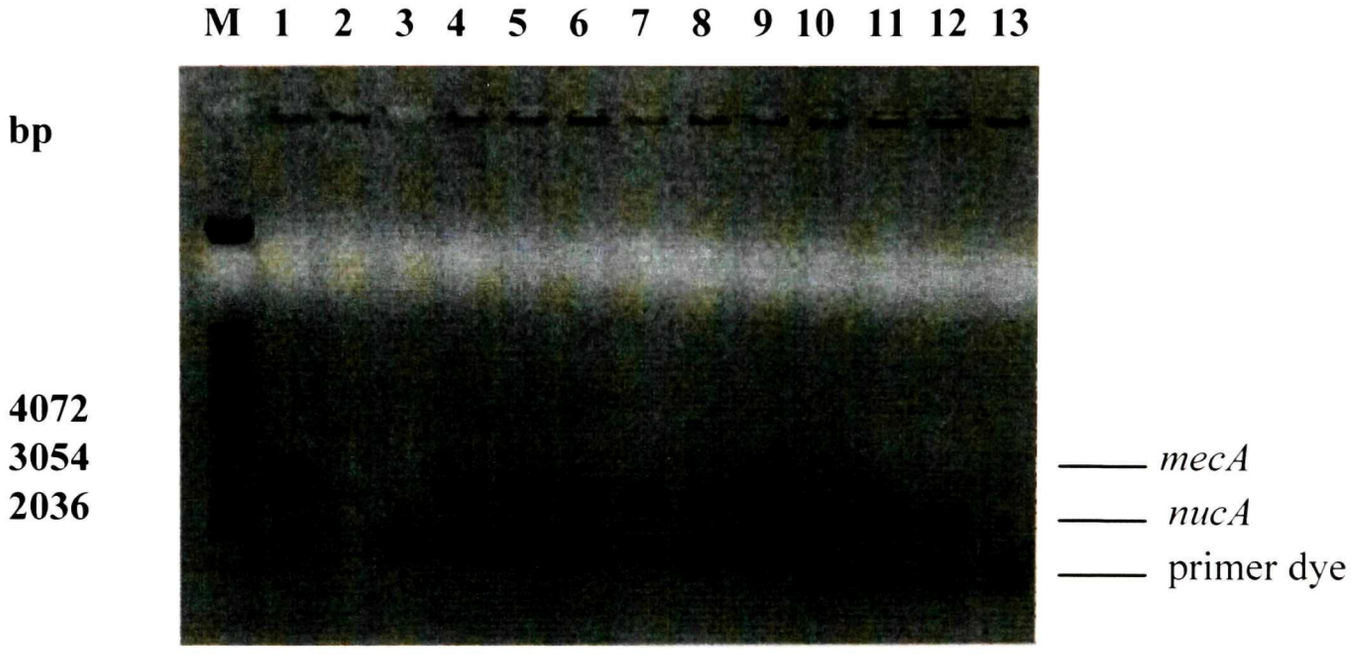

Figure 3.7: An ethidium bromide-stained agarose gel demonstrating the banding patterns observed with the multiplex PCR assay. Lane M: 50-bp molecular weight ladder; lane 1: MRSA control; lane 3: negative control (*E. coli*); lanes 4-8: MSSA strains misclassified as MRSA by FTIR spectroscopy; lane 9: MRSA; lanes 10-12: BORSA strains misclassified as MRSA by FTIR spectroscopy; lane 13: negative control (*E. coli*).

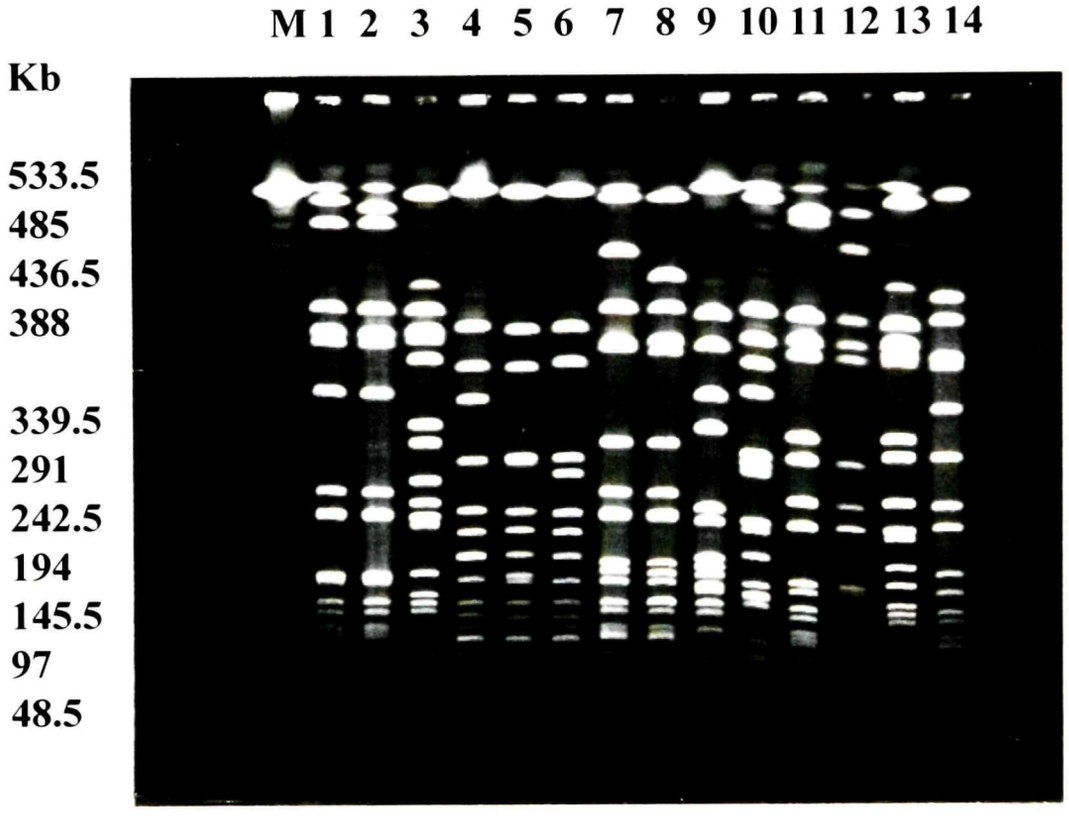

Figure 3.8: DNA representative patterns for MRSA, MSSA and BORSA strains obtained by PFGE.

Lane M, lambda DNA concatamers; lanes 1-5: MRSA; lanes 6-10: MSSA; lanes 11-14: BORSA

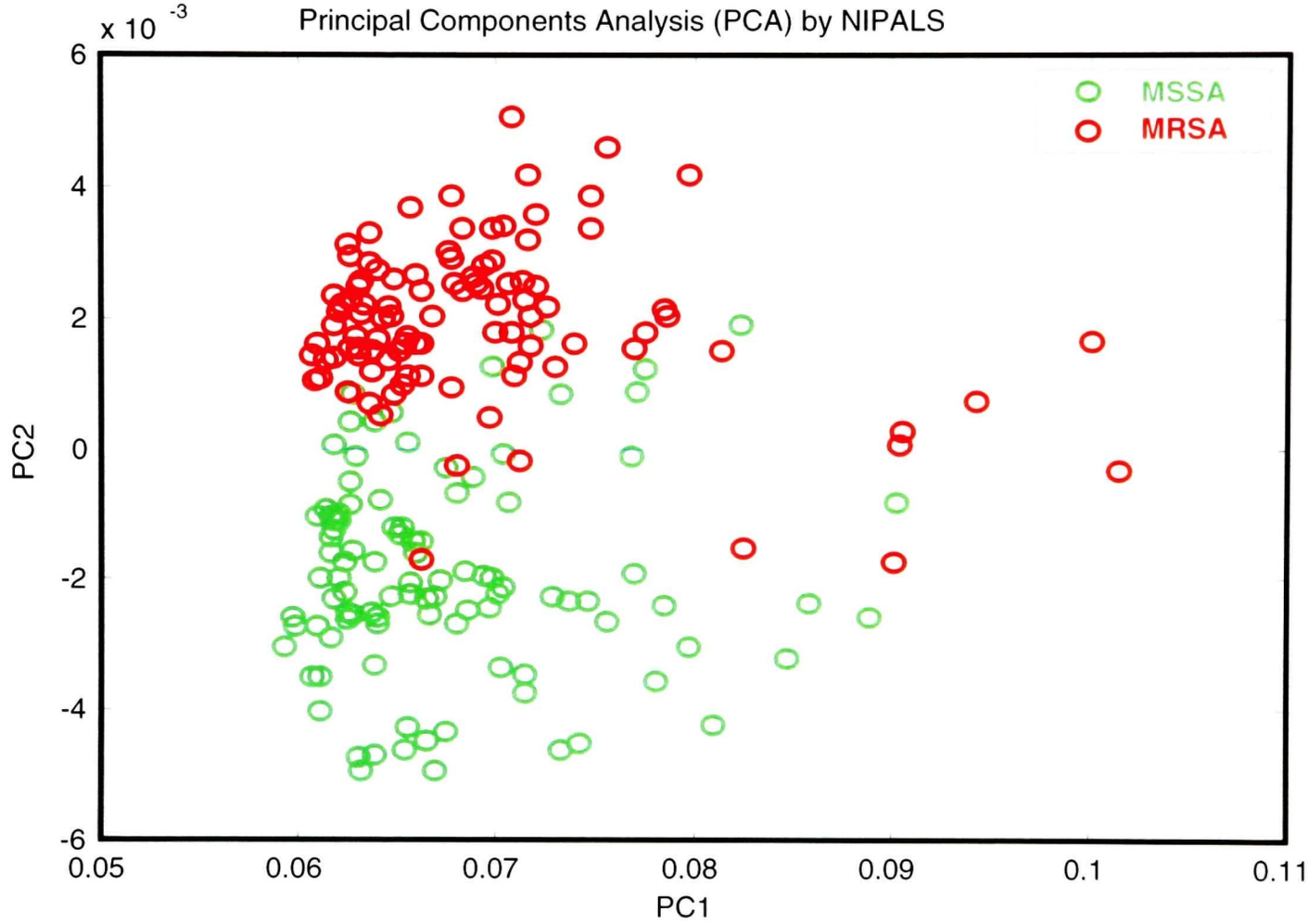

Figure 3.9: Scores plot for first two PCs obtained from the spectral data for 26 MRSA and 25 MSSA strains in the regions 1070-1000, 1732-1708 and 2968-2958 cm^{-1} by PCA using the NIPALS algorithm

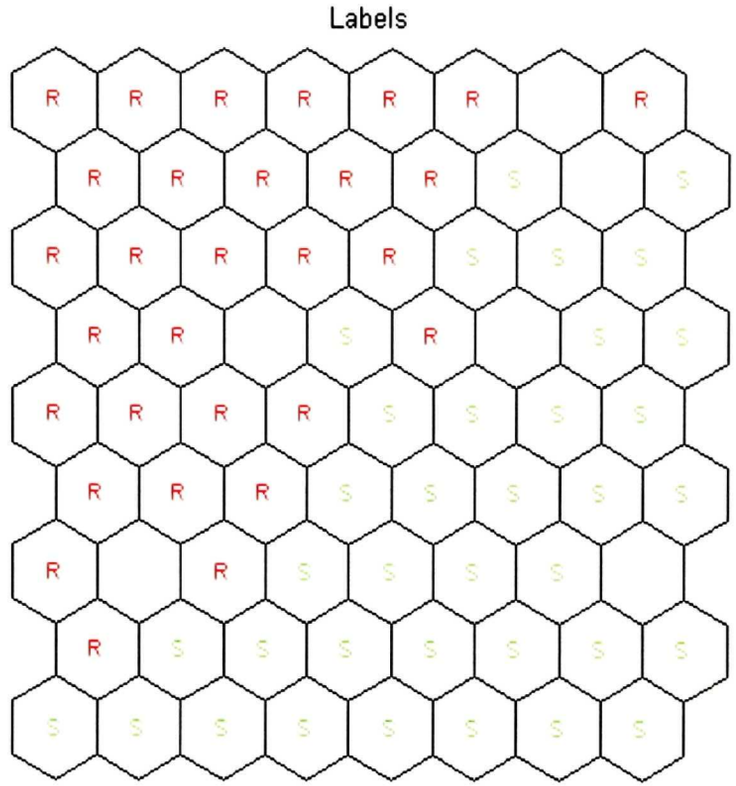

Figure 3.10: SOM obtained using the spectral data for 26 MRSA (R) and 25 MSSA (S) strains in the regions 1070-1000, 1732-1708, and 2968-2958 cm^{-1}

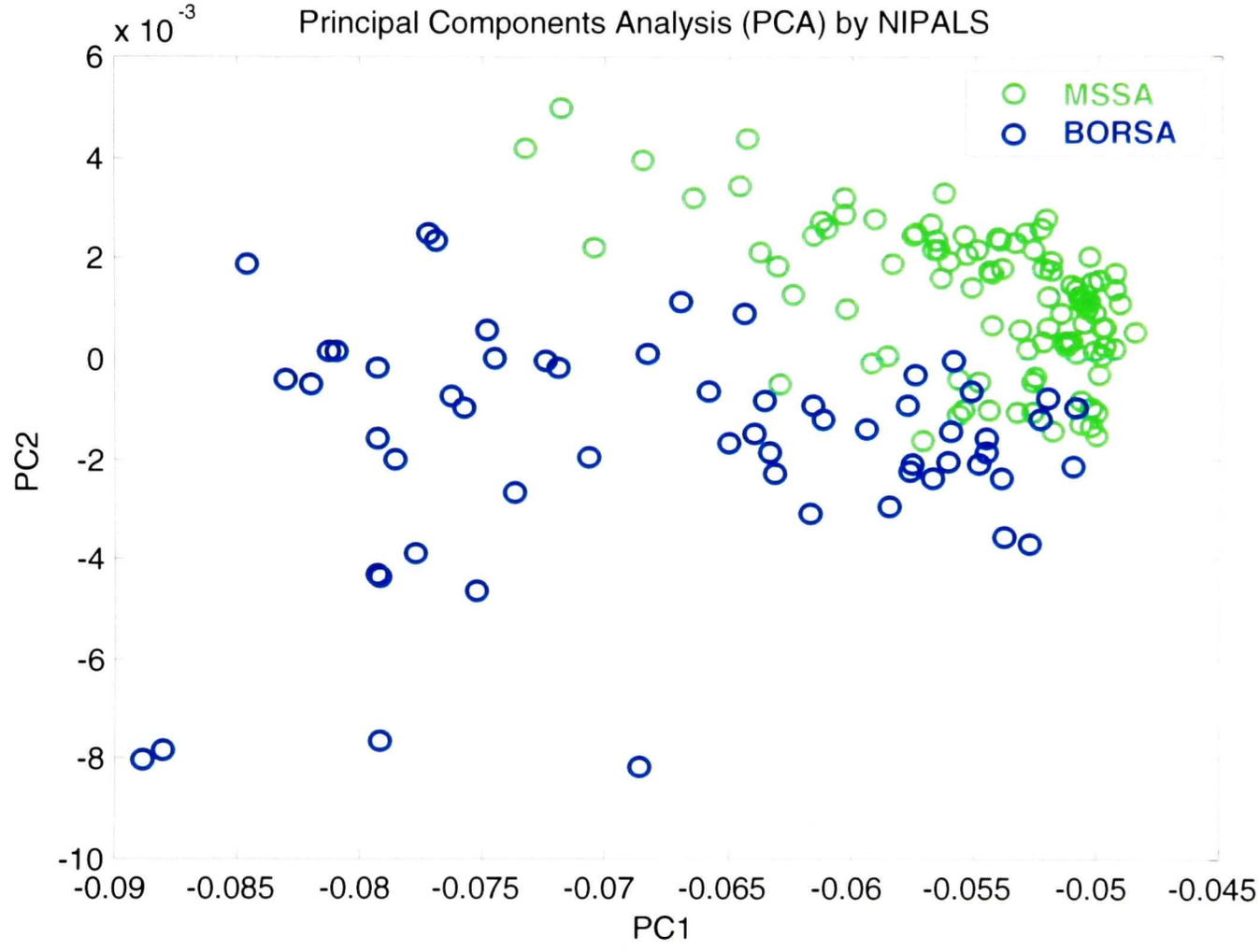

Figure 3.11: Scores plot for first two PCs obtained from the spectral data for 25 MSSA and 15 BORSA strains in the region 1732-1708 cm^{-1} by PCA using the NIPALS algorithm

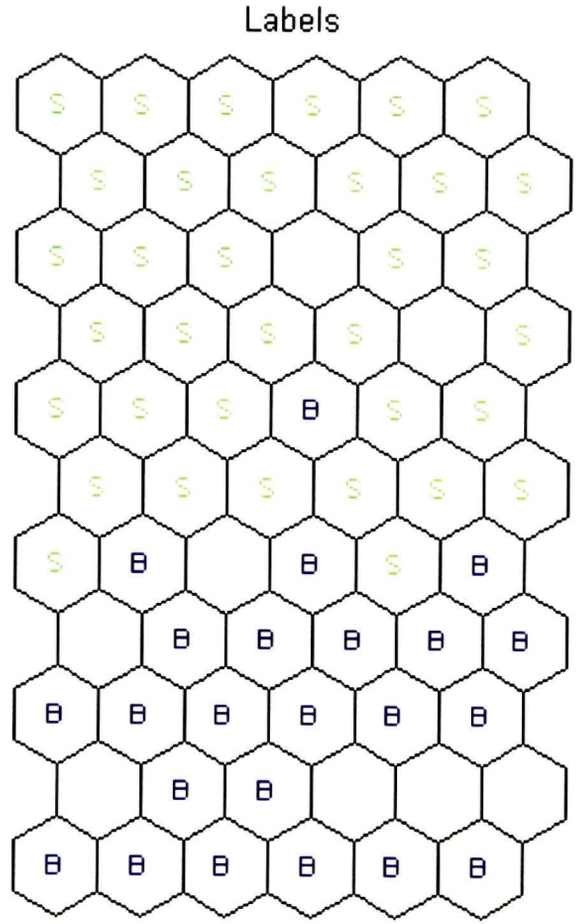

Figure 3.12: SOM obtained using the spectral data for 25 MSSA (S) and 15 BORSA (B) strains in the region 1732-1708 cm^{-1}

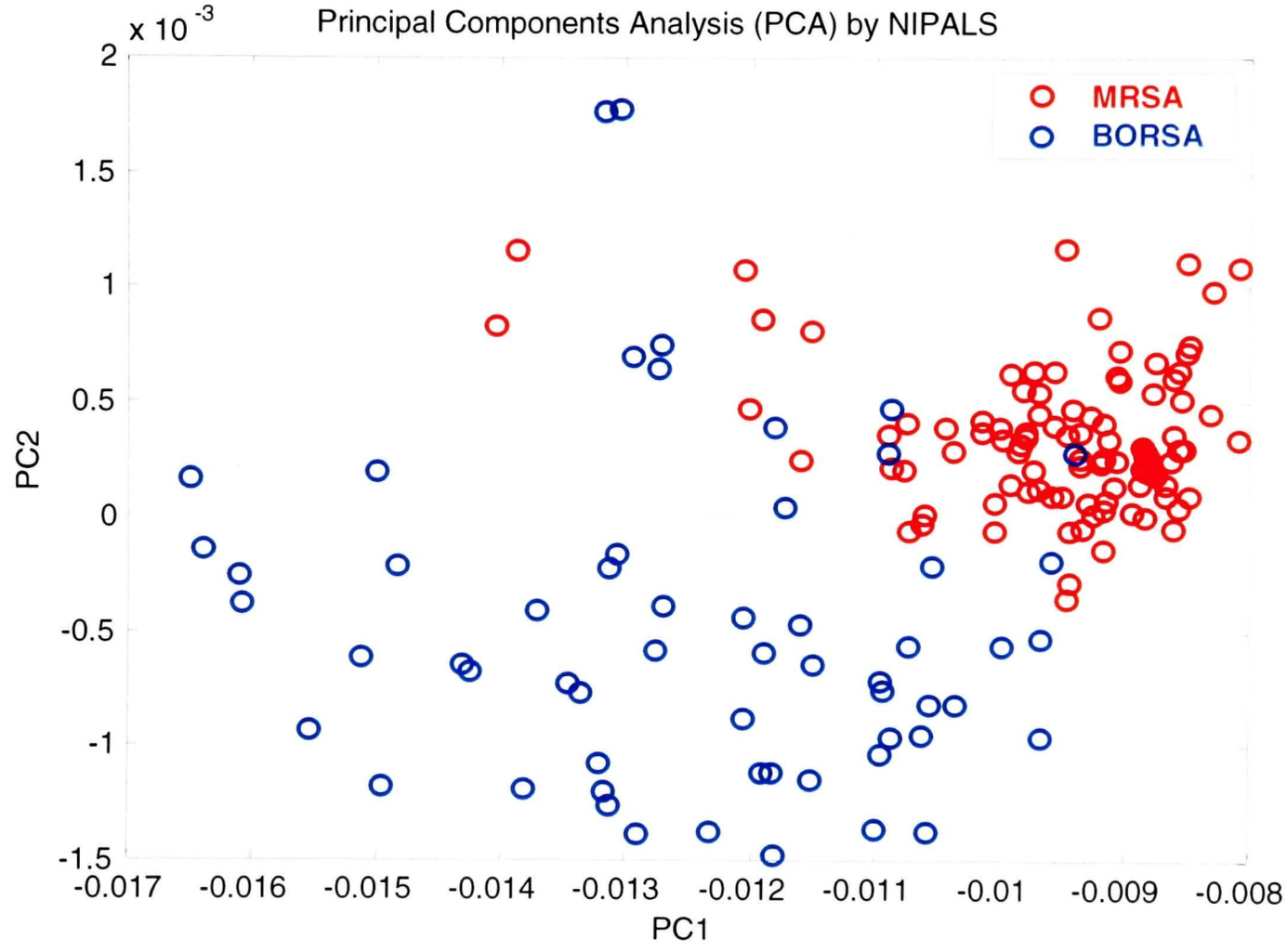

Figure 3.13: Scores plot for first two PCs obtained from the spectral data for 26 MRSA and 15 BORSA strains in the regions 1118-1112 and 2622-2552 cm^{-1} by PCA using the NIPALS algorithm

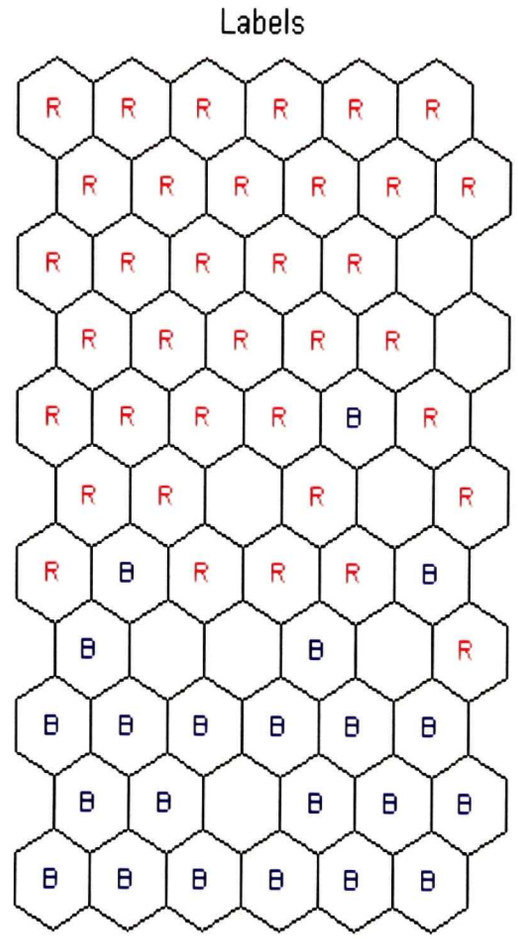

Figure 3.14: SOM obtained using the spectral data for 26 MRSA (R) and 15 BORSA (B) strains in the regions 1118-1112 and 2622-2552 cm^{-1}

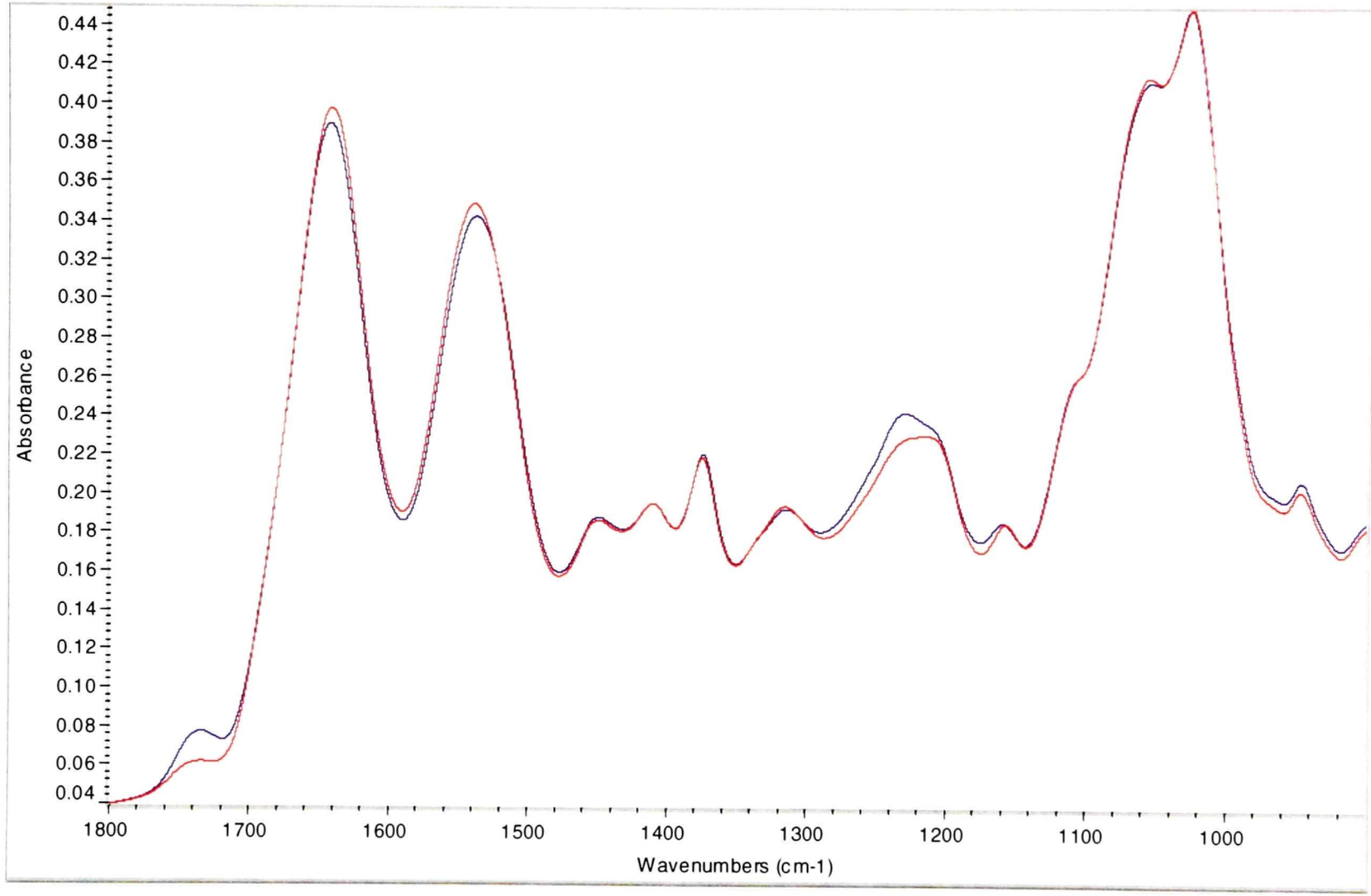

Figure 3.15: FTIR spectra of MRSA (BB270) and MSSA (BB255) cell walls in the region 1800-900 cm^{-1}. The major differences between the spectra were observed at 1018-978, 1074-1018, 1276-1214, 1540-1500, and 1756-1726 cm^{-1} and at 3190-3170 cm^{-1} (not shown)

CHAPTER 4

CONNECTING STATEMENT

In the previous chapter, an FTIR-based method for the discrimination of methicillin-resistant *S. aureus* (MRSA) from methicillin-sensitive *S. aureus* (MSSA) and from borderline strains was described. It was shown that FTIR spectroscopy, in combination with the use of a universal growth medium and the application of various chemometric tools, could provide a routine method for the identification of MRSA clinical isolates among MSSA and BORSA isolates. Based on these findings, the research presented in Chapter 4 was undertaken to evaluate the potential use of FTIR spectroscopy for the discrimination of coagulase-negative staphylococci (CNS) from *S. aureus* (MRSA and MSSA) as well as the identification of methicillin-resistant CNS (MRCNS) among CNS isolates.

CHAPTER 4

RAPID AND ACCURATE IDENTIFICATION OF COAGULASE-NEGATIVE STAPHYLOCOCCI (CNS) AND METHICILLIN-RESISTANT CNS (MRCNS) BY FOURIER TRANSFORM INFRARED (FTIR) SPECTROSCOPY

4.1 ABSTRACT

Coagulase-negative staphylococci (CNS) are frequently associated with both community-acquired and nosocomial bloodstream infections. Rapid and accurate identification of methicillin-sensitive CNS (MSCNS) and methicillin-resistant CNS (MRCNS) among staphylococci species by a single-step simple assay is important for treatment decisions. However, conventional routine methods are too laborious and time-consuming and often lack sensitivity in detecting methicillin resistance in CNS. The feasibility of developing a simple, rapid single-step method employing Fourier transform infrared (FTIR) spectroscopy, combined with the use of a universal medium (UM™) and chemometrics, was evaluated in this study. The FTIR spectra of 22 CNS strains, including 11 MRCNS and 11 MSCNS strains, 25 methicillin-resistant *Staphylococcus aureus* (MRSA) strains, and 25 methicillin-sensitive *S. aureus* (MSSA) strains were obtained from dried films of stationary-phase cells grown on UM™. Principal component analysis (PCA), self-organizing maps (SOM), and the K-nearest neighbor (KNN) algorithm were employed to cluster the different phenotypes of staphylococci species based on the similarity of their FTIR spectra. PCA of the first-derivative normalized spectral data from a single narrow region of the infrared spectrum (1442-1439 cm^{-1}) allowed for 100% correct classification of CNS and *S. aureus* species. When data from four spectral regions were combined, MRSA and MSSA strains were fully discriminated from each other as well as from CNS. For the discrimination of MRCNS from MSCNS, 92% correct classification was obtained with the use of a single narrow spectral region (2880-2860 cm^{-1}). Thus, FTIR spectroscopy provides a simple and accurate means for the identification of CNS species and is a promising method for discrimination of MRCNS from MSCNS strains.

4.2 INTRODUCTION

Coagulase-negative staphylococci (CNS) have been known for decades as commensal organisms of human skin flora and viewed mostly as clinically non-relevant contaminants in blood cultures among staphylococci species. Only recently, CNS strains have been recognized as a major cause of both community-acquired and nosocomial bloodstream infections [1], and an increasing proportion (60-90%) of methicillin resistance in CNS in hospitalized patients [2,3] has been ascertained within the past decade.

This emergence of CNS as human pathogens and reservoirs of antimicrobial-resistance determinants, especially for methicillin resistance, requires that rapid and reliable means for the differentiation of CNS from *S. aureus* and for the identification of methicillin-resistant CNS (MRCNS) strains be available to guide antimicrobial therapy and to clarify the clinical significance of CNS species. The accuracy of biochemical tests conventionally employed for the identification of CNS is low, ranging from 50 to 70% [4-7], and phenotypic detection of methicillin resistance in CNS is more difficult than in *S. aureus*, making disk diffusion methods unreliable [8]. Commercial automated systems are rapid but often lack sensitivity and may give false-positive results due to the heterogeneous expression of methicillin resistance. On the other hand, PCR assays based on the detection of the *nuc* gene [9], which is responsible for the production of the thermostable nuclease of *S. aureus* and is not present in other staphylococcal species, and the *mecA* gene [10], which confers methicillin resistance in staphylococci, are reliable and specific but are too laborious and time-consuming to be performed on a routine basis. For these reasons, significant efforts have been made to develop alternative identification methods that combine speed and reliability of identification at a lower cost per sample.

FTIR spectroscopy is one of several whole-organism fingerprinting techniques whose potential as simple, rapid, and accurate methods for characterization and identification of microorganisms has recently been investigated. As illustrated in Figure 4.1, FTIR spectroscopy measures the vibrations of chemical bonds within all the biochemical constituents of cells, i.e., proteins, lipids, polysaccharides, and nucleic acids,

and thus provides quantitative information about the total biochemical composition of the intact whole microbial cell [11]. Furthermore, because the FTIR spectra of microorganisms consist of distinct and unique patterns that are highly reproducible, the spectra effectively serve as "fingerprints", allowing for their successful use in taxonomic discrimination [12]. FTIR spectroscopy has been demonstrated to be a highly sensitive and reproducible method for microbial analysis and process control [13] that provides rapid identification within 19 h, starting from a single colony, without the use of any reagents. This simple and nondestructive technique has also been shown to have sufficient resolving power for the detection of antibiotic resistance in clinical isolates [14-17]. For example, in our previous work, the discrimination of methicillin-resistant *S. aureus* (MRSA) from methicillin-sensitive *S. aureus* (MSSA) and even from borderline strains was achieved [17]. Based on these findings, the present study was undertaken to evaluate the potential use of FTIR spectroscopy for the discrimination of CNS from *S. aureus* (MRSA and MSSA) and of MRCNS from methicillin-sensitive CNS (MSCNS).

4.3 MATERIALS AND METHODS

4.3.1 Clinical specimens

A total of 72 clinical isolates, consisting of 22 coagulase-negative staphylococci and 50 strains of *S. aureus*, were selected for this study. Eleven MSCNS (*mecA*-negative) strains, consisting of *S. hemolyticus* (n=1), *S. epidermidis* (n=2), *S. warneri* (n=2), *S. saprophyticus* (n=2), *S. hominis* (n=1), *S. xylosus* (n=1), *S. schleiferi* (n=1), and *S. lugdunensis* (n=1), and 11 MRCNS (*mecA*-positive) strains, including *S. hemolyticus* (n=1), *S. capitis* (n=2), *S epidermidis* (n=4), *S. sciuri* (n=1), *S. hominis* (n=1), *S. simulans* (n=1), and *S. cohnii* (n=1), were obtained from the collection of the microbiology laboratory of the Sunnybrook & Women's College, Health Sciences Centre (Toronto, ON, Canada). Strains of MRSA (n=25) and MSSA (n=25) were obtained from the Royal Victoria Hospital (Montreal, PQ, Canada).

4.3.2 Microbiological methods

All CNS strains were identified using the API Staph ID 32 system (bioMérieux Inc., Marcy-l'Etoile, France). The MRSA-Screen™ (Denska-Seiken, Tokyo, Japan) latex

agglutination test, oxacillin susceptibility testing, and multiplex PCR assays for the simultaneous detection of the *mecA* and *nucA* gene sequences were performed as described below.

4.3.2.1 MRSA-Screen™ assay

The MRSA-Screen latex agglutination test for the detection of penicillin-binding protein PBP2a [18], the product of the *mecA* gene, was performed according to the manufacturer's instructions with one modification. A large "heaping" 1-μl-loopful of the test microorganism was used (approximately 30-50 colonies, depending on colony size) instead of the standard 1-μl-loopful and was emulsified in 4 drops of an extraction reagent and boiled for 3 min. After cooling to room temperature, 1 drop of a second extraction reagent was added and mixed. The suspension was then centrifuged at 1500 × g for 5 min. A 50-μl aliquot of the supernatant was added to each of two circles on a disposable test card and mixed with 1 drop of the anti-PBP2a monoclonal antibody-sensitized latex and 1 drop of the negative control latex, respectively. The samples were then mixed for 3 min on a shaker, and agglutination was observed visually. Any agglutination was considered positive for the presence of PBP2a [18].

4.3.2.2 Antimicrobial susceptibility testing

Antimicrobial susceptibility testing of isolates using an oxacillin agar screen (Mueller-Hinton agar supplemented with 4% NaCl and 6 μg/ml of oxacillin), disk diffusion, and broth microdilution were performed in accordance with current National Committee for Clinical Laboratory Standards (NCCLS) guidelines. E test (AB Biodisk, Solna, Sweden) oxacillin MIC determination was performed according to the manufacturer's instructions. Breakpoint MIC testing using Vitek GPS-SV and GPS-107 (bioMérieux Inc., Hazelwood, MO) susceptibility cards was performed as per manufacturer's instructions.

4.3.2.3 Multiplex polymerase chain reaction (PCR)

Multiplex PCR assays were performed for the detection of the *nuc* gene for the differentiation of CNS from *S. aureus* and the *mecA* gene encoding for methicillin resistance in staphylococci. Bacterial DNA was extracted using two to three colonies of a test organism grown on 5% sheep blood agar plate and then boiled for 10 min in 100 µl of Triton X-100 lysis buffer (100 mM NaCl, 10 mM Tris-HCl [pH 8], 1 mM EDTA [pH 9], and 1% Triton X-100). The suspension was cooled at room temperature for 5 min and centrifuged at 14,000 rpm for 1 min. With the use of 1 µl of the supernatant as template. PCR was performed in a 25-µl volume, with 1×PCR buffer containing 10 mM Tris–HCl [pH 8.3], 50 mM KCl, 1.5 mM $MgCl_2$, 200 µM concentrations of each deoxynucleoside triphosphate, 2.5 U of *Taq* polymerase, and 0.2 µM concentrations of each primer (*mecA*1: AAA ATC GAT GGT AAA GGT TGG C. *mecA*2: AGT TCT GCA GTA CCG GAT TTG C. *nucA*1: GCG ATT GAT GGT GAT ACG GTT. *nucA*2: AGC CAA GCC TTG ACG AAC TAA AGC). Thermocycling conditions in a Gene-Amp 9600 thermocycler (PE Biosystems, Mississauga, ON, Canada) were as follows: 94 °C for 2 min followed by 30 cycles of 94 °C for 1 s and 55 °C for 15 s, with a final 10-min extension at 72 °C. The control organisms included *S. aureus* ATCC 25923 and *S. epidermidis* ATCC 12228. Electrophoresis at 100 V for 40 min was performed to separate the products on 1% 1× TBE (8.9 M boric acid and 0.2 M EDTA) agarose gels. Gels were stained with ethidium bromide and photographed under UV illumination.

4.3.3 FTIR spectroscopic methods

4.3.3.1 Sample preparation

All bacterial strains were grown from frozen stocks, kept at –70 °C in brain heart infusion (BHI) broth containing 15% glycerol, by overnight subculture on tryptic soy with sheep blood agar (Quelab Laboratories Inc., Montreal, PQ, Canada) at 37 °C. A single bacterial colony was then collected from the agar plate and cultured on Universal Medium (UM™) agar (Quelab Laboratories Inc., Montreal, PQ, Canada) for 18 h at 37 °C. Four loops-full of stationary-phase cells were then carefully collected from four different culture plates on UM™ using a 10-mm-diameter loop and suspended in 200-µl

aliquots of sterile physiological saline (0.9% NaCl). A 25-μl aliquot of the 10-fold diluted bacterial suspension, containing approximately 5×10^{11} cells ml^{-1}, was deposited onto a zinc selenide (ZnSe) optical window and then oven-dried at 48 °C for 1 hour to form a thin and transparent homogeneous dried film suitable for FTIR measurements.

4.3.3.2 Spectral acquisition

All FTIR spectra were acquired in the transmission mode using a Bomem MB-104 (ABB-Bomem, Quebec, PQ, Canada) FTIR spectrometer equipped with a deuterated triglycine sulfate (DTGS) detector and a KBr beamsplitter and operating under Bomem-Grams/386 software (Galactic, Salem, NH). The spectrometer was purged with dry, CO_2-free air from a Balston dryer (Balston, Lexington, MA) to minimize interferences from atmospheric water vapor and CO_2. To enhance the signal-to-noise ratio, 64 scans were co-added at 4 cm^{-1} resolution over the wavenumber range of 4000-400 cm^{-1} and ratioed against an open-beam background to produce an absorbance spectrum. For each strain, spectra were recorded in quadruplicate by depositing samples from four different culture plates on four different optical windows.

4.3.4 Mathematical preprocessing and processing

Spectral data (acquired in Grams SPC format) were converted into comma-separated values (CSV) files and then into MATLAB files by MATLAB version 5.1 (The MathWorks, Inc. Natick, MA). Spectra over the whole spectral range (4000-400 cm^{-1}) were normalized to unit height by vector transformation and were transformed to first-derivative spectra using the Savitzky-Golay algorithm to maximize peak separation, enhance apparent resolution, and minimize problems arising from baseline shifts [19]. Prior to data processing, spectral feature selection was performed using the singular-value decomposition (SVD) algorithm. Exploratory data analysis was performed using principal component analysis (PCA) based on the nonlinear iterative partial least squares (NIPALS) algorithm and self-organizing maps (SOM) clustered by the *k*-means algorithm. Cluster analysis of spectral data was accomplished using the K-nearest neighbors (KNN) algorithm. Programs were written in MATLAB version 5.1 to implement the data preprocessing and processing algorithms.

4.4 RESULTS

4.4.1 Classification strategy

The strategy employed to evaluate the potential utility of FTIR spectroscopy for the rapid and accurate identification of CNS and MRCNS strains involved three stages:

- Discrimination between 50 coagulase-positive (*S. aureus*) and 22 coagulase-negative staphylococci (CNS) strains
- Discrimination between 22 CNS, 25 MRSA, and 25 MSSA strains
- Discrimination between 11 MSCNS and 11 MRCNS strains

In each case, three chemometric techniques (PCA, SOM, and KNN) were employed to examine the clustering of the different phenotypes of staphylococci based on the similarity of their FTIR spectra in narrow spectral regions selected by the application of SVD to individual pairs of spectra.

4.4.2 Discrimination between *S. aureus* and CNS species

4.4.2.1 Spectral region selection

The capability of an FTIR-based method to differentiate between *S. aureus* and CNS was investigated with the use of a set of 288 spectra, comprising four replicate spectra of each of 25 MSSA, 25 MRSA, 11 MSCNS, and 11 MRCNS isolates. Regions for the classification of *S. aureus* and CNS were selected by applying the SVD algorithm to the spectral data for three randomly chosen *S. aureus*/CNS pairs. Based on this analysis, the single narrow region of 1442-1439 cm^{-1}, in which spectral differences between the *S. aureus* and CNS isolates could be visually discerned (Figure 4.2), was selected.

4.4.2.2 Principal component analysis (PCA)

PCA was performed on the data in the region 1442-1439 cm^{-1} using the complete data set of 288 spectra, transformed to first-derivative spectra. A plot of the first two PC scores (PC1 versus PC2) showed two distinct clusters (Figure 4.3), representing complete separation of *S. aureus* from CNS. Accordingly, the spectral data in this very narrow

region were sufficient to allow 100% differentiation between *S. aureus* and CNS isolates by PCA.

4.4.2.3 Self-organizing map (SOM)

The first and second PC scores were utilized as input data to generate an SOM of size [18×5]. A rough training phase of 4 epochs and a fine-tuning phase of 13 epochs resulted in a final quantization error of 0.137 and a final topographic error of 0.034. Visual examination of the SOM indicated two distinct clusters (Figure 4.4). The number of clusters was confirmed by partitioning of the map with the use of the *k*-means algorithm and calculation of the Davies-Bouldin index (Figure 4.5). The labeled SOM in Figure 4.4 shows 100% correct classification of the CNS and *S. aureus* isolates, as in the case of PCA.

4.4.2.4 K-Nearest neighbors (KNN) algorithm

Supervised cluster analysis using the KNN algorithm was performed on the spectral data in the 1442-1439 cm^{-1} region, employing half of the data set (n = 144) as a training set and the other half as a prediction set. All test points were correctly classified, with K= 4. Hence, the results obtained by PCA, SOM, and KNN all demonstrate that the spectral region between 1442 and 1439 cm^{-1} is highly sensitive and selective for the differentiation between *S. aureus* and CNS (Table 4.1).

4.4.3 Discrimination of CNS species from MRSA and MSSA strains

The same data set of 288 spectra employed in the previous stage of the classification strategy was used to investigate the possibility of classifying staphylococcal isolates as CNS, MSSA, or MRSA in a single step, i.e., without their prior classification as CNS or *S. aureus*. For this investigation, the spectral data in the region 1442-1439 cm^{-1} were combined with those from three spectral regions that were successfully employed in previous work [17] for differentiation between MRSA and MSSA (1080-1050, 1732-1709, and 2969-2958 cm^{-1}). The following results were obtained by analysis of the combined spectral data for these four regions.

4.4.3.1 Principal component analysis (PCA)

PCA was performed on the transformed (normalized and first-derivative) spectral data in the combined regions of 1080-1050, 1442-1439, 1732-1709, and 2958-2969 cm^{-1}. Figure 4.6 presents the scores plot for PC1 versus PC2, which clearly shows three clusters corresponding to MRSA, MSSA, and CNS. However, two CNS strains fall in the MSSA cluster, and four MSSA and four MRSA strains were misclassified as MRSA and MSSA, respectively, yielding an overall correct classification rate of 87%.

4.4.3.2 Self-organizing map (SOM)

The first and second PC scores were utilized as input data to generate an SOM of size [13×7]. A rough training phase of 4 epochs and a fine-tuning phase of 13 epochs resulted in a final quantization error of 0.166 and a topographic error of 0.027. Three distinct clusters were discerned by visual examination of the map (Figure 4.7); however, when the *k*-means algorithm was applied to partition the map, the Davies-Bouldin index indicated four clusters instead of the expected three clusters.

4.4.3.3 K-Nearest neighbors (KNN) algorithm

Supervised cluster analysis using the KNN algorithm was performed using half of the data set as a training set (n = 144) and the other half as a prediction set. The highest number of correctly classified test points (92%) was obtained with K= 1. Thus, the performance of the KNN algorithm was superior to that of PCA, and all CNS isolates were correctly classified. However, three MSSA and three MRSA strains were misclassified.

4.4.4 Discrimination between MSCNS and MRCNS strains

A data set of 88 spectra, consisting of four replicate spectra of 11 MSCNS and 11 MRCNS isolates, was used in this stage of the study. Based on the application of SVD to randomly chosen spectral pairs, four spectral regions of potential utility for the discrimination between MSCNS and MRCNS were selected: 2880-2860, 1479-1475, 1403-1393, and 1380-1375 cm^{-1}.

4.4.4.1 Principal component analysis (PCA)

A plot of the scores of the first two PCs (PC1 and PC2) for the normalized and first-derivatized data in the spectral region between 1403 and 1393 cm^{-1} showed partial clustering of the MRCNS and MSCNS isolates (Figure 4.8). Three MRCNS isolates were within the MSCNS cluster and three MSCNS isolates were within the MRCNS cluster, yielding a correct classification rate of only 73%. The use of the 2880-2860 cm^{-1} region in place of the 1403-1393 cm^{-1} region improved the rate of correct classification, with only two misclassified MRCNS isolates. With the use of the combined data from two regions (1380-1375 and 1479-1475 cm^{-1}), a single MRCNS isolate was misclassified. The use of other combinations of the spectral regions did not increase the rate of correct classification by PCA.

4.4.4.2 Self-organizing map (SOM)

Exploratory analysis using the SOM algorithm was investigated for the discrimination of MRCNS from MSCNS based on the use of the scores of the first three PCs from the spectral regions employed above. A better organization of the map units into two clusters was obtained by using the spectral region 1403-1393 cm^{-1} than the combined regions of 1380-1375 and 1479-1475 cm^{-1} or the single region 2880-2860 cm^{-1}. For the optimal spectral region (1403-1393 cm^{-1}), the [8 × 6] map was trained using a rough training phase of 6 epochs and a fine-tuning phase of 22 epochs with a final quantization error of 0.522 and topographic error of 0.0001, yielding two distinct clusters. However, application of the *k*-means algorithm and the Davies-Bouldin index failed to partition the map into two clusters of MRCNS and MSCNS.

4.4.4.3 K-Nearest neighbors (KNN) algorithm

The KNN algorithm was employed for cluster analysis of the spectral data from the four spectral regions examined in the exploratory data analysis described above. Half of the 88 spectra were put into the training set, and the rest into the prediction set. The rate of correct classification was evaluated by comparing the actual to the predicted category for the spectra in the prediction set. For the region between 1403 and 1393 cm^{-1},

the highest rate of correct classification was 73%, obtained with K = 1. In this case, three strains each of MRCNS and MSCNS were misclassified. The use two combined spectral regions (1380-1375 and 1479-1475 cm^{-1}) improved the rate of classification to 83% (with K = 1), with two misclassified MSCNS and two misclassified MRCNS strains. The best rate of correct classification (92%) was achieved by using the spectral data from the region between 2880 and 2860 cm^{-1} with K = 1. All MRCNS isolates were correctly classified, and only two MSCNS isolates were misclassified.

4.5 DISCUSSION

As stated in previous studies [12,17,20], correct classification of microorganisms by FTIR spectroscopy cannot be expected to be achieved if the variance within spectra of the same taxon is greater than the variance among spectra of different taxa. The FTIR spectra of microorganisms are highly influenced by the plating methods employed in growing the bacteria (growth conditions, growth media), spectral artifacts (incomplete baseline correction, instrumental noise), and sample-associated factors, such as variations in sample thickness and particle size. Thus, a standard procedure has been established in our laboratory to minimize these sources of variation and optimize spectral reproducibility in order to enhance the potential for accurate classification [17]. This procedure includes the use of a single growth medium (UM™) with a defined biochemical composition and rigorously controlled culture conditions. For FTIR spectral acquisition, a diluted drop of each sample (with approximately comparable concentration of bacteria in saline solution) was deposited on the dry polished surface of a ZnSe optical window of fixed diameter to yield a constant film thickness. The FTIR spectra obtained by this procedure in the present study were considered reproducible as assessed by the consistency between the relative peak intensities. Variations in absolute peak intensities resulting from minor differences in film thickness among replicate samples were minimized using peak height normalization. All spectra were subsequently transformed to their first-order spectral derivatives using the Savitzky-Golay algorithm, in order to delineate subtle changes in absorption bands and to correct for baseline shifts. Both of these preprocessing tools have been widely used in previous studies on the classification of microorganisms by FTIR spectroscopy [12,21,22].

The evaluation of an FTIR-based method for the accurate differentiation of CNS and *S. aureus* was investigated using PCA and SOM as exploratory data analysis tools and supervised cluster analysis based on the KNN algorithm. The search for spectral regions that could be suitable for differentiation between the two groups of staphylococci was carried out by visual inspection aided by the use of the SVD algorithm. Differences between typical spectra of CNS and *S. aureus* were readily discerned between 1442 and 1439 cm^{-1} (Figure 4.2), and the data in this single narrow spectral region were found to be appropriate for the differentiation between CNS and *S. aureus*. The discrimination of a small number of *S. aureus* isolates from CNS strains as well as *Streptococcus* and *Clostridium* species was reported previously based on the use of the combined data in three broad spectral regions (3000-2800, 1200-900, and 900-700 cm^{-1}) [24]. However, the use of narrow spectral regions has been found to be optimal in the discrimination between closely related bacteria, and, in the present work, it was demonstrated that the data from a single, very narrow region was highly effective for discrimination between CNS and *S. aureus*. Furthermore, the use of this region in combination with other regions, in an attempt to discriminate among CNS, MRSA, and MSSA, resulted in some misclassification of CNS isolates as *S. aureus* by PCA. This result highlights the importance of optimal region selection and the superiority of a hierarchical classification strategy, involving classification of isolates as CNS or *S. aureus* prior to differentiation between MRSA and MSSA. Finally, differentiation between methicillin-resistant and methicillin-sensitive CNS by FTIR spectroscopy was investigated for the first time. The most promising region for differentiation between the two groups was 2880-2860 cm^{-1}, with application of the KNN algorithm to the data in this region yielding 92% correct classification with no false negatives. The selection of additional or alternative spectral regions by the use of more sophisticated region selection tools, such as genetic algorithms, should be investigated to improve the rate of correct classification.

4.6 CONCLUSION

This study indicates that FTIR spectroscopy combined with the use of a universal growth medium is a rapid and simple method for the differentiation between *S. aureus* and CNS, yielding 100% correct classification of 50 *S. aureus* and 22 CNS isolates. In

addition, FTIR spectroscopy may be considered a promising tool for the differentiation between MSCNS and MRCNS.

Acknowledgments

We thank Quelab Laboratories Inc. for supporting the project and the Canadian Nosocomial Infection Surveillance Program (CNISP) for participating in this research.

4.7 REFERENCES

1. Grosserode, M.H., and R.P. Wenzel, 1991. The continuing importance of staphylococci as major hospital pathogens. *J. Hosp. Infect.* 19 (Suppl. B):3-17

2. Archer, G.L., and M.W. Climo, 1994. Antimicrobial susceptibility of coagulase-negative staphylococci. *Antimicrob. Agents Chemother.* 38:2231-2237

3. Tomasz, A., 1994. Multiple antibiotic resistant pathogenic bacteria. *N. Engl. J. Med.* 330:1247-1251

4. Grant, C.E., D.L. Sewell, M. Pfaller, R.V. Bumgardner, and J.A. Williams, 1994. Evaluation of two commercial systems for identification of coagulase-negative staphylococci to species level. *Diagn. Microbiol. Infect. Dis.* 18:1-5

5. Ieven M., J. Verhoeven, S.R. Pattyn, and H. Goossens, 1995. Rapid and economical method for species identification of clinically significant coagulase-negative staphylococci. *J. Clin. Microbiol.* 33:1060-1063

6. Perl, T.M., P.R. Rhomberg, M.J. Bale, P.C. Fuchs, R.N. Jones, F.P. Koontz, and M.A. Pfaller, 1994. Comparison of identification systems for *Staphylococcus epidermidis* and other coagulase-negative *Staphylococcus* species. *Diagn Microbiol. Infect. Dis.* 18:151-155

7. Renneberg, J., K. Rieneck, and E. Gutschik, 1995. Evaluation of Staph ID 32 system and staph-Zym system for identification of coagualse-negative staphylococci. *J. Clin. Microbiol.* 33:1150-1153

8. York, M.K., L. Gibbs, F. Chehab, and G.F. Brooks, 1996. Comparison of PCR detection of *mec A* with standard susceptibility testing methods to determine methicillin-resistance in coagulase-negative staphylococci. *J. Clin. Microbiol.* 34:249-253

9. Brakstad, O.G., K. Aasbakk, and J.A. Maeland, 1992. Detection of *Staphylococcus aureus* by PCR amplification of the *nuc* gene. *J. Clin. Microbiol.* 30:1654-1660

10. Murakami, K., W. Minamide, K. Wada, N. Nakamura, H. Teraoka, and S. Watanabe, 1991. Identification of methicillin-resistant staphylococci by polymerase chain reaction. *J. Clin. Microbiol.* 29:2240-2244

11. Naumann, D., D. Helm, and H. Labischinski, 1991. Microbiological characterization by FT-IR spectroscopy. *Nature* 351:81-82

12. Naumann, D., D. Helm, H. Labischinski, and P. Giesbrecht, 1991. The characterization of microorganisms by Fourier-transform infrared spectroscopy, *in* W.H. Nelson (ed.), *Modern Techniques for Rapid Microbiological Analysis*. New York: VCH Publishers. p. 43.

13. Mariey, L., J.P. Signolle, C. Amiel, and J. Travert, 2001. Discrimination, classification, identification of microorganisms using FTIR spectroscopy and chemometrics. *Vibr. Spectrosc.* 26:151-159

14. Bouhedja, W., G.D. Sockalingum, P. Pina, P. Allouch, C. Bloy, R. Labia, J.M. Millot, and M. Manfait, 1997. ATR-FTIR spectroscopy investigation of *E. coli* transconjugants β-lactams-resistance phenotype. *FEBS Lett.* 412:39-42

15. Kirschner C., Ngoc Anh Ngo Thi, and D. Naumann, 1999. FT-IR spectroscopic investigations of antibiotic sensitive and resistant microorganisms. *2nd Workshop on FT-IR Spectroscopy in Microbiology and Medical Diagnostics*. Robert Koch-Institute, Berlin

16. Sockalingum, G.D., W. Bouhedja, P. Pina, P. Allouch, C. Mandray, R. Labia, J.M. Millot, and M. Manfait 1997. ATR-FTIR spectroscopic investigation of imipenem-susceptible and -resistant *Pseudomonas aeruginosa* isogenic strains. *Biochem. Biophys. Res. Commun.* 232:240-246

17. Amiali, M.N., B. Berger-Bächi, K. Ehlert, M.R. Mulvey, A.A. Ismail, J. Sedman, and A.E. Simor, 2003. Rapid identification of methicillin-resistant *Staphylococcus aureus* (MRSA) by Fourier transform infrared (FTIR) spectroscopy. *Submitted*

18. Louie, L., A. Majury, J. Goodfellow, M. Louie, and A.E. Simor, 2001. Evaluation of a latex agglutination test (MRSA-Screen) for detection of oxacillin resistance in coagulase-negative staphylococci. *J. Clin. Microbiol.* 39:4149-4151

19. Savitzky, A., and M.J.E. Golay, 1964. Smoothing and differentiation of data by simplified least squares procedures. *Anal. Chem.* 36:1627-1633

20. Kansiz, M., P. Heraud, B. Wood, F. Burden, J. Beardall, and D. McNaughton, 1999. Fourier transform infrared microspectrometry and chemometrics as a tool for the discrimination of cyanobacterial strains. *Phytochemistry* 52:407-417

21. Curk, M.C., F. Peladan, and J.C. Hubert, 1994. Fourier transform infrared (FTIR) spectroscopy for identifying *Lactobacillus* species. *FEMS Microbiol. Lett.* 123:241-248

22. Goodacre, R., E.M. Timmins, P.J. Rooney, J.J. Rowland, and D.B. Kell, 1996. Rapid identification of *Streptococcus* and *Enterococcus* species using diffuse reflectance-absorbance Fourier transform infrared spectroscopy and artificial neural networks. *FEMS Microbiol. Lett.* 140:233-239.

23. Davies, D.L., and D.W. Bouldin, 1979. A cluster separation measure. *IEEE Trans. Patt. Anal. Machine Intell.*, Vol. PAMI-1, pp. 224-227

24. Helm, D., H. Labischinski, G. Schallehn, and D. Naumann, 1991. Classification and identification of bacteria by Fourier transform spectroscopy. *J. Gen. Microbiol.* 137:69-79

Table 4. 1. Percentage of correct classification of the three categories of species employing three different chemometric methods and obtained using regions selected by SVD

Species differentiated	**Spectral region (s) (cm^{-1})**	**Percent correct classification**		
		PCA	SOM*	KNN
S. aureus vs. CNS	1442-1439	100	100	100
CNS vs. MRSA vs. MSSA	1080-1050 1442-1439 1732-1709 2969-2958	87	<70	92
MRCNS vs. MSCNS	2880-2860	78	<70	92

*Based on clustering of the SOM with the *k*-means algorithm and the Davies-Bouldin index.

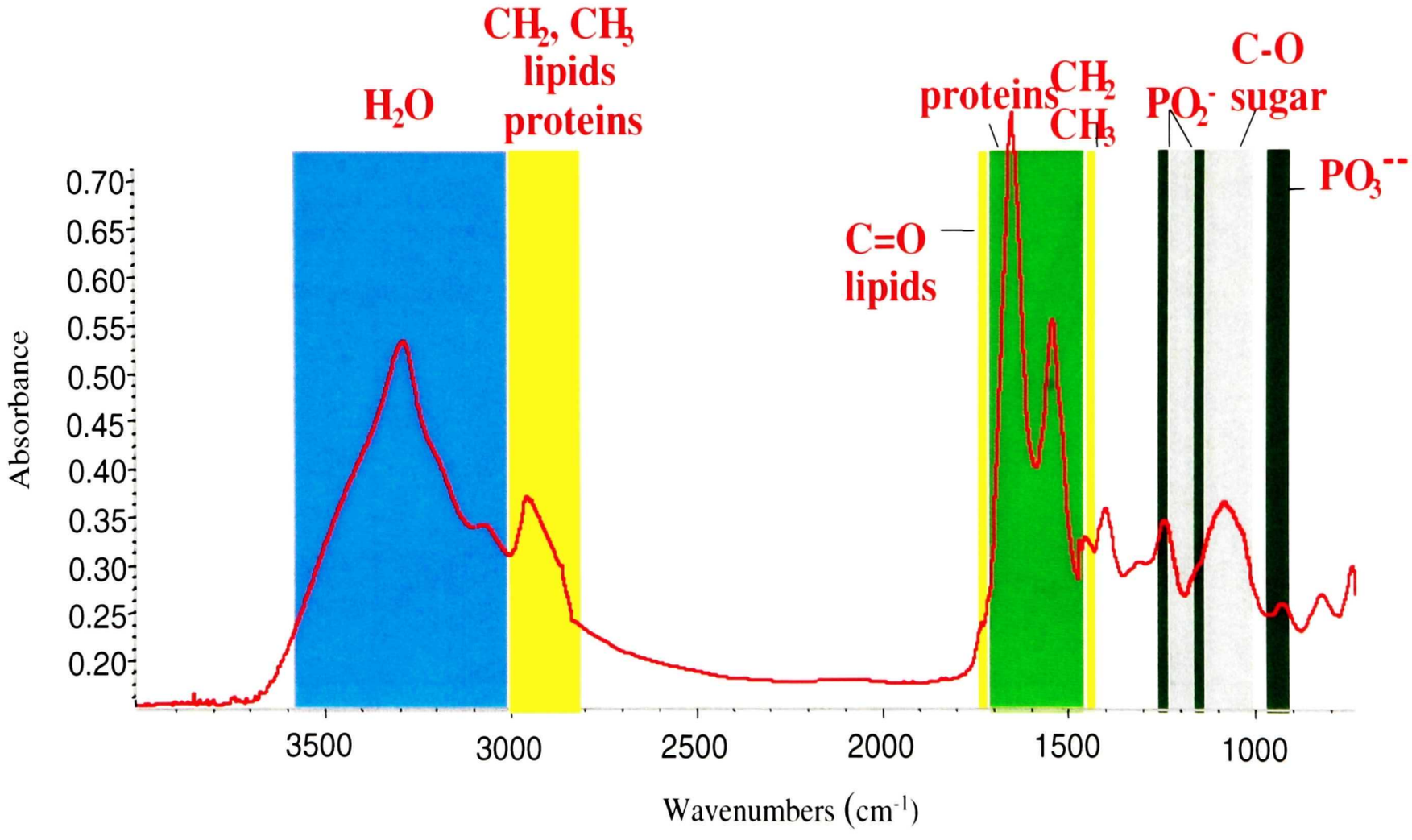

Figure 4.1: Typical FTIR spectrum of bacteria cells

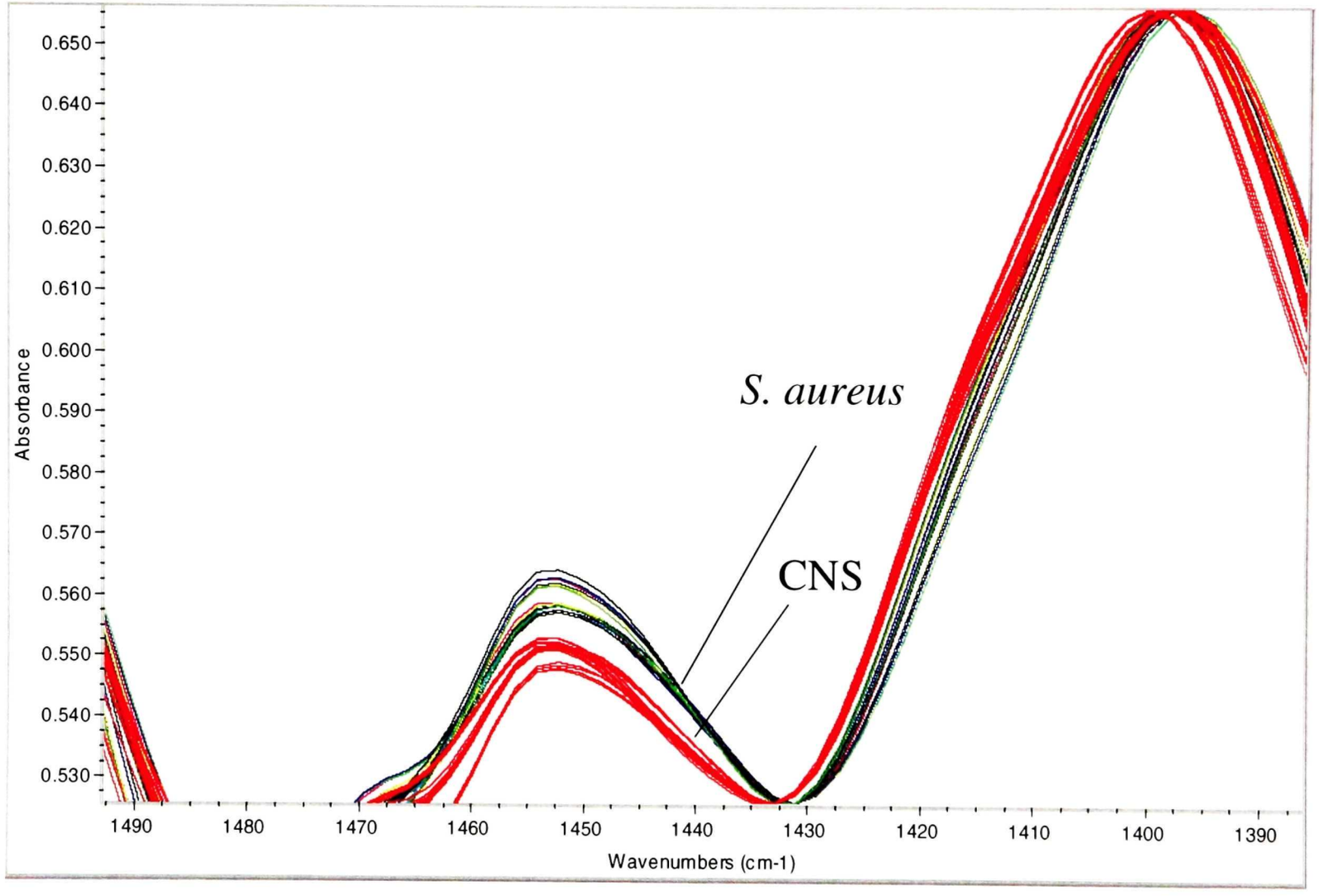

Figure 4.2: FTIR spectra of *S. aureus* and CNS strains in the region 1490-1390 cm^{-1}

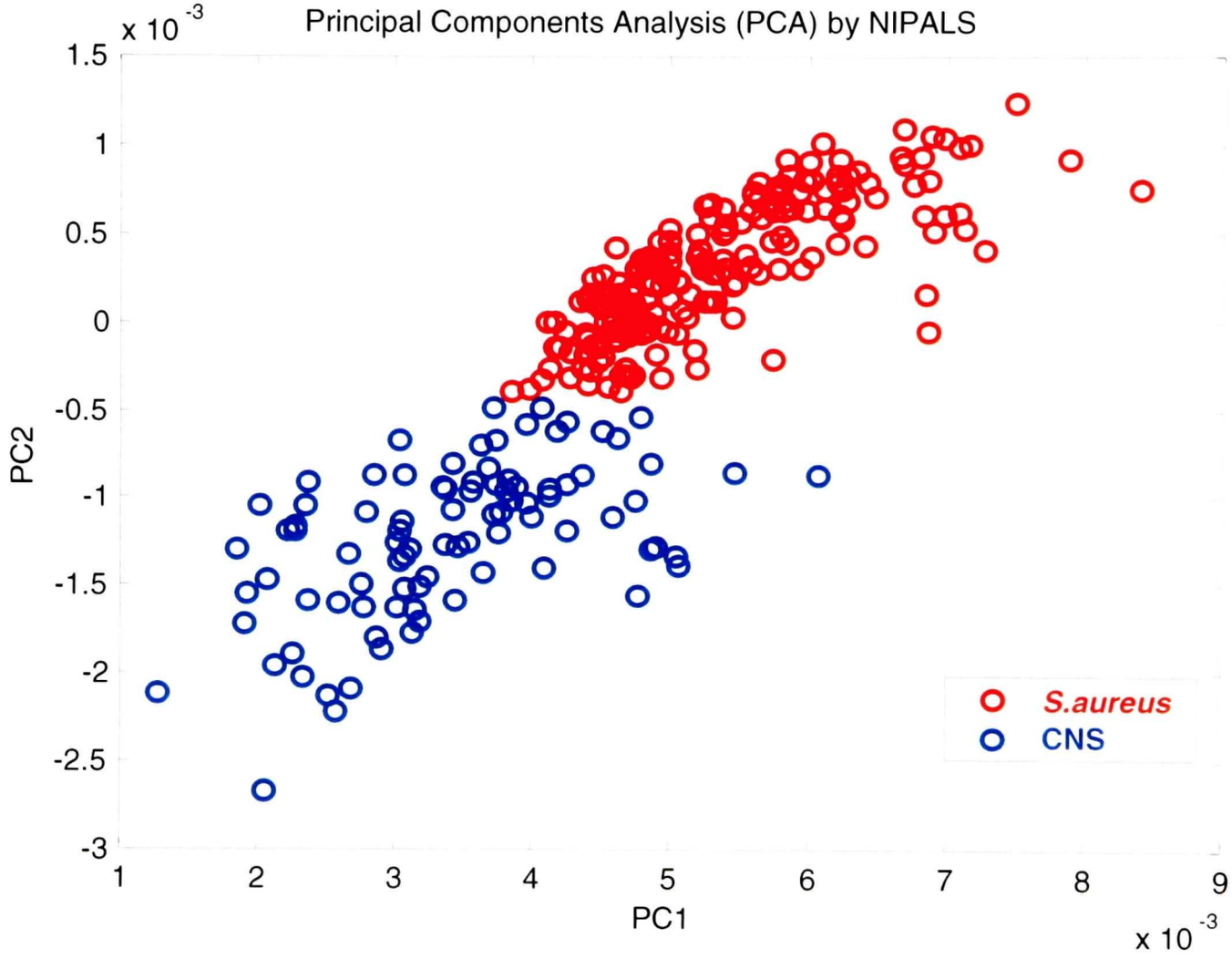

Figure 4.3: Scores plot for first two PCs obtained from the spectral data for 50 *S. aure*us and 22 CNS strains in the region 1442-1439 cm^{-1} by PCA using the NIPALS algorithm

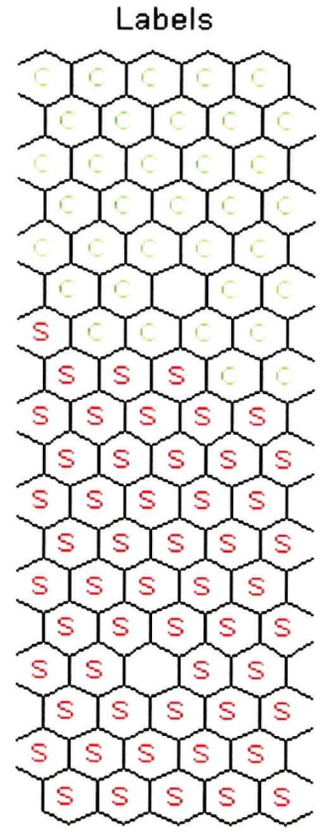

Figure 4.4: SOM obtained using the spectral data for 50 *S. aure*us (S) and 22 CNS (C) strains in the region 1442-1439 cm^{-1}

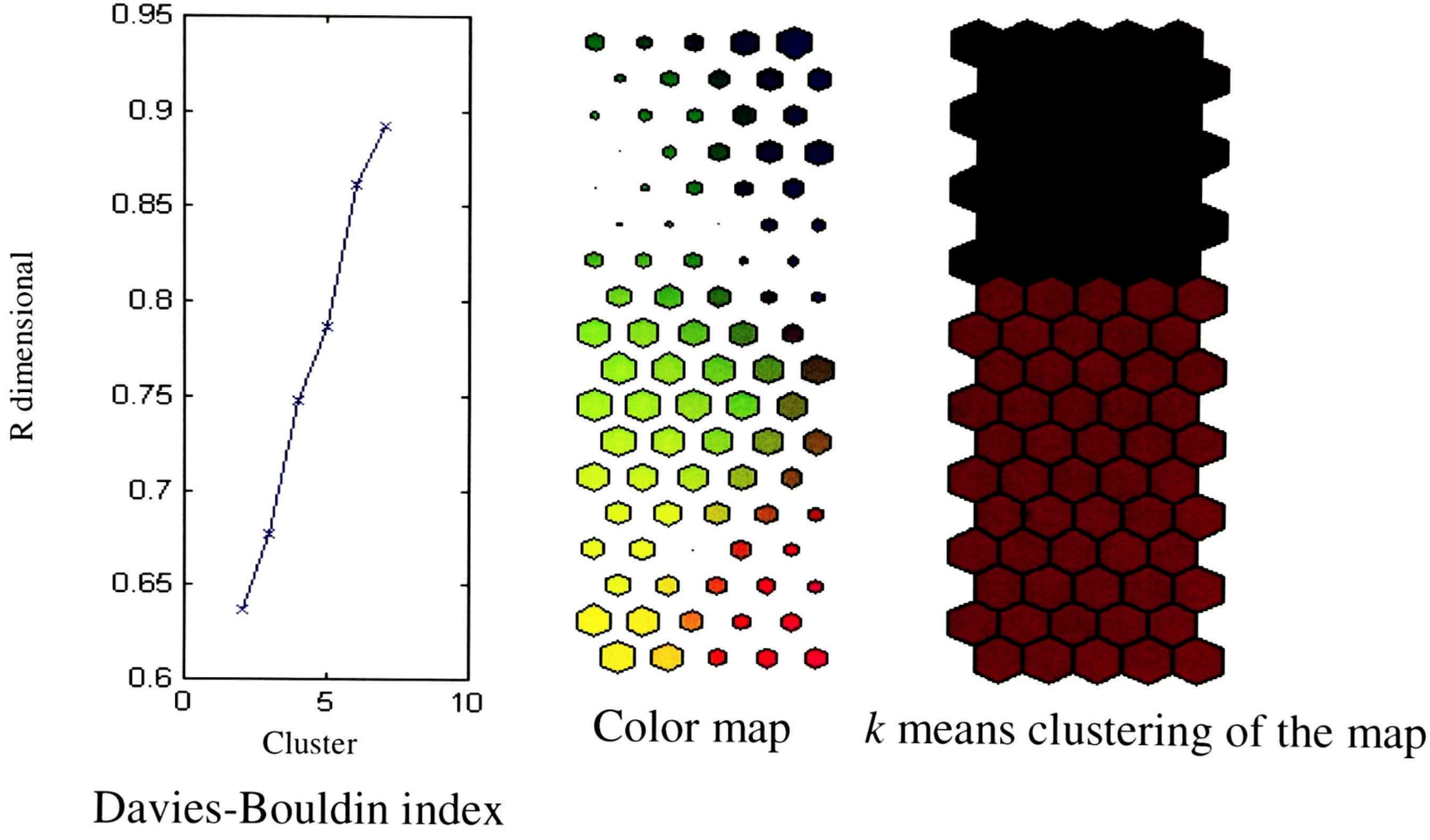

Figure 4.5: Partitioned SOM for the spectral data in the region 1442-1439 cm^{-1} obtained by applying the *k*-means algorithm and the Davies-Bouldin index

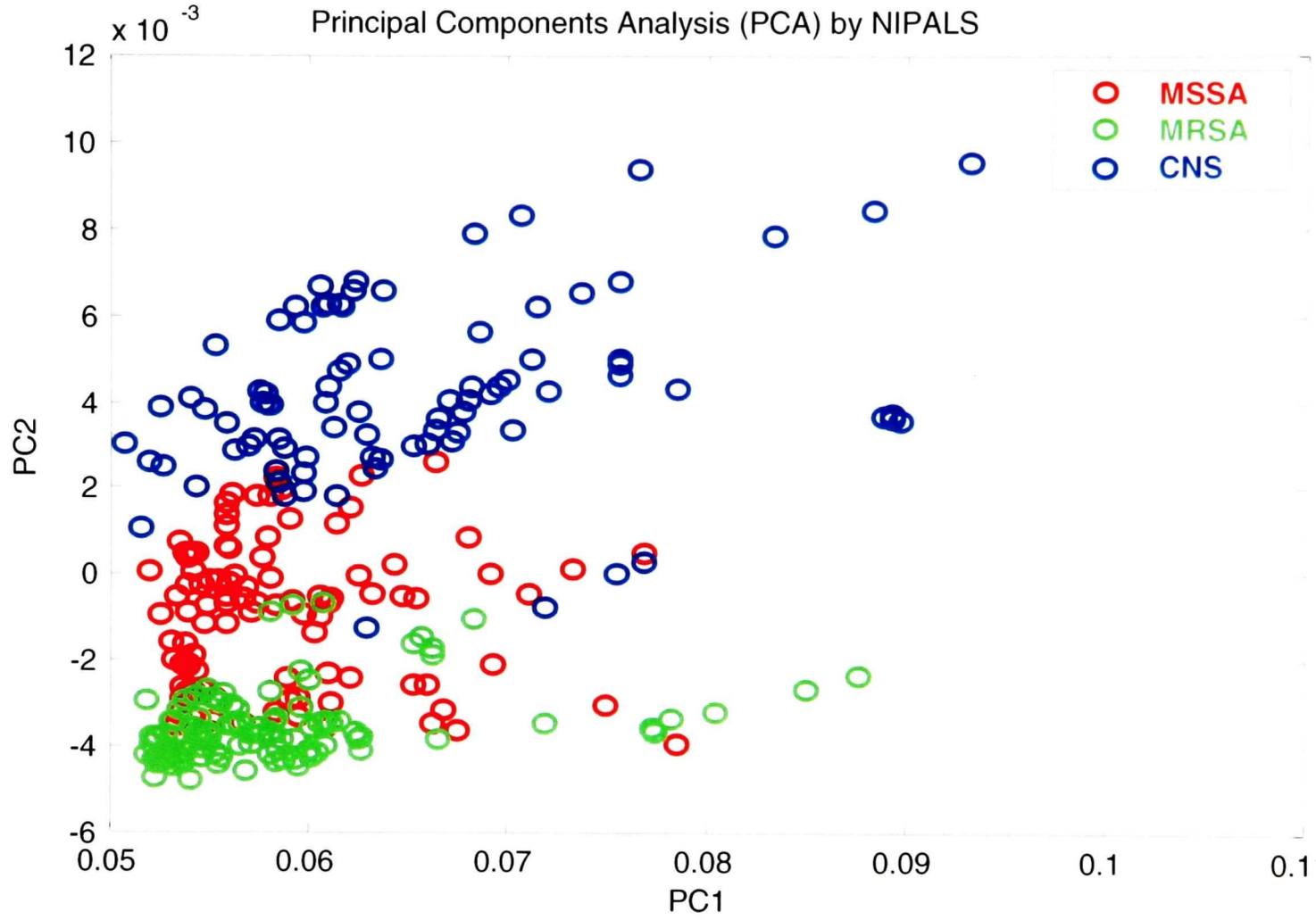

Figure 4.6: Scores plot for first two PCs obtained from the spectral data for 22 CNS, 25 MRSA and 25 MSSA strains in the regions 1080-1050,1442-1439, 1732-1708, and 2969-2958 cm^{-1} by PCA using the NIPALS algorithm

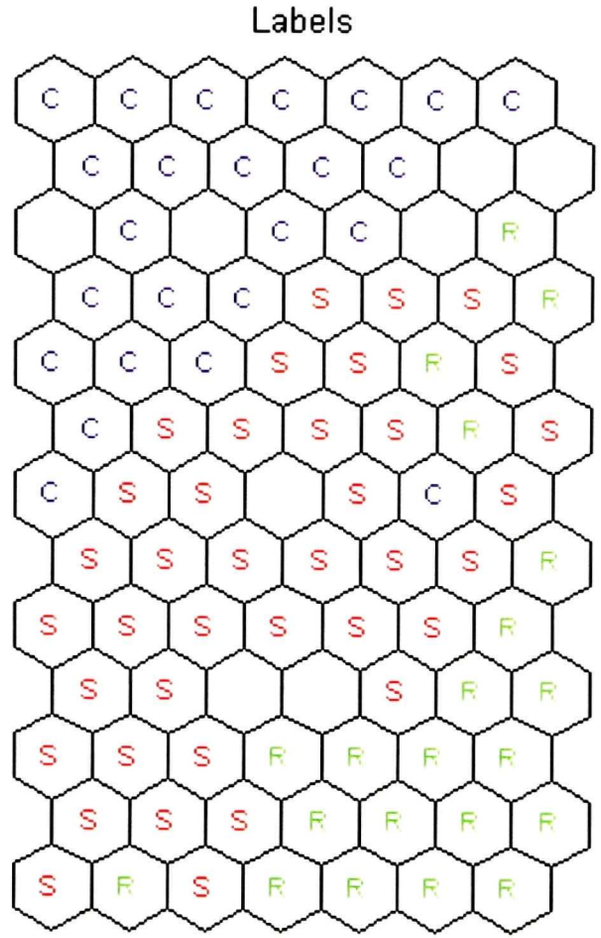

Figure 4.7: SOM obtained using the spectral data for 22 CNS (C), 25 MRSA (R) and 25 MSSA (S) strains in the regions 1080-1050, 1442-1439, 1732-1708, and 2969-2958 cm^{-1}

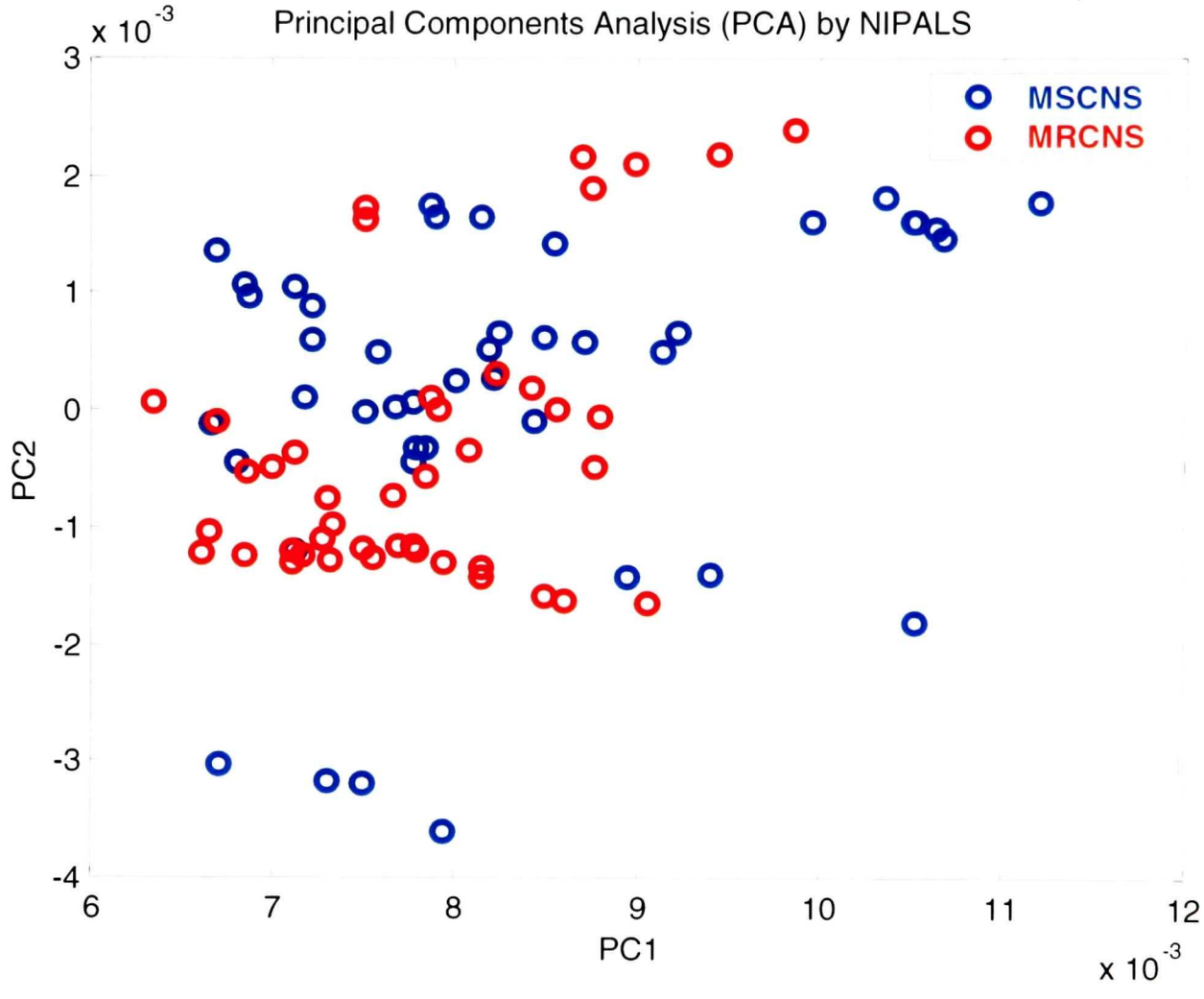

Figure 4.8: Scores plot for first two PCs obtained from the spectral data for 11 MRCNS and 11 MSCNS strains in the region 2880-2860 cm^{-1} by PCA using the NIPALS algorithm

CHAPTER 5

CONNECTING STATEMENT

In Chapters 3 and 4, research on the discrimination of methicillin-resistant *S. aureus* (MRSA) from methicillin-sensitive *S. aureus* (MSSA) and borderline oxacillin-resistant *S. aureus* (BORSA) strains and from coagulase-negative (CNS) species as well as for the discrimination of methicillin-resistant CNS from methicillin-sensitive CNS strains was presented. In view of the increasing emergence of MRSA with reduced susceptibility to glycopeptides such as vancomycin, which is the antibiotic of choice for treatment of MRSA, further research on the capability of FTIR spectroscopy for the detection of glycopeptide-intermediate *S. aureus* strains among MRSA strains was conducted and is described in the following chapter.

CHAPTER 5

EVALUATION OF FOURIER TRANSFORM INFRARED (FTIR) SPECTROSCOPY FOR THE RAPID IDENTIFICATION OF GLYCOPEPTIDE-INTERMEDIATE *STAPHYLOCOCCUS AUREUS* (GISA)

5.1 ABSTRACT

Methicillin-resistant *Staphylococcus aureus* (MRSA) isolates with reduced susceptibility to glycopeptides (vancomycin or teicoplanin), so-called GISA, have emerged with increasing frequency, making therapy for staphylococcal infections more difficult. Rapid and reliable identification of GISA and heterogeneous-GISA (h-GISA) strains by a single-step assay is of utmost importance for the prediction of inefficacy of glycopeptide treatment at normal dosage levels and prevention of emergence of GISA. However, GISA and h-GISA strains are difficult to detect by conventional routine diagnostic assays. FTIR spectroscopy was investigated as a rapid and accurate single-step method to identify 35 GISA and h-GISA strains from the Network on Antimicrobial Resistance in *Staphylococcus aureus* (NARSA) collection and to distinguish these 35 strains from 22 sporadic MRSA (SMRSA) and 25 Canadian epidemic MRSA (CMRSA) strains. Principal component analysis (PCA), self-organizing maps (SOM), and the K-nearest neighbor (KNN) algorithm were employed to cluster the GISA/h-GISA and MRSA strains based on the FTIR spectral data obtained from dried films of stationary-phase cells grown on a universal growth medium (UM™). PCA and SOM plots obtained for the GISA/h-GISA and CMRSA strains by employing the first-derivative normalized spectral data from either of two narrow regions of the IR spectrum (1352-1315 cm^{-1} and 1480-1460 cm^{-1}) showed two distinct clusters, the first region allowing for 99% correct classification and the second for 96% correct classification of GISA/h-GISA and CMRSA strains. However, the spectral data from only one of these regions (1480-1460 cm^{-1}) was appropriate for the discrimination of GISA/h-GISA strains from SMRSA as well as CMRSA strains, yielding a correct classification rate of 92%. Thus, FTIR spectroscopy may provide a means for the rapid and accurate identification of GISA and h-GISA among MRSA species.

5.2 INTRODUCTION

Methicillin-resistant *S. aureus* (MRSA) is one of the most common pathogens responsible for community-acquired and nosocomial infections worldwide, causing high morbidity and mortality. Over the past three decades, glycopeptides (teicoplanin and vancomycin) have been considered the antibiotics of choice for the treatment of MRSA infections. However, in recent years, the emergence of clinical isolates of MRSA with reduced susceptibility to glycopeptides (teicoplanin MIC 8-16 μg/ml and vancomycin MIC ≥8 μg/ml), so-called GISA, has been increasing [1]. Therefore, a convenient method for routine screening of GISA strains is of critical importance for the prediction of inefficacy of glycopeptide treatment at normal dosage levels and the institution of key measures for the prevention of the emergence of GISA strains.

Since the mechanisms of glycopeptide resistance in *S. aureus* strains are not completely elucidated, the detection of glycopeptide resistance in *S. aureus* strains continues to rely mainly on susceptibility testing methods. Efficient detection of GISA strains by routine diagnostic assays [2] is often difficult due to the low levels of glycopeptide resistance of the heterogeneous phenotypes within GISA (h-GISA: vancomycin MIC of 1-4 μg/ml and teicoplanin MIC of 16 μg/ml [2], with resistant subpopulations that can grow in the presence of >4 μg/ml vancomycin being present at a frequency of 10^{-6}) [1]. It has been suggested that h-GISA strains are best detected and quantified by means of population analysis [1], a method unsuited to routine practice. Accordingly, it has been recommended that quantitative susceptibility testing should be used routinely and confirmatory testing using population analysis profile testing should be done only on isolates with MICs of ≥4 μg/ml [2]. Currently, no standardized single method to screen for GISA/h-GISA in the clinical microbiology laboratory exists.

Because GISA is associated with alterations in the cell-wall peptidoglycan synthesis pathway and increased levels of penicillin-binding proteins (PBP2), resulting in thickened or aggregated cell walls [3], the possibility of developing a single reliable assay based on detection of these biochemical changes should be assessed. In this context, an FTIR-based assay emerges as a possible candidate. FTIR spectroscopy is a biophysical

technique that probes the total biochemical composition of intact microbial cells nondestructively and without the use of any reagents, producing complex, yet distinct and reproducible spectral signatures that serve as the "fingerprint" of a microorganism (Figure 5.1). FTIR spectroscopy has been extensively applied during the past decade for the identification and typing of microorganisms at the subspecies level [4,5]. Some recent studies have also demonstrated that FTIR spectroscopy has sufficient resolving power to detect antibiotic-resistant phenotypes in various clinical bacteria [6-10]. In our previous work, FTIR spectroscopy was successfully employed for the discrimination of MRSA from methicillin-sensitive *S. aureus* (MSSA) and borderline oxacillin-resistant *S. aureus* (BORSA) strains [9] and from CNS species as well as for the discrimination of MRCNS from MSCNS species [10]. Based on these results, the present study was undertaken to evaluate the potential use of FTIR spectroscopy for the discrimination of GISA/h-GISA strains from epidemic CMRSA and SMRSA strains.

5.3. MATERIALS AND METHODS

5.3.1 Clinical specimens and microbiological analysis

A total of 82 *S. aureus* clinical isolates, consisting of 31 methicillin-resistant and 4 methicillin-sensitive GISA strains and 22 sporadic and 25 epidemic MRSA strains, were selected for this study. The 35 GISA strains were obtained from the collection of the Network on Antimicrobial Resistance in *Staphylococcus aureus* (NARSA) Program. The 47 MRSA strains were provided from the collection of the National Microbiology Laboratory of Health Canada (Winnipeg, MB, Canada).

Susceptibility testing for the screening of glycopeptide intermediate resistance in all GISA strains was performed by NARSA using broth microdilution (with the use of frozen and dried panels), conventional E-test (MHA, 0.5 McFarland inoculum, 24 h at 35 °C) and modified E-BHI agar, 2 McFarland inoculum, 48 h at 35 °C), BHI agar screen assay (growth of 10-µl spot on BHI + 6 µg/ml vancomycin after 24, 48, and 72 h), and the conventional disk diffusion method.

5.3.2 FTIR spectroscopic methods

5.3.2.1 Sample preparation

All bacterial strains were grown from frozen stocks, kept at –70 °C in brain heart infusion (BHI) broth containing 15% glycerol, by overnight subculture on tryptic soy with sheep blood agar (Quelab Laboratories Inc., Montreal, PQ, Canada) at 37 °C. A single bacterial colony was then collected from the plate and cultured on Universal Medium™ (UM™) agar for 18 h at 37 °C. Four loops-full of stationary-phase cells were then carefully collected using a 10-mm-diameter loop and suspended in 200-µl aliquots of sterile physiological saline (0.9% NaCl). A 25-µl aliquot of the 10-fold diluted bacterial suspension (approximately 5×10^{11} cells ml^{-1}) was deposited onto a clean zinc selenide (ZnSe) optical window, which was then oven-dried at 48 °C for 1 h to form a thin and transparent homogeneous dried film suitable for FTIR measurements.

5.3.2.2 Spectral acquisition

All FTIR spectra were acquired in the transmission mode using a Bomem MB-104 (ABB-Bomem, Québec, QC, Canada) FTIR spectrometer equipped with a deuterated triglycine sulfate (DTGS) detector and a KBr beamsplitter and operating under Bomem-Grams/386 software (Galactic, Salem, NH). The spectrometer was purged with dry CO_2-free air from a Balston dryer (Balston, Lexington, MA) to minimize interferences from atmospheric water vapor and CO_2. To enhance the signal-to-noise ratio, 64 scans were co-added at 4 cm^{-1} resolution over the wavenumber range of 4000-400 cm^{-1} and ratioed against an open-beam background to produce an absorbance spectrum (Figure. 5.1). For each strain, spectra were recorded in quadruplicate by depositing samples from four different culture plates on four different optical windows.

5.3.3 Mathematical preprocessing and processing

Spectral data (acquired in Grams SPC format) were converted into comma-separated values (CSV) files and then into MATLAB files using MATLAB version 5.1 (The MathWorks, Inc., Natick, MA). Because band intensity varies as a function of film thickness, the spectral data over the whole spectral range (4000-400 cm^{-1}) were

normalized to unit height by vector transformation to compensate for differences in film thickness. They were then transformed to first-derivative spectra using the Savitzky-Golay algorithm to maximize peak separation, enhance apparent resolution, and minimize problems arising from baseline shifts.

Prior to data processing, spectral feature selection was performed by singular-value decomposition (SVD) using individual pairs of spectra and confirmed by visual examination of the normalized spectra. Data analysis was performed using principal component analysis (PCA) employing the nonlinear iterative partial-least-squares (NIPALS algorithm, self-organizing maps (SOM) clustered by the *k*-means algorithm, and cluster analysis using the K-nearest neighbors (KNN) algorithm, as described previously [9]. Programs were written in MATLAB version 5.1 to implement the data preprocessing and processing algorithms.

5.4 RESULTS

5.4.1 Examination of spectral differences between CMRSA and GISA/h-GISA

Investigation of differences between randomly selected spectra within a data set consisting of 240 spectra acquired from four replicate test portions of 25 CMRSA and 35 GISA/h-GISA strains revealed clear differences between CMRSA and GISA/h-GISA strains in two narrow regions of the IR spectrum: (i) 1352-1315 cm^{-1} (Figure 5.2) and (ii) 1480-1460 cm^{-1} (Figure 5.3).

5.4.2 Discrimination between CMRSA and GISA/h-GISA strains based on spectral data in the region 1352-1315 cm^{-1}

PCA was performed on the first-order derivatives of the peak height-normalized spectral data in the region of 1352-1315 cm^{-1} for all the CMRSA and GISA/h-GISA strains. The first five PCs accounted for over 99.9% of the total variance, with PC1 and PC2 alone accounting for 98.8% (PC1: 96.0%; PC2: 2.8%) of the total variance. The PCA scores plot (PC1 vs. PC2) showed two distinct clusters, corresponding to CMRSA and GISA/h-GISA (Figure. 5.4). A single GISA strain, namely NRS68, fell between the two clusters, yielding 99% correct classification of GISA/h-GISA strains. A similar rate

of correct classification was obtained by visual inspection of an SOM of size [16×5] generated by a nonlinear projection of the scores of the first two PCs derived from the spectral data in the region 1352-1315 cm^{-1}, using 4 training lengths for the rough training and 13 epochs for the fine-tuning phase. The final quantization error was 0.136 with a final topological error of 0.004. The U-matrix, the two component planes, and the labeled SOM are represented in Figure 5.5a along with an expanded view of the labeled SOM in Figure 5.5b. Referring to the SOM labels, two distinct clusters of GISA and CMRSA are clearly discerned on the map grid. The map was partitioned with use of the *k*-means algorithm, and the Davies-Bouldin index confirmed the existence of two distinct clusters (Figure 5.6). However, based on this partitioning; only 82% correct classification was achieved. On the other hand, application of the KNN algorithm using half of the data set (n = 120) as the training set and the other half as the prediction set yielded the same rate of correct classification (99%) as obtained by PCA. The value of K was varied from 1 to 10, with the best results being obtained with K = 4.

5.4.3 Discrimination between CMRSA and GISA/h-GISA strains based on spectral data in the region 1480-1460 cm^{-1}

A similar analysis of the spectral data in the 1480-1460 cm^{-1} region also allowed appreciable clustering of CMRSA and GISA/h-GISA strains but yielded a slightly lower overall correct classification rate of 96% (data not shown). Irrespective of the data analysis technique employed (PCA, SOM, or KNN), NRS68 and a second GISA strain (NRS3) were misclassified as CMRSA, and a single CMRSA strain (CMRSA 488) was misclassified as GISA.

5.4.4 Discrimination between CMRSA/SMRSA and GISA/h-GISA strains

An additional set of 22 SMRSA strains was subsequently added to the CMRSA set to investigate the capability of the FTIR method to discriminate both sporadic and epidemic MRSA strains from GISA/h-GISA. The expanded data set comprised 328 spectra, consisting of four replicate spectra of 35 GISA/h-GISA strains and 47 MRSA strains [CMRSA (n = 25) and SMRSA (n = 22) strains]. The region between 1352-1315 cm^{-1}, although suitable for the discrimination between CMRSA and GISA/h-GISA

strains, did not prove to be appropriate for discrimination between SMRSA and GISA/h-GISA strains, yielding an overall correct classification rate of 84% by PCA (data not shown). Some improvement was obtained when PCA was applied to the spectral data for the region of 1480-1460 cm^{-1}. The first three PCs were sufficient to explain over 99.9% of the overall total variance in the spectral data, the cumulative total variance explained being 98.18, 99.74 and 99.92% for PC1, PC2, and PC3, respectively. The scores plot (PC1 vs. PC2) showed two main distinct clusters, corresponding to GISA and MRSA strains (Figure 5.7). However, three SMRSA strains (SMRSA693, SMRSA715, and SMRSA864) fell within the GISA cluster, and five GISA strains (NRS4, NRS11, NRS19, NRS68, and NRS76) fell within the MRSA cluster, yielding an overall correct classification rate of 90%. Application of the SOM algorithm to the scores of the first two PCs also resulted in a clear clustering of the GISA/h-GISA and MRSA strains (Figure 5.8a,b). The map of size [13×7] was trained using a rough training phase of 3 and a fine-tuning phase of 11 epochs. The learning rate decreased linearly to zero during the fine-tuning phase with a final quantization error of 0.167 and a final topographic error 0.021. The U-matrix (Figure 5.8a) shows two distinct areas of dark blue (top of the map) and light blue (rest of the map), indicating the presence of two clusters, although there is no clear border (which would be represented by a yellow–red area) separating the top cluster from the rest of the map. Comparative visual inspection of the U-matrix and the labeled SOM revealed that the top dark blue cluster in the U-matrix corresponded to an SMRSA/CMRSA cluster and the light blue cluster to a GISA/h-GISA cluster. However, partitioning of the SOM with the use of the *k*-means algorithm and the Davies-Bouldin index indicated the presence of four clusters (data not shown).

Supervised classification performed with the KNN algorithm using half of the data set (n = 164) as the training set and the other half as the prediction set gave a 92% rate of correct classification with K = 6. Three SMRSA (SMRSA693, SMRSA715, and SMRSA864) and four GISA (NRS4, NRS11, NRS19, and NRS68) strains were misclassified. It may be noted that the strains misclassified when using KNN were the same as those misclassified by PCA and SOM.

5.5 DISCUSSION

Successful discrimination between CMRSA and GISA/h-GISA strains with a 99% correct classification rate was achieved by analysis of FTIR spectral data in a single narrow region of 1352-1315 cm^{-1} using either PCA, SOM, or KNN chemometric tools. However, with the inclusion of SMRSA strains in the data set, this region was no longer appropriate for classification, yielding an overall classification rate as low as 84%, indicating that the spectral differences between GISA/h-GISA and CMRSA strains observed in this region are not specific to glycopeptide-intermediate phenotypes. The spectral region of 1480-1460 cm^{-1}, containing primarily absorption bands assigned to CH_2 asymmetric bending vibrations of lipids and proteins [11], was found to be more appropriate for discrimination between CMRSA/SMRSA and GISA/h-GISA strains. Based on the spectral data in this region, 92% of the strains were correctly classified with the use of the KNN algorithm. All three SMRSA and four GISA/h-GISA strains that were misclassified (SMRSA693, SMRSA715 and SMRSA864; NRS4, NRS11, NRS19, and NRS68) were also misclassified [together with an additional GISA strain (NRS76)] when classification was based on visual examination of clusters on the PCA scores plot or the SOM. Since the same strains were misclassified using KNN, SOM, and PCA, the microbiological identification of these strains should be confirmed by quantitative susceptibility testing and confirmatory testing using routine population analysis profiles.

5.6 CONCLUSION

Based on the results of this study, FTIR spectroscopy combined with the use of UM™ and chemometrics is a promising alternative to susceptibility testing methods as a routine technique for the identification of GISA/h-GISA strains, and accordingly further validation studies are warranted to confirm the suitability of this technique for the rapid screening of GISA/h-GISA strains. In addition, further investigation of the spectral differences between MRSA and GISA strains observed in this study may aid in the elucidation of the mechanisms of glycopeptide resistance in *S. aureus* strains.

Acknowledgments

We thank Quelab Laboratories Inc. for supporting the project and the Canadian Nosocomial Infection Surveillance Program (CNISP) for participating in this research. GISA isolates were obtained through the Network on Antimicrobial Resistance in *Staphylococcus aureus* (NARSA) Program supported under NIAID, NIH Contract No. N01-AI-95359 (Focus Technologies, Herndon, VA).

5.7 REFERENCES

1. Hiramatsu, K., N. Aritaka, H. Hanaki, S. Kawasaki, Y. Hosoda, S. Hori, Y. Fukuchi, and I. Kobayashi, 1997. Dissemination in Japanese hospitals of strains of *Staphylococcus aureus* heterogeneously resistant to vancomycin. *Lancet.* 350:1670-1673

2. Tenover, F.C., M.V. Lancaster, B.C. Hill et al., 1998. Characterization of staphylococci with reduced susceptibilities to vancomycin and other glycopeptides. *J. Clin. Microbiol.* 36:1020-1027

3. Sieradzki, K., and A. Tomasz, 1999 Gradual alterations in cell wall structure and metabolism in vancomycin-resistant mutants of *Staphylococcus aureus*. *J. Bacteriol.* 181:7566-7570

4. Naumann, D., D. Helm, H. Labischinski, and P. Giesbrecht, 1991. The characterization of microorganisms by Fourier-transform infrared spectroscopy, *in* W.H. Nelson (ed.), *Modern Techniques for Rapid Microbiological Analysis.* New York: VCH Publishers. p. 43

5. Mariey, L., J.P. Signolle, C. Amiel, and J. Travert, 2001. Discrimination, classification, identification of microorganisms using FTIR spectroscopy and chemometrics. *Vibr. Spectrosc.* 26:151-159

6. Bouhedja, W., G.D. Sockalingum, P, Pina, P. Allouch, C. Bloy, R. Labia, J.M. Millot. and M. Manfait, 1997. ATR-FTIR spectroscopy investigation of *E. coli* transconjugants β-lactams-resistance phenotype. *FEBS Lett.* 412:39-42

7. Kirschner C., Ngoc Anh Ngo Thi, and D. Naumann, 1999. FT-IR spectroscopic investigations of antibiotic sensitive and resistant microorganisms. *2nd Workshop on FT-IR Spectroscopy in Microbiology and Medical Diagnostics*, Robert Koch-Institute, Berlin

8. Sockalingum, G.D., W. Bouhedja, P, Pina, P. Allouch, C. Mandray, R. Labia, J.M. Millot, and M. Manfait, 1997. ATR-FTIR spectroscopic investigation of imipenem-susceptible and -resistant *Pseudomonas aeruginosa* isogenic strains. *Biochem. Biophys. Res. Commun.*. 232:240-246

9. Amiali, M.N., B. Berger-Bächi, K. Ehlert, M.R. Mulvey, A.A. Ismail, J. Sedman, and A.E. Simor, 2003. Rapid identification of methicillin-resistant *Staphylococcus aureus* (MRSA) by Fourier transform infrared (FTIR) spectroscopy. *Submitted*

10. Amiali, M.N., B. Berger-Bächi, M.R. Mulvey, A.A. Ismail, L. Louie, J. Sedman, and A.E. Simor, 2003. Rapid and accurate identification of coagulase-negative staphylococci (CNS) and methicillin-resistant CNS (MRCNS) by Fourier transform infrared (FTIR) spectroscopy. *Submitted*

11. Alban, J.O., and F.G. Fiamingo, 1984. Fourier transform infrared spectroscopy, *in* D.L. Rousseau (ed.), *Optical Techniques in Biological Research.* New York: Academic Press. pp. 133-179

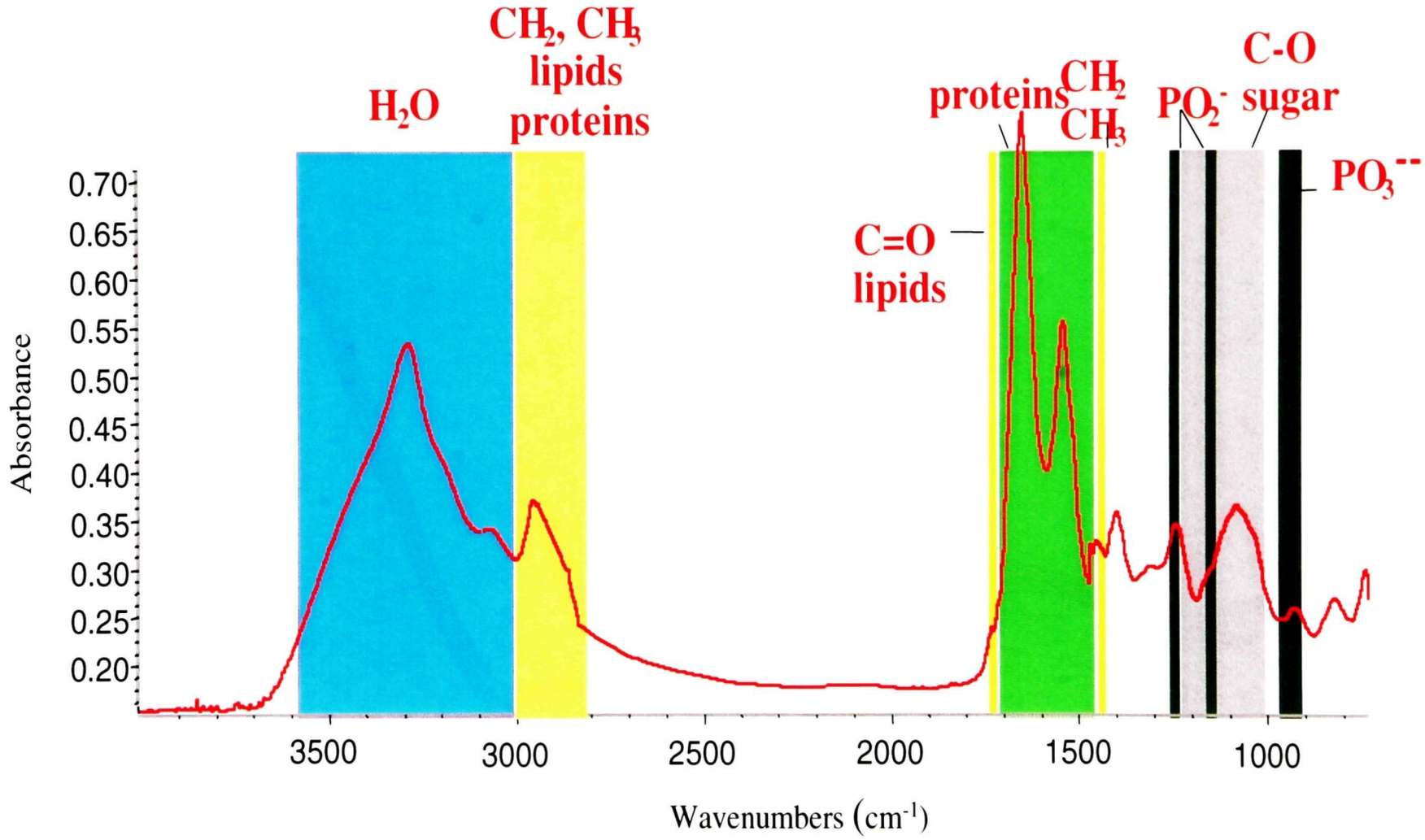

Figure 5.1: Typical FTIR spectrum of bacteria cells

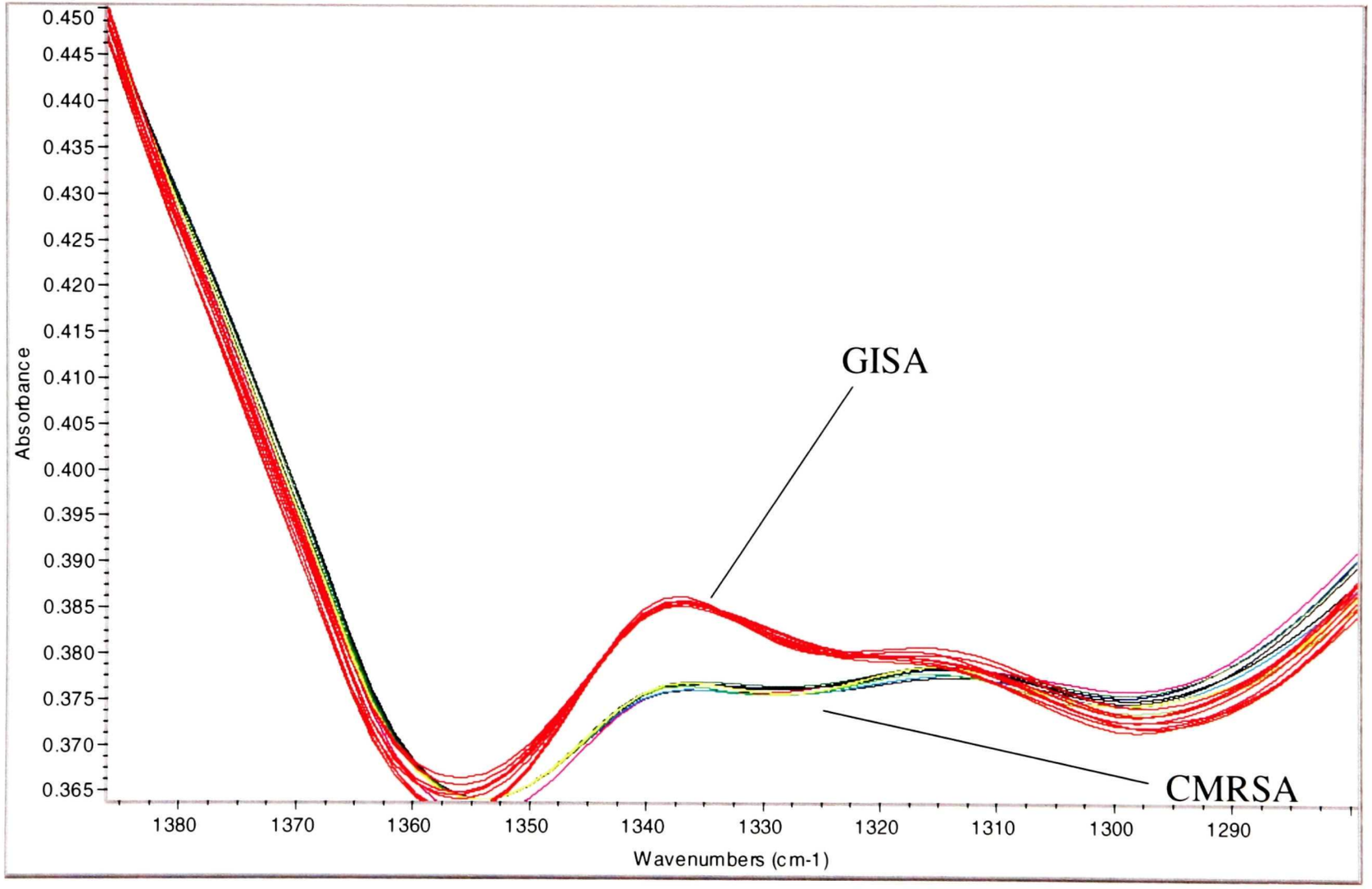

Figure 5.2: FTIR spectra of GISA and CMRSA strains in the region 1360-1300 cm^{-1}

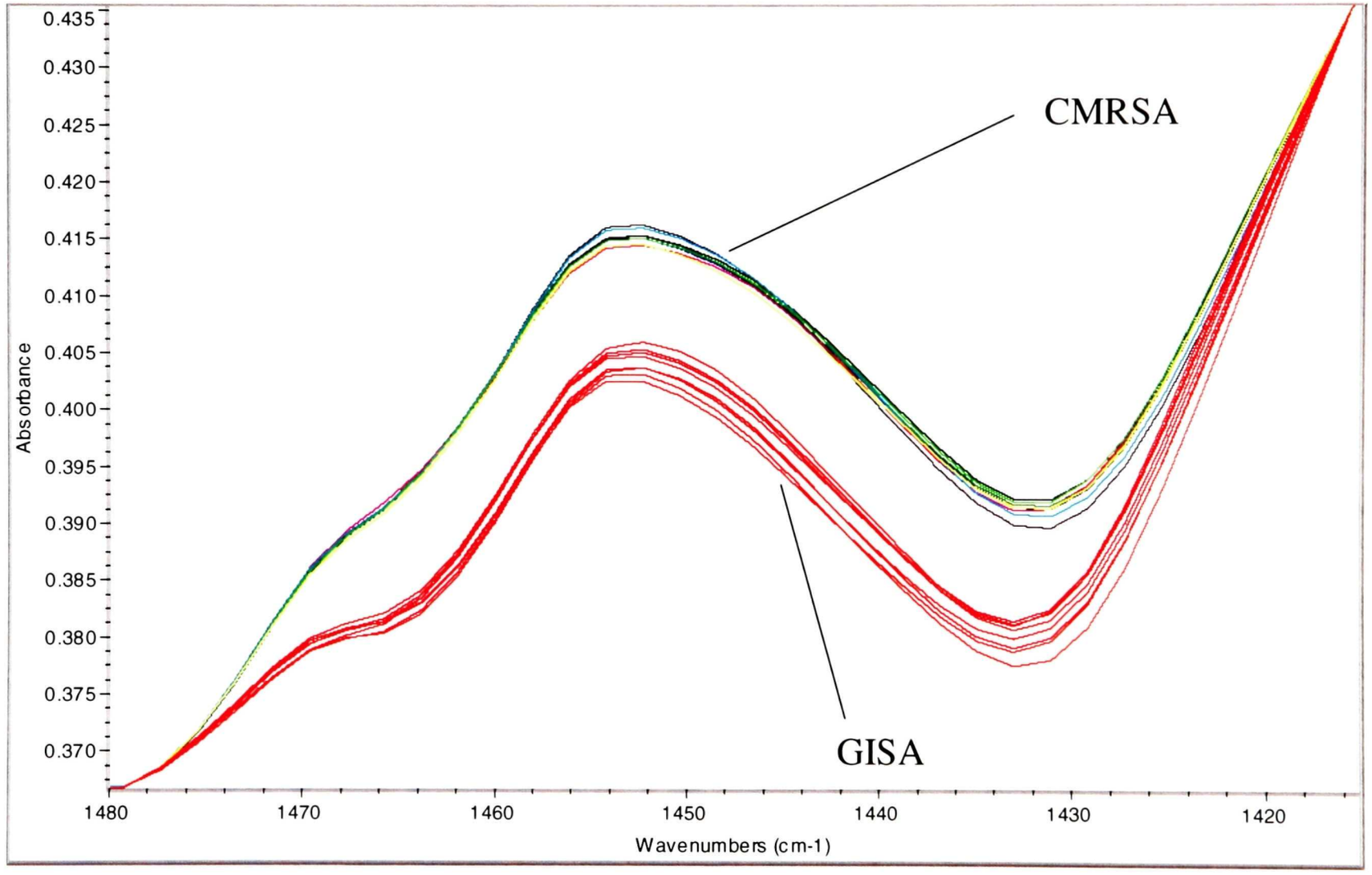

Figure 5.3: FTIR spectra of GISA and CMRSA strains in the region 1480-1420 cm^{-1}

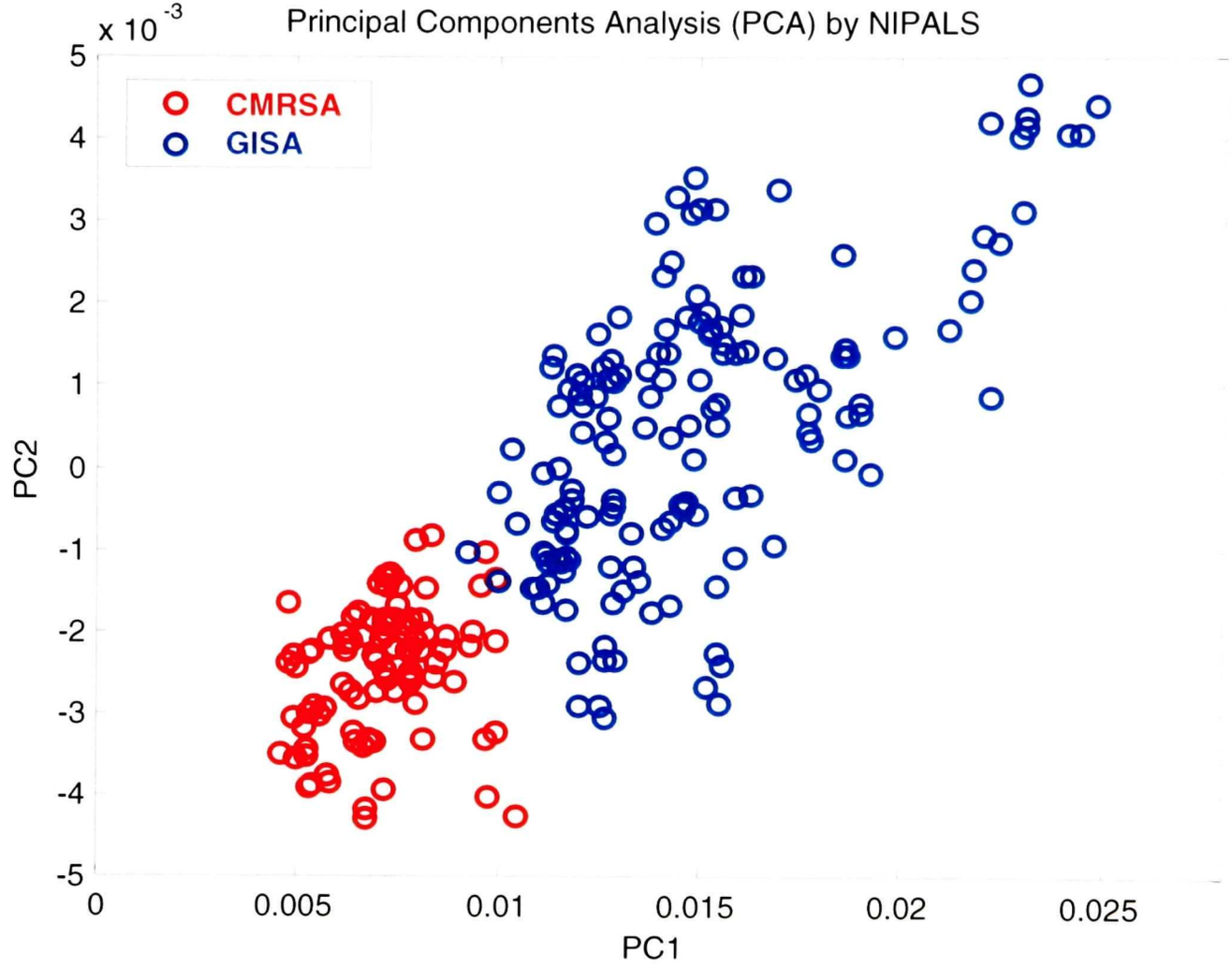

Figure 5.4: Scores plot for first two PCs obtained from the spectral data for 35 GISA and 25 CMRSA strains in the region 1352-1315 cm^{-1} by PCA using the NIPALS algorithm

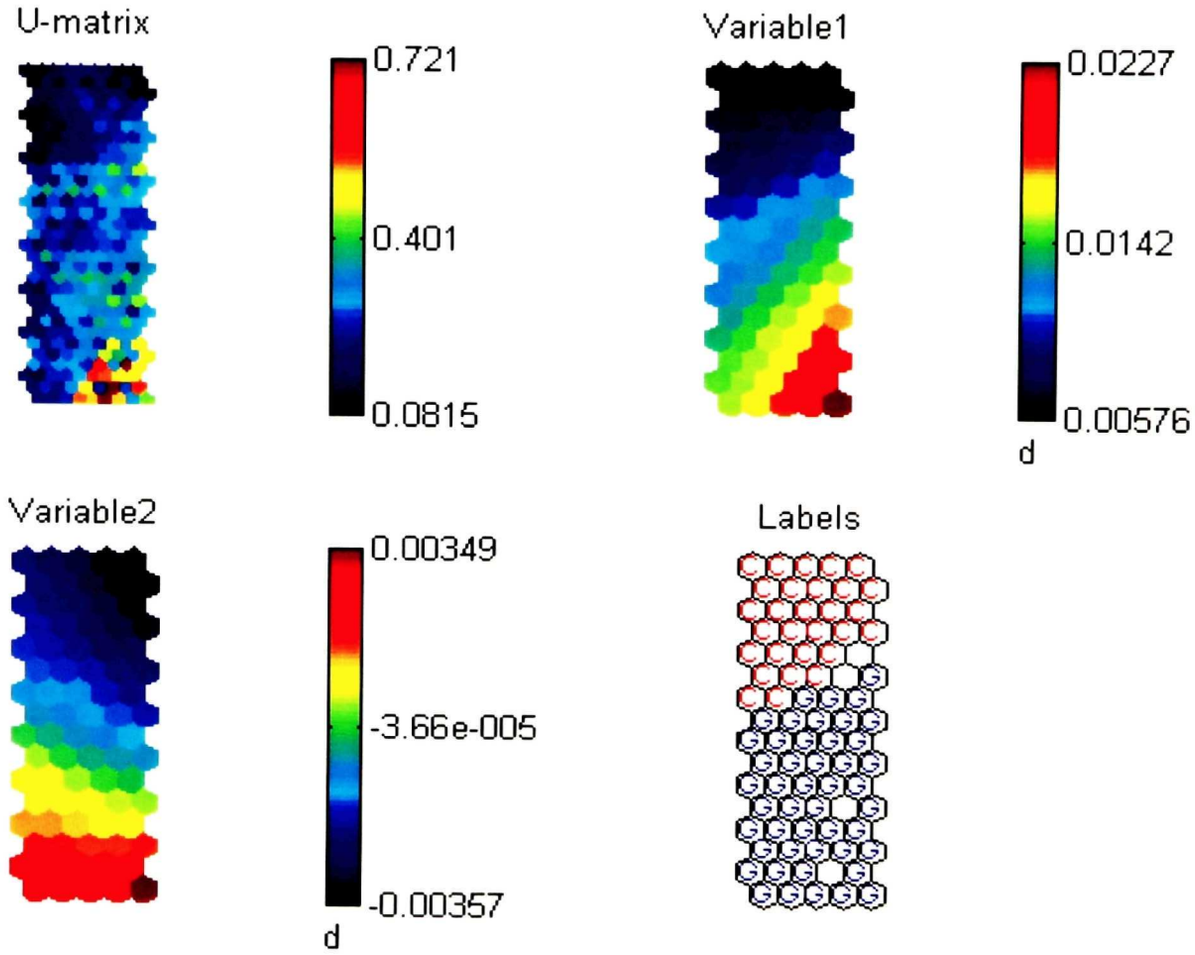

Figure 5.5a: U-matrix, component planes, and SOM obtained by application of the SOM algorithm using the spectral data for 35 GISA (G) and 25 CMRSA (C) strains in the region 1352-1315 cm^{-1}

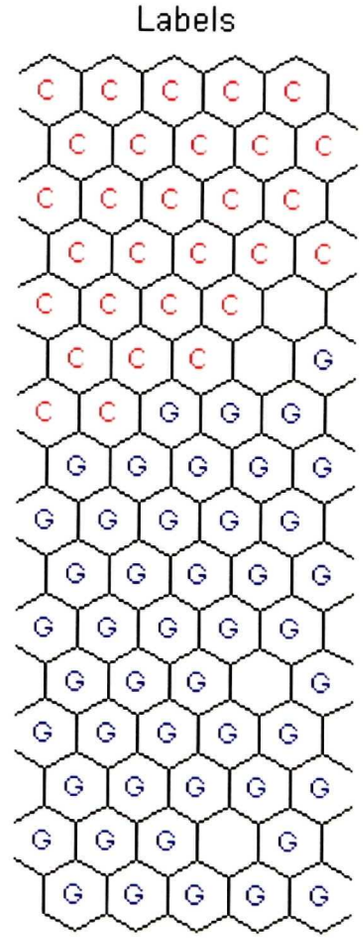

Figure 5.5b: Expanded view of the SOM shown in Figure 5.5a.

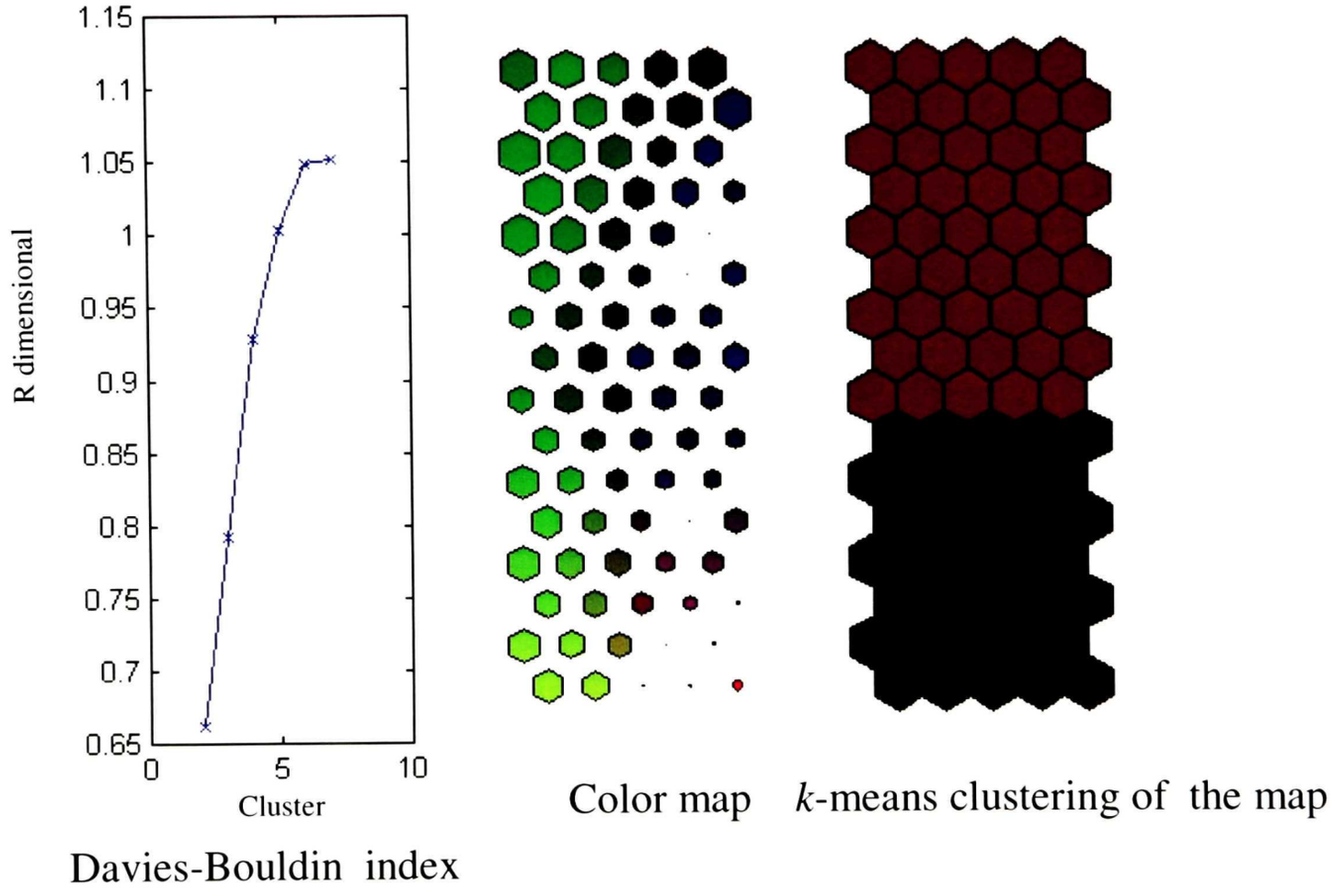

Figure 5.6: Partitioned SOM for the spectral data in the region 1352-1315 cm^{-1} obtained by applying the *k*-means algorithm and the Davies-Bouldin index

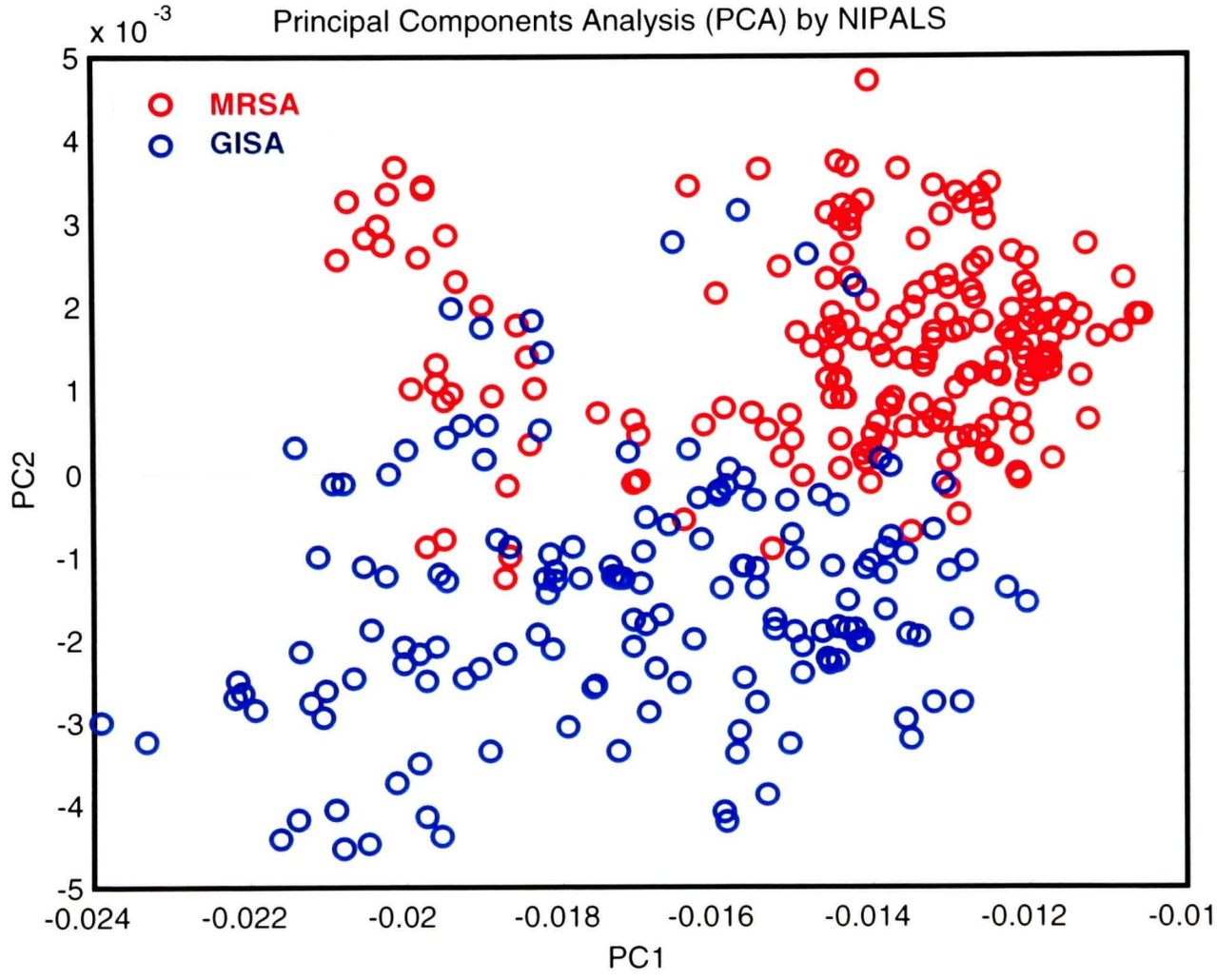

Figure 5.7: Scores plot for first two PCs obtained form the spectral data for 35 GISA and 47 MRSA (SMRSA and CMRSA) strains in the region 1480-1460 cm^{-1} by PCA using the NIPALS algorithm

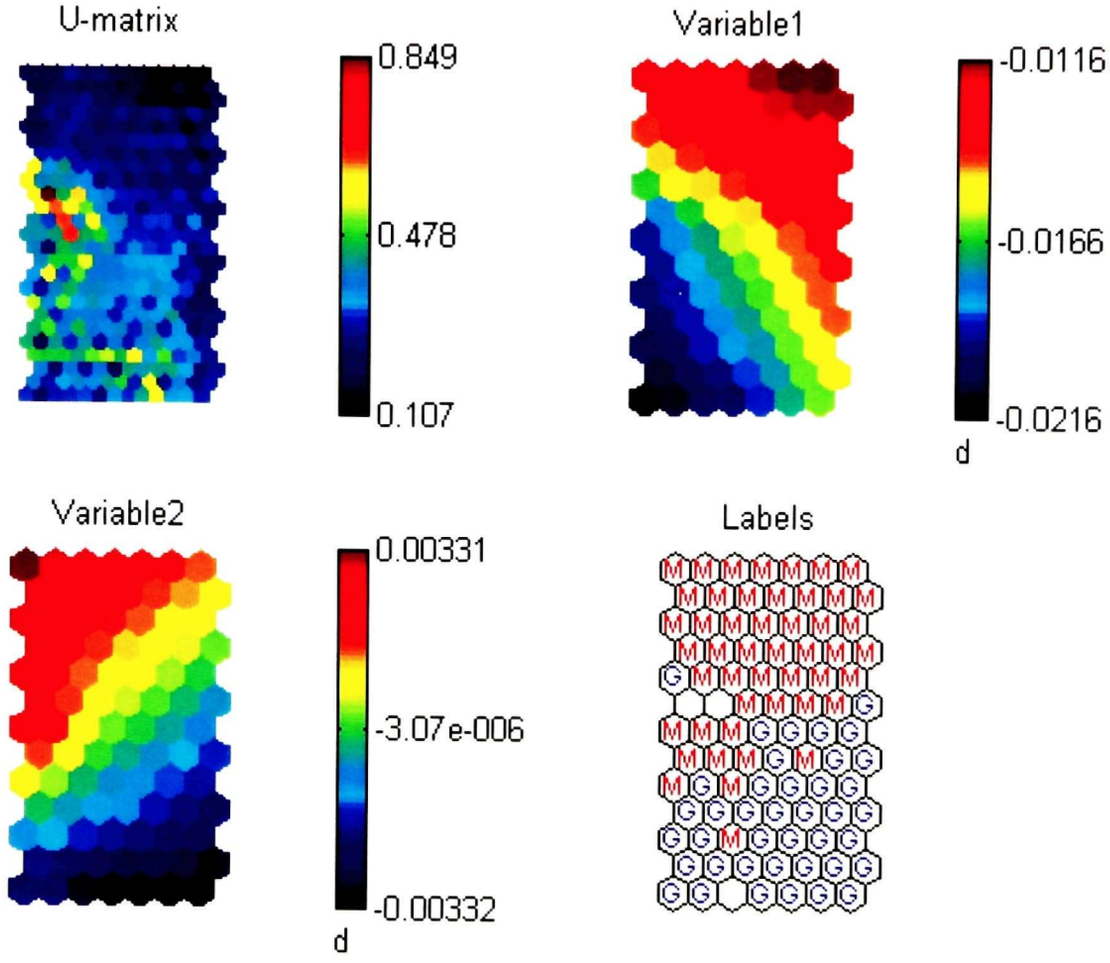

Figure 5.8a: U-matrix, component planes, and SOM obtained by application of the SOM algorithm using the spectral data for 35 GISA (G) and 47 MRSA (M) strains in the region 1480-1460 cm^{-1}

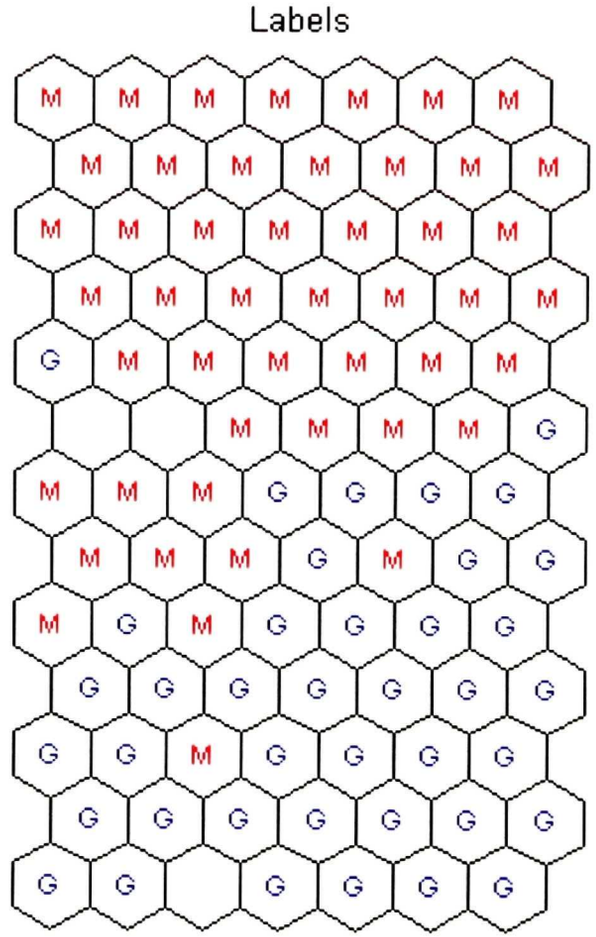

Figure 5.8b: SOM obtained using the spectral data for 35 GISA (G) and 47 MRSA (M) strains in the region 1480-1460 cm^{-1}

CHAPTER 6

CONNECTING STATEMENT

Chapters 3-5 have concerned the application of FTIR spectroscopy for the identification of antibiotic-resistant staphylococci. The FTIR-based methods developed in this research are of potential utility in a clinical setting as they would provide a simple, rapid, and reliable means for the detection of antibiotic-resistant strains so that appropriate therapy and intervention for cross-infection control can be initiated in a timely manner. In recent years, a limited number of studies on the subtyping of microorganisms by FTIR spectroscopy have been reported. Accordingly, the discriminatory power of FTIR spectroscopy for epidemiological typing of five Canadian epidemic MRSA clones was evaluated in order to determine whether FTIR spectroscopy could be employed for epidemiological surveillance purposes. The results of this investigation are presented in the following chapter.

CHAPTER 6

EPIDEMIOLOGICAL TYPING OF METHICILLIN-RESISTANT *STAPHYLOCOCCUS AUREUS* (MRSA) STRAINS BY FOURIER TRANSFORM INFRARED (FTIR) SPECTROSCOPY

6.1 ABSTRACT

Methicillin-resistant *Staphylococcus aureus* (MRSA) is one of the most widespread multidrug-resistant nosocomial pathogens in Canada. A rapid, efficient, and simple routine epidemiologic typing system is crucial for monitoring and limiting intra- and interhospital spread of epidemic MRSA strains. Molecular subtyping methods such as pulsed-field gel electrophoresis (PFGE) are reliable discriminatory methods, but they are technically demanding and time-consuming. In the present study, FTIR spectroscopy was employed to subtype 85 strains of epidemic Canadian MRSA clones (CMRSA-1, CMRSA-2, CMRSA-3, CMRSA-4, and CMRSA-5) based on their infrared spectral fingerprints obtained from whole cells (stationary-phase cells grown on UM™). Potentially suitable spectral regions for the differentiation of CMRSA-1 through CMRSA-5 were selected by visual inspection of randomly chosen spectra, aided by singular-value decomposition (SVD) of the spectral data matrix. The spectral regions 1080-1050 and 1170-1140 cm^{-1} appeared to be suitable for discrimination of CMRSA-4 and CMRSA-2, respectively, from the other CMRSA strains while CMRSA-1, CMRSA-5, and CMRSA-3 each exhibited distinctive spectral profiles in the 1120-1080 cm^{-1} region. The clustering of the different subtypes of CMRSA based on these spectral differences in the region of 1170-1050 cm^{-1} by principal component analysis (PCA), self-organizing maps (SOM), and supervised cluster analysis employing the K-nearest neighbor (KNN) algorithm was investigated with a data set of 850 spectra, comprising the first derivatives of the peak-height normalized spectra of 10 replicates of each of the 85 strains. While use of the spectral data from this region did not result in clear separation of the five CMRSA subtypes, five clusters were obtained when the data from the spectral region 2914-2880 cm^{-1} were combined with the data from the narrow regions 1096-1066 and 1114-1099 cm^{-1}. An overall correct classification rate of 86% was obtained by visual examination of the PCA scores plot (PC1 vs. PC2) or by partitioning

an SOM with the use of the *k*-means algorithm, whereas the supervised cluster analysis yielded a correct classification rate of 97%. These results demonstrate that FTIR spectroscopy has considerable potential as an alternative rapid (1-hour) and simple method for epidemiological typing investigations and monitoring transmission of MRSA strains at both local and interregional levels.

6.2 INTRODUCTION

MRSA is recognized as the most important worldwide multidrug-resistant pathogen causing nosocomial infections, and the incidence of MRSA in Canadian hospitals has dramatically increased in recent years. A rapid, accurate, and simple routine epidemiologic typing system is essential for institution of appropriate infection control procedures and epidemiological surveillance purposes in health-care facilities. Several DNA-based typing methods have been developed for typing MRSA strains. Standardized pulsed-field gel electrophoresis (PFGE) systems provide fingerprinting of the chromosomal background with high discriminatory power and accurate typability for comparing distant clonal MRSA lineages [1,2]. PFGE is widely used by many hospitals and laboratories and has been suggested as the gold standard for the molecular typing of MRSA [3,4]. However, it is labor-intensive and has a long turnaround time (2–3 days), reducing a laboratory's ability to analyze large numbers of samples and therefore making this technique difficult to perform on a routine basis in a hospital setting.

Ideally, laboratories routinely conducting regional epidemiological surveillance of MRSA infections would have available to them a rapid, simple, and accurate typing system with high discriminatory potential, easily interpretable results, and good intra-laboratory reproducibility. With recent developments in analytical instrumentation, these requirements may potentially be fulfilled by "whole-organism fingerprinting" using spectroscopic techniques. Such biophysical methods may offer several advantages over conventional biochemical methods, including speed, simplicity, and unambiguous data interpretation, as well as not requiring the use of any reagents.

In this context, the application of FTIR spectroscopy for the identification and classification of microorganisms has been extensively investigated [3-14]. FTIR spectroscopy measures the vibrations of chemical bonds within all the biochemical constituents of cells, i.e., proteins, lipids, polysaccharides, and nucleic acids, and thus provides quantitative information about the total biochemical composition of the intact whole microbial cell [13]. Furthermore, because the FTIR spectra of microorganisms consist of distinct and unique patterns that are highly reproducible, the spectra effectively serve as "fingerprints", allowing for their successful use in taxonomic discrimination [13]. Thus, various studies have shown that FTIR spectroscopy provides a powerful tool with sufficient discriminatory power to distinguish between microbial cells even at the strain level, without any preclassification on the basis of other taxonomic criteria [8].

In recent years, several studies have been reported on the application of FTIR spectroscopy for the discrimination of some pathogenic species of the genera *Staphylococcus* [8], *Clostridium* [6], *Listeria* [9], *Klebsiella* [7], *Bacillus* [5], *Pseudomonas* [10], and *Enterococcus* [11]. In addition, the subtyping of microorganisms by FTIR spectroscopy has recently been reported for food-borne yeasts [12] and in an epidemiological typing study of nosocomial yeasts [14], for bacteria such as *Salmonella enteritidis* [15], *Serratia marcescens* [16], and *Acinetobacter baumannii* [17], and for algae [14]. Only one study to date has addressed the typing of five *S. aureus* strains by FTIR spectroscopy [18]. The goal of the present study was to evaluate the discriminatory power of FTIR spectroscopy for epidemiological typing of CMRSA clones.

6.3. MATERIALS AND METHODS

6.3.1 Strains

Eighty-five strains of epidemic CMRSA clones (CMRSA-1, CMRSA-2, CMRSA-3, CMRSA-4, and CMRSA-5) were generously provided by the Canadian Nosocomial Infection Surveillance Program from the National Microbiology Laboratory (Winnipeg, MB, Canada). All strains were stored in cryovials containing brain heart infusion (BHI) broth supplemented with 15% glycerol at –70 °C.

6.3.2 Microbiological methods

6.3.2.1 Phage typing

Phage typing of MRSA was performed according to the standard method of Blair and Williams [19] with the basic international set of 23 phages. The set of phages included the lytic groups I (29, 52, 52A, 79 and 80), II (3A, 3C, 55 and 71), III (6, 42E, 47, 53, 54, 75, 77, 83A, 84 and 85), and V (94, 96), and miscellaneous or non-allocated phages 81 and 95. Susceptibility to phages was determined at the standard routine test dilution (RTD) and at 100 × RTD concentrations. Bacterial isolates were considered to belong to different phage types if they differed in their sensitivity to two or more phages.

6.3.2.2 Pulsed-field gel electrophoresis (PFGE) analysis

Isolates were characterized by PFGE following DNA extraction and digestion with *Sma*I [2]. The digitized PFGE DNA profiles were input into the Molecular Analyst software, Version 1.6 (BioRad; Hercules, CA) for analysis. DNA fragments on each gel were normalized using lambda molecular weight standards run on each gel to allow comparisons between different gels. Cluster analysis was performed by the unweighted pair group method using arithmetic averages (UMPGA), and DNA relatedness was calculated based on the Dice coefficient. Genetic relatedness was calculated based on criteria recommended by Bannerman *et al.* [1] and Tenover *et al.* [4]. Isolates were considered to be genetically related if their macrorestriction DNA patterns differed by six bands or less and the Dice coefficient of correlation was 75% or greater.

6.3.3 FTIR spectroscopic methods

6.3.3.1 Sample preparation

After an overnight subculture on tryptic soy with sheep blood agar (Quelab Laboratories Inc., Montreal, PQ, Canada) at 37 °C, followed by culture on Universal Medium™ agar (Quelab Laboratories Inc., Montreal, PQ, Canada) for 18 h at 37 °C, four loops-full of stationary-phase cells were carefully collected using a 10-mm-diameter loop and suspended in 200-µl aliquots of sterile physiological saline (0.9%). A 25-µl aliquot of the 10-fold diluted bacterial suspension (approximately 5×10^{11} cells ml^{-1}) was evenly

applied onto a zinc selenide (ZnSe) optical window and then oven-dried at 50 °C for 1 hour (Figure 6.1).

6.3.3.2 Spectral acquisition

All FTIR spectra were recorded using a Bomem MB-104 (ABB-Bomem, Quebec, QC, Canada) FTIR spectrometer equipped with a KBr beamsplitter and a deuterated triglycine sulfate (DTGS) detector and operating under Bomem-Grams/386 software (Galactic, Salem, NH). Ten replicate spectra were collected for each of the 85 samples. The procedure for spectral acquisition is schematically represented in Figure 6.2. For each FTIR spectrum, 64 interferograms were co-added at 4 cm^{-1} resolution in the mid-IR region (4000-400 cm^{-1}) and ratioed against an open-beam background to produce an absorbance spectrum. The spectrometer was continuously purged with dry air from a Balston dryer (Balston, Lexington, MA) to reduce the spectral contributions of atmospheric water vapor and CO_2.

6.3.4 Mathematical preprocessing and processing

The collected spectral data, stored in Grams SPC format, were converted into CSV format and then into MAT format using Matlab version 5.1 (The MathWorks, Inc., Natick, MA). Spectra were normalized to unit peak height to compensate for variations in sample thickness, autoscaled to unit variance (all spectral ranges equally weighted), and transformed to first-order derivative spectra using the 9-point Savitzky-Golay filter to enhance the separation of partially superimposed bands and to minimize problems arising from unavoidable baseline drift. Singular-value decomposition (SVD) was employed to investigate the spectral differences between different clones. Exploratory data analysis was performed using principal component analysis (PCA) based on the NIPALS algorithm and self-organizing maps (SOM) clustered by applying the *k*-means algorithm and the Davies Bouldin index [20]. Cluster analysis was performed using the K-nearest neighbors (KNN) algorithm.

6.4 RESULTS AND DISCUSSION

The representative DNA profiles obtained by PFGE of *Sma*I digests from CMRSA-1, CMRSA-2, CMRSA-3, CMRSA-4, and CMRSA-5 isolates show that the five CMRSA strains have different DNA pattern profiles (Figure 6.3). The phylogenetic relatedness of these strains is shown in a dendrogram (Figure 6.4).

The data set employed to evaluate the possibility of differentiating these five CMRSA strains by FTIR spectroscopy comprised 850 spectra, consisting of 10 replicate spectra of each of the 85 CMRSA isolates. The difficulty of extracting the relevant discriminatory information from a spectral data set of this size is compounded by the inherent complexity of the spectra, as they are the superposition of the infrared-active vibrational spectroscopic features of all biochemical components present in the whole cell [21-24]. Thus, appropriate spectral preprocessing and region selection, use of data reduction techniques to compress the data while preserving the important information, and application of pattern recognition techniques are mandatory. The principles of the strategy employed in the present work have been described in a previous publication [25].

6.4.1 Spectral reproducibility

A prerequisite for successful typing of CMRSA isolates by FTIR spectroscopy is sufficient spectral reproducibility to ensure that spectral differences between strains are not obscured by the variance within the spectra of each individual strain. The selection of an appropriate growth medium and rigorous control of growth conditions are of prime importance in this regard since changes in spectral profiles occur with changes in growth media and/or time of growth [26-29]. The reproducibility of the IR spectra depends also on the sample homogeneity, particle size, and film thickness. The way in which bacteria are transferred from an agar plate to the IR sample holder and even the method used to dry the bacterial suspension after deposition on the sample holder can affect the level of spectral reproducibility. Excellent spectral reproducibility thus requires rigorous control and standardization of both plating and sampling methodology. The first requirement was addressed in this study by the use of a standard universal medium (UM^{TM}) developed by Quelab Laboratories Inc. and a strict control of the growth conditions (18-h incubation at

37 °C) to ensure that all samples were taken from an early stationary-phase culture. In terms of sampling methodology, a precise volume of diluted bacterial suspension was deposited on a ZnSe optical window and dried for 1 hour at 48 °C. This procedure produced a transparent and homogeneous film of uniform dryness suitable for FTIR measurements, avoiding the anomalous diffraction effects seen in inhomogeneous samples with too large particles. The level of spectral reproducibility achieved was evaluated by examining replicate spectra obtained by taking 10 individual samples from four different culture agar plates. Excellent reproducibility was indicated by the consistency of the relative peak intensities. However, the integrated area (measured between 1800 and 800 cm^{-1}) varied somewhat among replicate spectra ($r = 0.97$) due to baseline shifts and variations in sample thickness. These variations in integrated area were minimized by the use of pea-height normalization and first-order spectral derivatives.

6.4.2 Spectral differences among the 5 CMRSA strains

Prior to multivariate analysis, randomly chosen spectra of each of the five CMRSA strains were examined in an attempt to identify spectral features that might be employed for the differentiation of the CMRSA strains. Visual inspection of the spectra, aided by the application of singular-value decomposition (SVD), revealed clear differences between the spectra of CMRSA-4 and those of the other CMRSA strains in the spectral region between 1080 and 1050 cm^{-1} (Figure 6.5). The region 1120-1080 cm^{-1} allowed a clear distinction between CMRSA-1, CMRSA-3, and CMRSA-5 strains (Figure 6.6), and. CMRSA-2, CMRSA-1, and CMRSA-4 were each distinguishable from CMRSA-3 and CMRSA-5 in the region 1175-1140 cm^{-1} (Figure 6.7). Finally, CMRSA-2 was distinguishable from the four other CMRSA strains in the region between 2940 and 2865 cm^{-1} (Figure 6.8). A summary of these readily observed differences between typical spectra of the five CMRSA strains is presented in Table 6.1.

It would clearly be of interest to interpret the spectral differences observed in these regions in relation to specific biochemical markers. However, although it can be stated that the bands in the region between 2940 and 2865 cm^{-1} are due to C-H stretching

vibrations, and those in the other regions may be assigned to polysaccharide or phosphate-containing compounds, more definitive band assignments cannot be made owing to the extensive overlap of vibrational bands of the various biochemical components of the cell. Further information regarding the origin of the observed spectral differences could potentially be obtained through the application of isotope-edited FTIR spectroscopic techniques, which take advantage of the band shifts produced by isotopic substitution owing to the dependence of infrared absorption frequencies on atomic mass. For example, by growing bacteria on media containing ^{13}C-sugars, the infrared bands due to polysaccharide components of the cell would shift to lower wavenumbers [30], and thus the effects of such isotopic substitution on the spectral differences among the five CMRSA strains observed in Figures 6.5-6.8 could help in elucidating the biochemical basis for these differences. Also, data obtained by pyrolysis mass spectrometry could further help in band assignment and identification of biomarkers. This approach has been successfully implemented by Goodacre and co-workers [31] for the detection of dipicolinic acid as the characteristic biomarker for the identification of *Bacillus* spores.

6.4.3 Principal component analysis (PCA)

PCA was performed on the first derivatives of the 850 peak-height-normalized spectra in the data set, using only the information contained in the narrow spectral regions shown in Figures 6.5-6.8. The combined data from the regions 1096-1066, 1114-1099, and 2914-2880 cm^{-1} were selected for differentiation of the five CMRSA strains through an iterative process. A plot of the scores of the first two principal components, PC1 (accounting by itself for 97% of the total variance) versus PC2, derived from these data shows five distinct clusters corresponding to CMRSA-1, CMRSA-2, CMRSA-3, CMRSA-4, and CMRSA-5 (Figure 6.9). The CMRSA-1, CMRSA-2, and CMRSA-4 isolates give rise to fairly well separated clusters on the scores plot, whereas there is some overlap between the CMRSA-3 and CMRSA-5 isolates. Classification of the 850 spectra in the data set on the basis of the scores plot yielded an overall correct classification rate of 86%.

6.4.4 Self-organizing map (SOM)

The generation of an SOM by an unsupervised neural network algorithm using the scores of the first two PCs as input data was subsequently investigated as a possible means of improving the rate of correct classification. The map of size [12×9] was trained using a rough training phase of 3 and a fine-tuning phase of 9 epochs. The learning rate decreased linearly to zero during the fine-tuning phase with a final quantization error of 0.149 and a final topographic error of 0.008. Figure 6.10a shows the U-matrix, the component planes, and the labeled SOM, which is also shown in an expanded view in Figure 6.10b. The U-matrix shows two large clusters (dark blue areas), two medium-sized clusters (light blue areas), and one small cluster (light green area). Visual inspection of the labeled SOM indicated that these clusters correspond to CMRSA-1, CMRSA-3, CMRSA-2, CMRSA-5, and CMRSA-4, respectively, and classification of all the spectra in the data set based on these clusters yielded a correct classification rate of 97%. For quantitative analysis, the map was partitioned by partitive clustering using the *k*-means algorithm and the number of clusters was confirmed to be five by calculating the Davies-Bouldin index (Figure 6.11). Classification based on the clustered SOM yielded the same percentage of correct classification (86%) as PCA.

6.4.5 K-Nearest neighbors (KNN) algorithm

Supervised cluster analysis using the KNN algorithm was based on the spectral data (normalized and transformed to first derivatives) in the same spectral regions as employed in PCA. Half of the 850 spectra in the data set served as the training set, with the remaining 425 spectra serving as the test set. Each member of the test set was classified among the five CMRSA clones by computing its K nearest neighbors (K = 1-10) in the training set in multidimensional space and assigning it to the class to which the majority of its K nearest neighbors belonged. The highest percentage of correctly classified test points (97%) was achieved with K = 5.

6.5 CONCLUSION

The work presented here demonstrates that differences in the biochemical composition of various CMRSA strains are reflected in differences in their infrared spectra. The use of three narrow spectral regions (1096-1066, 1114-1099, and 2936-2880 cm^{-1}) allowed for differentiation among five CMRSA strains by PCA, SOM, and KNN, with the latter technique yielding the highest percentage of correct classification (97%). Accordingly, FTIR spectroscopy has considerable potential as an alternative rapid (1-hour) method for the differentiation of CMRSA strains and would be useful for monitoring transmission of epidemic MRSA at both local and interregional levels. Extensive validation studies and elucidation of the origin of the spectral differences on which differentiation is based would facilitate adoption of the FTIR method in clinical diagnostics.

6.6 REFERENCES

1. Bannerman, T.L., G.A. Hancock, F.C. Ternover, and J.M. Miller, 1995. Pulsed-field gel electrophoresis as a replacement for bacteriophage typing of *Staphylococcus aureus*. *J. Clin. Microbiol.* 33:551-555

2. Mulvey, M.R., L. Chui, J. Ismail, L. Louie, C. Murphy, N. Chang, M. Alfa, and Canadian Committee for the Standardization of Molecular Methods, 2001. Development of a Canadian Standardization Protocol for Subtyping Methicillin-Resistant *Staphylococcus aureus* (MRSA) using pulsed-field gel electrophoresis. *J. Clin. Microbiol.* 39:3481-3485

3. Tenover, F.C., R. Arbeit, G. Archer, J. Biddle, S. Byrne, R. Goering, G. Hancock, G. A. Hebert, B. Hill, and R. Hollis, 1994. Comparison of traditional and molecular methods of typing isolates of *Staphylococcus aureus*. *J. Clin. Microbiol.* 32:407-415

4. Tenover, F.C., D. Arbeit, R.V. Goering, P.A. Mickelsen, B.E. Murray, D.H. Persing, and B. Swaminathan, 1995. Interpreting chromosomal DNA restriction patterns produced by pulsed-field gel electrophoresis: criteria for bacterial strain typing. *J. Clin. Microbiol.* 33:2233-2239

5. Beattie, S.H., C. Holt, D. Hirst, and A.G. Williams, 1998. Discrimination among *Bacillus cereus*, *B. mycoides* and *B. thuringiensis* and some other species of the genus *Bacillus* by Fourier transform infrared spectroscopy. *FEMS Microbiol. Lett.* 164:201-206

6. Franz, M, 1994. Identifizierung von Clostridien mittels FT-IR-Spektroskopie. *Dtsch. Milchwirtsch.* 3:130-132

7. Goodacre, R., E.M. Timmins, R. Burton, N. Kaderbhai, A.M. Woodward, D.B. Kell, and P.J. Rooney, 1998. Rapid identification of urinary tract infection bacteria using hyperspectral whole-organism fingerprinting and artificial neural networks. *Microbiology* 144:1157-1170

8. Helm, D., H. Labischinski, G. Schallehn, and D. Naumann, 1991. Classification and identification of bacteria by Fourier transform spectroscopy. *J. Gen. Microbiol.* 137:69-79

9. Holt, C., D. Hirst, A. Sutherland, and F. MacDonald, 1995. Discrimination of species in the genus *Listeria* by Fourier transform infrared spectroscopy and canonical variate analysis. *Appl. Environ. Microbiol.* 61:377-378

10. Johnesen, K., and P. Nielsen, 1998. Diversity of *Pseudomonas* strains isolated with King's B and Gould's S1 agar determined by repetitive extragenic palindromic-polymerase chain reaction, 16S rDNA sequencing and Fourier transform infrared spectroscopy characterization. *FEMS Microbiol. Lett.* 173:155-162

11. Kirschner, C., K. Maquelin, P. Pina, N.A. Ngo Thi, L-P. Choo-Smith, G.D. Sockalingum, C. Sandt, D. Ami, F. Orsini, S.M. Doglia, P. Allouch, M. Manfait, G.J. Puppels, and D. Naumann, 2001. Classification and identification of *Enterococci*: a comparative phenotypic, genotypic, and vibrational spectroscopic study. *J. Clin. Microbiol.* 39:1763-1770

12. Kümmerle, M., S. Scherer, and H. Seiler, 1998. Rapid and reliable identification of food-borne yeasts by Fourier-transform infrared spectroscopy. *Appl. Environ. Microbiol.* 64:2207-2214

13. Naumann, D., D. Helm, and H. Labischinski, 1991. Microbiological characterization by FTIR spectroscopy. *Nature* 351:81-82

14. Schmalrek, A., P. Tränkle, E. Vanca, and R. Blaschke-Hellmessen, 1998. Differentiation and characterization of *Candida albicans*, *Exophila dermatidis* and *Prototheca* spp. by Fourier-transform infrared spectroscopy (FTIR) in comparison with conventional methods. *Mycoses* 41:71-77

15. Seltmann, G., W. Voigt, and W. Beer, 1994. Application of physico-chemical typing methods for the epidemiological analysis of *Salmonella enteritidis* strains of phage type 25/17. *Epidemiol. Infect.* 113:411-424

16. Irmscher, H-M., R. Fischer, W. Beer, and G. Seltmann, 1999. Characterization of nosocomial *Serratia marcescens* isolates: Comparison of Fourier-trransform infrared spectroscopy with pulsed-field gel electrophoresis of genomic DNA fragments and multilocus enzyme electrophoresis. *Zbl. Bakteriol.* 289:249-263

17. Seltmann, G., W. Beer, H. Claus, and H. Seifert 1995. Comparative classification of *Acinetobacter baumannii* strains using seven different typing methods. *Zentbl. Bakteriol.* 282:372-383

18. Ngo Thi, N.A., C. Kirschner, and D. Naumann, 1999. FTIR microscopy: a rapid method for classifying microorganisms, *in* J. Greve, G.J. Puppels, and C. Otto (eds.), *Spectroscopy of Biological Molecules: New Directions*. Dordrecht: Kluwer. pp. 557-558.

19. Blair, J.E., and R. E. O. Williams, 1961. Phage typing of staphylococci. *Bull. WHO* 24:771-784

20. Vesanto, J., and E. Alhoniemi, 2000. Clustering of the self-organized map. *IEEE Trans. Neural Networks.* 11(3):586-600

21. Helm, D., H. Labischinski, and D. Naumann, 1991. Elaboration of a procedure for identification of bacteria using Fourier-rransform IR spectral libraries: a stepwise correlation approach. *J. Microbiol. Methods* 14:127-142

22. Helm, D., H. Labischinski, G. Schallehn, and D. Naumann, 1991. Classification and identification of bacteria by Fourier transform spectroscopy. *J. Gen. Microbiol.* 137:69-79

23. Naumann, D., D Helm, and H. Labischinski, 1991. Microbiological characterization by FT-IR spectroscopy. *Nature* 351:81-82

24. Naumann, D., 1998. Infrared and NIR Raman spectroscopy in medical microbiology. *Proc. SPIE* 3257 (*Infrared Spectroscopy: New Tool in Medicine*):245-257

25. Amiali, M.N., B. Berger-Bächi, K. Ehlert, M.R. Mulvey, A.A. Ismail, J. Sedman, and A.E. Simor, 2003. Rapid identification of methicillin-resistant *Staphylococcus aureus* (MRSA) by Fourier transform infrared (FTIR) spectroscopy. *Submitted*

26. Naumann, D., 1984. Some ultrastructural information on intact, living bacterial cells and related cell-wall fragments as given by FTIR. *Infrared Phys.* 24:233-238

27. Kummerle, M., S. Sherer, and H. Seiler, 1998. Rapid and reliable identification of food-borne yeast by Fourier-transformed infrared spectroscopy. *Appl. Environ. Microbiol.* 64:2207-2214

28. Magee, J., 1993. Whole-organism fingerprinting, *in* M. Goodfelow and A.G. O'Donnel (eds.), *Handbook of New Bacterial Systematics*. New York: Harcourt Brace, pp. 383-427

29. Bourne, R., U. Himmelreich., A. Sharma., C. Mountford, and T. Sorrel, 2001. Identification of *Enterococcus*, *Streptococcus*, and *Staphylococcus* by multivariate analysis of proton magnetic resonance spectroscopic data from plate cultures. *J. Clin. Microbiol.* 39:2916-2923

30. Torres, J., A. Kukol, J. Goodman, M, T. and Arkin, 2001. Site-specific examination of secondary structure and orientation determination in membrane proteins: the peptidic $^{13}C=^{18}O$ group as a novel infrared probe. *Biopolymers* 59:396-401.

31. Goodacre, R., B. Shann, R.J. Gilbert, E. Timmins, M. McGovern, C. Aoife, B. Alsberg, K. Kell, B. Douglas, and A. Niall, 2000. Detection of the dipicolinic acid biomarker in *Bacillus* spores using curie-point pyrolysis mass spectrometry and Fourier transform infrared spectroscopy. *Anal. Chem.* 72:119-127.

Table 6. 1. Spectral regions for differentiation of five Canadian epidemic MRSA (CMRSA) strains selected by visual inspection

Spectral regions (cm^{-1})	**Distinguishable CMRSA strain(s)**
1086-1049	CMRSA- 4
1123-1078	CMRSA-1 CMRSA-3 CMRSA-5
1174-1137	CMRSA-1 CMRSA-2 CMRSA-4
2904-2864	CMRSA-2

Figure 6.1: Sample preparation

a: Overnight subculture of CMRSA strains on tryptic soy with sheep blood agar at 37 °C

b: Culture of CMRSA strains on Universal Medium for 18 h at 37 °C

c: Collection of stationary-phase cells with 10-mm disposable loop

d: Four loops-full of stationary-phase cells suspended in 200 µl of physiological saline (0.9%)

e: 10-fold dilution of bacterial suspension in 100 µl of physiological saline

f: Drop of suspension (25 µl; ~5×10^{11} cells ml^{-1}) deposited on a ZnSe optical window

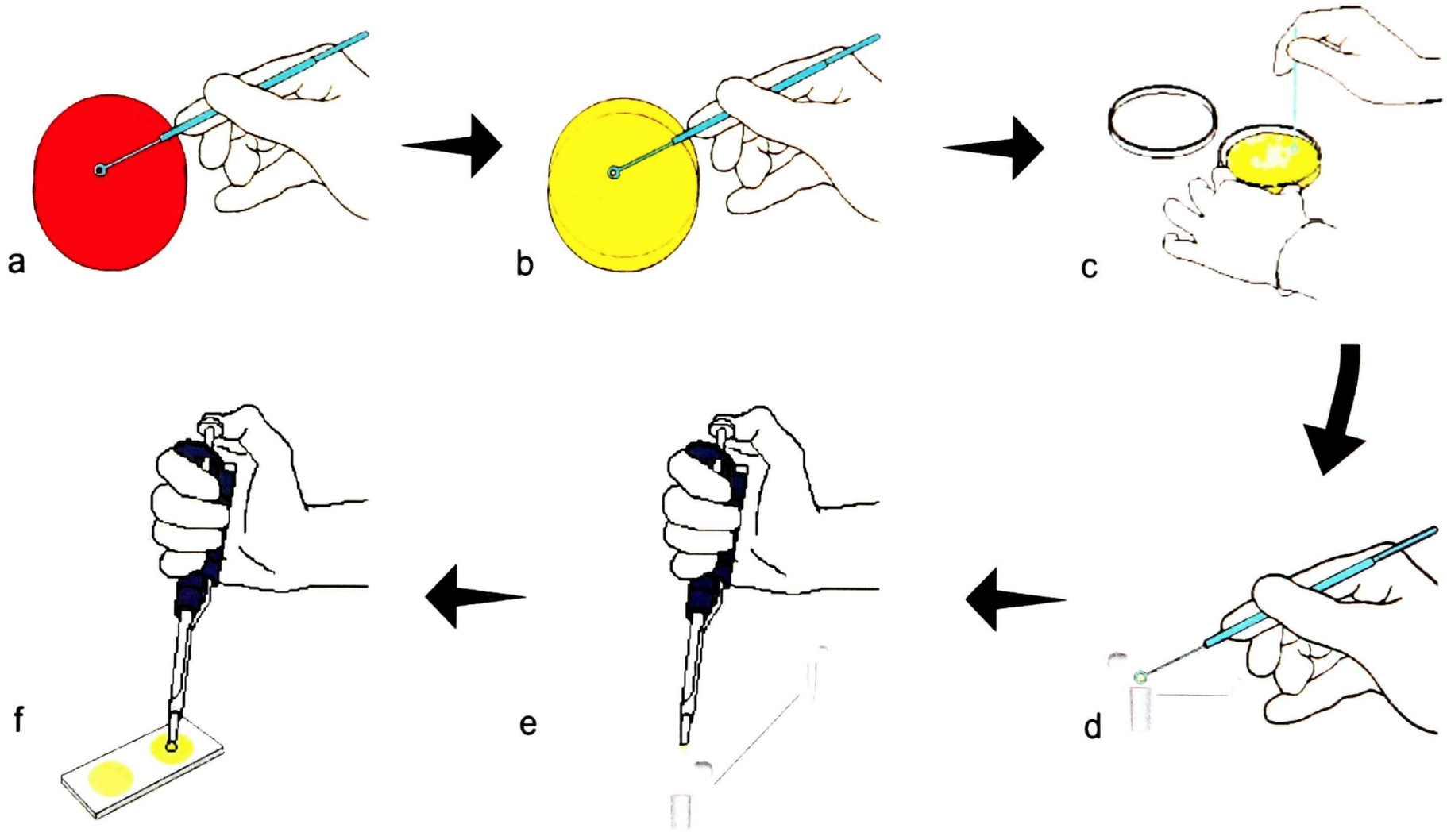
a
b
c
d
e
f

Figure 6.2: FTIR spectral acquisition

Light emitted from the IR source (**1**) is passed into an interferometer (**2**), where "spectral encoding" takes place, producing an interferogram signal. The beam enters the sample compartment, where it is transmitted through the surface of the sample (**3**). The interferogram signal is altered by absorption of energy of specific frequencies by the sample. The beam then passes to the detector (**4**), which measures the interferogram signal. The measured signal is digitized and sent to the computer (**5**), where it is Fourier transformed to yield an FTIR spectrum

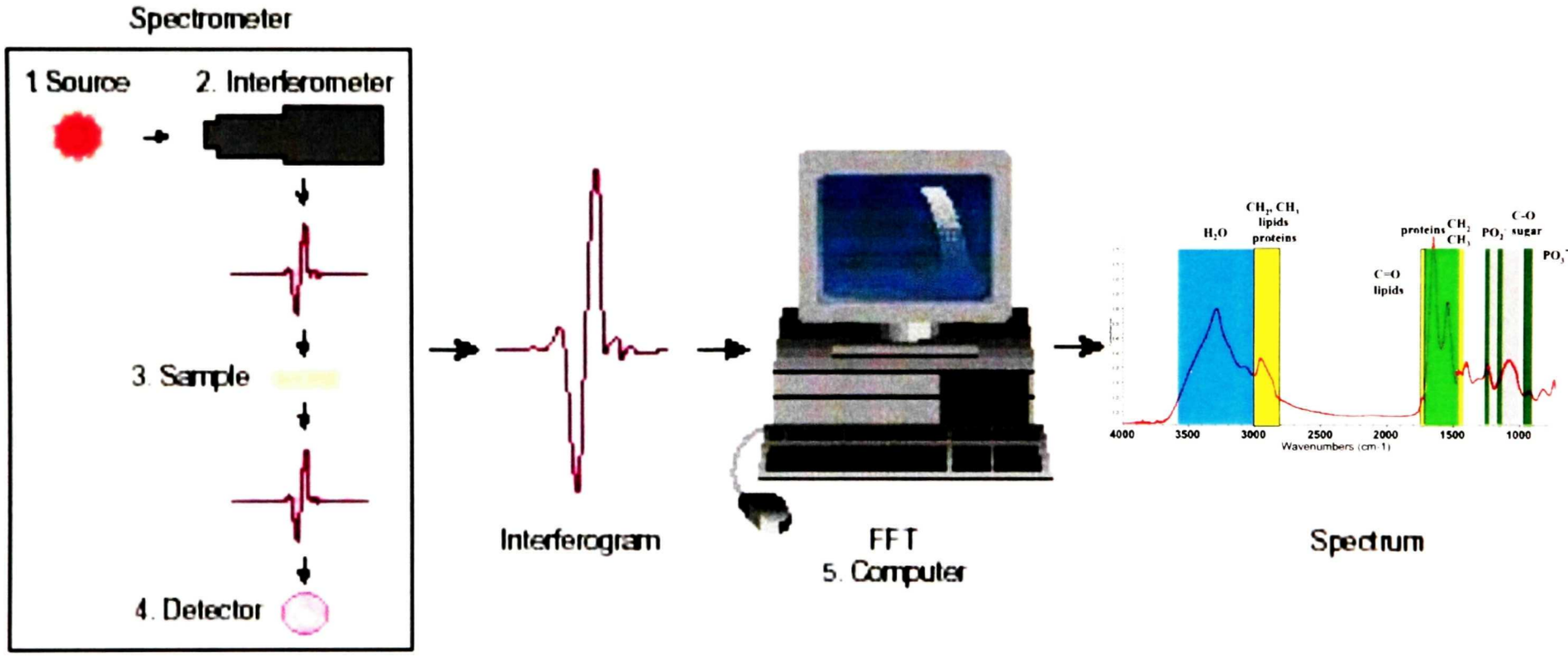
Spectrometer
1 Source
2. Interferometer
3. Sample
4. Detector
Interferogram
FFT
5. Computer
H_2O
CH_2, CH_3 lipids proteins
proteins CH_2 CH_3
C=O lipids
PO_2^-
C-O sugar
PO_3^{--}
4000
3500
3000
2500
2000
1500
1000
Wavenumbers (cm-1)
Spectrum

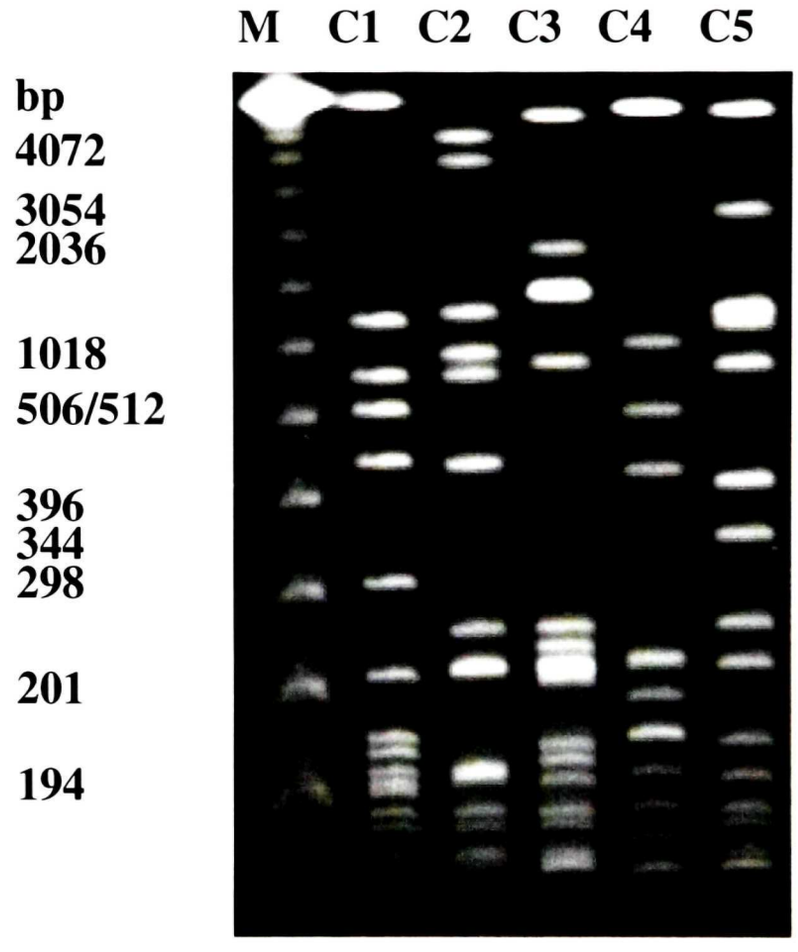

Figure 6.3: Representative DNA profiles obtained by PFGE of *SmaI* digests from five Canadian epidemic strains of MRSA (CMRSA). Lane 1, lambda DNA concatamers; lane 2, CMRSA-1; lane 3, CMRSA-2; lane 4, CMRSA-3; lane 5, CMRSA-4; lane 6, CMRSA-5

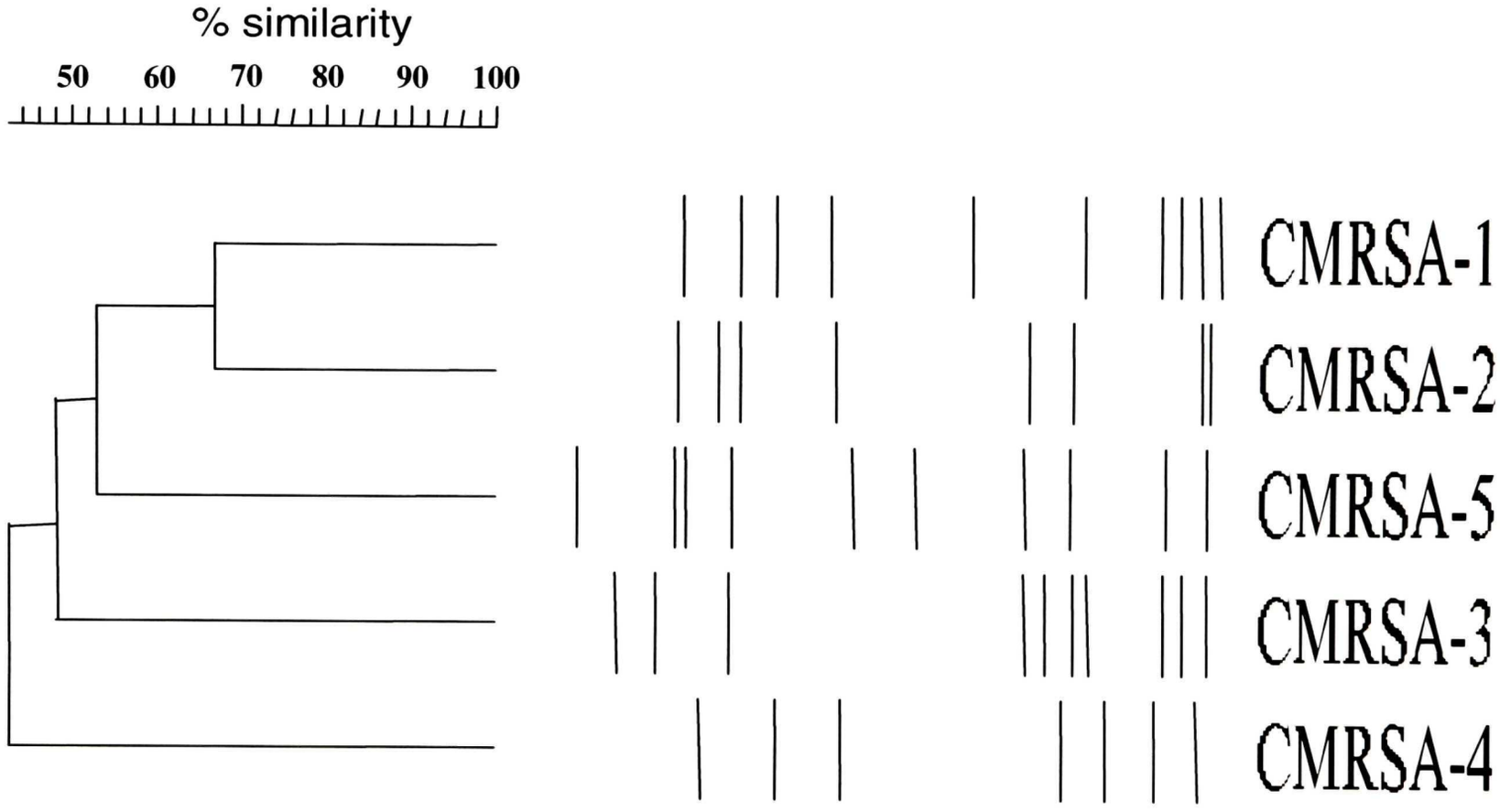

Figure 6.4: Dendrogram generated for DNA profiles obtained by PFGE of *SmaI* digests from five CMRSA strains

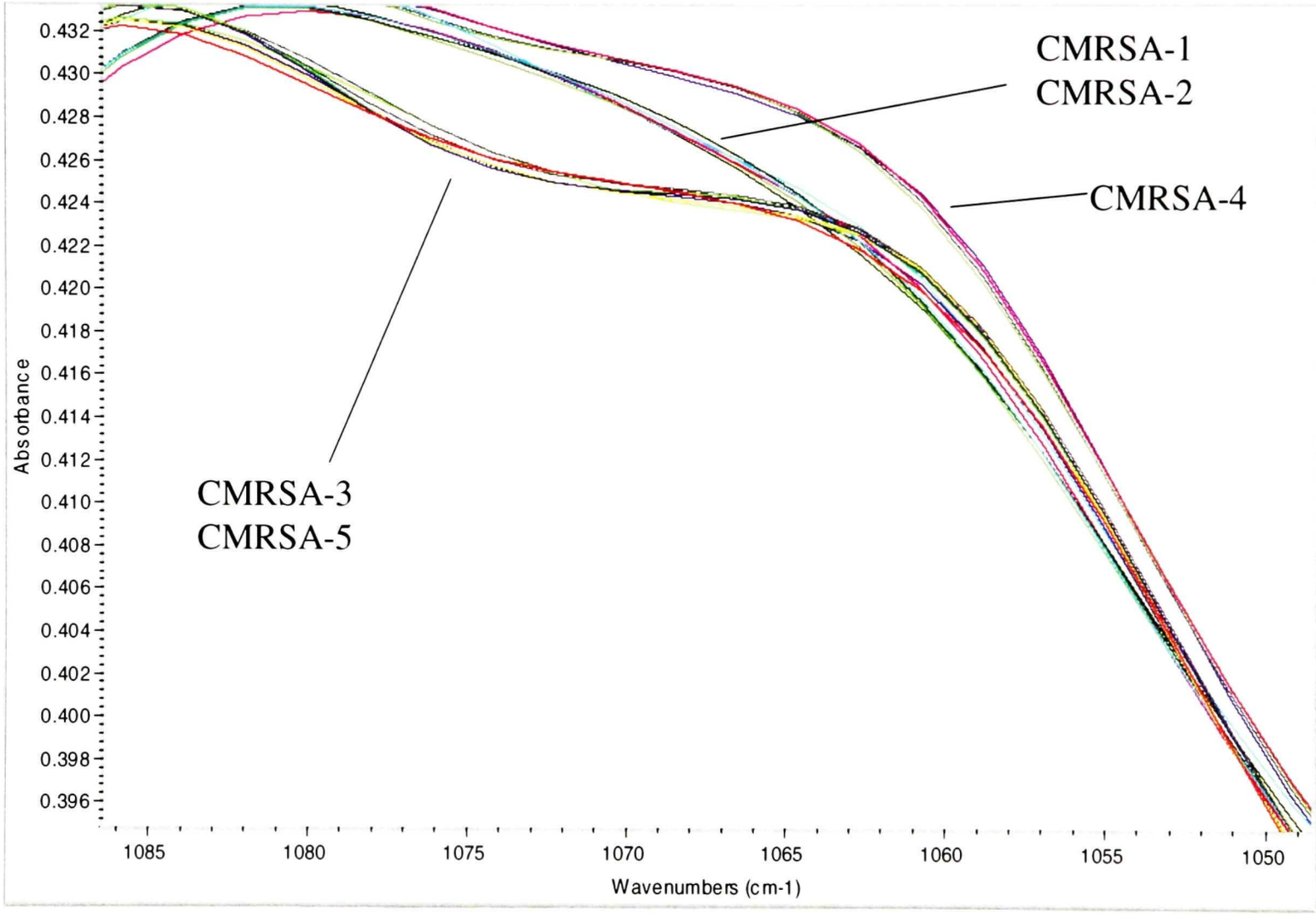

Figure 6.5: FTIR spectra of five CMRSA strains in the region 1086-1049 cm^{-1}

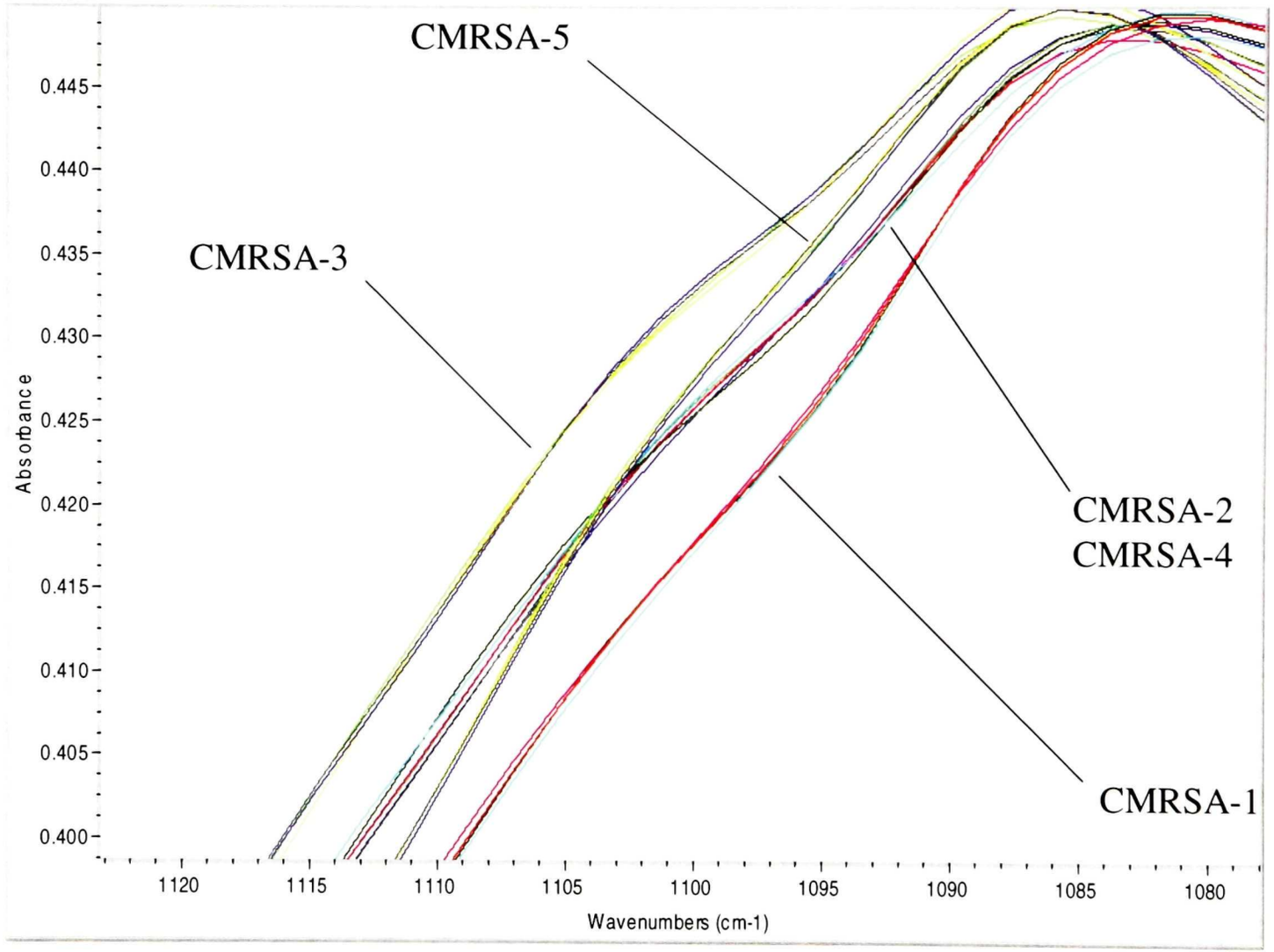

Figure 6.6: FTIR spectra of five CMRSA strains in the region 1116-1080 cm^{-1}

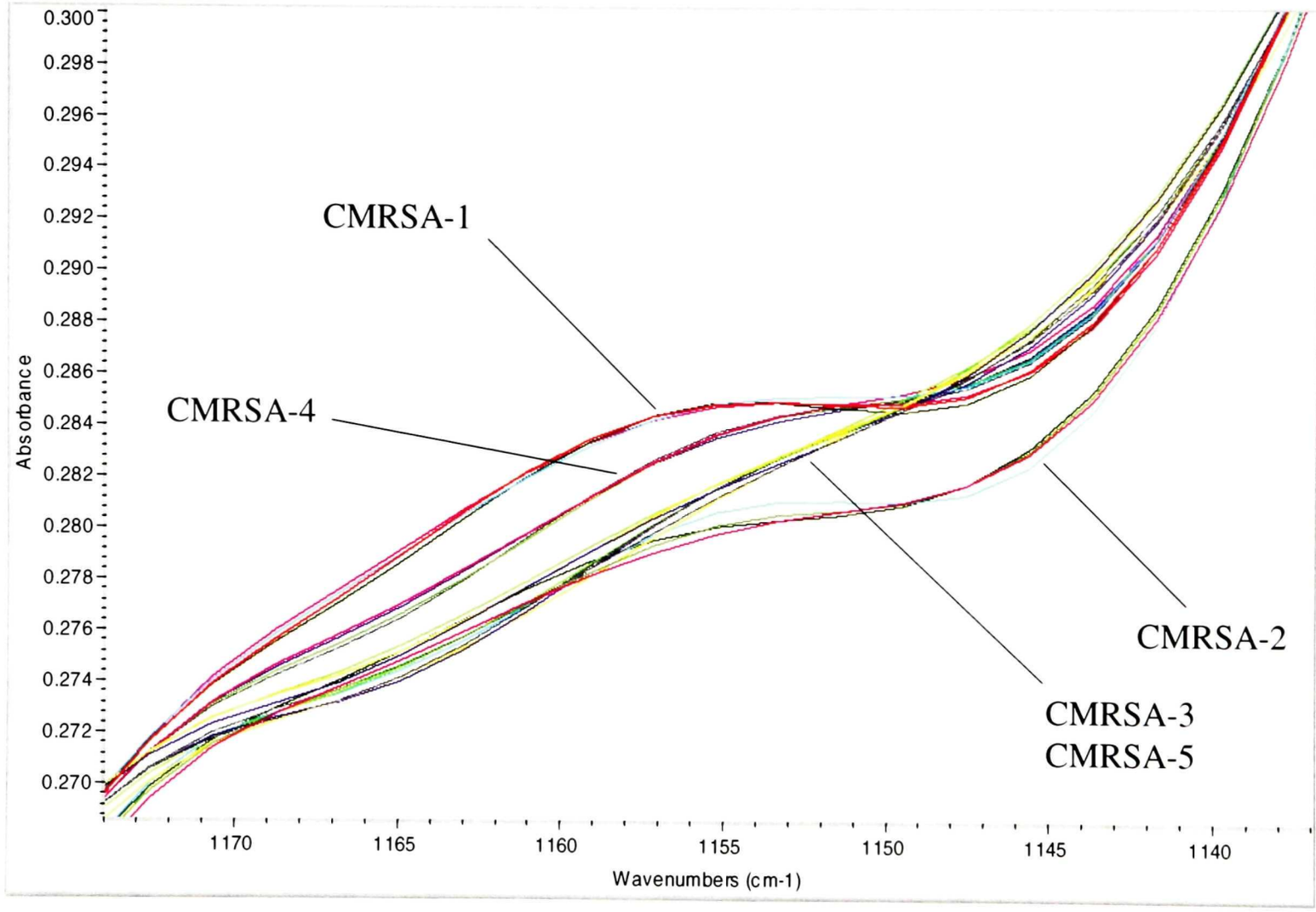

Figure 6.7: FTIR spectra of five CMRSA strains in the region 1174-1140 cm^{-1}

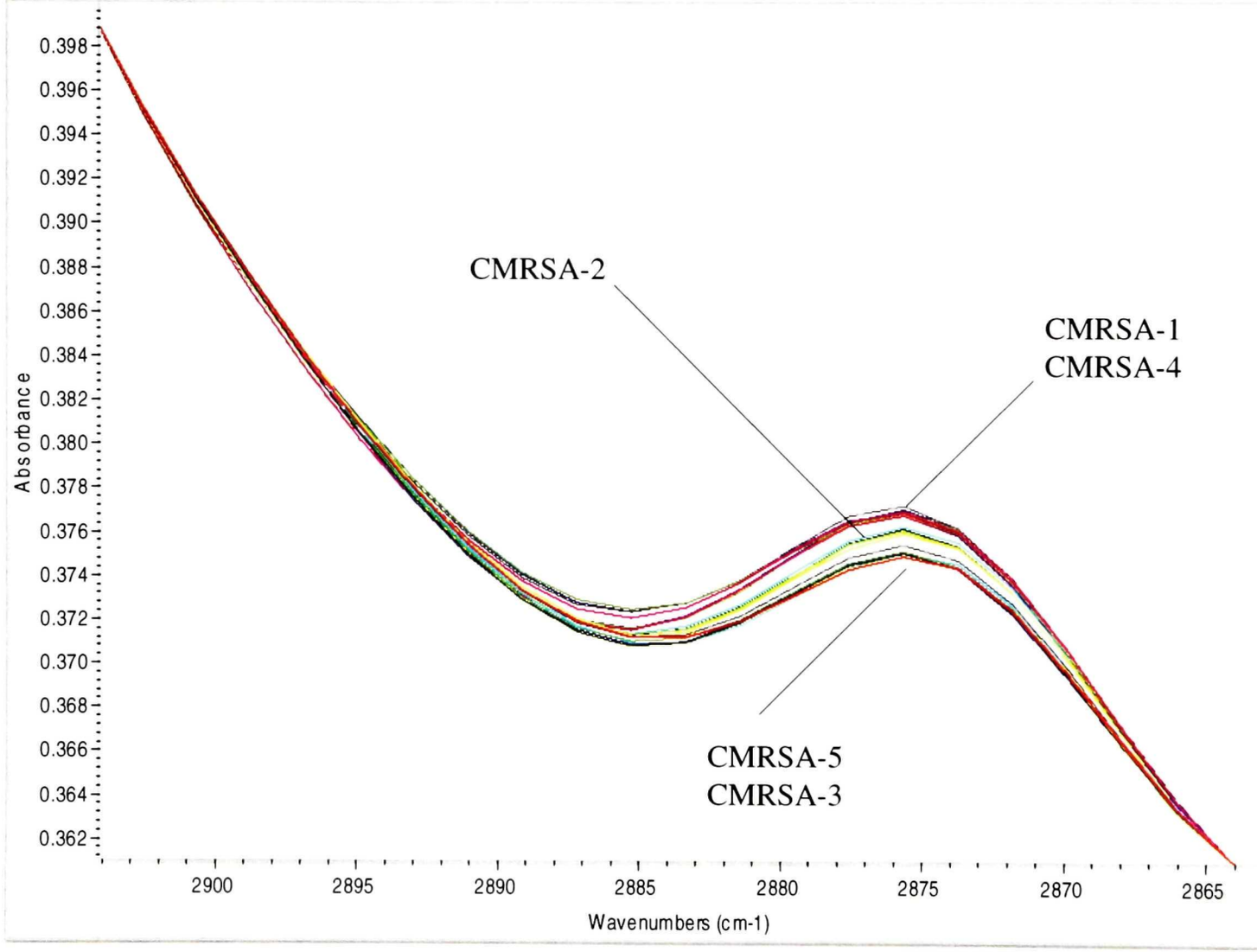

Figure 6.8: FTIR spectra of five CMRSA strains in the region 2904-2864 cm^{-1}

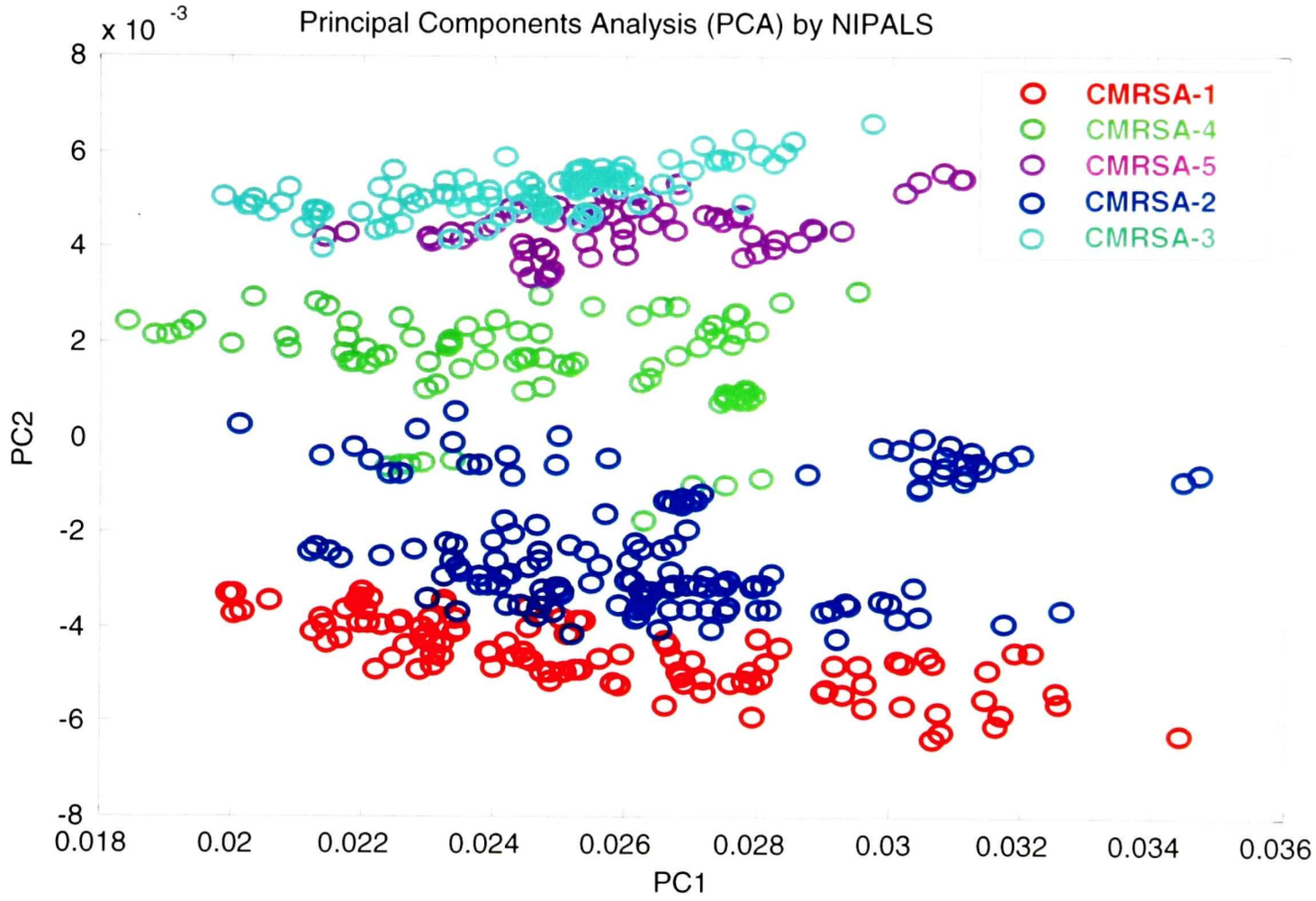

Figure 6.9: Scores plot for first two PCs obtained from the spectral data for 24 CMRSA-1, 26 CMRSA-2, 15 CMRSA-3, 12 CMRSA-4 and 8 CMRSA-5 strains in the regions 1096-1066, 1114-1099 and 2914-2880 cm^{-1} by PCA using the NIPALS algorithm

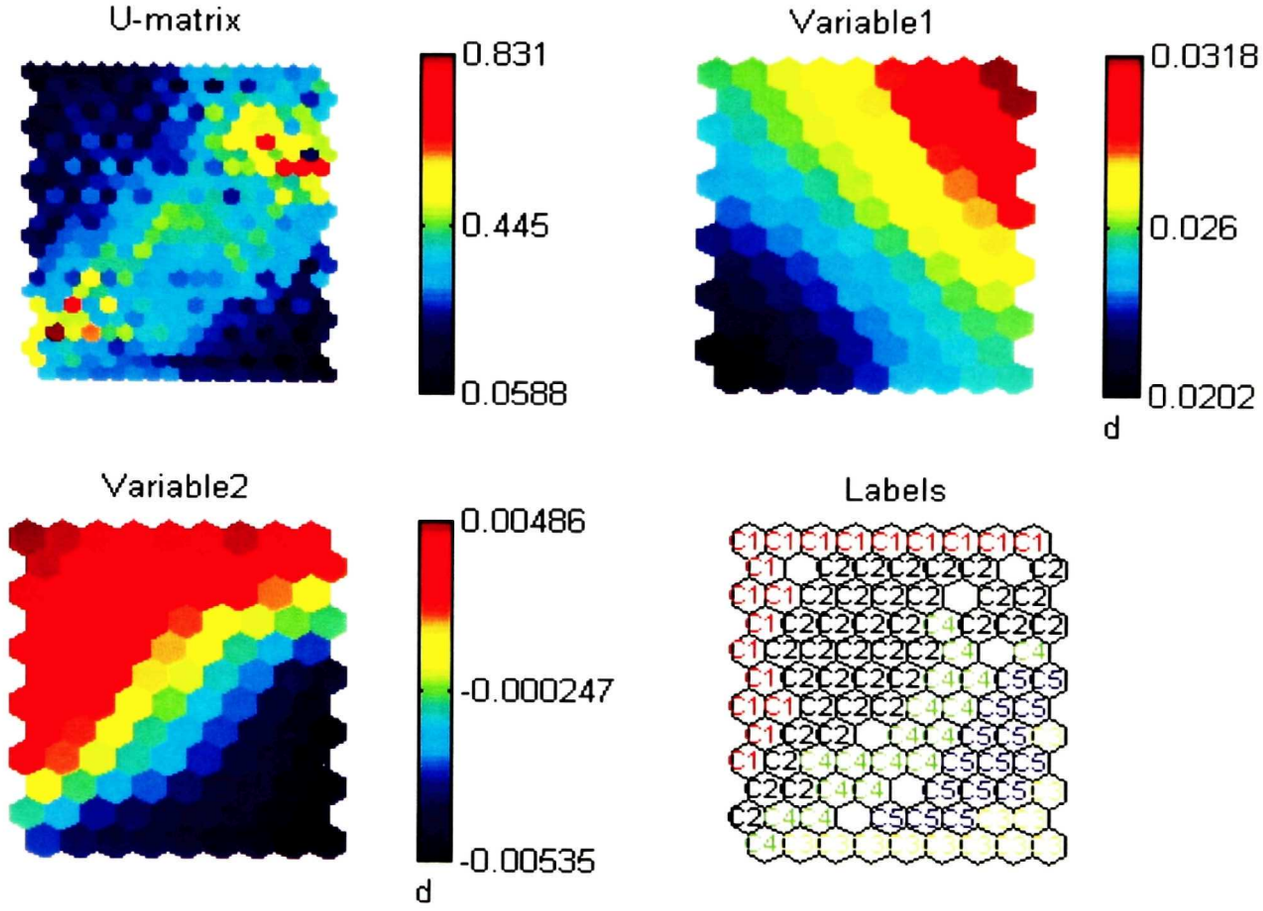

Figure 6.10a: U-matrix, component plane, and SOM obtained by application of the SOM algorithm using the spectral data for 24 CMRSA-1 (C1), 26 CMRSA-2 (C2), 15 CMRSA-3 (C3), 12 CMRSA-4 (C4) and 8 CMRSA-5 (C5) strains in the regions 1096-1066, 1114-1099 and 2914-2880 cm^{-1}

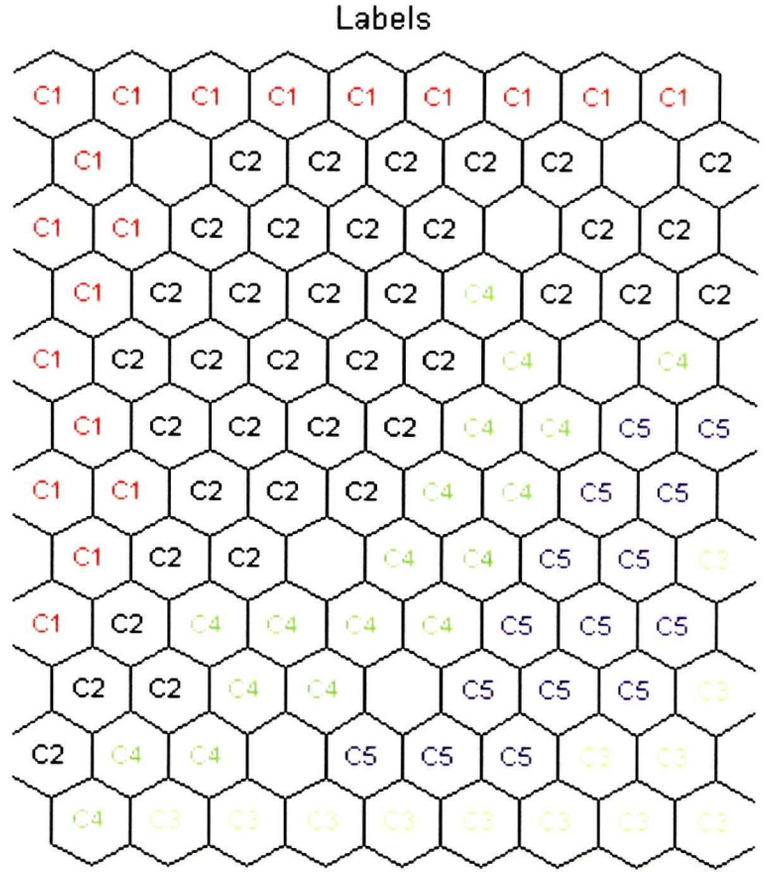

Figure 6.10b: Expanded view of the SOM shown in Figure 6.10a

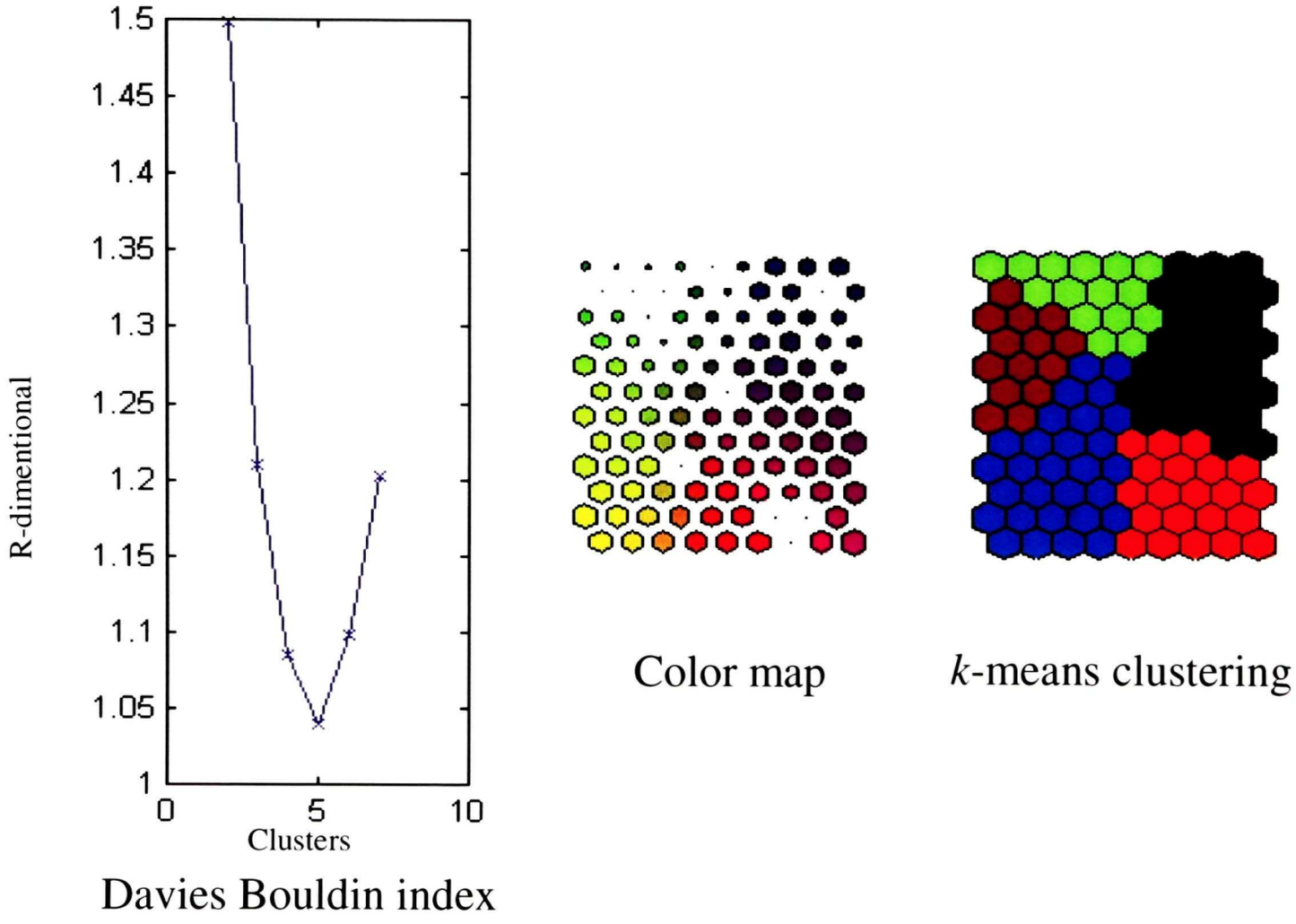

Figure 6.11: Partitioned SOM for the spectral data in the regions 1096-1066, 1114-1099 and 2914-2880 cm^{-1} obtained by applying the *k*-means algorithm and the Davies-Bouldin index

CHAPTER 7

CONNECTING STATEMENT

In Chapter 3, the potential utility of FTIR spectroscopy for the detection of methicillin-resistant *S. aureus* (MRSA) strains was demonstrated, and the advantage of implementing such a method in a clinical setting so that appropriate therapy and intervention for cross-infection control can be initiated in a timely manner was described. In the latter context, the capability to differentiate between epidemic (EMRSA) and sporadic (SMRSA) strains is important as the institution of strict infection control measures is only required in the case of EMRSA infections. In the research described in Chapter 6, five epidemic Canadian MRSA clones (CMRSA-1 to CMRSA-5) were differentiated by FTIR spectroscopy. The extension of this work to the differentiation of these CMRSA strains from SMRSA is described in the following chapter.

CHAPTER 7

DISCRIMINATION BETWEEN EPIDEMIC AND SPORADIC ISOLATES OF METHICILLIN-RESISTANT *STAPHYLOCOCCUS AUREUS* (MRSA) STRAINS BY FOURIER TRANSFORM INFRARED (FTIR) SPECTROSCOPY

7.1 ABSTRACT

The incidence of methicillin-resistant *Staphylococcus aureus* (MRSA) has been increasing throughout the world over the past few decades, causing outbreaks or epidemics of hospital infections. Epidemic strains (EMRSA) are differentiated from nonepidemic or sporadic strains (SMRSA) by their ease of transmission, long-term persistence, rapid interhospital spread, and ability to cross geographic and continental boundaries. Therefore, an efficient diagnostic test for the accurate detection of MRSA strains with epidemic spreading capacity is essential to be able to apply appropriate infection control and prevention measures most effectively. However, no specific diagnostic assay for the discrimination of EMRSA from SMRSA based on genetic or biochemical markers is yet available. To investigate the potential utility of FTIR spectroscopy for the identification of EMRSA clones, the FTIR spectra of 25 EMRSA and 22 SMRSA strains were recorded from dried films of stationary-phase cells grown on UM™. Spectra were normalized and transformed to first-derivative spectra prior to exploratory data analysis, performed using principal component analysis (PCA) and self-organizing maps (SOM), and cluster analysis based on the K-nearest neighbor (KNN) algorithm. Although visual inspection of selected spectra suggested that the SMRSA and EMRSA strains could be differentiated on the basis of either of two narrow regions of their FTIR spectra (940-929 and 1346-1306 cm^{-1}), only the 940-929 cm^{-1} region proved suitable for accurate classification of MRSA isolates as sporadic or epidemic. The use of the spectral data in the 940-929 cm^{-1} yielded 100% correct classification of the spectra in an independent test set, confirming that FTIR spectroscopy is a promising diagnostic tool for the discrimination of EMRSA from SMRSA.

7.2 INTRODUCTION

Outbreaks of hospital-acquired infections due to methicillin-resistant *Staphylococcus aureus* (MRSA) are being reported with increasing frequency, challenging clinicians and infection control teams throughout the world [1,2]. Based on epidemiological evidence, it has been suggested that some MRSA strains have properties that enable them to disseminate particularly well [3], the term epidemic MRSA (EMRSA) being used to designate clinically or epidemiologically relevant strains that have been identified in patients or staff members from five or more hospitals sites or from three or more geographic regions within the country. By comparison to non-epidemic or sporadic (SMRSA) strains, EMRSA strains appear to be able to spread more rapidly or easily among patients within hospitals and, once introduced into an institution, mainly in intensive care units (ICU), are difficult to control and eradicate. SMRSA strains are mostly acquired in hospitals by long-term-care patients and lack the capacity to spread extensively [4].

Accurate discrimination between EMRSA and SMRSA strains and detection of a discriminative biochemical marker by a single reliable assay would allow a more selective implementation of strict infection control measures to prevent dissemination of MRSA strains within hospitals. It may also provide insight into the bacterial factors involved in epidemic spread. Several attempts to identify markers for the discrimination of EMRSA and SMRSA using antibiotyping, protein A (*spaA* typing) gene polymorphism analysis [5], coagulase gene restriction fragment length polymorphism (RFLP) analysis [6], or binding to extracellular matrix proteins [7] were investigated in the past decades. Epidemic MRSA strains were reported to have a lower level of protein A expression and a higher level of coagulase expression than non-epidemic SMRSA strains [5]. Protein A gene polymorphism analysis indicated that strains with more than seven repeats in the X region of protein A tended to be epidemic, while the presence of seven or fewer repeats was indicative of non-epidemic MRSA strains [8]. EMRSA was found to bind significantly less to extracellular protein fibrinogen and Fc fragments of immunoglobulin G [7]. However, none of these methods were able to differentiate between EMRSA and SMRSA [4]. Traditional phenotypic typing methods such as phage

typing have also been used in attempts to discriminate between EMRSA and SMRSA. However, although there is a preponderance of certain phage types in epidemic strains [9], the association of phage type and epidemic character is not rigorous enough to be of prognostic value [9]. The only available genotyping methods for the recognition of epidemic MRSA strains are macrorestriction *Sma*I digest DNA using pulsed–field gel electrophoresis (PFGE) and *mec* DNA characteristics using ribotyping. The recognition of EMRSA and SMRSA strains is based on arbitrary comparison of genetic characteristics (*Sma*I DNA digest-PFGE patterns, genomic background or *mec* DNA) of the unknown to those of already known epidemic and sporadic strains [10,11] and does not rely on any genetic or biochemical markers. Both genotyping techniques are appropriate and adequate to define MRSA clones and enable the detection of widely spread MRSA clonal lineages rather than for discrimination of EMRSA from SMRSA. Therefore, efforts should be directed at the development of a diagnostic tool for differentiation of SMRSA and EMRSA based on genetic or biochemical markers.

In the present work, an evaluation of the use of FTIR spectroscopy for differentiating between EMRSA and SMRSA strains and for the detection of appropriate biochemical markers was undertaken. The applicability of FTIR spectroscopy as an analytical tool in the field of microbiology has already been persuasively demonstrated [12-17]. This biophysical technique allows the differentiation of intact microbial cells nondestructively and without the use of any reagents by producing complex, reproducible and distinct fingerprint-like spectral signatures (Figure 7.1). Because FTIR spectroscopy measures molecular vibrations, the spectral fingerprint signatures represent the overlap of the spectral signatures of all vibrationally active biochemical components (including DNA, RNA, proteins, membrane and cell wall components) of the whole cell. Thus, the differences in biochemical composition among different strains result in differences in the FTIR spectra of the strains, with sufficient discriminatory power to distinguish microbial cells at different taxonomic levels, at the strain level and even down to the subtype level [12,18].

FTIR spectroscopy has been shown to be a rapid, reliable, and highly sensitive method for microbial analyses and process control [14,18]. It is also considered a promising diagnostic tool in clinical microbiology. FTIR spectroscopy was recently employed for epidemiological typing of nosocomial yeasts [19-21], algae [19], *Salmonella enteritidis* [22], *Serratia marcescens* [23], and *Acinetobacter baumannii* [24]. Subtyping of yeasts by FTIR spectroscopy has also been reported for food-borne yeasts [25]. Moreover, only recently, epidemiological typing of epidemic MRSA strains was reported [26]. In this latter work, five epidemic Canadian MRSA clones (CMRSA-1 to CMRSA-5) were differentiated by FTIR spectroscopy, enabling the detection of widely spread epidemic MRSA clonal lineages such as MRSA phage type 95 among the clonal lineages [27]. The present study extends this work to the differentiation of EMRSA from SMRSA.

7.3 MATERIALS AND METHODS

The feasibility of employing FTIR spectroscopy for the differentiation between EMRSA and SMRSA strains was evaluated using 47 clinical isolates of MRSA, consisting of 25 EMRSA (CMRSA) and 22 SMRSA strains (set I). These strains were kindly provided by the Canadian Nosocomial Infection Surveillance Program (CNISP). An additional set of 25 MRSA strains obtained from the Laboratoire de Santé Publique du Québec (LSPQ) and 25 subtypes of CMRSA-1 to CMRSA-5 obtained from CNISP were employed as an independent test set (set II). Stock cultures were stored at -70 °C in brain heart infusion (BHI) broth containing 15% glycerol.

7.3.1 Microbiological methods

7.3.1.1 Antimicrobial susceptibility testing

Resistance to oxacillin was confirmed by growth on an oxacillin agar screen plate (Mueller-Hinton agar supplemented with 4% NaCl and oxacillin, 6 μg/ml) incubated at 35 °C for 24 h [28]. MICs to oxacillin, clindamycin, erythromycin, ciprofloxacin, fusidic acid, mupirocin, rifampin, vancomycin, teicoplanin, tetracycline, and trimethoprim-

sulfamethoxazole (TMP-SMZ) were determined by broth microdilution in accordance with National Committee for Clinical Laboratory Standards guidelines [28].

7.3.1.2 MRSA screen assay

All isolates were confirmed as MRSA by simultaneous detection of the *mecA* and *nucA* genes by multiplex polymerase chain reaction (PCR). Primer sequences designed to detect the *mecA* gene and PCR conditions were as described by Louie *et al.* [29] Thermocycling conditions, using a GeneAmp 9600 thermocycler (Perkin-Elmer Cetus), were as follows: 95 °C for 2 min followed by 25 cycles of 94 °C for 15 s, 55 °C for 15 s, and 72 °C for 15 s. PCR amplicons were visualized on a 1% agarose gel after staining with ethidium bromide and were photographed under UV illumination.

7.3.1.3 Molecular typing by PFGE

MRSA isolates were typed by PFGE following DNA extraction and digestion with *SmaI* [30]. PFGE-generated DNA profiles were digitized into the GelCompar computer software program (Version 4.1; GelCompar, Kortrijk, Belgium) for analysis. DNA fragments of each gel were normalized using the molecular weight standard run on each gel to allow comparisons between different gels. A 1.8% band tolerance was selected for use during comparisons of DNA profiles. Cluster analysis was performed by the unweighted pair group method, using arithmetic averages (UPGMA), and DNA relatedness was calculated on the basis of the Dice coefficient. Isolates were considered to be genetically related if their macrorestriction DNA patterns differed by <7 bands [31] and the Dice coefficient of correlation was ≥75%.

Definition of EMRSA versus SMRSA and analysis of strain relatedness

MRSA strains were classified as EMRSA if isolates were recognized to be clinically or epidemiologically significant (e.g., associated with outbreaks of infection in health care facilities and spread among patients), the strain was identified among patients or staff members from ≥5 hospital sites or from ≥3 geographic regions in Canada, and all

the isolates were genetically related and had been characterized by standard methods [32]. Strains were classified as SMRSA if they were recovered from only one patient.

Genetic relatedness was based on the results of DNA macrorestriction analysis [30]. Identification of EMRSA and SMRSA strains was based on comparison of their *SmaI*-DNA pattern to those of already known EMRSA and SMRSA strains. Isolates were classified as genetically closely related to an EMRSA strain if their macrorestriction pattern differed from that of the EMRSA strain by changes consistent with a single genetic event, which typically results in a two- to three-band difference. These isolates showed a Dice coefficient of correlation of 80% or more with EMRSA. Isolates were classified as possibly genetically related to an EMRSA strain if their macrorestriction pattern differed from that of the EMRSA strain by changes consistent with two independent genetic events, i.e., a four- to six-band or greater difference and a Dice coefficient of correlation of 60% or less.

Banding patterns were compared visually by two independent observers and by calculating the Dice coefficient of correlation (number of shared fragments × 2 × 100/total number of fragments in the two samples; [33]) with the GelCompar software (Applied Maths, Kortrijk, Belgium). Epidemiological relatedness was based on data obtained by analysis of patients' charts. The isolates were considered epidemiologically related to EMRSA when they were recovered during the same time frame or from the same area during the patient's hospital stay, according to the guidelines proposed by Tenover *et al.* [31].

7.3.1.4 Phage typing

MRSA strains were phage typed according to the method of Blair and Williams [34], using the basic international set of typing phages. All phages were used at 100 × routine test dilution.

7.3.2 FTIR spectroscopic methods

7.3.2.1 Sample preparation

Following an overnight subculture on tryptic soy with sheep blood agar (TSB; Quelab Laboratories Inc., Montreal, PQ, Canada) at 37 °C, a single bacterial colony was collected from the TSB plate and streaked onto a universal medium (UM™) agar plate (Quelab Laboratories Inc., Montreal, PQ, Canada) with the use of a four-quadrant streak pattern. After 18 h at 37 °C, four loops-full of stationary-phase cells were carefully collected using a 10-mm-diameter disposable loop from the third quadrant of the agar surface and suspended in 200-µl aliquots of sterile physiological saline (0.9% NaCl). A 25-µl aliquot of the 10-fold diluted bacterial suspension (~5×10^{11} cells ml^{-1}) was deposited onto the center of a zinc selenide (ZnSe) optical window and then oven-dried at 48 °C for 1 hour to form a thin and transparent homogeneous dried film suitable for FTIR spectral acquisition in the transmission mode. The ZnSe window was placed in a custom-made holder that shielded the spectrometer optics from the bacteria to prevent contamination.

7.3.2.2 FTIR spectral acquisition

Spectra were recorded in quadruplicate for each strain in the region between 4000 and 400 cm^{-1} on a Bomem MB FTIR spectrometer (ABB-Bomem, Quebec, PQ, Canada) equipped with a deuterated triglycine sulfate (DTGS) detector and a KBr beam splitter and operating under Bomem-Grams/386 software (Galactic, Salem, NH). The spectrometer was continuously purged by dry air from a Balston dryer (Balston, Lexington, MA) to reduce the spectral contributions of atmospheric water vapor and CO_2. Spectra were acquired by co-addition of 64 scans collected at 4 cm^{-1} resolution and ratioed against an open-beam background to produce absorbance spectra.

7.3.3 Multivariate data processing and preprocessing

The collected spectral data, stored in Grams SPC format, were converted into CSV format and then into MAT format using Matlab version 5.1 (The MathWorks, Inc., Natick, MA). Prior to data pre-processing and processing, optimal spectral features selection was performed by singular-value decomposition (SVD) using randomly

selected EMRSA/SMRSA pairs of spectra. Spectra over the whole spectral range (4000-400 cm^{-1}) were normalized to unit height by vector transformation and were transformed to first-derivative spectra using a 5-point Savitzky-Golay filter to maximize peak separation, enhance apparent resolution of superimposed bands, and minimize problems arising from unavoidable baseline shifts. Exploratory data analysis was performed using principal component analysis (PCA) employing the NIPALS algorithm and self-organizing maps (SOM) clustered by the *k*-means algorithm. Cluster analysis was applied to normalized and first-derivatized spectral data using the K-nearest neighbor (KNN) algorithm. A program was written in Matlab to implement the preprocessing and processing algorithms of the spectral data.

7.4 RESULTS AND DISCUSSION

7.4.1 Spectral feature selection

Optimal differentiation of closely related strains by FTIR spectroscopy is generally achieved by basing the analysis of the spectral data on specific spectral features or narrow spectral regions that reflect the differences between the strains rather than on the whole spectrum, or large regions of it. Spectral regions of potential use for the differentiation of SMRSA from EMRSA were selected by the application of SVD in order to discover subtle differences in the spectra that would be difficult to detect by the naked eye. SVD of randomly chosen pairs of spectra of SMRSA and EMRSA isolates showed significant differences in two narrow regions, 940-929 cm^{-1} and 1346-1306 cm^{-1}. Visual inspection of the spectra confirmed that there were distinct differences in the absorption bands of SMRSA and EMRSA strains in both spectral regions as shown in Figures 7.2 and 7.3, respectively.

7.4.2 Differentiation between SMRSA and EMRSA using the infrared spectral region between 940 and 929 cm^{-1}

7.4.2.1 Principal component analysis (PCA)

PCA is commonly employed to reduce the dimensionality of spectral data and obtain preliminary information about the distribution of the data. PCA was applied to the

first-derivative spectral data in the region 940-929 cm^{-1} for set I, comprising the normalized spectra of 25 EMRSA (CMRSA) and 22 SMRSA isolates recorded in quadruplicate. The eigenvalue plot indicated that the first three principal components (PCs) were significant (Figure 7.4). When the scores of the first two PCs were plotted against each other (PC1 vs. PC2), two distinct clusters could be detected on the plot (Figure 7.5) and were confirmed to represent the complete separation of the SMRSA and EMRSA isolates. Since PCA is an unsupervised technique, this separation was obtained without the use of information about the class assignment of the samples and is indicative of definitive spectral differences between the EMRSA and SMRSA isolates. Furthermore, 100% correct classification of the strains in the independent test set (set II) was subsequently achieved based on these spectral differences.

7.4.2.2 Self-organizing map (SOM)

Information about the spatial relationships and clustering of the data can be obtained by visual inspection of an SOM generated by using an unsupervised neural network algorithm. The scores of the first two PCs from set I were input into an SOM algorithm, and the network was trained using a rough training phase of 3 epochs and a fine-tuning phase of 10 epochs with initial learning rates 0.5 and 0.05, respectively. The learning rate decreased linearly to zero during the fine-tuning phase. Visual inspection of the labeled SOM, shown in Figure 7.6, indicated the presence of two clusters corresponding to SMRSA and EMRSA. Partitioning of the SOM by applying the *k*-means algorithm and the Davies-Bouldin index confirmed the presence of two clusters (Figure 7.7), although the Davies-Bouldin index plot had several local minima. However, the rate of correct classification of SMRSA and EMRSA strains based on the partitioned SOM was only 85%.

7.4.2.3 Clustering by K-nearest neighbors (KNN) algorithm

Supervised cluster analysis was performed by applying the KNN algorithm to the spectral data in the region 940-929 cm^{-1} using half of the spectra in set I as the training set (n = 94) and the other half as the prediction set. All the spectra in the prediction set

were correctly classified with all K values used (K = 1-10). In addition, 100% correct classification was also obtained with the independent test set (set II).

7.4.3 Differentiation of SMRSA and EMRSA using the region 1346-1306 cm^{-1}

7.4.3.1 Principal component analysis (PCA)

As described above, the first step in the data processing was to apply PCA to the normalized first-derivative spectral data for set I (Figure 7.8). PC1 accounted for 88.9% of the total variance, and a scores plot for PC1 vs. PC2 (Figure 7.9) revealed a clustering of the data that corresponded to a clear separation of the EMRSA and SMRSA isolates into two distinct groups. However, one EMRSA isolate fell within the SMRSA cluster, and one SMRSA isolate fell within the EMRSA cluster, yielding a rate of correct classification of 96%. This result indicated that the 940-929 cm^{-1} region is more appropriate for the differentiation of SMRSA and EMRSA.

7.4.3.2 Self-organizing map (SOM)

The eigenvalue plot obtained by PCA for the region 1346-1306 cm^{-1} showed a plateau at seven PCs (Figure 7.8). Accordingly, the scores of the first seven PCs for set I were input into an SOM algorithm, and the network was again trained using a rough training phase of 3 epochs and a fine-tuning phase of 10 epochs with initial learning rates 0.5 and 0.05, respectively. Based on visual inspection of the labeled SOM (Figure 7.10), the SMRSA and EMRSA isolates were fairly well separated into two clusters, corresponding to a rate of correct classification of 87%. However, the Davies-Bouldin index plot obtained upon partitioning of the SOM by the *k*-means algorithm indicated the presence of five clusters (data not shown). Accordingly, the SOM results confirmed that use of spectral data in the 1346-1306 cm^{-1} region is not effective for the differentiation between SMRSA and EMRSA isolates.

7.5 CONCLUDING REMARKS

The results obtained in this study indicate that FTIR spectroscopy can provide a rapid and accurate means for the discrimination between EMRSA and SMRSA strains,

thereby allowing timely implementation of measures to minimize the spread of EMRSA among patients within hospitals. The successful differentiation between EMRSA and SMRSA isolates achieved in this study was based solely on spectral differences in a very narrow region of the infrared spectrum (940-929 cm^{-1}). As seen in Figure 7.2, which shows the range between 955 and 925 cm^{-1} in the normalized spectra of a set of four SMRSA and four EMRSA isolates, this region contains a single band centered at ~936 cm^{-1}, the intensity of which is higher in the spectra of the SMRSA isolates. Such an intensity difference likely indicates differences in the relative amounts of a specific biomarker. Although it may also arise from differences in absorptivity resulting from interactions of the biomarker with its surroundings, such changes in the absorptivity of an infrared absorption band are often accompanied by a shift of the peak maximum. Thus, since the difference in the band intensity at 936 cm^{-1} seen in Figure 7.2 is not accompanied by any significant shift of the peak maximum, it is likely that the spectral differences that allowed for the differentiation between EMRSA and SMRSA isolates can be attributed to changes in the concentration of the biomarker. However, the assignment of the 936 cm^{-1} band to a specific biochemical component of the cell is extremely difficult owing to the numerous possible origins of spectral absorptions in this region of the infrared spectrum and was beyond the scope of the present work.

In this context, it is also of interest to note that although band intensity differences between randomly selected SMRSA and EMRSA strains were also apparent in the region 1346-1306 cm^{-1}, as seen in Figure 7.3, the use of spectral data in this region was not effective for the differentiation between SMRSA and EMRSA isolates..This finding highlights the critical importance of region selection in the development of FTIR methods for the differentiation of closely related strains.

7.6 REFERENCES

1. Brumfit, W., and J. Hamilton-Miller, 1989. Methicillin-resistant *Staphylococcus aureus*. *N. Engl. J. Med.* 320:1188-1196

2. Struelens, M.J., O. Ronveaux, B. Jans, and R. Mertens, 1996. Methicillin-resistant *Staphylococcus aureus* epidemiology and control in Belgium, 1991 to 1995. *Infect. Control Hosp. Epidemiol.* 17:503-508

3. Phillips, I., 1991. Epidemic potential and pathogenicity in outbreaks with EMRSA and EMREC. *J. Hosp. Infect.* 18(Suppl. A):197-201

4. Hoefnagels-Schuremans, A., W.E. Peetermans, M.J. Struelens, S. Van Lierde, and J. Van Eldere, 1997. Clonal analysis and identification of epidemic strains of methicillin-resistant *Staphylococcus aureus* by antibiotyping and determination of protein A gene and coagulase gene polymorphisms. *J. Clin. Microbiol.* 35:2514=2520

5. Roberts, J.I.S., and M.A. Gaston, 1987. Protein A and coagulase expression in epidemic and non epidemic *Staphylococcus aureus*. *J. Clin. Pathol.* 40:837-840

6. Goh, S., S.K. Byrne, J.L. Zhang, and A.W. Chow, 1992. Molecular typing of *Staphylococcus aureus* on the basis of coagulase gene polymorphism. *J. Clin. Microbiol.* 30:1642-1645.

7. Voss, A., D. Milatovic, C. Wallrauch-Schwarz, V.T. Rosdahl, and I. Braveny, 1994. Methicillin resistant *Staphylococcus aureus* in Europe. *Eur. J. Clin. Microbiol. Infect. Dis.* 13:50-55.

8. Frénay, H.M.E., J.P.G. Theelen, L.M. Schouls, C.M.J.E. Vandenbrouke-Grauls, J. Verhoef, W.J. van Leeuwen, and F.R. Mooi, 1994. Discrimination of epidemic and non epidemic methicillin-resistant *Staphylococcus aureus* strains on the basis of protein A gene polymorphism. *J. Clin. Microbiol.* 32:846-847

9. Marples, R.R., and S. Reith, 1992. Methicillin-resistant *Staphylococcus aureus* in England and Wales. *Commun. Dis. Res.* 2:25-29

10. Salmenlinna, S., and J. Vuopio-Varkila, 2001. Recognition of two groups of methicillin-resistant *Staphylococcus aureus* strains based on epidemiology, antimicrobial susceptibility, hypervariable-region type, and ribotype in Finland. *J. Clin. Microbiol.* 39:2243-2247

11. Simor, A.E., M. Ofner-Agostini, E Bryce, A. McGeer, S. Paton, M.R. Mulvey, and Canadian Hospital Epidemiological Committee and Canadian Nosocomial Infection Surveillance Program, Health Canada, 2002. Laboratory characterization of methicillin-resistant *Staphylococcus aureus* in Canadian hospitals: Results of 5 years of national surveillance, 1995-1999. *J. Infect. Dis.* 186:652-660

12. Helm, D., H. Labischinski, and D. Naumann, 1991. Classification and identification of bacteria by Fourier transform spectroscopy. *J. Gen. Microbiol.* 137:69-79

13. Naumann, D., D. Helm, and H. Labischinski, 1991. Microbiological characterization by FT-IR spectroscopy. *Nature* 351:81-82

14. Naumann, D., D. Helm, H. Labischinski, and P. Giesbrecht, 1991. The characterization of microorganisms by Fourier-transform infrared spectroscopy, *in* W.H. Nelson (ed.), *Modern Techniques for Rapid Microbiological Analysis.* New York: VCH Publishers. p. 43

15. Goodacre, R., E.M. Timmins, P.J. Rooney, J.J. Rowland, and D.B. Kell, 1996. Rapid identification of *Streptococcus* and *Enterococcus* species using diffuse reflectance-absorbance Fourier transform infrared spectroscopy and artificial neural networks. *FEMS Microbiol. Lett.* 140:233-239

16. Bouhedja, W., G.D. Sockalingum, P. Pina, P. Allouch, C. Bloy, R. Labia, J.M. Millot, and M. Manfait, 1997. ATR-FTIR spectroscopy investigation of *E. coli* transconjugants ß-lactams-resistance phenotype. *FEBS Lett.* 412:39-42

17. Sockalingum, G.D., W. Bouhedja, P, Pina, P. Allouch, C. Mandray, R. Labia, J.M. Millot, and M. Manfait, 1997. ATR-FTIR spectroscopic investigation of imipenem-susceptible and-resistant *Pseudomonas aeruginosa* isogenic strains. *Biochem. Biophys. Res. Commun.* 232:240-246

18. Mariey, L., J.P. Signolle, C. Amiel, and J. Travert, 2001. Discrimination, classification, identification of microorganisms using FTIR spectroscopy and chemometrics. *Vibr. Spectrosc.* 26:151-159

19. Schmalrek, A., P. Tränkle, E. Vanca, and R. Blaschke-Hellmessen, 1998. Differentiation and characterization of *Candida albicans*, *Exophila dermatidis* and *Prototheca* spp. by Fourier-transform infrared spectroscopy (FTIR) in comparison with conventional methods. *Mycoses* 41:71-77

20. Sockalingum, G.D., C. Sandt, D. Gomez, P. Pina, I. Beguinot, F. Witthuhn, D Aubert, P. Allouch, J.M. Pinon, and M. Manfait, 2002. FTIR characterization of *Candida* species: a study on some reference strains and pathogenic *C. albicans* isolates from HIV+ patients. *Vibr. Spectrosc.* 28:137-146

21. Tintelnot, K., G. Haase, M. Seibold, F. Bergmann, M. Staemmler, T. Franz, and D. Naumann, 2000. Evaluation of phenotypic markers of selection and identification of *Candida dubliniensis*. *J. Clin. Microbiol.* 38:1599-1608

22. Seltmann, G., W. Voigt, and W. Beer, 1994. Application of physico-chemical typing methods for the epidemiological analysis of *Salmonella enteritidis* strains of phage type 25/17. *Epidemiol. Infect.* 113:411-424.

23. Irmscher, H-M., R. Fischer, W. Beer, and G. Seltmann, 1999. Characterization of nosocomial *Serratia marcescens* isolates: Comparison of Fourier-transform infrared spectroscopy with pulsed-field gel electrophoresis of genomic DNA fragments and multilocus enzyme electrophoresis. *Zbl. Bakteriol.* 289:249-263

24. Seltmann, G., W. Beer, H. Claus, and H. Seifert, 1995. Comparative classification of *Acinetobacter baumannii* strains using seven different typing methods. *Zbl. Bakteriol.* 282: 372-383

25. Kümmerle, M., S. Scherer, and H. Seiler, 1998. Rapid and reliable identification of food-borne yeasts by Fourier-transform infrared spectroscopy. *Appl. Environ. Microbiol.* 64:2207-2214

26. Amiali, M.N., B. Berger-Bachi,, K. Ehlert, M.R. Mulvey, A.A. Ismail, J. Sedman, and A.E. Simor, 2003. Rapid identification of methicillin-resistant *Staphylococcus aureus* (MRSA) by Fourier transform infrared (FTIR) spectroscopy. *Submitted.*

27. Amiali, M.N., M.R. Mulvey, B. Berger-Bächi, A.A. Ismail, J. Sedman, and A.E. Simor, 2003. Epidemiological typing of methicillin-resistant *Staphylococcus aureus* (MRSA) strains by Fourier transform infrared (FTIR) spectroscopy. *Submitted.*

28. National Committee for Clinical Laboratory Standards, 1999. Performing Standards for Antimicrobial Sucseptibility Testing-Eighth Informational Supplement: Approved Standards M7-A4. NCCLS, Wayne, PA.

29. Louie, L., S.O. Matsumura, E. Choi, M. Louie, and A.E. Simor, 2000. Evaluation of three rapid methods for detection of methicillin resistance in *Staphylococcus aureus*. *J. Clin. Microbiol.* 38:2170-2173

30. Mulvey, M.R., L. Chui, J. Ismail, L. Louie, C. Murphy, N. Chang, M. Alfa, and Canadian Committee for the Standardization of Molecular Methods, 2001. Development of a Canadian standardization protocol for subtyping methicillin-resistant *Staphylococcus aureus* (MRSA) using pulsed-field gel electrophoresis. *J. Clin. Microbiol.* 39:3481-3485

31. Tenover, F.C., D. Arbeit, R.V. Goering, P.A. Mickelsen, B.E. Murray, D.H. Persing, and B. Swaminathan, 1995. Interpreting chromosomal DNA restriction patterns produced by pulsed-field gel electrophoresis: criteria for bacterial strain typing. *J. Clin. Microbiol.* 33:2233-2239

32. Simor, A.E., D. Boyd L. Louie, A. McGeer, M.R. Mulvey, and B.M. Willey for the Canadian Hospital Epidemiology Committee and the Canadian Nosocomial Infection Surveillance Program, 1999. Characterization and proposed nomenclature of epidemic strains of MRSA in Canada. *Can. J. Infect. Dis.* 10:333-336

33. Dice, L.R., 1945. Measures of the amount of ecological association between species. *Ecology* 26:297-302

34. Blair, J.E., and R.E.O. Williams, 1961. Phage typing of staphylococci. *Bull. WHO* 24:771-784

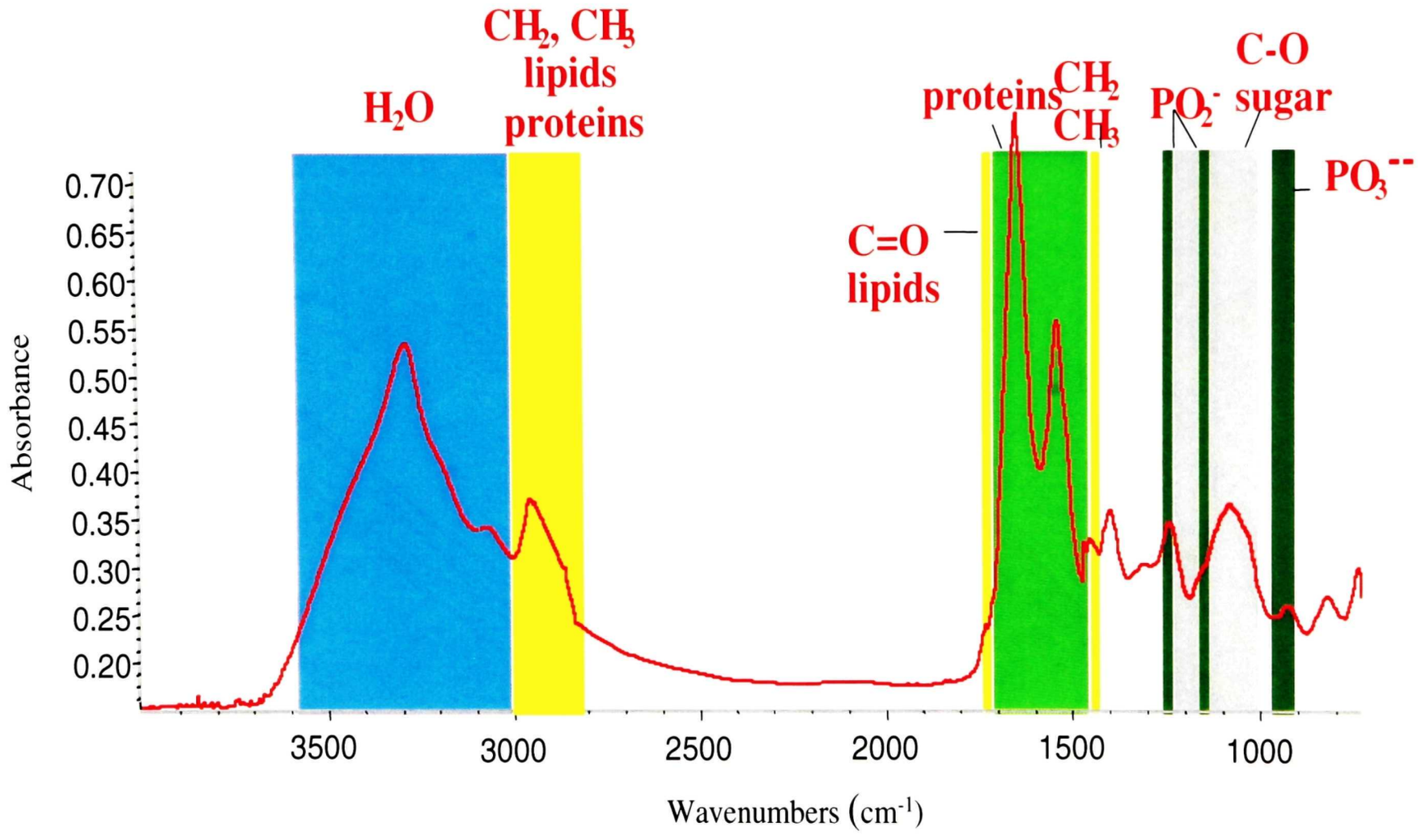

Figure 7.1: Typical FTIR spectrum of bacteria cells

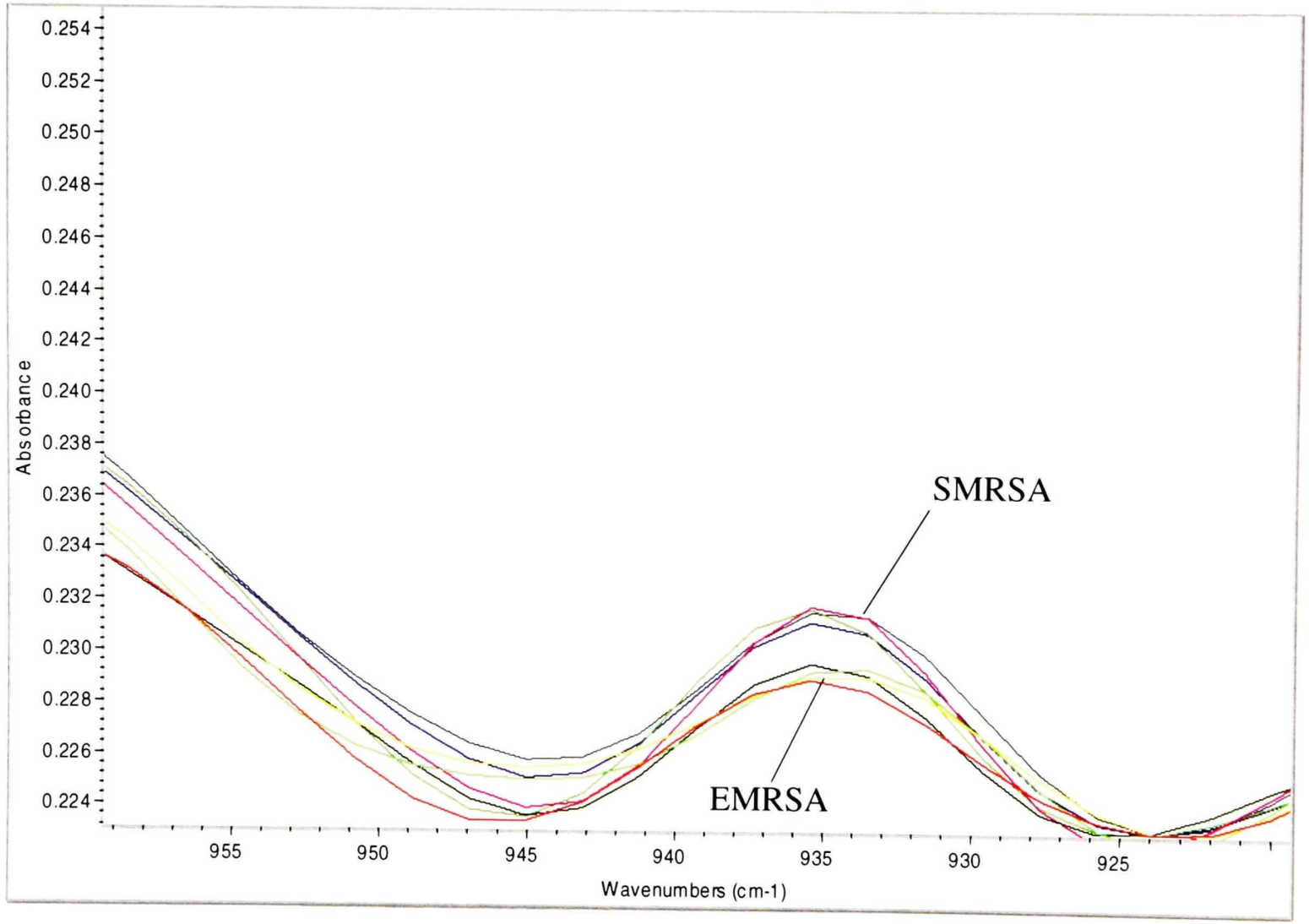

Figure 7.2: FTIR spectra of EMRSA and SMRSA strains in the region 955-915 cm^{-1}

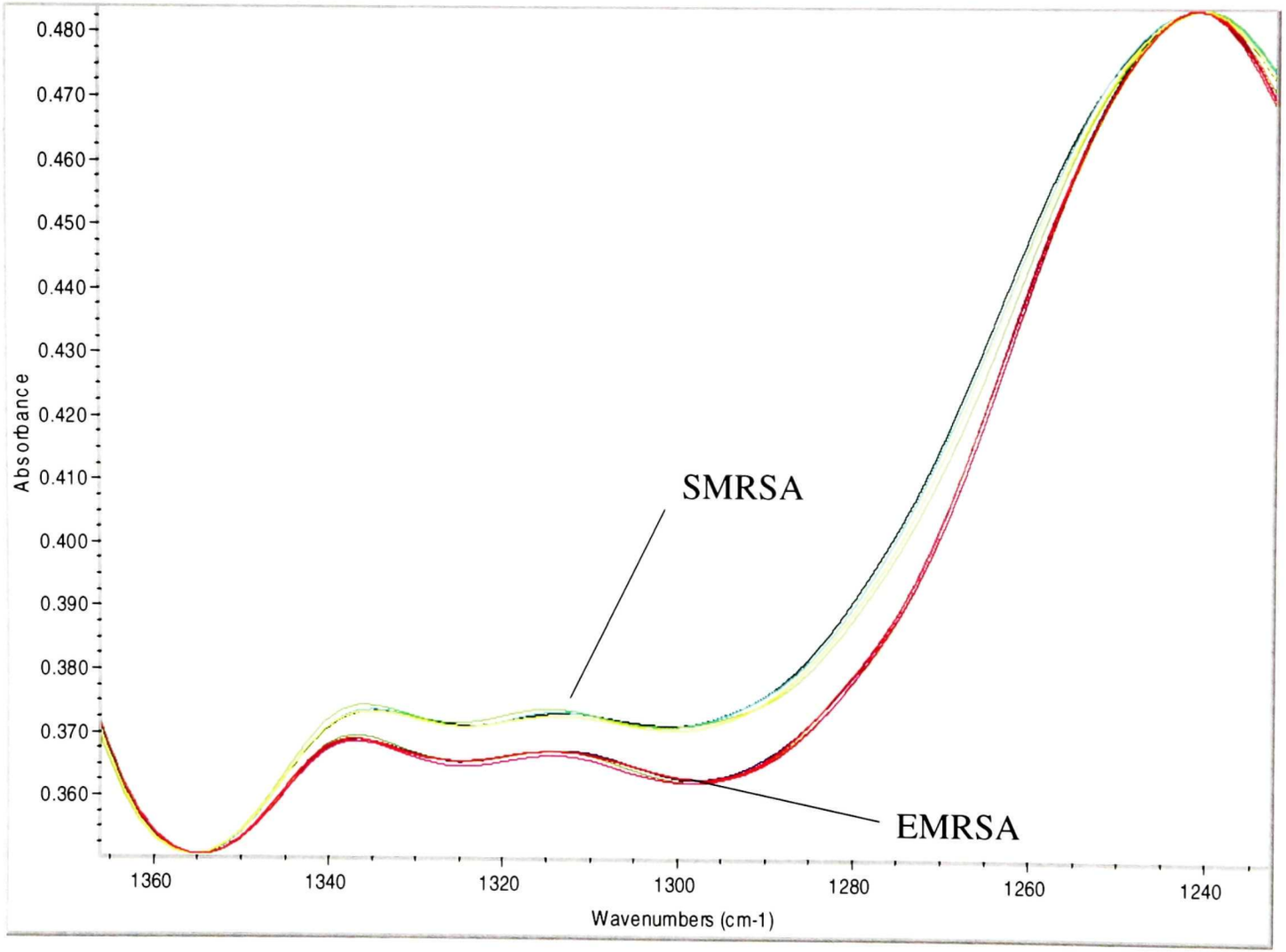

Figure 7.3: FTIR spectra of EMRSA and SMRSA strains in the region 1360-1240 cm^{-1}

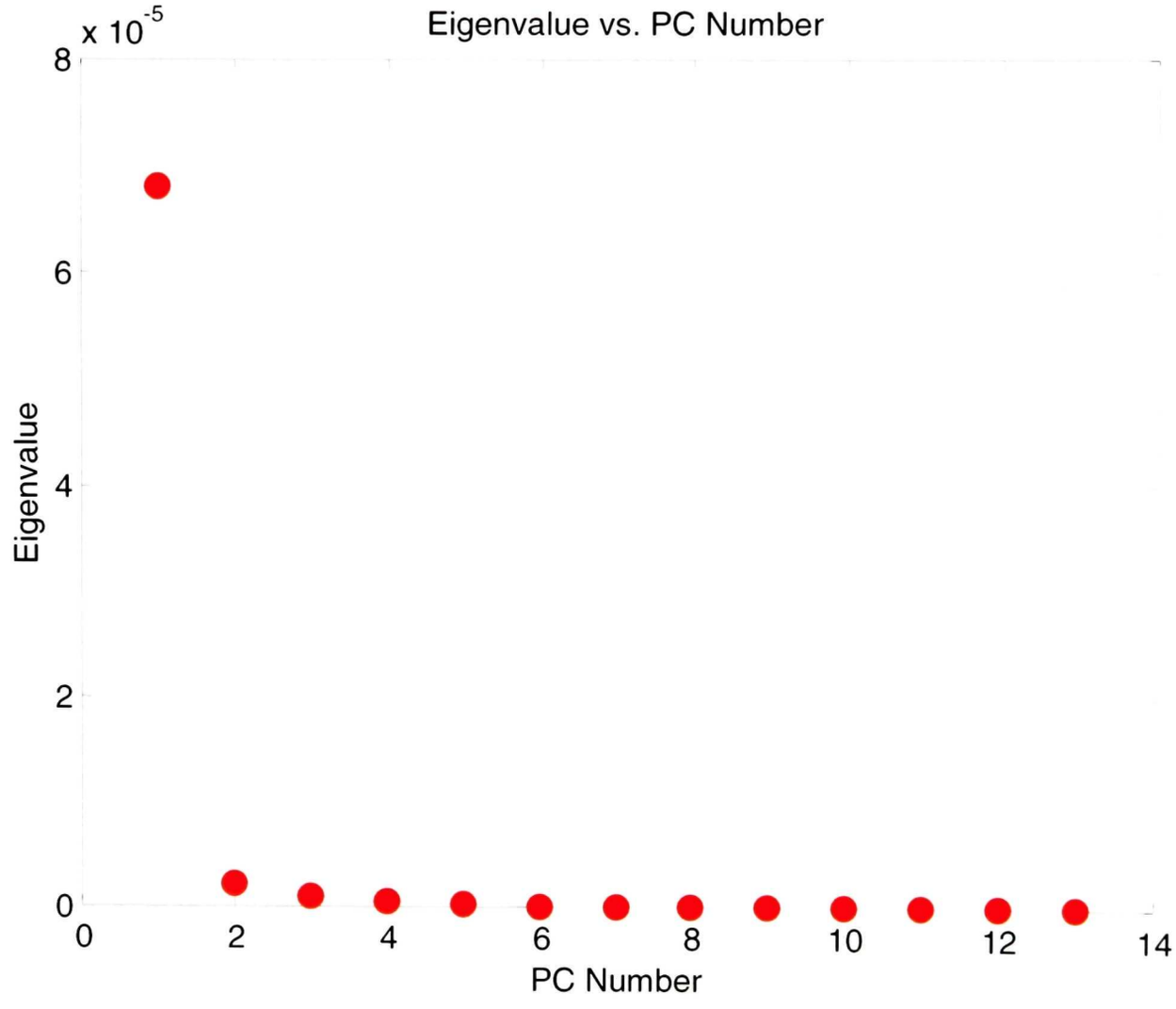

Figure 7.4: Eigenvalue plot obtained by PCA based on the spectral data for 25 EMRSA and 22 SMRSA strains in the region 940-929 cm^{-1}

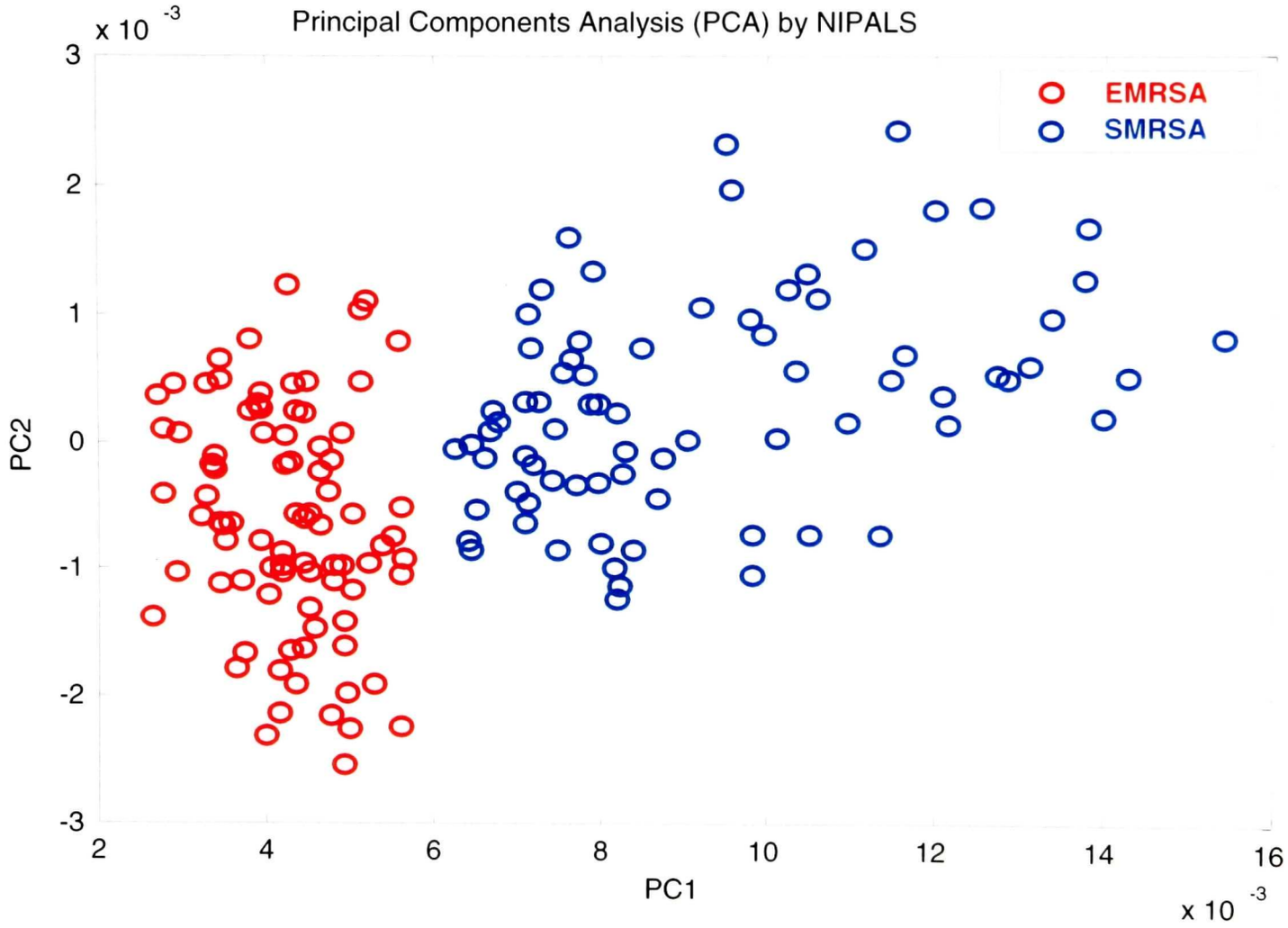

Figure 7.5: Scores plot for first two PCs obtained from the spectral data for 25 EMRSA and 22 SMRSA strains in the region 940-929 cm^{-1} by PCA using the NIPALS algorithm

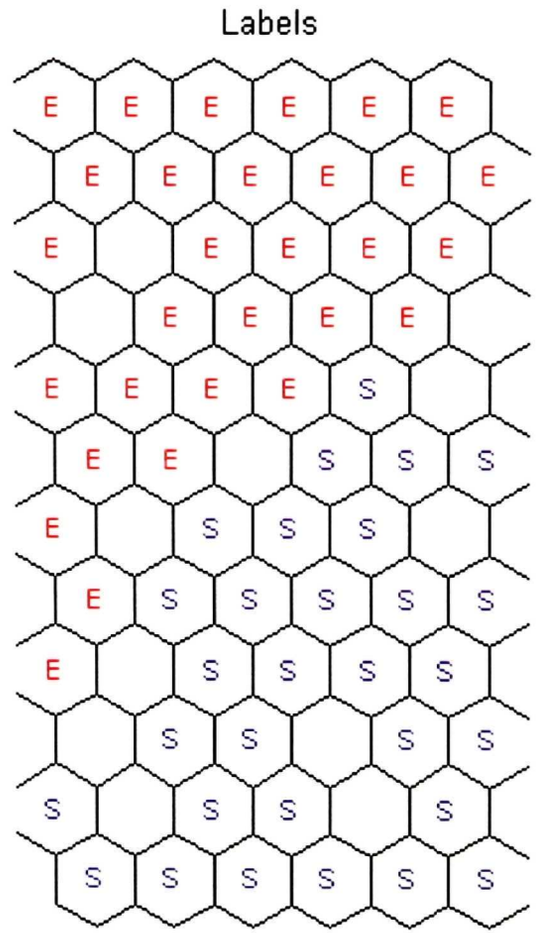

Figure 7.6: SOM obtained using the spectral data for 25 EMRSA (E) and 22 SMRSA (S) strains in the region 940-929 cm^{-1}

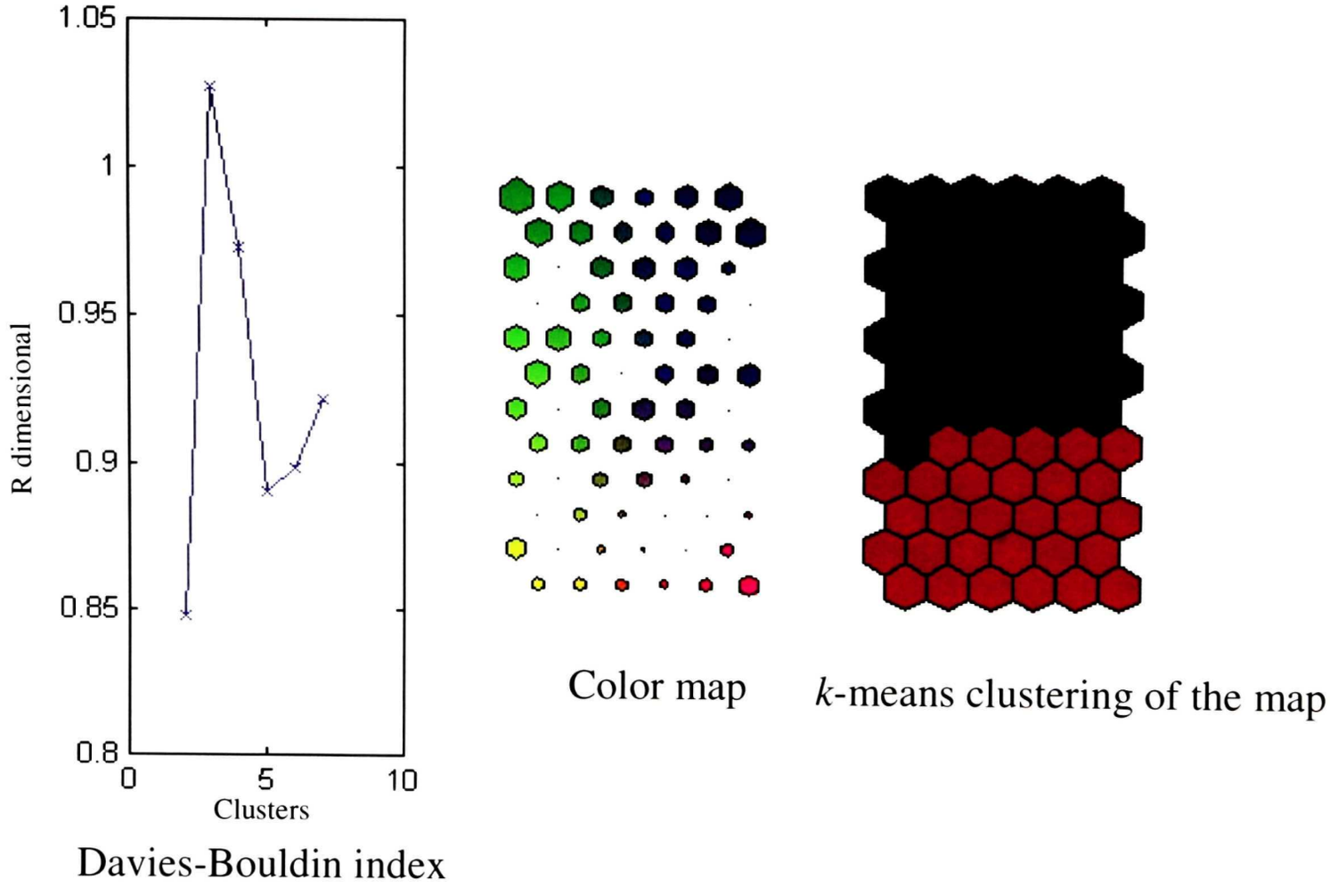

Figure 7.7: Partitioned SOM for the spectral data in the region 940-929 cm^{-1} obtained by applying the *k*-means algorithm and the Davies-Bouldin index

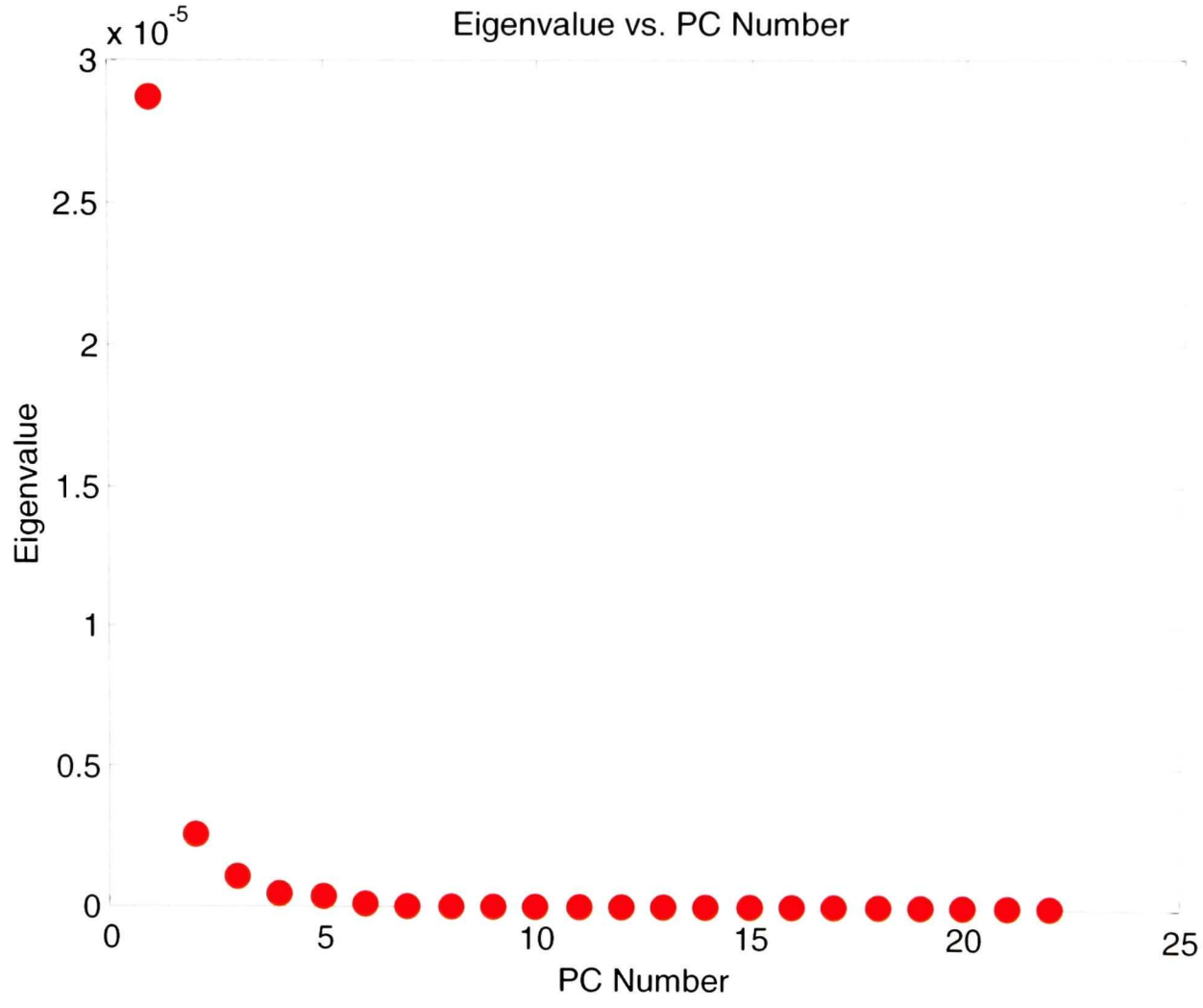

Figure 7.8: Eigenvalue plot obtained by PCA based on the spectral data for 25 EMRSA and 22 SMRSA strains in the region 1346-1306 cm^{-1}

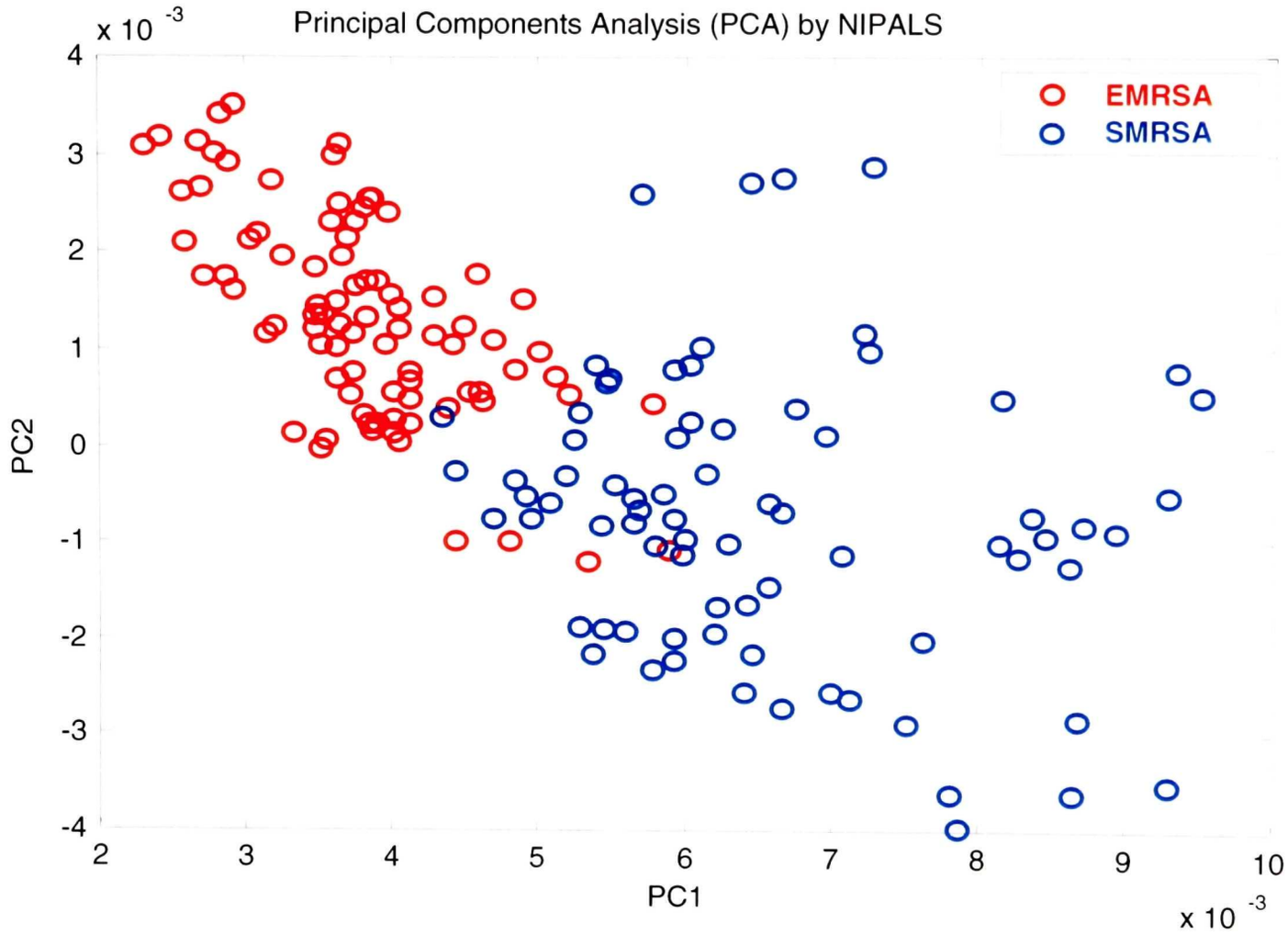

Figure 7.9: Scores plot for first two PCs obtained from the spectral data for 25 EMRSA and 22 SMRSA strains in the region 1346-1306 cm^{-1} by PCA using the NIPALS algorithm

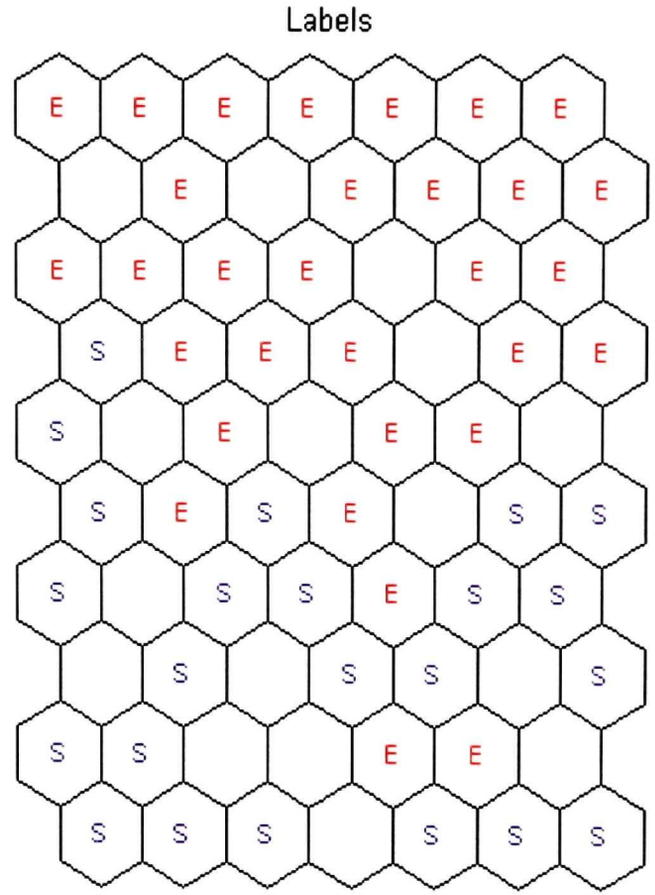

Figure 7.10: SOM obtained using the spectral data for 25 EMRSA (E) and 22 SMRSA (S) strains in the region 1346-1306 cm^{-1}

CHAPTER 8

CONCLUSION AND CONTRIBUTIONS TO KNOWLEDGE

Research conducted primarily during the past decade has demonstrated that the information about the total biochemical composition of the cell contained in the infrared spectrum of a microorganism can be widely exploited for the classification, differentiation, and identification of microorganisms. In the research presented in this thesis, FTIR spectroscopy was utilized for the first time in the identification of the different phenotypes of antibiotic-resistant staphylococci strains and in the epidemiological typing of methicillin-resistant *S. aureus* strains. The major contributions to knowledge resulting from this research may be summarized as follows.

1. **Demonstrated the capacity of FTIR spectroscopy, combined with the use of a universal growth medium and chemometrics, for the discrimination of methicillin-resistant** *Staphylococcus aureus* **(MRSA) strains from methicillin-sensitive** *S. aureus* **(MSSA) and from borderline oxacillin-resistant** *S aureus* **(BORSA)**

Subtle differences in the infrared spectra of *Staphylococcus aureus* strains were identified and shown to be useful for the accurate identification of MRSA among MSSA and BORSA strains. The accurate differentiation between BORSA, MSSA and MRSA strains would allow physicians to avoid prescribing vancomycin unnecessarily, thereby reducing both cost of care and the risk of side effects and the development of bacterial resistance to vancomycin.

2. **Provided experimental evidence that information inherent in the infrared spectra can successfully differentiate coagulase-negative staphylococci (CNS) from** *S. aureus* **and from MSSA and MRSA strains**

Excellent agreement between PCR and agglutination tests and an FTIR-based method developed in this thesis provides the means for the rapid discrimination between *S.*

aureus and CNS strains and for the determination of whether strains from a patient represent contamination or infection.

3. **Developed the first simple technique to reliably detect glycopeptide-intermediate *Staphylococcus aureus* (GISA) strains**

FTIR spectroscopy was shown to potentially serve as an alternative to antibiotic susceptibility testing for detection of GISA/h-GISA among MRSA isolates. The increasing emergence of clinical isolates of MRSA with reduced susceptibility to glycopeptides.has led to a critical need for such a routine screening method for the detection of GISA

4. **Demonstrated the utility of FTIR spectroscopy for the differentiation between the five Canadian epidemic MRSA (CMRSA) strains and as a means of epidemiological monitoring of MRSA in surveillance programs**

Exhaustive analysis of infrared spectra of CMRSA revealed subtle but reproducible differences between the infrared spectra of various strains of CMRSA. This led to the development of an FTIR method for the differentiation and epidemiological typing of MRSA that may potentially serve as a rapid, simple and cost-effective alternative to the gold standard technique (PFGE) in MRSA surveillance programs.

5. **Developed the first biophysical technique for the differentiation of epidemic MRSA (EMRSA) from sporadic MRSA (SMRSA)**

The FTIR method can be employed in a clinical setting for the identification of epidemic strains of MRSA through the differentiation of epidemic MRSA from sporadic MRSA, allowing for a more selective implementation of infection control measures in order to prevent dissemination of MRSA strains within hospitals. The adoption of the FTIR method could play a critical role in controlling the spread of epidemic MRSA.

6. Identification of spectral differences linked to the biochemical variability in the different phenotypes of staphylococci and in the five CMRSA strains

With the aid of the SVD algorithm, appropriate spectral regions allowing for differentiation between the different phenotypes of staphylococci and the separation of the five CMRSA strains were identified. These spectral regions are listed in Table 8.1 together with the results achieved using the three chemometric techniques employed in this work. In the majority of cases, higher rates of correct classification were achieved when differentiation of strains was based on the combined data from several spectral regions. In several cases, however, the best results were obtained by restricting the analysis to the data from a single narrow spectral region. In particular, it is noteworthy that the information contained in single spectral regions was sufficient for the complete differentiation of CNS from *S. aureus* and of SMRSA from EMRSA. In the latter case, the use of an alternative spectral region in which spectral differences between randomly selected SMRSA and EMRSA strains were also apparent gave a somewhat lower rate of correct classification. This finding highlights the importance of region selection in the development of FTIR methods for the differentiation of closely related strains. In contrast, the choice of the chemometric approach was not critical since similar rates of correct classification were achieved with exploratory (unsupervised) data analysis using PCA, an unsupervised artificial neural network approach (SOM), and supervised cluster analysis based on the KNN algorithm.

Although beyond the scope of the research described in this thesis, it would clearly be of interest to elucidate the origin of the spectral differences observed in the regions that were successfully employed for differentiation between the different phenotypes of staphylococci and the separation of the five CMRSA strains. However, such an undertaking would be exceedingly complex since the FTIR spectra represent the superposition of contributions from all the biochemical components in the cell and would require the application of a multitude of separation and analytical techniques.

In conclusion, the results presented in this thesis demonstrate that FTIR spectroscopy has considerable potential as an alternative rapid (1-hour) discriminative method for the differentiation between staphylococci strains and identification of antibiotic-resistant strains as well as epidemiological typing of methicillin-resistant *S. aureus* strains (Figure 8.1). It may thus be recommended that extensive validation studies of the FTIR methods developed in this thesis be undertaken.

Table 8.1. Infrared spectral regions allowing for differentiation of various phenotypes of staphylococci by FTIR spectroscopy

Strains differentiated	**Spectral region(s) (cm^{-1})**	**Percentage of correct classification based on:**		
		PCA	SOM	KNN
MRSA vs. MSSA	1070-1000 1732-1708 2968-2958	94	95	95
MSSA vs. BORSA	1732-1708	83	82	90
MRSA vs. BORSA	1118-1112 2622-2552	94	93	97
CNS vs. *S. aureus*	1442-1439	100	100	100
CNS vs. MSSA vs. MRSA	1080-1050 1442-1439 1732-1709 2969-2958	87	93	92
MSCNS vs. MRCNS	2880-2860	78	75	92
GISA/hGISA vs. MRSA	1480-1460	90	88	92
SMRSA vs. EMRSA	940-929	100	100	100
	1346-1306	96	87	98
CMRSA-1 CMRSA-2 CMRSA-3 CMRSA-4 CMRSA-5	1096-1066 1114-1099 2936-2880	86	86	97

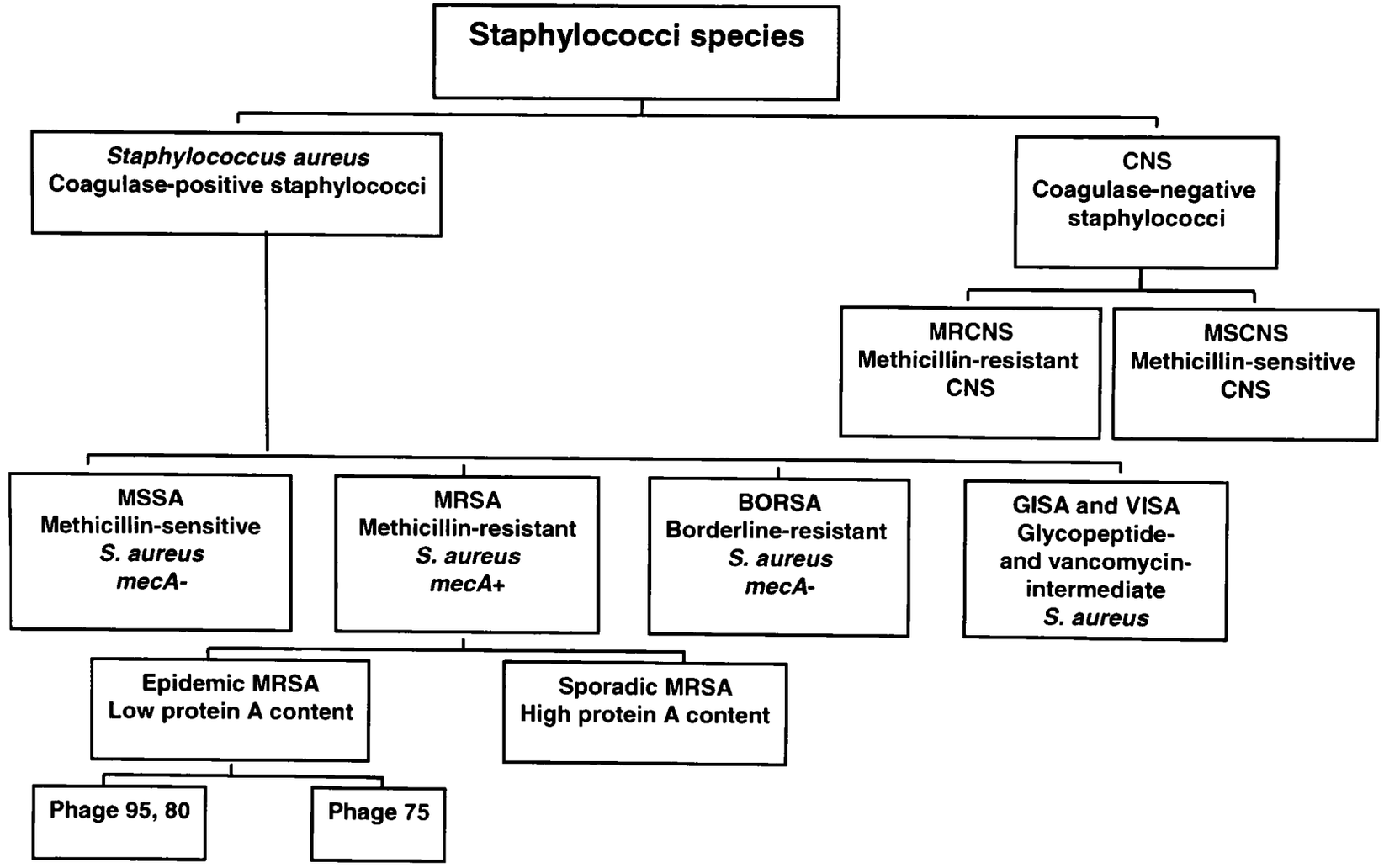

Figure 8. 1. Diagram illustrating hierarchical differentiation of staphylococci species by FTIR spectroscopy